# Mitochondrial voltage-dependent anion-selective channel (VDAC): A global player in cells.

By

**Sabbir Rahman Shuvo**

A Thesis submitted to the Faculty of Graduate Studies of the University of Manitoba

partial fulfilment of the requirements of the degree of

**DOCTOR OF PHILOSOPHY**

Department of Microbiology

Faculty of Science

University of Manitoba

Winnipeg, Manitoba

Canada

**Abstract:**

Mitochondria are primary ATP producing organelles and are involved in many cellular signalling pathways. Mitochondrial porin, which forms voltage-dependent anion-selective channels (VDAC) in the mitochondrial outer membrane (MOM), can be folded into a 19 β-stranded barrel. The N-terminus of the protein is external to the barrel, and contains α-helical structure. VDAC play roles in the transport of metabolites across the MOM and influences mitochondrial bioenergetics.

Here, *Neurospora crassa* VDAC was used as a model to investigate the effects of a partial deletion of the N-terminal segment. The protein, ΔN2-12porin, is assembled into the outer membrane, albeit at lower levels than the wild-type (WT) protein. The resulting strain displays electron transport chain deficiencies, concomitant expression of alternative oxidase, and decreased growth rates. Most of the genes that are expressed in high levels in porin-less *N. crassa* are expressed at levels like WT or are slightly increased in ΔN2-12porin strain. Thus, although the N-terminal segment of VDAC is required for complete function *in vivo*, low levels of a protein lacking part of the N-terminus can rescue some of the defects associated with the absence of porin.

In the second study, in comparison with WT, the VDAC-less mitochondria display lower complex I and respiratory control ratio, but higher ROS production capacity under non-phosphorylating conditions. Membrane depolarization by subsequent addition of ADP was significantly lower than that observed in wild-type organelles. Mitochondria harbouring about 50% of the wild-type amount of VDAC have elevated complex II activity and ROS production capacity compared to wild-type. Similarly, in mitochondria expressing low levels of an N-terminally truncated VDAC (ΔN2-12porin), higher ROS production capacity was detected compared to wild-type.

Lastly, proteomic analyses of cytosolic proteins in a VDAC-less *N. crassa* and *Saccharomyces cerevisiae* strains revealed proteins related to protein synthesis are less abundant; this includes those involved in amino acid and nucleotide metabolism. In contrast, proteins involved in aerobic respiration, in the TCA cycle, carbohydrate and sugar metabolism and oxidative stress responses were more abundant. Additionally, the absence of VDAC influences the composition of mitochondrial membrane, unfolded protein response and target of rapamycin pathways.

Overall these studies revealed the functions associated with the N-terminal of VDAC and the global roles of VDAC.

**Acknowledgements:**

First, I would like to thank GOD, for his blessing and mercy.

A special thanks to my supervisor, Dr. Deborah Court, for providing me the opportunity to work in her lab. I am honoured to work under her guidance. Without her support and guidance, this work won't be possible.

I would like to thank, my committee members, Dr. Georg Hausner, Dr. Ayush Kumar, Dr. Jason Treberg for their valuable comments and for providing training with different instruments.

I would like to express my gratitude to Fraser Ferens. His support and ideas help me a lot. I will miss our discussion on different topics.

I would like to thank my previous lab colleague Anna Motnenko and all the summers and project students in the lab. My gratitude towards the people at the Department of Microbiology, University of Manitoba.

I would like to acknowledge the support from my mother Sahida Nasrin and my father Hafizur Rahman. Without their encouragement and sacrifice, I won't be able to reach here.

Last, but not the least, I would like to show gratitude to the funding agencies NSERC and University of Manitoba for providing financial support to finish this work.

# Table of Contents

**List of Tables:**

**List of Figures:**

**List of Abbreviations:**

| | |
|---|---|
| a. u. | arbitrary unit |
| ADP | adenosine diphosphate |
| AOX | alternative oxidase |
| ATP | adenosine triphosphate |
| bp | base pair |
| $Ca^{2+}$ | Calcium |
| CD | circular dichroism |
| cDNA | complimentary deoxyribonucleic acid |
| CL | cardiolipin |
| COX | cytochrome c oxidase |
| Da | Dalton |
| DFC | dichlorofluorescein |
| DMSO | dimethyl sulfoxide |
| EDTA | ethylenediamine-tetraacetic acid |
| ER | endoplasmic reticulum |
| ETC | electron transport chain |

| | |
|---|---|
| F | Fluorescence |
| FAD | flavin adenine dinucleotide |
| GFP | green fluorescent protein |
| GPU | graphics processing unit |
| hVDAC | human voltage-depended anion-selective channel |
| IMS | intermembrane space |
| Ire1 | inositol-requiring enzyme-1 |
| LC | liquid chromatography |
| M | molar |
| m/z | m stands for mass and z stands for charge number of ions |
| MD | molecular dynamic |
| mg | milligram |
| MGF | mascot generic format |
| MIM | mitochondrial inner membrane |
| min | minute |
| ml | milliltre |
| mM | millimolar |

| | |
|---|---|
| MOM | mitochondrial outer membrane |
| MS | mass spectrometry |
| mVDAC | mouse VDAC |
| NADH | nicotinamide adenine dinucleotide |
| ng | nanogram |
| NMR | nuclear magnetic resonance |
| NTB | nitrotetrazolium blue |
| N-terminus | amino terminus |
| OD | optical density |
| ORF | open reading frame |
| OSCP | oligomycin sensitivity-conferring protein |
| OXPHOS | oxidative phosphorylation |
| PC | phosphatidylcholine |
| PCR | polymerase chain reaction |
| PE | phosphatidylethanolamine |
| PI | phosphatidylinositol |
| PMSF | phenylmethylsulfonyl fluoride |

| | |
|---|---|
| RNA | ribonucleic acid |
| ROS | reactive oxygen species |
| rpm | rotation per minute |
| SDH | succinate dihydrogen |
| SDS-PAGE | sodium dodecyl sulfate polyacrylamide gel electrophoresis |
| SHAM | salicylhydroxamic acid |
| SPR | surface plasmon resonance |
| TCA | tricarboxylic acid cycle |
| TIC | total ion count |
| TMRM | tetramethylrhodamine methyl ester |
| TOR | target of rapamycin |
| tRNA | Transfer RNA |
| UPR | unfolded protein response |
| UTR | untranslated region |
| VM | Vogel's minimal medium |
| zfVDAC | zebra fish VDAC |
| Δ | deletion |

| | |
|---|---|
| µg | microgram |
| µl | microlitre |
| µm | micrometer |
| VDAC | voltage-dependent anion-selective channel |

## Copyright information:

This Agreement between Mr. Sabbir Rahman ("You") and NRC Research Press ("NRC Research Press") consists of your license details and the terms and conditions provided by NRC Research Press and Copyright Clearance Center.

| | |
|---|---|
| License Number | 4164420588402 |
| License date | Aug 08, 2017 |
| Licensed Content Publisher | NRC Research Press |
| Licensed Content Publication | Canadian Journal of Microbiology |
| Licensed Content Title | Functional characterization of an N-terminally-truncated mitochondrial porin expressed in Neurospora crassa |
| Licensed Content Author | Sabbir R. Shuvo, Uliana Kovaltchouk, Abdullah Zubaer, et al |
| Licensed Content Date | Aug 1, 2017 |
| Licensed Content Volume | 63 |
| Licensed Content Issue | 8 |
| Type of Use | Thesis/Dissertation |
| Requestor type | Author (original work) |
| Format | Print and electronic |
| Portion | Full article |
| Order reference number | |
| Title of your thesis / dissertation | VDAC- a global player of the cells |
| Expected completion date | Dec 2017 |
| Estimated size(pages) | 250 |

This Agreement between Mr. Sabbir Rahman ("You") and Elsevier ("Elsevier") consists of your license details and the terms and conditions provided by Elsevier and Copyright Clearance Center.

| | |
|---|---|
| License Number | 4164420243615 |
| License date | Aug 08, 2017 |
| Licensed Content Publisher | Elsevier |
| Licensed Content Publication | Biochimica et Biophysica Acta (BBA) - Biomembranes |
| Licensed Content Title | The N-terminus of VDAC: Structure, mutational analysis, and a potential role in regulating barrel shape |
| Licensed Content Author | Sabbir R. Shuvo,Fraser G. Ferens,Deborah A. Court |
| Licensed Content Date | Jun 1, 2016 |
| Licensed Content Volume | 1858 |
| Licensed Content Issue | 6 |
| Licensed Content Pages | 12 |
| Start Page | 1350 |
| End Page | 1361 |
| Type of Use | reuse in a thesis/dissertation |
| Portion | full article |
| Format | both print and electronic |
| Are you the author of this Elsevier article? | Yes |
| Will you be translating? | No |
| Title of your thesis/dissertation | VDAC- a global player of the cells |
| Expected completion date | Dec 2017 |
| Estimated size (number of pages) | 250 |

**Authors' contributions:**

**Chapter 1:** Literature review. Part of the literature review (1.2, 1.2.1,1.2.3-1.2.3.3) was adapted from (Shuvo et al., Biochim. Biophys. Acta - Biomembr. 1858 (2016) 1350–1361). Fraser Ferens wrote the section "Role of the N-terminus in nucleotide binding". Deborah Court designed the reviewed and edited the manuscript. Sabbir Shuvo designed and wrote the manuscript.

**Chapter 2:** "Functional characterization of an N-terminally-truncated mitochondrial porin expressed in *Neurospora crassa*. (Shuvo et al., Can. J. Microbiol. 68 (2017) 730–738)". Uliana Kovaltchouk performed growth rate experiments. William A.T. Summers generated the ΔN2-12porin strain. Abdullah Zubaer and Georg Hausner helped with genome analysis. Lynda J. Donald contributed with mass spectrometry. Ayush Kumar provided intellectual assistance with qRT-PCR. Deborah Court designed the project, reviewed and edited the manuscript.

**Chapter 3: "**The impact of changes to VDAC levels and expression of an N-terminally truncated VDAC on mitochondrial bioenergetics and reactive oxygen species production in *Neurospora crassa"*. Lilian M. Wiens contributed to respiration and membrane potential experiments. She also did the ANOVA test. Jason R. Treberg contributed to the design of the experiments and reviewed the manuscript. Deborah Court reviewed and edited the manuscript (submitted).

**Chapter 4**: "The absence of VDAC from *Neurospora crassa* influences differential protein expression profile, mitochondrial membrane composition and UPR pathway". Anna Motnenko analyzed mitochondrial 2D LC-MS/MS proteomic data. Oleg Krokhin and Victor Spicer performed LC-MS/MS analysis. Deborah Court designed the project, reviewed and edited the manuscript (in revision).

**Chapter 5:** "The absence of Por1p in *Saccharomyces cerevisiae* associated with differential cytosolic protein expression profile and downregulation of TOR pathway". Sabbir Shuvo designed

the experiments, analyzed data and wrote the manuscript. Deborah Court designed the project, reviewed and edited the manuscript (in preparation).

# Chapter 1: Literature review

## 1. Introduction:

The voltage dependent anion-selective channel (VDAC) is the most abundant mitochondrial outer membrane (MOM) protein [1]. It is a pore forming β-barrel containing protein that has a flexible N-terminus (Figure 1.1A) [2], and works as a channel in the MOM for the transport of metabolites. In addition, studies have proposed that the N-terminus of VDAC influences the movement of the metabolites [2]. There are several aims for this study (Figure 1.1). First, the elucidation of the *in vivo* roles of the N-terminus of VDAC. For these studies, a VDAC with a truncated N-terminus was generated in a model organism *Neurospora crassa* (Figure1.1A). Secondly, the roles of VDAC in mitochondrial bioenergetics and ROS production were studied (Figure 1.1B). Here, the differences between mitochondrial bioenergetics, electron transport chain complexes and the expression of alternative oxidase (AOX) in different VDAC variants was investigated. Lastly, in the absence of VDAC, cellular stress responses were studied by using proteomic studies as a tool (Figure 1.1C). Overall, these studies will help us to understand cellular responses in the absence of VDAC and in presence of the N-terminally truncated VDAC.

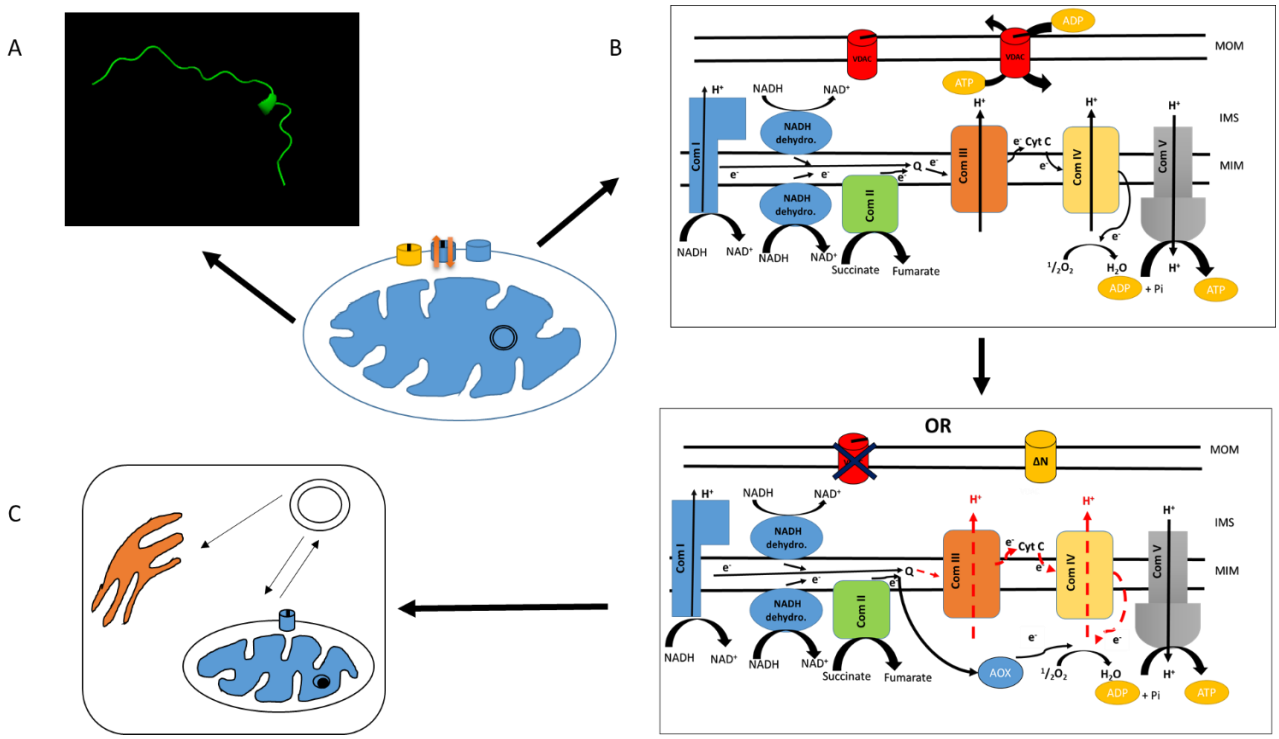


Figure 1.1: Graphical abstract of the thesis.

A) The elucidation of the *in vivo* roles of the N-terminus of VDAC. 1-21 residues of *N. crassa* VDAC is shown**.** Stucture was drown following the structure (PDB: 2JK4) B) The influence of VDAC on mitochondrial bioenergetics and ROS production. Upper panel is WT and lower panel represents the situation in mitochondria with VDAC defects. The complete figure legend linked to Figure 3.1 and Figure 3.2 in the thesis. C) The global impact of VDAC deficiencies was studied by using proteomic analysis. The arrows between mitochondria and nucleus indicate bidirectional communication between mitochondria and nucleus. The arrow between nucleus to endoplasmic reticulum (ER) indicates signal transfer between nucleus and ER.

**1.1 Mitochondrion:**

The mitochondrion is the primary energy transforming organelle in the most eukaryotic cells. Mitochondrion originated from α-proteobacteria through endosymbiosis process. Mitochondria are 0.5- 1μm in diameter and are represented as elongated cylinders shaped like bacteria; they reside in the cytoplasm of the cells [3]. However, structure of mitochondria is constantly changing because of fusing and fissioning with other mitochondria.

A mitochondrion is a double membrane bound organelle. The MOM covers the organelle and the mitochondrial inner membrane (MIM) folds over many times to form cristae. The space between two membranes is the intermembrane space (IMS) and the space bounded by the MIM is the matrix, which contains mitochondrial DNA. The mitochondrial genome of the model organism used in these studies, *N. crassa,* is 64,800 bases and contains 28 protein coding genes, as well as 2 rRNAs and 28 tRNA genes [4,5]. Although mitochondria contain their own DNA, they require nuclear-encoded proteins for their functions [6]. One of the MOM proteins is VDAC, which works as a tunnel for the transport of metabolites across the MOM, and is the focus of this thesis.

Mitochondria are an essential parts of normal physiological functions; they are accountable for energy transformation in most eukaryotes. Mitochondria transform cellular energy to ATP through oxidative phosphorylation (OXPHOS). They are also involved in the synthesis of phospholipids, amino acids and heme and play roles in calcium homeostasis, β-oxidation of fatty acids and activation of apoptosis [7].

**1.2 Voltage dependent anion-selective channel (VDAC):**

The VDAC, also known as mitochondrial porin, is a β-strand-rich protein that resides in the MOM. It is a highly abundant protein, and is responsible for the passage of most of the small molecules that are exchanged between the cytosol and the IMS [8]. In artificial membranes, the channel is slightly anion-selective and sensitive to partial closure, or gating, upon application of an electrical potential of around 30-50 mV. The partially closed pore is slightly cation-selective [9,10].

### 1.2.1 VDAC structure:

It was long assumed that this protein folded in a way analogous to that of bacterial porins, i.e. in a β-barrel comprised of an even number of β-strands [11–13]. Alternatively, a mixed structure of 13 β-strands and the N-terminal α-helix was proposed, based on the electrophysiological properties of engineered VDAC variants [14]. Direct structural analysis of isolated VDAC for the most part was limited to characterization by circular dichroism spectropolarimetry [15], proteolysis [16] and antibody binding [17] , until the use of recombinant VDAC, expressed in *E. coli* was optimized [18–20]. The protein, purified in denatured form and subsequently folded in detergent or lipid/detergent bicelles was analyzed by NMR [21], x-ray crystallography, [22,23] or a mixture of the two methods [24]. Human VDAC1 (hVDAC1), the highly similar mouse VDAC1 (mVDAC1) and human and zebrafish VDAC2 (zfVDAC2) folded into novel structures comprised of an odd number of β-strands (19) and an N-terminal α-helix that adopted several conformations. In most analyses, it was rich in α-helix [24,25], but in one form it was unfolded [26]. Homologous modelling of *N. crassa* mitochondrial VDAC also predicted 19 β-strands and an N-terminal α-helix (Figure 2).

A.

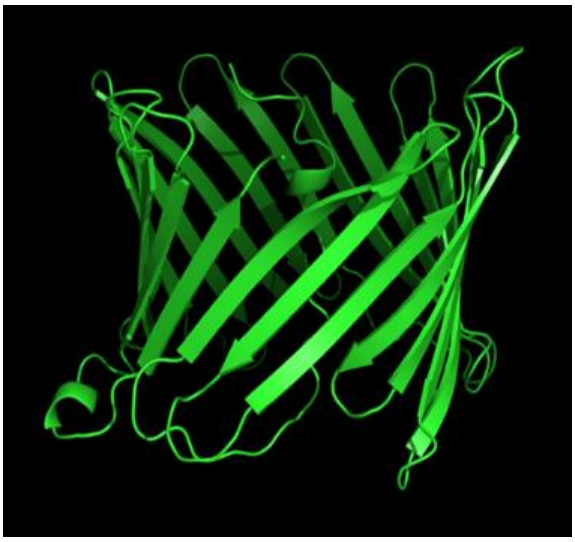

B.

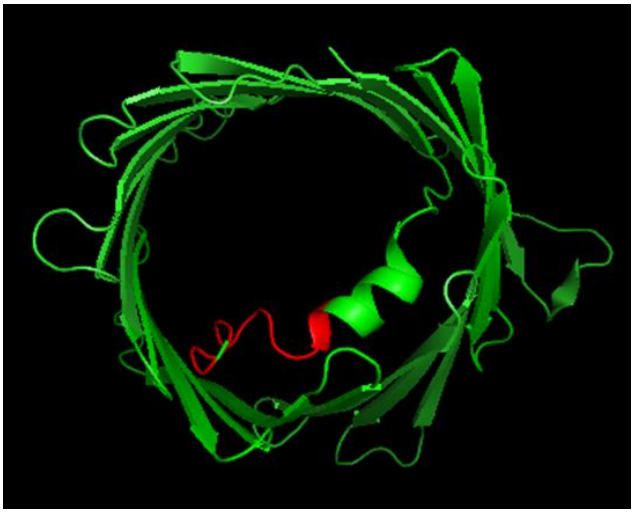

Figure 1.1: Predicted structure of a *N. crassa* VDAC.

The structure was predicted in Phyre2 [27] following template PDB: 2K4T and created in PyMOL (https://www.pymol.org/). Side view of VDAC (A). Top view of the VDAC (B). Red indicates deleted N-terminal segment of VDAC.

### 1.2.2 VDAC interactions with other proteins:

VDAC interacts with numerous proteins in cells for performing different cellular functions and for maintaining cellular homeostasis [28–30]. In the absence of VDAC, some proteins were differentially expressed compared to WT (Chapters 4 and 5). Therefore, VDAC interactions with a subset of these different proteins are discussed below.

#### 1.2.2.1 VDAC-hexokinase:

The first step of glycolysis is catalyzed by hexokinase through phosphorylation of glucose to glucose-6-phosphate. This is the rate limiting step in glycolysis. Different studies have suggested that mammalian hexokinases I and II can bind to the MOM, specifically to VDAC [31,32]. The hydrophobic tails of the N-terminal domains of mammalian hexokinase I and II may interact with one or more transmembrane domains of VDAC [1]. The interaction between VDAC and hexokinase is important for the survival of cells, possibly because hexokinase can prevent apoptosis by closing the mitochondrial permeability transition pore [32–34].

#### 1.2.2.2 VDAC-cytoskeleton proteins:

The cytoskeletal proteins actin and tubulin have been proposed to control mitochondrial distribution and localization [35–37]. Interaction of VDAC with actin was shown in bilayer experiments [38], through enzymology [38], co-immunoprecipitation [1], and surface plasmon resonance (SPR) methods [28]. Moreover, it has been proposed that actin can modulate the gating of VDAC [36] and that dimeric tubulin can cause reversible closure of VDAC reconstituted in artificial bilayers [37]. The negatively charged C-terminus of tubulin was proposed to interact with VDAC and block the channel conductivity [1]. VDAC-actin interaction may be involved in

mitochondrial distribution. Therefore, interactions between cytoskeleton proteins and VDAC may be important for proper cellular functions.

#### 1.2.2.3 VDAC- adenine nucleotide translocator (ANT):

It has been proposed that VDAC-ANT complexes are important for the transport of ADP and ATP [39]. These complexes work as a rate limiting step for the movement of ADP/ATP [39]. For example, decreased levels of cytosolic ATP and ADP were detected in T-Rex-293 cells when VDAC1 was knocked down by shRNA [40]. Similarly, when human VDAC1 was blocked by itraconazol the ADP/ATP pool was disrupted compared to non-treated cells [41]. Furthermore, when nucleotide binding sites were mutated, in murine VDAC1, lower levels of cellular ATP were detected [42]. However, other proteins also interact with VDAC-ANT complexes, such as hexokinase, creatine kinase and cytochrome *c*. VDAC-ANT-hexokinase complexes were isolated from mitochondrial membranes solubilized with TritonX-100. From the same membrane extracts, another complex composed of VDAC-ANT and creatine kinase was isolated [32].

#### 1.2.2.4 VDAC and members of the Bcl-2 family:

Recent studies have shown that both anti and pro-apoptosis proteins can interact with VDAC to control mitochondrial mediated apoptosis. In the proteoliposomes assay, efflux of sucrose increased in the presence of Bax through human VDAC1; in contrast, in the presence of Bcl-xL efflux was stopped. Therefore, Bax may influence the opening of VDAC and Bcl-xL may influence the closing of VDAC. Moreover, the pore size of VDAC1 was increased in the presence of Bax, although, oligomeric Bax has no effect on the function of VDAC [1]. Another study found that, Bax and Bim interact with VDAC to release cytochrome c; on the other hand, Bcl-xL inhibits the release [33]. Different studies strongly support the connection of VDAC with the activity of

pro- and anti-apoptotic proteins. However, this kind of involvement is dependent on different cell types and apoptosis stimulus.

### 1.2.3 N-terminus of VDAC:

Structural studies have suggested that VDAC has an N-terminal α-helix [24,25] and *in vitro* studies suggest that the N-terminus of VDAC is involved in modulating VDAC functions. The *in vivo* roles of the N-terminus of VDAC were studied in this thesis. The following sections describe different aspects of the N-terminus of VDAC.

#### 1.2.3.1 Sequence and structure of the N-terminal segment:

The α-helical nature of the N-terminus was predicted with the first reports of the primary sequences of fungal mitochondrial porins [12,13]. The N-terminal sequence of VDAC is usually defined as the sequence preceding the first β strand (β1), and can range from 24 residues in *N. crassa* to over 77 residues in *Drosophila melanogaster* (isoform CG31722_B; [43]. Many organisms harbour paralogues of the VDAC gene; for example, mammalian cells express three VDAC isoforms, while fungi may have one (*N. crassa*) or two (*S. cerevisiae*) and plants may express over five [10,11]. In most VDAC, the N terminal sequence is around 25 residues in length. Exceptions include VDAC2 from mammals, including humans, on which there is an N terminal extension of 11 residues (Figure 3).

The α-helical nature of the N-terminus was subsequently confirmed by circular dichroism (CD) spectropolarimetry of N-terminal peptides in non-polar solutions [44] or detergents [45]. CD and infrared spectroscopy analyses and Molecular Dynamic (MD) simulations of peptides

corresponding to the α helical region (residues 1-25 for hVDAC1 and hVDAC3 and 12-36 for hVDAC2; see Figure 3) supported an equilibrium between random coil and partially folded α-helices in phosphate buffer. The N-terminus of hVDAC1 showed the highest helical propensity. However, as noted by the authors, folding of the N-terminus is likely directed and stabilized by the whole VDAC molecule [46].

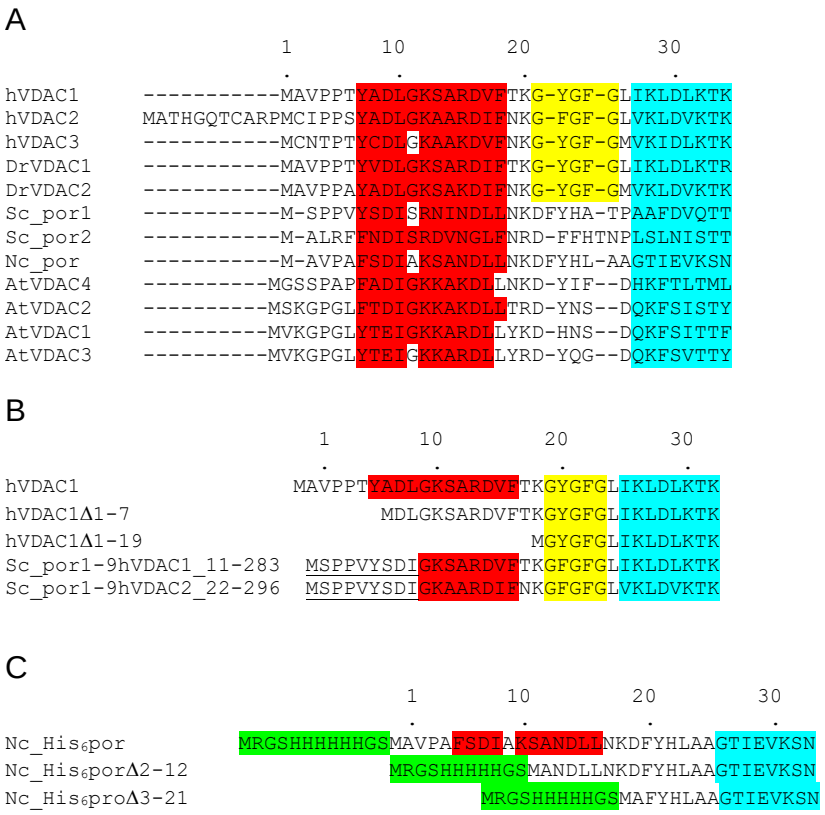


Figure 1.2: N-terminal sequences of different species of VDAC.

A) Alignment of N-termini of VDAC isoforms from *Homo sapiens* (h), *Danio rerio* (Dr), *S. cerevisiae* (Sc), *N. crassa* (Nc) and *Arabidopsis thaliana* (At). Alignments were carried out with PRALINE [42], and secondary structure predictions with the linked PSIPRED function [43]. Sequences were obtained from Swiss-Prot (hVDAC1 (P12796), hVDAC2 (P45880), hVDAC3 (Q9Y277), DrVDAC1 (Q6NWC1), DrVDAC2 (Q8AWD0), Sc_Por1 (P04840), Sc_Por2 (P40478), Nc_Por (P07144), AtVDAC1 (Q9SRH5), AtVDAC2 (Q9FJX3), AtVDAC3 (Q9SMX3), AtVDAC4 (Q9FKM2). B) Alignment of N-termini from variants of hVDAC1. The N-terminal sequences of variants lacking the first 7 (Δ7, [44]) and 20 (Δ20, [23]) residues of hVDAC1 are shown. The N-terminal sequences of two chimeric proteins composed of the N-terminal nine residues (underlined) of *S. cerevisiae* porin (Sc) and the indicated residues of

hVDAC1[45] are shown. C) Alignment of the N-terminal sequences of the wild-type (Nc_por) and two N-terminal truncation variants of *N. crassa* VDAC [46]. In all panels, sequences in red and blue are predicted to form α-helix and β-strand, respectively. Yellow indicates the glycine-rich-segment in mammalian VDAC, and $H_6$-tags and the additional residues introduced through cloning into the pQE-9 vector [46] are highlighted in green. Figure is taken from [1] with permission.

In studies of full-length VDAC, the folded state of the N-terminal segment varies from one rich in α-helix to an unstructured state. A flexible, unstructured N-terminus was predicted for C-terminally tagged hVDAC1 (hVDAC1-$H_6$) from the nuclear magnetic resonance (NMR) data of [26], but subsequent studies have not led to similar observations. NMR [25] and x-ray crystallographic [22] analyses of hVDAC1-$H_6$ and N-terminally tagged mVDAC1 ($H_6$-VDAC1), respectively, support the presence of two short α-helices (residues 6-9 and 12-20), as does NMR analysis of zebrafish [23] and human [47] VDAC2. In the structure determined by crystallography [22], a bidentate hydrogen bond between the carbonyl oxygens of A8 and L10 (helix 1) and R15 (helix 2) was detected in mVDAC1. In general agreement with the structural information described above [22], Molecular Dynamic simulations of a peptide comprised of residues 1-25 predicts two peaks of helical structure, one centred around residue 8 and the other around residue 16 in hVDAC isoforms 1 and 3. α-helical structure was also detected in the NMR/x-ray diffraction studies of hVDAC1-$H_6$ although in this case a single helix (residues 7-17) was positioned horizontally along the midpoint of the barrel. Information regarding A2 was not available to support or preclude the bidentate hydrogen bond detected in the mVDAC1 structure. The observed variation in structure likely indicates, not unexpectedly, that the structure and resulting flexibility of the N-terminus is dependent on the conditions for refolding and crystallization, and may also reflect the presence or absence of an N-terminal his-tag, or additional resides resulting from the cloning strategy used.

.

### 1.2.3.2. Role of the N-terminus in oligomerization:

Dimers, trimers and multimers of VDAC have been detected in mitochondria or purified outer membranes [48,49], and in detergent-solubilized recombinant proteins[19,23,50]. The role of the N-terminus in dimerization was investigated using T6C-ΔCys-rVDAC1, a variant lacking all native cysteines, and in which T6 was replaced by a cysteine [51]. Upon treatment of cells harbouring this variant with the crosslinker BMOE, VDAC dimers, and monomers resulting from intramolecular crosslinking, were observed. Dimer formation was increased if the second α-helical region was disrupted (R15P/D16P-rVDAC1), and was decreased in molecules with alterations in the glycine-rich-segment (G21V/G23VrVDAC1). Together, these results were interpreted to indicate that the N-terminal segment leaves the lumen and participates in intermolecular interactions that lead to dimerization [51]. Other *in vivo* studies suggest that the N-terminus is not required for oligomerization. In cultured human cells, in which hVDAC1 expression is suppressed, over-expressed mVDAC1 forms oligomers that can be isolated following chemical cross-linking of isolated mitochondria with the hydrophobic cross-linking agent [52]. N-terminally truncated Δ(26)VDAC1 also forms multimers under these conditions. Although these results suggest that the N-terminal region is not required for VDAC1 oligomerization *in vivo* [52], crowding due to high concentrations of Δ(26)VDAC1 in the MOM may have contributed to the levels of oligomers detected.

### 1.2.3.3 The mammalian VDAC N-terminus, hexokinase binding and apoptosis:

VDAC contributes to the regulation of cellular metabolism and cell death through its interactions with kinases, including hexokinase, and apoptotic regulators of the Bcl-2 family, respectively. Both activities contribute to the characteristics of rapidly growing cancer cells that

avoid apoptosis [1]. Its interactions with hexokinases I and II allow these proteins preferential access to ATP generated through oxidative phosphorylation. The role of the N-terminus in hexokinase binding has been investigated using peptides corresponding to the N-terminus [74], and with VDAC variants lacking the N- terminal segment [66]. Surface plasmon resonance (SPR) studies reveal that mVDAC1 peptide A2-I27 interacts with immobilized hexokinase I (HKI). *In vivo,* overexpression of the 26-residue mVDAC1 N-terminal peptide can cause release of HKI-GFP fusion protein from the mitochondria [53] and blocks the anti-apoptotic effect of overexpressed HKI, HKII or Bcl-2 *in vivo* [52]. These effects were not specific to the N-terminal peptide, but were also observed for several internal peptides. Analysis of the N-terminus in the context of the full-length protein also implicates the N-terminus in regulation of apoptosis. Overexpression of mVDAC1, but not of Δ(26)mVDAC1, in hVDAC1-depleted cells (TREx-293) triggers apoptosis. Further, normal responses to a variety of apoptosis inducers are observed when full-length mVDAC1 is over-expressed in these cells, while Δ(26)mVDAC1-over-expressing cells are resistant to apoptosis and cytochrome c release is inhibited [52].

### 1.3 Mitochondrial respiration:

In the absence of VDAC, mitochondrial ETC complexes and mitochondrial respiration are impaired [54–56]. In the following section, mitochondrial ETC complexes and the proteins that are involved in the respiration process are discussed.

#### 1.3.1 Mitochondrial OXPHOS:

Mitochondrial OXPHOS is a set of metabolic reactions and processes inside the mitochondria. In this process energy stored in nutrients is converted to adenosine triphosphate (ATP), where oxygen works as a terminal electron acceptor. The coupling process of oxidation of

nutrient substrates to produce ATP was first described by Mitchell in his chemiosmotic theory in 1961 [57]. Mitochondrial ETC complexes (complexes I-IV) are present in the MIM and these enzymes use nicotinamide adenine dinucleotide (NADH) and succinate as substrates to generate electrons that are passed to the final electron acceptor, oxygen (Figure 1.1). During this process, protons are pumped from the mitochondrial matrix to the intermembrane space through these complexes. Thus, an electrochemical gradient, also known as the proton-motive force (PMF), is generated across the MIM. Later, protons return to the mitochondrial matrix through ATP synthase (complex V) to convert ADP and inorganic phosphate (Pi) to ATP. The flow of electrons and the process of ATP synthesis are maintained by the oxidation of the substrates and the use of oxygen. However, leakage of protons from the intermembrane space to mitochondrial matrix can alter this proton gradient [57].

### 1.3.2 Mitochondrial ETC complex I:

Mitochondrial complex I, also known as NADH: ubiquinone oxidoreductase, is one of the largest membrane-bound complexes in mitochondria. This enzyme complex is present in most eukaryotic organisms and catalyzes the oxidation of NADH. Although, most of the members of the fungal kingdom have complex I; some of the notable exceptions are *S. cerevisiae, Saccharomyces carlsbergii and Kluyveromyces lactis* [58]. Through NADH oxidation, protons are translocated across the MIM to generate a transmembrane proton gradient [58–61]. In the mammalian system, 45 protein subunits with a combined weight of 1 MD form complex I, whereas, only 14 protein subunits are needed for the formation of complex I in bacteria [62,63]. Complex I of *N. crassa* is composed of at least 39 peptide subunits, of which, 7 subunits are encoded in the mitochondrial genome (Table 1.1) and the rest are encoded in the nuclear genome. The complex I in *N. crassa* is an L-shaped structure: a hydrophilic peripheral arm that supplies

electrons to ubiquinone with the help of different prosthetic groups and a hydrophobic membrane arm resides the proton-translocating-P-module [64]. The pathways for formation of these two arms in *N. crassa* are independent from each other [65]. The complex procedure of transfer of electrons is initiated by the oxidation of NADH by a flavin mononucleotide; subsequently electrons move through an FeS (iron-sulphur) cluster to the ubiquinone. Protons are translocated through four proton-transfer routes that are distinct from the electron transfer process. Coupling between redox reactions and proton translocation happens near the junction of peripheral arm and the membrane arm [62].

### 1.3.3 Mitochondrial ETC Complex II:

ETC complex II, also termed as succinate:ubiquinone oxidoreductase, is present in both eukaryotes and bacteria. This complex is the simplest respiratory complex with respect to the number of protein subunits that form the complex [66]. Complex II is also part of the TCA cycle and catalyzes the conversion of succinate to fumarate. In eukaryotic systems, complex II is mostly encoded by nuclear genome (exception*: Porphyra purpurea*) and does not translocate protons [58,66,67]. The whole structure of complex II can be divided into a hydrophilic head and a hydrophobic tail, which resemble a "q" shape. The hydrophilic head group is highly conserved throughout mitochondria and bacteria, but distinct sequences for the hydrophobic arm have been observed between different domains of life [58]. Complex II also contains five prosthetic groups, such as FAD, three distinct iron-sulfur complexes and heme group. These prosthetic groups are important for electron transfer; as well as, they are also essential for the formation of the complex II [66,67]. Electron transfer in complex II is mediated by the oxidation of succinate to FAD, followed by the movement through iron-sulfur complexes to quinone or heme groups [67].

### 1.3.4 Mitochondrial ETC complex III:

Mitochondrial complex III, also known as ubiquinol cytochrome *c* oxidoreductase, is also referred to as cytochrome *bc1* complex. This complex facilitates the transfer of electrons from the low potential substrate ubiquinol to the high potential electron carrier cytochrome *c*. Simultaneously, it moves protons from the mitochondrial matrix side to the intermembrane space, thus, contributing to PMF. This complex was first isolated in 1962 from bovine heart mitochondria and the crystal structure of complex III was first published in 1997 [68]. Complex III is composed of 10-11 nuclear-encoded proteins subunits, but the *cyt b* subunits are encoded by mitochondria. The functional form of this complex is a dimer [69]. In *N. crassa*, the absence of complex III is not associated with the absence of complex I and complex IV [70]. Furthermore, deletion of complex III caused increases the complex I dimer and the formation of supercomplex I+IV. Moreover, deletion of this complex from mitochondria causes expression of AOX [70].

### 1.3.5 Mitochondrial ETC complex IV:

Mitochondrial complex IV, also known as cytochrome c oxidase (COX) is the last enzyme of the mitochondrial respiratory chain. Three mitochondrial DNA encoded protein subunits form the core of the complex and contain the prosthetic groups (heme and copper). An additional 10 protein subunits are encoded in the nuclear DNA and form the barrier around the core subunit. Moreover, 20 supplementary nuclear-encoded genes are required for the processing of COX. Expression of mitochondria-encoded protein subunits and nuclear encoded protein subunits, import and insertion of those subunits in the inner membrane, and the addition of prosthetic groups in the complex are tightly regulated nuclear-mitochondrial-coordinated fashion [71]. The

functional form of COX is a dimer that faces both mitochondrial matrix and mitochondrial intermembrane space. COX plays the role in electron transport chain by catalyzing the reduction of oxygen to water and the oxidation of reduced cytochrome c. This whole process is coupled with the transfer of protons across the MIM [71,72].

### 1.3.6 Mitochondrial ETC complex V:

Mitochondrial complex V, also known as ATP synthase, is a multi-subunit complex. This complex is composed of two functional domains: $F_1$ situated in the matrix site of mitochondria, and $F_0$ situated in the MIM. It has been proposed that the hydrophobic $F_0$ domain contains a protein channel and the hydrophilic $F_1$ domain contains the adenine nucleotide processing polypeptides. A mechanism has been proposed for the function of complex V, where, through the rotation of the $F_0$ section, protons from intermembrane space translocate to the matrix of mitochondria [73,74]. This rotation causes a conformational change of $F_1$ and helps to synthesize and release ATP from the complex. $F_1$ is formed by three copies of each of the subunits α and β, and one copy of each the subunits of γ, δ and ε. The central core of complex V is composed of $F_1$ subunits γ, δ and ε. Three subunits of this complex are encoded in the mitochondrial DNA and the rest are encoded in the nuclear DNA. Subunits of the c-ring and single copy of each of the a, b, d, F6 proteins and the oligomycin sensitivity-conferring protein (OSCP) form the $F_0$ segment of complex V [75].

Table 1.1: *N. crassa* mitochondria encoded ETC proteins

(http://www.fgsc.net/2000compendium/2000appendix4.html)

| **Gene name** | **Description** | **Present in the ETC complexes** |
|---|---|---|
| Nad1 | NADH dehydrogenase subunit 1 | Complex I |
| Nad2 | NADH dehydrogenase subunit 2 | |
| Nad3 | NADH dehydrogenase subunit 3 | |
| Nad4 | NADH dehydrogenase subunit 4 | |
| Nad4L | NADH dehydrogenase subunit 4L | |
| Nad5 | NADH dehydrogenase subunit 5 | |
| Nad6 | NADH dehydrogenase subunit 6 | |
| Cob | Apocytochrome b | Complex III |
| Cox1 | Cytochrome c oxidase subunit 1 | Complex IV |
| Cox2 | Cytochrome c oxidase subunit 2 | |
| Cox3 | Cytochrome c oxidase subunit 3 | |
| Atp6 | ATP synthase subunit 6 | Complex V |
| Atp8 | ATP synthase subunit 8 | |
| Atp9 | ATP synthase subunit 9 | |

### 1.3.7 Alternative NADH dehydrogenase:

Alternative NADH dehydrogenase, also known as class 2 NADH: ubiquinone oxidoreductase, is a non-proton pumping, rotenone-insensitive, single nuclear-encoded polypeptide with a molecular mass of 50-65 kDa [58,76–78]. In *N. crassa*, four alternative dehydrogenase enzymes are present (Figure 1.3) and flavin adenine dinucleotide (FAD) is the only prosthetic group in those enzymes [76]. NDE-1 (External alternative NADH dehydrogenase) can use NADPH as a substrate; however, NDE-2 and NDE-3 can utilize both NADH and NADPH as a substrate (Figure 1.4 ) [78,79]. NDI-1 (Internal NADH dehydrogenase) resides on the matrix side of the mitochondria and can catalyze NADH to produce $NAD^+$ [79]. Although they are encoded by a single peptide, a small N-terminal motif is proposed to determine mitochondrial import and the localization of enzymes to either side of the inner membrane [58,78]. The presence of a class 2 NADH dehydrogenase may help *N. crassa* survive when complex I becomes abnormal. These class 2 NADH dehydrogenases are proposed to work as overflow systems to maintain mitochondrial and cytosolic NADH and NADPH levels so that the tricarboxylic cycle can function normally and excessive reactive oxygen species cannot be produced [78]. However, knockout of different NADH dehydrogenases from *N. crassa* resulted in defective growth phenotypes, suggesting that they have roles in the growth and development of *N. crassa* [78]. In *S. cerevisiae,* three rotenone-insensitive NADH dehydrogenases are present. NDE1, NDE2 are external and NDI1 is the internally localized enzyme. It has been proposed that class 2 NADH dehydrogenases in *S. cerevisiae* compensate for the natural absence of complex I to maintain normal electron flow [58].

.

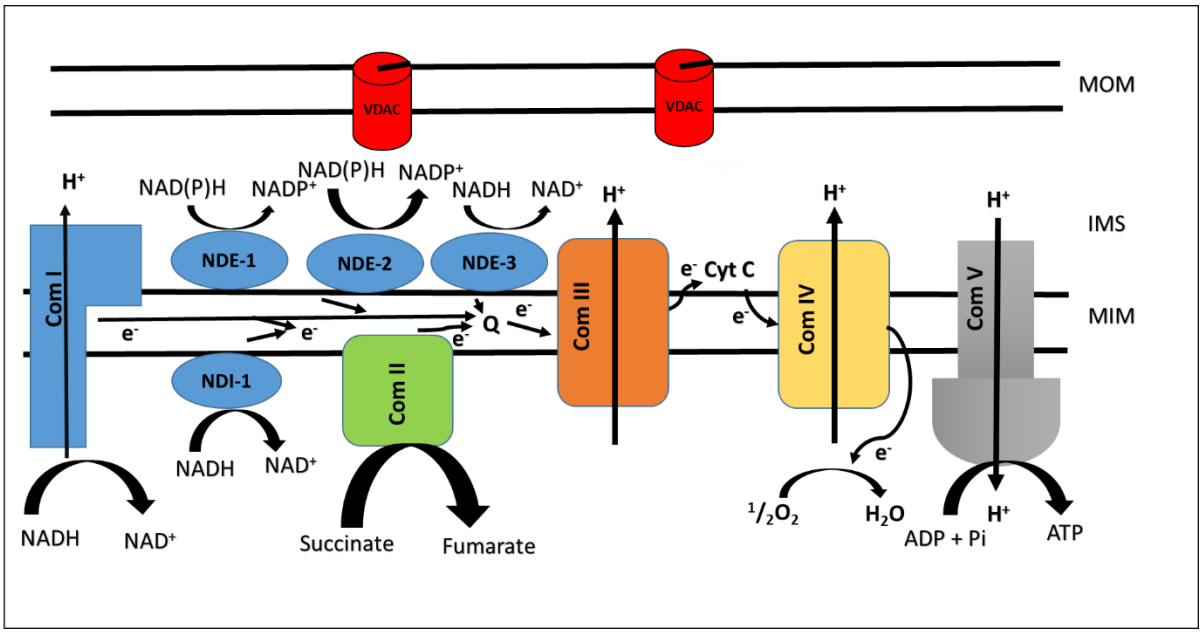


Figure 1.3: Electron transport and OXPHOS in *N. crassa* mitochondria.

In WT cells CoQ (Q) shuttles electrons from complex I and complex II to complex III. Cytochrome c collects electrons from complex III and transports them to complex IV. Electrons from complex IV react with the oxygen in the matrix of the mitochondria to produce $H_2O$. A proton gradient is generated across the MIM because of this mechanism. These protons return to the mitochondrial matrix through complex V (ATP synthase) and in the process ADP and inorganic phosphate (Pi) are converted to ATP. *N. crassa* has four alternative NADH dehydrogenases: one on the matrix side (NDI-1) and three (NDE-1, NDE-2, NDE-3) in the MIM. VDAC molecules are shown as red cylinders with black sticks that indicate the N-terminus of VDAC. MOM, mitochondrial outer membrane; MIM, mitochondrial inner membrane; IMS, intermembrane space.

### 1.3.8 Alternative oxidase:

Alternative oxidase is a cyanide-resistant enzyme that accepts electrons from ubiquinone and can bypass complex III and complex IV to donate electrons to the terminal oxygen [80]. Alternative oxidase transfers electrons, but those electrons do not participate in ATP production; hence, energy produced from the reaction is lost as heat [81]. Alternative oxidase can be found in the plants, fungi, and protists [82]. Moreover, expression of alternative oxidase is growth, tissue and stress specific [76]. In *N. crassa,* under normal conditions, insignificant or no alternative oxidase is expressed [56]*;* however, in the presence of different ETC complex inhibitors like antimycin A and chloramphenicol, immunoblot analysis showed alternative oxidase in WT *N. crassa* [83]. Furthermore, genetic mutations that induce abnormal ETC complex formation can also induce expression of alternative oxidase; for example, knockout of VDAC causes abnormal complex I and complex III that associated with high alternative oxidase expression [56]. Alternative oxidase in *N. crassa* is encoded by a nuclear gene *aod-1* [81]. Recently, five other genes *aod-2, aod-4, aod-5, aod-6,* and *aod-7* have been identified to be involved in the expression of alternative oxidase in *N. crassa* [84]. The mechanisms for the regulation of the expression of alternative oxidase in *N. crassa* are not elucidated yet; however, studies have shown that two zinc cluster transcription factors *aod-2* and *aod-5* are required for the expression of alternative oxidase in the cells that have abnormal electron transport chain complexes [85]. In *N. crassa* alternative oxidase transcription factors aod-2 and aod-5 also play roles in energy transformation and metabolism [33]. As mentioned before, alternative oxidase works as a channel to maintain electron flow, thereby, preventing the excessive reduction of the ETC complexes to reduce ROS production [58]. Moreover, alternative oxidase is also involved in the human pathogenicity of some fungi such as *Aspergillus fumigatus* [86], *Cryptococcus neoformans* [87], and *Paracoccidioides brasiliensis*

[88]. It has been speculated that, in those fungi, alternative oxidase works as a defence mechanism against the macrophage mediated oxidative stress and helps intracellular growth in the activated macrophage. In contrast, other eukaryotic model organism *S. cerevisiae* does not have alternative oxidase.

### 1.4 VDAC and oxidative stress:

In the absence of VDAC, mitochondrial ETC complexes were disrupted [55,56]. Moreover, increased intracellular reactive oxygen species (ROS) is associated with VDAC-less cells [1,30,41]. In the following section, mitochondrial ROS and cellular anti-oxidant mechanisms are discussed.

#### 1.4.1 Introduction to ROS:

In aerobic respiration, molecular oxygen is used as the terminal electron acceptor; however, molecular oxygen can be potentially toxic because of its capacity to become a free derived radical, which in the broad spectrum is known as a ROS [89]. Free radical means "any species capable of independent existence that contains one or more unpaired electrons, where an unpaired electron occupies an atomic orbital by itself" [90]. In the process of aerobic respiration, oxygen is converted to two molecules of water by accepting four electrons; however, partial reduction of oxygen results in potent oxidants such as $O_2^-$ (superoxide anion), $H_2O_2$ (hydrogen peroxide), or $HO^-$ (the hydroxyl radical). The term "mitochondrial ROS" defines a broad spectrum of oxyradical species produced from the organelles. Superoxide anion is the main ROS molecule that is produced in mitochondria by the enzymes involved in the Krebs cycle and in the ETC complexes [91].

### 1.4.2 Mitochondrial ROS formation sites:

Most of the mitochondrial ROS are produced by ETC complexes I and III. However, several other potential ROS production sites have been proposed in mitochondria. Until now, atleast 11 ROS producing sites have been proposed [38] (Figure1.5).

Those ROS producing sites can be divided into 2 isopotential groups, NADH/NAD and $QH_2$/Q, based on the redox properties (isopotential) of the electron donor involved in ROS production [92]. Complex I, 2-oxoglutarate dehydrogenase, and pyruvate dehydrogenase, and branched chain keto acid dehydrogenase are the part of the NADH/NAD isopotential group, while complex III, succinate dehydrogenase, dihydroorotate dehydrogenase, electron transfer flavoprotein oxidoreductase, proline dehydrogenase, succinate:quinone reductase, and sn-glycerol-3-phosphate dehydrogenase are the part of $QH_2$/Q group. In the first group, ROS production is dependent on the potential of NAD(H) pool; in contrast, ROS production in the second group depends on the reduction of Q to $QH_2$ [90].

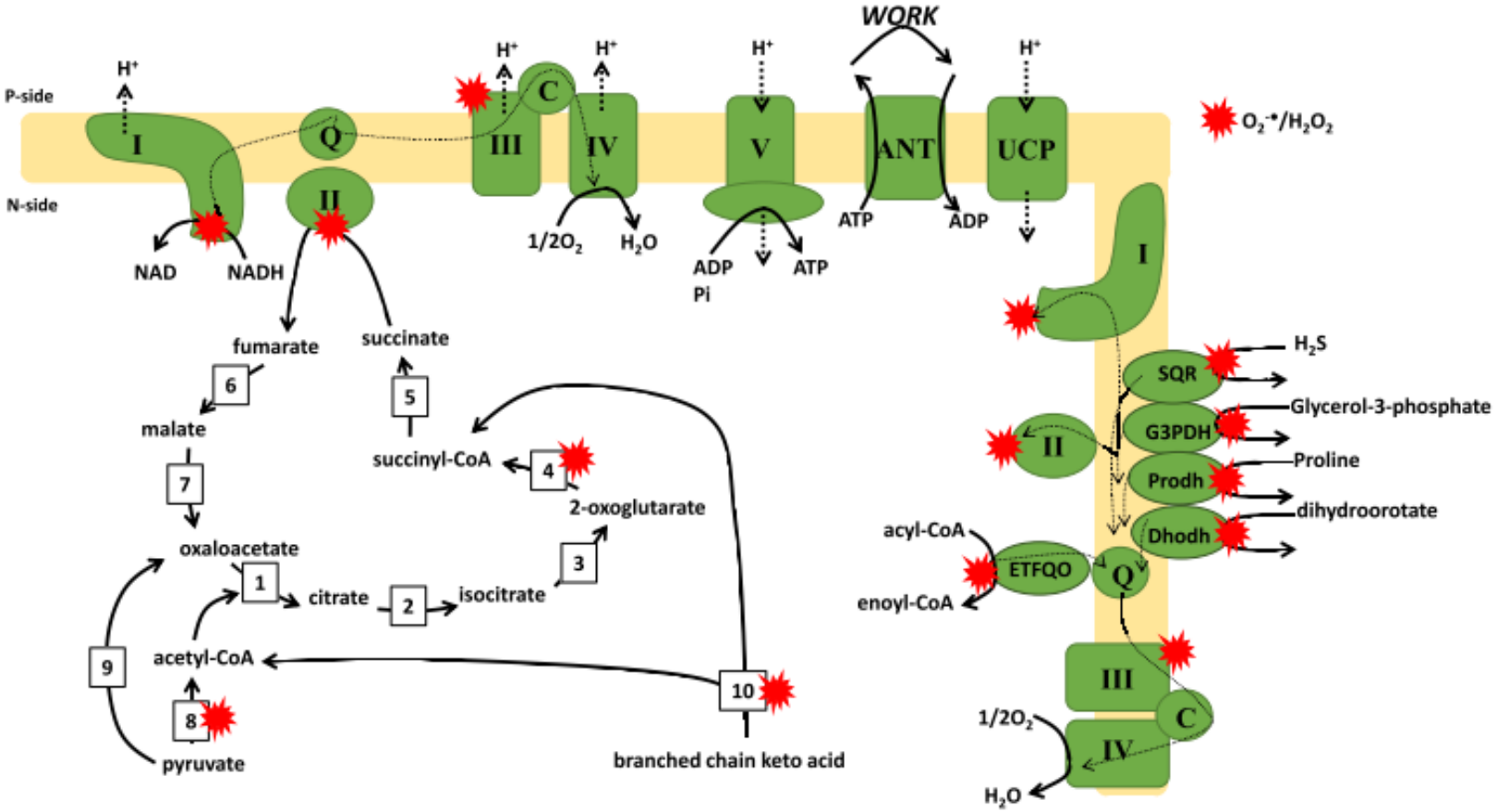
WORK
P-side
N-side
H+
I
Q
II
III
C
IV
V
ANT
UCP
NAD
NADH
1/2O2
H2O
ADP
Pi
ATP
ADP
ATP
O2-•/H2O2
fumarate
succinate
6
5
malate
7
succinyl-CoA
4
2-oxoglutarate
3
oxaloacetate
1
citrate
2
isocitrate
9
acetyl-CoA
8
pyruvate
10
branched chain keto acid
H2S
SQR
Glycerol-3-phosphate
G3PDH
Proline
Prodh
dihydroorotate
Dhodh
acyl-CoA
ETFQO
enoyl-CoA

Figure 1.4: Mitochondrial potential ROS producing sites.

Mitochondrial ROS is mainly produced from ETC complexes I-III. Other than that, electron transfer flavoprotein oxidoreductase (ETFQO), dihydroorotate dehydrogenase, proline dehydrogenase, succinate:quinone reductase (SQR), sn-glycerol-3-phosphate dehydrogenase (G3PDH) can also supply electrons into the Q pool subsequent to oxidation of their cognate substrates. Red stars indicate 11 potential sources of ROS. The flow of electrons are shown by thin dotted lines. Protons ($H^+$) flow is indicated by bold dotted lines. (1) Citrate synthase, (2) aconitase, (3) $NAD(P)^+$-isocitrate dehydrogenase, (4) 2-oxoglutarate dehydrogenase, (5) succinyl-CoA synthase, (6) fumarase, (7) malate dehydrogenase, (8) pyruvate dehydrogenase, (9) pyruvate carboxylase, (10) branched chain keto acid dehydrogenase [90]. The figure and legend were taken from [90]; creative common licence under CC BY-NC-ND 4.0.

### 1.4.3 Antioxidant enzymes:

To maintain the homeostasis of the oxidative environment, cells have various powerful antioxidant defences. However, antioxidant enzymes have distinct functions — such as, the superoxide dismutase (SOD) that acts only on superoxide. Catalase and peroxiredoxin (PRDX) catalyze the conversion of hydrogen peroxide to water. These enzymes not only act as pure scavengers but also work as sensors [93].

#### 1.4.3.1 Catalase:

Catalase is the enzyme that decomposes $H_2O_2$ to water. Different fungal species contain more than one isoform of catalase [94]. It has been proposed that multiple catalases are not spontaneously distributed inside fungal cells; in contrast, they may be in definite intracellular organelles, like peroxisomes. In peroxisomes, β-oxidation occurs and endogenous $H_2O_2$ is continuously formed [94]. In *S. cerevisiae*, there are two distinct varieties of catalase: type A catalase and type T catalase [95]. Two different genes encode the two different enzymes CTA1 and CTT1. Catalase T (CTT1) is localized in cytoplasm and catalase A (CTA1) is localized in the mitochondria and peroxisomes [96]. In *N. crassa*, four catalases have been identified [97]: CAT-1 is mainly found in conidia, CAT-2 is highly abundant in hyphae and conidia, and CAT-3 is detected in the exponential phase and in different stress conditions. However, the localization of CAT-4 has not been determined [97].

#### 1.4.3.2 Superoxide dismutase (SOD):

SOD works on superoxide and catalyzes conversion of superoxide to less toxic hydrogen peroxide and water. Based on the metal in the active sites, SOD enzymes can be divided into manganese SOD (Mn-SOD), Copper-Zinc SOD (Cu, Zn-SOD), and Nickel SOD (Ni-SOD) [94]. Mn-SOD is exclusively found in the mitochondria matrix and Cu, Zn-SOD, is predominant in the cytosol [94]. In *N. crassa* two distinct SOD have been found [98]. Cytosolic Cu, Zn-SOD and mitochondrial MnSOD, where Cu, Zn and Mn are cofactors respectively. Strains with mutation in those genes are highly sensitive to oxidative stress and their spontaneous mutation rate are higher compared to WT [98]. In S. *cerevisiae*, Mn-SOD is encoded by the SOD2 gene and around 5-15 % of total SOD activity in mitochondria is mediated by this enzyme [99]. Furthermore, Cu, Zn-SOD is encoded by the SOD2 gene and accounts for 90% of the total SOD activity. In the absence of either SOD, a slow aerobic growth rate, higher sensitivity to redox inducing drugs and higher mutation frequency were observed [98]. Another kind of extracellular superoxide dismutase (EC-SOD or SOD3) is also present in mammalian cells [100].

#### 1.4.3.3 Glutathione peroxidase:

Another antioxidant enzyme is glutathione peroxidase. The electron donor of this type of peroxidase is glutathione (GSH). The reaction catalyzed by glutathione peroxidase is the oxidation of glutathione to glutathione disulfide. In contrast to catalase, glutathione peroxidase can reduce organic peroxides such as, tert-butyl hydroperoxidase and cumene peroxide [94].

#### 1.4.3.4 Peroxiredoxins:

This enzyme is a thiol-specific peroxidase that is found in all kingdoms of living organisms. The activity of peroxiredoxins depends on the thiol-disulfide transition of cysteines and is supported by electron donors such as thioredoxin and cyclophilin [94].

### 1.5 VDAC and cellular dysfunctions:

VDAC is the most abundant MOM protein and absence of VDAC is associated with abnormal mitochondrial membranes properties (Chapter 4). In addition to that, the absence of VDAC is linked to the modulation of the endoplasmic reticulum (ER) unfolded protein response (UPR) (Chapters 4 & 5). In the following section, mitochondrial membrane properties and UPR are discussed:

#### 1.5.1 Mitochondrial lipid:

Mitochondria are membrane bound by the MOM and MIM. Mitochondrial membranes are mainly composed of lipid, proteins and sterols, and are arranged according to the fluid mosaic model [101]. The movement of the lipid molecules provides the fluidity of the membranes and is important for the function of the organelles.

MOM harbours metabolic enzymes and different protein complexes for protein transfer, lipid transfer and mitochondrial tethering. In mitochondrial MOM, different types of lipid are present: phosphatidylcholine (PC), phosphatidylethanolamine (PE) and phosphatidylinositol (PI) [102] are the main phospholipids in the MOM. Phosphatidylserine (PS), phosphatidylglycerol

(PG), cardiolipin (CL), phosphatidic acid (PA), lysophospholipids, sterols and sphingomyelin are the other components of the MOM.

The structure of MIM is more complex compared to MOM because of in-foldings of the membrane, which creates a large surface area. In the MIM, the ratio of lipids to proteins is lower compared to the MOM, although the MIM contains the machinery for OXPHOS to produce ATP. The MIM is also involved in ATP transport, lipid and protein trafficking, calcium transport, regulation of cellular metabolites, and signal transduction. In the MIM, PC and PE are the most abundant phospholipids, like in the MOM; however, the amount of CL is high in the MIM [103].

### 1.5.2 Yeast endoplasmic reticulum unfolded protein response:

Cellular protein homeostasis in endoplasmic reticulum (ER) is important for maintaining proper physiological conditions. Under certain stresses, accumulation of unfolded proteins in the ER induces the unfolded protein response (UPR) [104]. One UPR pathway which is present in yeast, is conserved in all the eukaryotes; however, mammals have two addition UPR pathways [104]. The yeast UPR pathway is induced by an ER sensor inositol-requiring enzyme-1 (Ire1) [105]. Ire1 is activate by disassociation of KAR2/BiP- or by the binding of unfolded proteins [106–110]. KAR2/BiP is a heat shock chaperone which can be released from Ire1 to bind with the unfolded proteins to active the Ire1. After activation, Ire1 oligomerizes, and subsequently, trans-autophosphorylation occure through its cytosolic kinase domain. In the activation stage, the cytosolic ribonuclease domain of Ire1 cleaves the intron of pre-mRNA of HAC1 and generate a mature HAC1, to recruit synthesis of transcription factor Hac1. After that, Hac1 is localized into the nucleus to control the expression of UPR target genes. The UPR can reduce stress through the up-regulation of around 400 genes. Those genes are ER chaperones, lipid biosynthesis enzymes

and ERAD (ER-associated degradation) machinery. The UPR can be adaptable and might be modified differently per the needs of the cells. This variance of the UPR, from different stresses, suggests the contribution of another unidentified regulatory factor(s) [105].

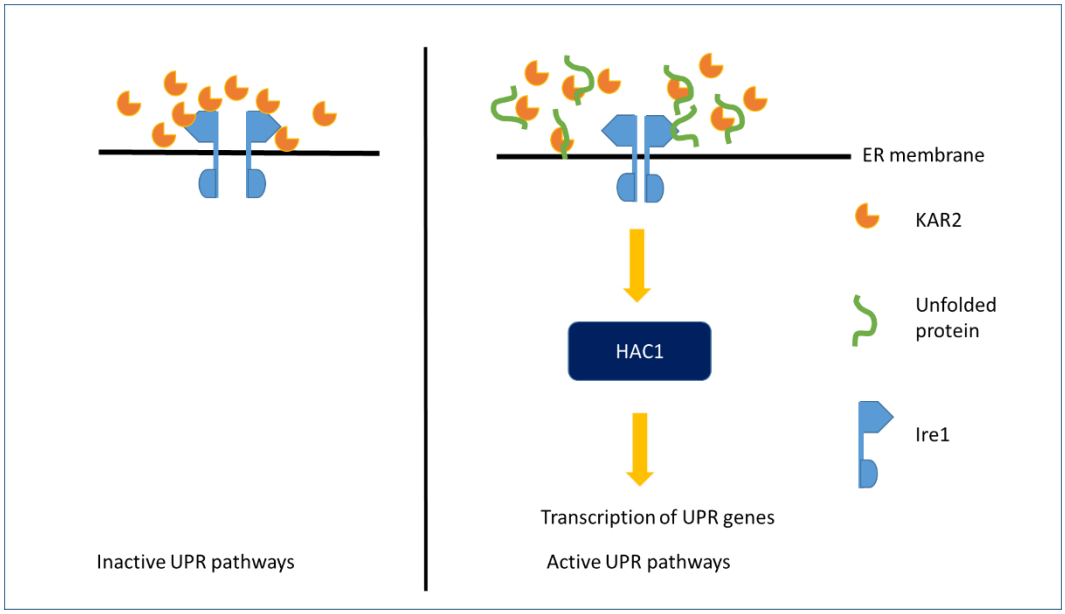


Figure 1.5: *S. cerevisiae* UPR pathway.

The black line separates the inactive and active UPR pathways. In the inactive stage KAR2 is in a complex with Ire1. In the presence of unfolded proteins, KAR2 disassociates from the complex and binds with the unfolded proteins. This disassociation actives the Ire1, followed by downstream activation of HAC1. HAC1 translocates to nucleus and actives UPR genes [104].

## 1.6 Model organisms:

To understand the roles of VDAC, two different model organisms, *N. crassa* and *S. cerevisiae*, were utilized. *N. crassa* has been used for mitochondrial studies by many groups [55,98,111–115]. Moreover, *N. crassa* has one VDAC isoform that makes it a straightforward model for VDAC studies. Another model organism *S. cerevisiae* was also used for mitochondrial and VDAC studies for a long time [116–118]. However, there are few differences between two model organisms (Table 1.2).

Table 1.2: Comparison between *N. crassa* and *S. cerevisiae* model systems for mitochondrial studies:

| | *N. crassa* | *S. cerevisiae* | References |
|---|---|---|---|
| Oxygen requirement | Obligate aerobe | Facultative aerobe | [111,119] |
| Expression of alternative oxidase | Yes | No | [58] |
| Presence of complex I | Yes | No | [58] |
| Cell type | Coenocytic | Uni-cellular | |
| Number of genes | ≈10000 | ≈6000 | [120,121] |

### 1.6.1 *Neurospora crassa:*

The filamentous *N. crassa* (Figure 1.6) is an ascomycete fungus, which was first described around 1843 as a contaminant in French bakeries. The fungus was becoming popular as a model organism when Beadle and Tatum were showing genetic control of the biochemical reactions and proving the "one gene- one enzyme" hypothesis by using *N. crassa* [111,122,123]. Between the 1940s and 1970s *N. crassa* was used as a model organism to address the questions regarding mitochondrial inheritance, gene conversion, and metabolic pathway regulation [123]. The genome sequence of *N. crassa* was first published in 2003 and it has seven chromosomes with an approximately 40 megabase genome encoding around 10000 proteins [120]. Recently, the use of *N. crassa* as a model organism was enhanced by the whole genome knockout program that created a knockout library, which is available from Fungal Genetic Stock Center (FGSC) [123].

*N. crassa* can be grown cheaply in laboratories in Vogel's Medium (VM) [124]. A vegetative culture of *N. crassa* is composed of hyphae - a branched filamentous structure (Figure 7). The hyphae grow from their tips and can fuse together. Hyphae contain many haploid nuclei and are separated into compartments by the incomplete cross-walls known as *septa*. Multiple nuclei can be present in each compartment as nuclei can traffic between the pores in the septa. Strains having genetically identical nuclei are called *homokaryons* and having distinct nuclei are designated as *heterokaryons* [111]. The *N. crassa* life cycle can be divided into two phases, the asexual life cycle and sexual life cycle. In the asexual life cycle conidia are formed from the aerial hyphae. However, in the sexual life cycle two different mating type *MAT a* and *MAT A* come into close interaction, conidia of two meting types are fused to generate diploid nuclei inside the perithecium. The resulting diploid nuclei undergo mitotic division to generate ascospores in the ascus.

As an obligate aerobe, *N. crassa* is a good model for mitochondrial biology; however, unlike yeast, mitochondrial DNA mutants - the $rho^-$ and $rho^0$ mutants - cannot be created in *N. crassa.* Mitochondrial DNA of *N. crassa* encode the essential subunits that participate in the formation of ETC complex formation. Furthermore, relatively inexpensive and large quantities of mitochondria can be easily isolated from *N. crassa;* hence, as a model organism *N. crassa* has been studied for the import and post transitional modification of mitochondrial complexes and proteins, such as TOM complex and VDAC [111].


Figure 1.6: *N. crassa* in a conidia flask.

### 1.6.2 *Saccharomyces cerevisiae:*

*Saccharomyces cerevisiae* is an unicellular and an eukaryotic model organism. *S. cerevisiae* contains many basic cellular functions that are conserved across in eukaryotic domain; therefore, those characteristics of yeast are used for genetics, biochemical and cell biological studies. Moreover, *S. cerevisiae* has a short doubling time and can be grown in an economic manner [119]. Thus, many studies can be performed in a short time.

Different auxotrophic and antibiotic resistant markers are available for *S. cerevisiae*. Furthermore, genetic manipulation can be performed with high efficiency by utilizing homologous recombination techniques [125]. In 1996, the genome sequence of *S. cerevisiae* was completed and around 6000 genes were detected. A library of different yeast plasmids for genetics studies and the availability of knockout strains enhance the yeast research [121,126]. Moreover, many viable knockout mutants are accessible for studying mitochondrial biogenesis [116].The mitochondrial genome of *S. cerevisiae* is around 80,000 bp in size and eight major proteins essential for OXPHOS are encoded by the mitochondrial genome [116].

## 1.7 Objectives of This Study:

The goal for this project is to understand the functions associated with the N-terminus of VDAC and the global roles of VDAC in cells. Therefore, a *N. crassa* strain expressing N-terminally truncated VDAC was studied. Mitochondrial bioenergetics and ROS production were studied in cells expressing different levels of VDAC. Moreover, proteomic analysis was performed to understand the cellular stress responses in the absence of VDAC. These studies give us some insights about VDAC roles in the cells. The general approaches for this project were:

The first goal of this thesis was to understand the biological role of the N-terminus of VDAC in *N. crassa*. *In vitro* experiments led to proposals that the N-terminus of VDAC is involved in the gating of VDAC, oligomerization of VDAC, and binding with hexokinase and ATP [2]. However, the biological roles of N-terminus of VDAC have not been elucidated completely. To understand the biological roles of N-terminus of VDAC in *N. crassa*, a truncated variant of N-terminus of VDAC (ΔN2-12porin) was created. Moreover, as control of low level of VDAC, a strain expressing almost half of amount of VDAC (LoPo) was generated. Characterization of LoPo was also performed.

The second goal was to understand the influence of VDAC levels and expression of an N-terminally truncated VDAC on mitochondrial bioenergetics and ROS production in *N. crassa.* The primary function of mitochondria is energy production through OXPHOS. VDAC is functionally conserved most abundant mitochondrial MOM proteins [1,10,11]. Moreover, VDAC has been proposed to maintain the flow of small metabolites, like succinate, pyruvate, ATP/ADP, calcium across the MOM. Furthermore, VDAC interactions with ANT has been proposed as a rate liming

step for the movement of ADP/ATP [39,127]. Therefore, the influence of VDAC on mitochondrial bioenergetics and ROS production was tested.

The third goal of this project was to study the cytosolic proteome of the VDAC-less mitochondria to identify alterations in expression of proteins in response to the lack of VDAC. The *N. crassa* strain expressing VDAC-less mitochondria has a slow growth rate, expresses alternative oxidase, and has increased mitochondrial ROS production capacity and abnormal ETC complexes [56]. Therefore, the absence of VDAC is associated with cellular stresses. Moreover, VDAC has been proposed to interact with different cytosolic and mitochondrial proteins to maintain cellular homeostasis. To understand the global role of VDAC in the cells, cytosolic proteomic analysis of *N. crassa* was performed. To validate the proteomic analysis different biochemical tests and mitochondria membrane properties were studied. Similarly, *S. cerevisiae* cytosolic proteomic analysis was performed to understand the global role of VDAC; subsequently, various biochemical tests were utilized to validate those findings.

Together these studies will help us the elucidate the roles of VDAC and the functions associated with N-terminus of VDAC.

# Chapter 2: Functional characterization of an N-terminally truncated mitochondrial porin expressed in *Neurospora crassa*

Sabbir R. Shuvo, Uliana Kovaltchouk, Abdullah Zubaer, Ayush Kumar, William A.T. Summers, Lynda J. Donald, Georg Hausner, Deborah A. Court*

Department of Microbiology, University of Manitoba, Winnipeg, MB R3T 2N2

*corresponding author

Department of Microbiology

University of Manitoba

Winnipeg, MB Canada R3T 2N2

Phone (204) 474 8263

Fax (204) 474-7603

Chapter has been published in Can. J. Microbiol. 68 (2017) 730–738.

**Abstract:**

Mitochondrial porin, which forms voltage-dependent anion-selective channels (VDAC) in the outer membrane, can be folded into a 19 β-stranded barrel. The N-terminus of the protein is external to the barrel, and contains α-helical structure. Targeted modifications of the N terminal region have been assessed in artificial membranes, leading to different models for gating *in vitro*. However, the *in vivo* requirements for gating and the N-terminal segment of porin are less well-understood. Using *N. crassa* porin as a model, the effects of a partial deletion of the N-terminal segment were investigated. The protein, ΔN2-12porin, is assembled into the outer membrane, albeit at lower levels than the wild-type protein. The resulting strain displays electron transport chain deficiencies, concomitant expression of alternative oxidase, and decreased growth rates. Nonetheless, its mitochondrial genome does not contain any significant mutations. Most of the genes that are expressed in high levels in porin-less *N. crassa* are expressed at levels similar to wild-type or are slightly increased in ΔN2-12porin strains. Thus, although the N-terminal segment of VDAC is required for complete function *in vivo*, low levels of a protein lacking part of the N-terminus are able to rescue some of the defects associated with the absence of porin.

## 2.1 Introduction:

Voltage-dependent anion-selective channels (VDAC, mitochondrial porins) reside in the outer membrane (MOM) of mitochondria, where they allow the flow of small solutes across the lipid bilayer. Incorporation of isolated or recombinant mitochondrial porins into artificial bilayers reveals features common to porins from a wide range of organisms: slight anion selectivity, conductances of 3-5 nS in the open state, and susceptibility to voltage-dependent gating to form a slightly cation-selective pore of reduced conductance ("closed state", see [11] for review).

Analysis of refolded, recombinant VDAC1 and VDAC2 from vertebrates has revealed a common structure, comprised of a 19-stranded β-barrel, and an N-terminal segment of about 25 residues that does not form part of the barrel [22–24,26,47]. The relatively uniform nature of gating by the VDACs characterized to date, suggests either a conserved process driven by voltage potentials *in vivo*, or a conserved structure and charge distribution that lead to similar effects on channels analyzed *in vitro*. Several studies using variants of fungal and human porins lacking most or part of the N-terminal segment indicate that these residues are involved in gating [128,129]. Other studies [130] have suggested that the N-terminus is not required for gating, but the molecules used in these studies carried N-terminal hexa-histidine tags, which may have partially compensated for the shortened N termini (see [2] for discussion).

One aspect of the role of the N-terminus that has been studied to a lesser extent is its essentiality *in vivo*. Mitochondrial porins lacking either 11 or 22 N-terminal residues are imported into isolated mitochondria of *N. crassa*, although they are assembled into a more protease-sensitive form [131]. Similarly, human VDAC1 (hVDAC1) variants lacking 7 or 19 N-terminal residues co-localize with mitochondria when expressed in transformed monkey kidney fibroblast (Cos-7) cells

[45]. In these cells, overexpression of the truncated hVDAC1 molecules abolished the pro-apoptotic effect associated with overexpression of the wild-type protein, indicating a direct or indirect role for the N-terminus in apoptosis. However, the native monkey VDACs were also expressed in those cells, precluding analysis of the participation of the N terminally deleted hVDAC in key cellular processes. The importance of this region *in vivo* is further suggested by experiments in which the N-terminal sequence of hVDAC3 was replaced with that of hVDAC1, resulting in a pore that complemented *S. cerevisiae Δpor1* mutant that lacked the main porin isoform [118]. This yeast is a facultative aerobe (use aerobic respiration to produce ATP in the presence of oxygen but capable to switch fermentation when oxygen is not present), and although these experiments indicate an important role for the N-terminus of VDAC in cellular function, they do not directly test the question of whether a porin lacking part of the N-terminus can complement a VDAC-less strain of an obligate aerobe.

To address this question, the *N. crassa* model system was used; in this organism porin is not essential, but its absence results in severe mitochondrial defects [56]. *N. crassa* possesses a single VDAC isoform, allowing for more straightforward interpretation of results. Electrophysiological analysis of variants of this porin revealed that the absence of part (Δ2-12porin) or all (Δ3-21porin) of the N-terminal segment did not preclude the formation of gated channels [130]. However, Δ3-21porin produced noisy channels (fluctuation of conductance) and, following import into isolated mitochondria, was more sensitive to externally added protease than wild-type and ΔN2-12porin [131]. Therefore, the latter protein was chosen for analysis and a strain of *N. crassa* was generated in which the wild-type porin gene was replaced with one encoding ΔN2-12porin. The mitochondrial function of the strain was assessed, and the relative levels of mRNA encoding several proteins that are up-regulated in porin-less cells were examined.

## 2.2 Materials and Methods:

### 2.2.1 Strains and growth conditions:

The strains used in this study are listed in (Table 2.1) and were maintained according to Davis and De Serres [124]. Growth rate of the cells were measured in "race tubes" following the method described in [124]. Strains harboring the VDAC (porin) variant genes were created using the homologous recombination strategy developed by [132] and [133] and the wild-type strain FGSC 9718. For ΔN2-12porin, the wild-type VDAC gene was replaced by that encoding a variant lacking residues 2-12. Conidia were transformed with a linear DNA fragment containing base pairs (bp) 1000 to 320 upstream of the native porin start codon (amplified from FSGC 9720), the hygromycin resistance cassette from pCNS44 [134] , bp 320 to 1 upstream of the porin gene, the cDNA sequence encoding ΔN2-12porin [130], and about 1400 bp of sequence downstream of the porin stop codon. The first and last sequences listed were designed to provide homologous sequences for the double recombination event that would replace the wild-type porin coding sequence with the ΔN2-12porin coding sequence flagged with an adjacent hygromycin-resistance marker. DNA sequence analysis of the integrated sequences revealed that the recombination event to the 3' side of the ORF occurred between exon 4 in the genome and the transformed cDNA. Thus, intron 4 is retained in the ΔN2-12porin strain.

A strain expressing a relatively low amount of VDAC (LoPo) was constructed from FGSC 9718 by replacing the native VDAC promoter region with that of the *N. crassa* tom40 gene. Wild-type conidia were transformed with a linear DNA fragment containing bp 1000 to 320 upstream of the native porin start codon (amplified from FSGC 9720), the hygromycin resistance cassette

from pCNS44, bp  300 to 1 upstream of the tom40 gene (from FGSC 9718), and the cDNA sequence encoding the wild-type VDAC [130]. Following confirmation of the correct insertion by DNA sequencing, homokaryotic strains were generated by 7 rounds of repeated sub-culturing in the presence of hygromycin A in VM and confirmed by PCR. Levels of VDAC were determined using an antibody against residues 7-20 (R. Lill and W. Neupert, Universität München) or residues 195-210 (GenScript, Piscataway, NJ).

Table 2.1: *N. crassa* strains used in this study.

| **Strain name** | **Genotype/Comments** | **Reference** |
|---|---|---|
| FGSC* 9718 (wild-type) | *mus-51::bar mat a* | [132] |
| ΔPor-1 | Δ*por::hph mus-51::bar mat a* transformant of FGSC 9718 | [56] |
| ΔN2-12porin | *hph+, por*Δ2-12 *mus-51::bar mat a* transformant of FGSC 9718 | this work |
| LoPo | *hph+, tom40prom:por, mat a* transformant of FGSC 9718 | this work |

* Strains bearing FGSC names were obtained from the Fungal Genetics Stock Center [135].

### 2.2.2 Mitochondrial analyses:

Mitochondria were isolated according to [136], following growth in Vogel's Medium (VM). The respiration control rate (RCR) was used to assess integrity as described in [137] and [138]. Mitochondrial MOM integrity was more than 70% for all experiments.

Growth rate, cytochrome spectra and $O_2$ consumption measurements were collected as described in [56], with the exception that an Oxygraph-2k (Oroboros Instruments, Innsbruck, Austria) was used. Microscopy was performed following the protocol described in [55].

### 2.2.3 RNA extraction and cDNA synthesis:

Cultures were grown for 21-25 hours at 30°C in VM. One gram (wet weight) of hyphae was flash frozen with liquid nitrogen and was ground with RNase-free sand in a mortar and pestle. One fifth of each sample was used for whole cell RNA extraction using a Plant RNA kit (Qiagen, Mississauga, ON, Canada) following manufacturer's instructions except that the initial volume of RLC buffer was 650 µl to which 6.5 µl of 2-mercaptoethanol were added. To remove the genomic DNA, the samples were treated with 1.5 Kunitz units of DNase I (Qiagen) for 30 min at 37° C, followed by heat inactivation at 65°C for 5 min. Next, 1 µg of total RNA (determined by NanoDrop 2000, ThermoFisher) was used to synthesize cDNA using the Bio-Rad iScript reverse transcriptase kit (Bio-Rad, Mississauga, ON, Canada). To ensure that all genomic DNA was removed by DNase treatment, a control reaction lacking reverse transcriptase (NRT) was set up using all the reaction components except the reverse transcriptase enzyme.

### 2.2.4 Quantitative Reverse Transcriptase PCR (qRT-PCR):

Analysis was carried out with the primers listed in (Table 2.2). The efficiency of the primers was tested with 10-fold serial dilutions of genomic DNA and ranged from 88-103%. The expression of genes was determined by quantitative PCR by using SsoFast Evagreen Supermix (Bio-Rad). The NRT control described above and a reaction lacking template (NTC) were used to control for the presence of genomic DNA in the sample, and for nucleic acid contamination in the reaction mixture, respectively. Reactions were set up using primer concentrations of 300 nM and 1.6 µl of cDNA (diluted 1:2) in 8-µl reaction mixtures. Actin (NCU04173) was used as a reference gene. Relative expression levels were determined using the cycle threshold method ($\Delta\Delta C_t$) on an Eco Real-Time PCR System (San Diego, California, USA). Relative expression (R) levels were calculated using the following equations:

$\Delta Cq$= Cq target-Cq reference

$\Delta\Delta Cq = \Delta Cq$ sample – $\Delta Cq$ control

$R= 2^{-\Delta\Delta Cq}$

where "Cq" is the PCR cycle in which fluorescence is detected, "target" to the mRNA under study, "reference" to actin, "sample" to the data obtained with ΔN2-12Porin cDNA and "control" to that from the wild type (FGS9718). Each measurement was carried out in triplicate, data analysis was performed using EcoStudy Software v 5.0.

Table 2.2: Primers used for qRT-PCR and sequencing reactions.

| ORF* | **Forward Primer (5'-3')** | **Reverse Primer (5'-3')** |
|---|---|---|
| NCU07953 | GGAGCGACGAAAAGTTTGAG | CCCTCGCCCTCCTTATAGTC |
| NCU06518 | TGCACAGTACCGAGCTCATC | TGACCATGAGCTCAACGAAG |
| NCU02157 | AATACCCTGTTGCCGATGAC | TTTACATCCCGCTCCAACTC |
| NCU05850 | CCCAAGATCAAGTGCAAGGT | AGCTTGCTGAGATCGGTCAT |
| NCU05633 | ACAGCAGCGACAACACAAAG | CTGCTGTCGAGGAGGAAGTC |
| NCU04173 | TTCTCTCGAGAAGTCCTACG | TGACAATGTTGCCATAGAGA |
| NCU08476 | ATCCCGAGGAACTGATTGTG | AACAGCCCCGTAAACTCTGA |
| NCU06550 | CGAGATTGCTCAGGCTAAGG | ACCCAAACTCCATCATGAGC |
| NCU11655/ NCU04304 | CACAAGGTCAACTCCCAGGT | ATCGAAAGAGGCACCAACAC |
| Nad2 sequencing primers | GTAGGTTTACATGGAGGTTTACTTC | CCTGAATTTGCTCATAGTAAACATG |
| Nad2_whole | GATCGAGTAGGACCAGAG | GCTCCATGAACATTATTAATTC |

*ORF numbers are taken from *Neurospora crassa* Sequencing Project, Broad Institute of Harvard and MIT (http://www.broadinstitute.org/)

### 2.2.4 Mitochondrial genome analysis:

Mitochondrial DNA (mtDNA) was isolated following the protocol described in [139]. Approximately 100 ng of DNA in 75 µl of $H_2O$ were supplied to Genome Quebec (Innovation Centre, McGill University, Quebec, Canada) for Illumina sequencing using the MiSeq platform. DNA samples were barcoded and combined on a MiSeq run. Average size reads were 250 bp, average quality was 35 and quality offset was 33, reconfirmed by FastQC. Paired-end reads were assembled de novo with the A5-MiSeq pipeline [140], which was updated for Illumina MiSeq from the A5 pipeline [141]. The scaffolds were sorted and joined to prepare the complete genome with the aid of our own Python script as well as manual inspection. The mtDNA sequence was annotated with the program Artemis [142] on the basis of the gene, intron, rRNA and tRNA coordinates predicted with the MFannot and RNAweasel online programs ( [143,144]; http://megasun.bch.umontreal.ca/cgi-bin/mfannot/mfannotInterface.pl). The comparison of the genome sequences of the wild type (GenBank KY213951), the ΔN2-12porin (KY498477) and ΔPor-1 (KY498478) mutants and the previously published mitochondrial genome of *N. crassa* (NC_026614.1) was done in MAFFT (multiple sequence alignment server selecting the progressive method of alignment; [145].

### 2.2.5 Determination of relative protein level by mass spectroscopy:

Mitochondria were washed with 1 M sodium carbonate (pH 10) as described in [131] to enrich for membrane proteins and proteins were separated via SDS-PAGE. Regions of the gel containing both VDAC (30 kDa) and adenine nucleotide translocator (ANT, 34 kDa) were excised from SDS-PAGE gels, and prepared for mass spectrometry analysis, essentially as described by [146]. Mass spectra were acquired on a prototype MALDI QqTOF instrument [147]. Relative porin

levels were estimated by normalizing total ion counts (TIC) for porin to the TIC for ANT obtained for each strain, and then comparing to the same value from the wild-type samples (see Appendix 7.1 Table 1).

### 2.2.6 SDS-PAGE gels and Western blot:

SDS-PAGE were cast with 0.1% SDS and 12% acrylamide:bisacrylamide (29:1) using a Mini-PROTEAN® 3 Cell kit (Bio-Rad Laboratories, Hercules, CA). Gels were loaded with 10 µl of Precision Plus Protein™ Unstained Standard ladder (Bio-Rad) and 20 µg of mitochondrial protein as samples. Electrophoresis was performed at 175 V for 45 minutes at room temperature. Western blot was performed following the protocol described in [148] with slight modification. Briefly, electrophoresis was performed at 100 V for 1 hour.

## 2.3 Results:

### 2.3.1 Porin lacking the N-terminal 12 amino acids is assembled poorly into the outer membrane:

*In vitro* synthesized ΔN2-12porin can form pores in artificial membranes [130] and can be imported into isolated mitochondria, where it assembles in a membrane-embedded form that is more accessible to externally added protease than the wild-type protein [131]. To investigate the function of this truncated porin *in vivo*, the gene for the wild-type porin was replaced with that encoding ΔN2-12porin. To determine if ΔN2-12porin was assembled into the mitochondria of the resulting strain, western blot analysis was performed (Figure 2.1). The truncated porin was present in significantly lower levels than in the wild-type. The relative level of ΔN2-12porin, normalized to that of the inner membrane adenine nucleotide translocator (ANT), was about one-tenth of that

in the wild-type strain, as estimated by mass spectroscopy (Appendix 7.1 Table 1) and quantitation of signals on the western blots (Figure 2.1).

One possible explanation for the low levels of ΔN2-12porin is a reduction in steady state levels of the corresponding mRNA. To investigate this possibility, porin (NCU04304) mRNA levels were analyzed using qRT PCR (Figure 2.2). In ΔN2-12porin strain mRNA levels were not reduced compared to wild-type. Thus, the low protein levels likely reflect suboptimal post-transcriptional processes.

The low levels of the variant protein complicate the analysis of the mutant strains, because phenotypic changes could result from reduced protein levels, or the partial truncation of the N-terminus, or both. In order to separate these factors, a control strain was generated in which the transcription of porin is driven by the tom40 promoter. Tom40 is significantly less abundant in the MOM than is porin [112]. The resulting strain, LoPo, harbours about half as much porin as does the wild-type strain (Figure 2.1, and Appendix 7.1 Table 1).

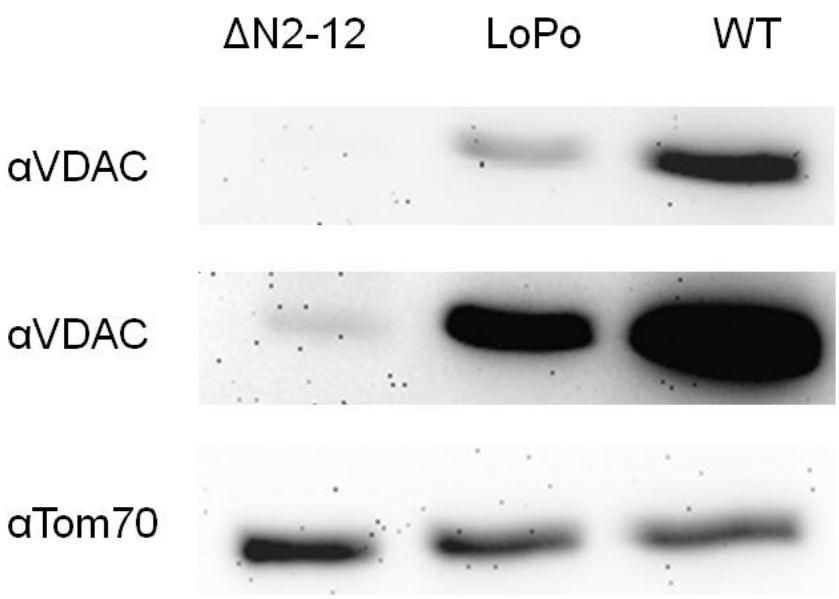


Figure 2.1: Western blot analysis of mitochondria purified from wild-type (WT), LoPo and ΔN2 12porin (ΔN2-12) strains.

20 µg of mitochondrial proteins were loaded in each lane. Blots were immunodecorated with antibodies against residues 195-210 of porin (αVDAC) or αTom70 (Translocase of the outer membrane 70). The top and middle panels represent 30s- and 5-minute exposures of the blot probed with αVDAC, and the lower panel was probed with the loading control, Tom70 and exposed for 30s.

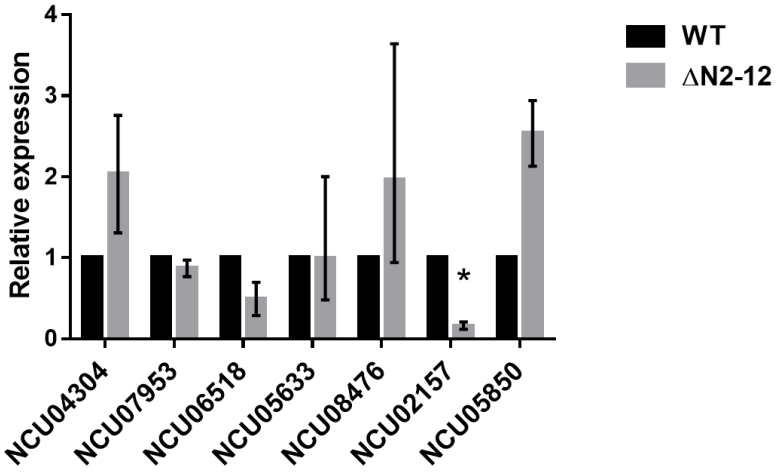


Figure 2.2. RT-qPCR analysis of selected genes in ΔN2-12porin.

The expression profiles of seven genes [(NCU04304, por encoding porin), (NCU07953, aod-1 encoding alternative oxidase-1), (NCU06518, NADH-cytochrome b5 reductase 2), (NCU05633, stomatin family protein), (NCU08476, conserved hypothetical protein), (NCU02157, coq4), (NCU05850, aif-1, apoptosis-inducing factor, annotated in the Broad Institute database as rubredoxin-NAD+ reductase 2)] were analyzed by RT-qPCR, normalized to actin (ΔΔCq). These normalized expression values are shown relative to the wild-type, which was set to 1. The data represent an average of at least two biological replicates and the error bars indicate the range of relative expression levels obtained. * indicates $P < 0.05$ based on a students' t-test.

### 2.3.2 Strains expressing porin lacking the N-terminal 12 amino acids display electron transport chain deficiencies and altered staining with MitoTracker:

Strains of *N. crassa* lacking mitochondrial porin (ΔPor-1) exhibit deficiencies in cytochromes *b* and *aa3*, and express alternative oxidase, indicating reduced mitochondrial function [56]. To determine if the Δ2-12porin strain possesses similar characteristics, cytochrome spectra (Figure 2.3A) and oxygen consumption (Figure 2.3B) were analyzed. Levels of cytochromes *b* and *aa3* were reduced in ΔN2-12porin strain and enhanced expression of cytochrome *c* was observed, which is common in Neurospora strains with deficiencies in cytochromes *b* and *aa3* (for example see [149]). As expected from these results, the ΔN2-12porin strain expresses cyanide-insensitive, salicylhydroxamic acid (SHAM)-sensitive oxygen consumption, indicative of expression of alternative oxidase [150]. To exclude the possibility that the defects in cytochromes *aa3* and *b* resulted from spontaneous mutations in the mitochondrial genes encoding some of the proteins they associate with, this DNA was sequenced from the wild-type, ΔPor-1 and ΔN2-12porin strains. The only mutation detected was in ΔN2-12porin, and was a short deletion in a segment containing a partial duplication of the ND2 gene (bp 59634-59638 of the FGSC 9718 mtDNA sequence). This duplication does not encode a functional ND2 polypeptide [5,151]. Mutations in nuclear genes may also be responsible for these mutations, but analysis of these genomes are beyond the scope of the current study.

LoPo, the strain harbouring a lower level of wild-type porin (50% of wild-type) is similar to wild-type in terms of growth (Table 2.3) and electron transport chain (Figure 2.3A). Thus, while it cannot be excluded that the level of porin is insufficient in ΔN2-12porin variant, the data obtained with LoPo suggest that the defects in ΔN2-12porin are due to the truncated porin rather than reduced porin levels.

Hyphae were stained with MitoTracker to assess the overall abundance and distribution of mitochondria in the strain harbouring ΔN2-12porin. Compared to the wild-type and LoPo strains, the variant strain displayed lower numbers of fluorescent mitochondrial punctate (Figure. 2.4).

A.

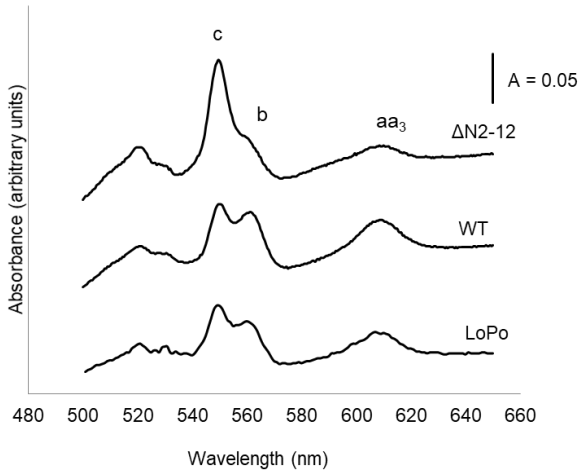


B.

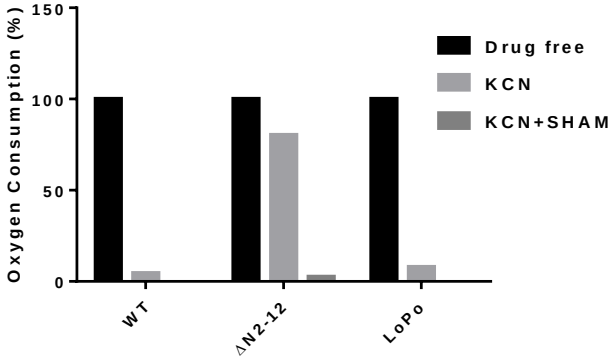


Figure 2.3: (A) Cytochrome spectra obtained from ΔN2-12porin, WT and LoPo.

Peaks representing absorbance by cytochromes c, b, and $aa_3$ are indicated. (B) Alternative oxidase expression in wild-type, ΔN2-12porin and LoPo strains. Cultures were grown at 30◦C for 14 hours for wild-type, and LoPo and 16 hours for ΔN2-12porin. The first bar in each set represents the oxygen consumption in the drug-free state. Second and third bars indicate consumption of oxygen after addition of inhibitor of the standard electron transport chain (KCN) alone, or in combination with the alternative oxidase pathway (SHAM), respectively.

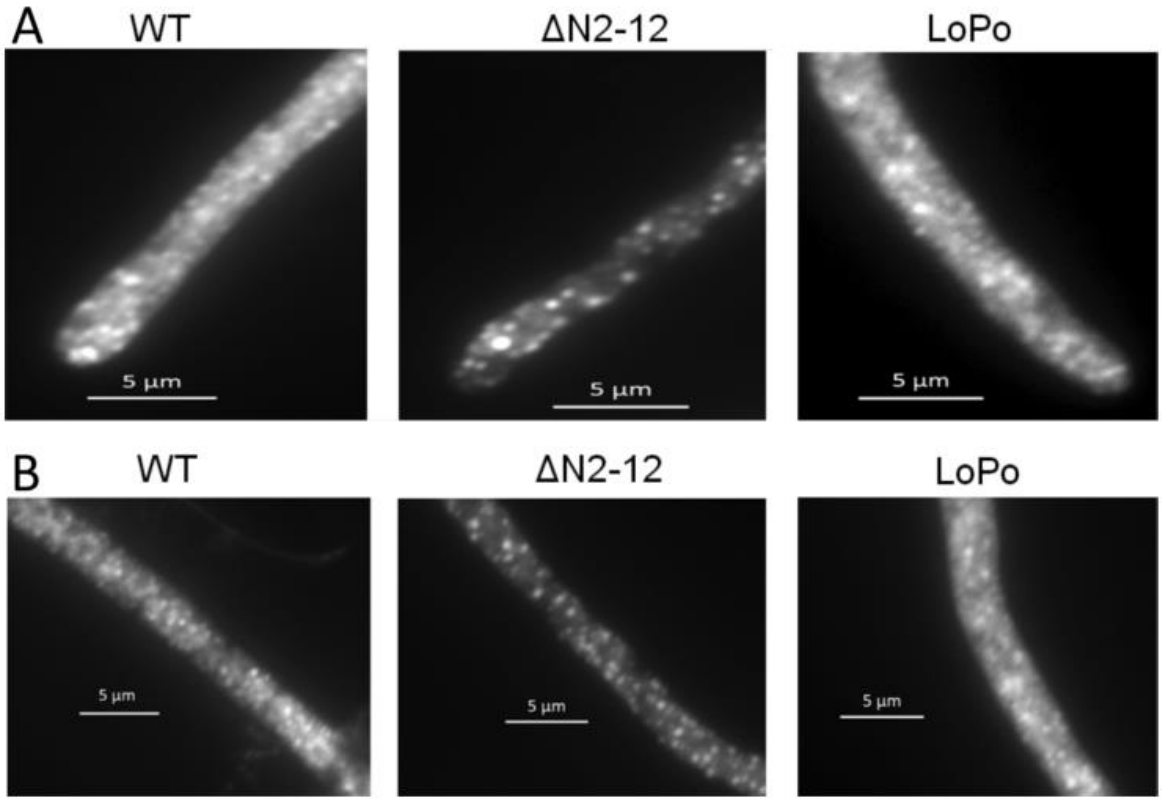


Figure 2.4: Morphology of mitochondria in wild-type, LoPo, and ΔN2-12porin strains. Cultures were grown on glass slides on solidified VM medium at 30$^{o}$C for 12 hours for wild-type, 13 hours for LoPo and 16 hours for ΔN2-12porin, followed by staining with MitoTracker Green$^{FM}$. Stained material was observed at 1630X magnification. Mitochondria at the hyphal tips (A) and distal regions of hyphae (B) are shown. Scale bar represents 5 µm.

Table 2.3: Growth rates and relative porin levels of strains expressing wild-type or variants of porin. Growth rates were determined at 22°C on VM.

| **Strain** | **Growth rate (cm/24hr)** | **Porin relative to ANT*** **(%)** |
|---|---|---|
| FGSC† 9718 (wild-type) | 7.7 ± 0.4‡ | 100 |
| ΔPor-1 | 1.6 ± 0.1‡ | 0 |
| ΔN2-12porin | 6.6 ± 0.3§ | 10 |
| LoPo | 7.1 ± 0.3 | 46 |

*based on MS analysis as described in Materials and Methods (see Appendix 7.1 Table 1)

†FGSC, Fungal Genetics Stock Center

‡taken from [56]

§taken from [114] and this work

### 2.3.4 Gene expression associated with Δ2-12porin:

Analysis of the mitochondrial proteome of the ΔPor-1 strain revealed a subset of proteins and corresponding mRNAs that were overexpressed in that strain compared to the wild-type FGSC 9718 ([56], Appendix 7.1 Table 2). To evaluate whether ΔN2-12porin can compensate for the loss of porin, quantitative PCR of cDNA derived from ΔN2-12porin RNA was used to determine if the same set of genes are upregulated in this strain. RNA levels corresponding to proteins present in lower relative amounts in ΔPor-1 were similar for both wild-type and ΔPor 1 strains [56], and were therefore excluded from the current analysis. These proteins are constituents of the intermembrane space, suggesting that damage to the MOM during mitochondrial preparation resulted in their loss.

The results of the RT-qPCR analysis for alternative oxidase in ΔN2-12porin was similar to wild-type (Figure. 2.2). In contrast to the previous study [56], alternative oxidase (*aod-1*) mRNA was detected in wild-type RNA samples (Appendix Table 2), likely due to the use of a more sensitive qPCR detection system. This observation agrees with the detection of mRNA for *aod-1* in wild-type strains using RNAseq [152], even though alternative oxidase activity, and mRNA and protein are not readily detectable in wild-type by northern and western blot methods, respectively [81]. Given the apparent similarities in *aod-1* mRNA levels in wild-type and ΔN2-12porin strains, it is unexpected that cyanide-insensitive respiration is detected only ΔN2-12porin. Similarly, incongruous results were obtained with the 238porin strain, which expresses low levels of porin lacking residues 238-242. In this strain, alternative oxidase activity was detected although the protein was not [55]. In contrast, both *aod-1* mRNA and protein were observed in the ΔPor-1 strain. The reasons for these observations are not clear, but may include regulation at the post-transcriptional level.

The expression levels of several other genes that are upregulated in ΔPor-1 were not distinguishable from wild-type ($P > 0.05$; Figure. 2.2). The only exception was the RNA for *coq4* (NCU02157), which is involved in ubiquinone biosynthesis, and was present in much lower levels than in wild-type ($P < 0.05$).

**2.4 Discussion:**

The N-terminus may contribute to several aspects of porin function, including gating and/or changes to barrel shape that may influence ion selectivity and pore size [2] and interactions with metabolic enzymes such as hexokinase [53]. The current study indicates that porin lacking part of the N-terminal segment is not assembled at normal levels in the membrane, and the associated mitochondria do not maintain a normal electron transport chain.

In spite of these low levels of porin, the growth rate of the ΔN2-12porin strain is over 85% of the wild-type rate (Table 2), in comparison to less than 30% for the porin-less strain [56]. Similarly, a variant expressing 238porin at levels less than 5% of wild-type porin, also grows at more than 85% of the wild-type rate [55]. Thus, low levels of two different porin variants partially rescue the growth rate defect associated with the absence of porin. Taken together, these results suggest that ΔN2-12porin is at least partially functional, as 238porin contains a wild-type N terminus and is associated with a similar phenotype when expressed at low levels. Both proteins are capable of generating wild-type sized pores in artificial membranes [130].

Nonetheless, the reduced levels of ΔN2-12porin complicate the interpretation of the phenotypes associated with the mutant. In an attempt to separate the effects of the N-terminal truncation and the low level of porin, a strain expressing low levels of wild-type porin was generated by replacing the porin promoter with that of Tom40. The resulting strain expressed

~50% of wild-type levels of porin and is phenotypically wild-type, although it cannot be excluded that a further reduction in wild-type porin levels would lead to mitochondrial defects.

ΔN2-12porin is present at lower levels in mitochondria than the wild-type protein, although the amounts of mRNA are not lower than in wild-type. Therefore, reduced levels of ΔN2-12porin are most likely linked to one or more defects in translation, nascent protein stability and subsequent targeting and assembly of the protein in the outer membrane. *In vitro*-synthesized ΔN2-12porin can be imported and assembled into isolated mitochondria [131], indicating that the molecule retains a mitochondrial targeting signal. Once it has crossed the MOM through the TOM complex, assembly of porin into the membrane requires the sorting and assembly complex (SAM, reviewed in [153]). The "β signal" recognized by the SAM complex is located in the C-terminal β-strand of the protein (see [15] for the predicted *N. crassa* signal), so it is unlikely that targeting to the SAM complex is defective. Nonetheless, inefficient release from the TOM or assembly via the SAM complex cannot be ruled out.

Sampling of mRNA for genes overexpressed in ΔPor-1 strains revealed levels closer to wild-type in the ΔN2-12porin-expressing strain. This result suggests that low levels of ΔN2-12porin can partially compensate for the absence of wild-type porin. Among those 7 tested genes the only under-expressed mRNA in ΔN2-12por was for *coq4* (NCU02157), involved in ubiquinone biosynthesis. The reason for this reduction is not clear. Although statistical support was not strong, the mRNA putatively encoded by NCU05850 was increased two-fold. Although this gene is annotated as a rubredoxin-$NAD^{(+)}$ reductase, recent work has identified it as a homologue of the apoptosis-related oxidoreductase (aif-1, [154]). However, unlike its mammalian counterpart, AIF 1 does not appear to be required for assembly of complex I and therefore the reason for its abundance in ΔPor-1 is not clear.

## 2.5 Conclusion:

The N-terminus of porin is required for the efficient assembly of the protein in mitochondria, and maintenance of the standard electron transport chain and lower levels of mitochondria are observed in the ΔN2-12por strain. The expression of low levels of ΔN2-12porin is associated with only some of the changes in gene expression observed in the ΔPor-1 strain.

## 2.6 Acknowledgement:

This work was funded through Discovery Grants from NSERC to DAC, AK and GH. UK received a URSA from NSERC and SRS and WATS were supported in part by the Faculty of Science, University of Manitoba. SRS was the recipient of a University of Manitoba Graduate Fellowship and SRS and AZ were supported in part by the GETS program of the Faculty of Graduate Studies. Initial analyses of the strains were completed as part of the BSc Honours thesis of Justine Gallardo. We thank Ameet Bharaj for excellent technical assistance, and Dr. Jason Treberg and Mr. Andre Dufresne, Department of Biological Sciences, for use of the Oxygraph and for assistance with fluorescence microscopy, respectively. We acknowledge Drs. W. Ens and K.G. Standing for use of the instruments in the Department of Physics and Astronomy and we appreciate the assistance from Dr. Neil J. Holliday, Department of Entomology, with statistical analysis of the MS data. We also thank Mr. Manu Singh and Mr. Malaka de Silva (Department of Microbiology) for their help with RT-qPCR.

# Chapter 3: The impact of changes to VDAC levels and expression of an N-terminally truncated VDAC on mitochondrial bioenergetics and reactive oxygen species production in *Neurospora crassa.*

Sabbir R. Shuvo [a], Lilian M. Wiens [b], Jason R. Treberg [b, c], Deborah A. Court [a] *

[a]Department of Microbiology, University of Manitoba, [b]Department of Biological Sciences, University of Manitoba, [c]Department of Food and Human Nutritional Sciences, University of Manitoba, Winnipeg, MB, Canada, R3T 2N2

*corresponding author
Deborah.Court@umanitoba.ca

Department of Microbiology

University of Manitoba

Winnipeg, MB Canada R3T 2N2

Phone (204) 474-8263

Fax (204) 474-7603

**Abstract:**

Mitochondria are primary ATP producing organelles and are involved in many cellular signalling pathways. Mitochondrial porin, also known as the voltage-dependent anion-selective channel (VDAC) is a highly functionally conserved protein in the mitochondrial outer membrane and functions as a channel to transport metabolites. In this study, the influence of VDAC on mitochondrial bioenergetic pathways and reactive oxygen species (ROS) production in *Neurospora crassa* was investigated. In comparison with wild-type, the VDAC-less mitochondria display lower complex I and respiratory control ratio, but higher ROS production capacity under non-phosphorylating conditions. Membrane depolarization by subsequent addition of ADP was significantly lower than that observed in wild-type organelles. Mitochondria harbouring about 50% of the wild-type amount of VDAC have elevated complex II activity and ROS production capacity compared to wild-type. Similarly, in mitochondria expressing low levels of an N-terminally truncated VDAC (ΔN2-12porin), higher ROS production capacity was detected compared to wild-type. Thus, VDAC affects mitochondrial electron transport chain complexes, the flux of ADP, and ROS production capacity. Abnormal ROS production may trigger redox signalling pathways and contribute to phenotypes that have been observed in VDAC knockout cells and those expressing ΔN2-12porin.

## 3.1 Introduction:

Mitochondria can transform cellular energy to the form of ATP through oxidative phosphorylation (OXPHOS). Important to these processes are mitochondrial porins, also known as voltage dependent anion-selective channels (VDAC), which are proposed to regulate calcium, metabolite and ATP/ADP flow through the mitochondrial outer membrane (MOM) from the intermembrane space to the cytosol and vice-versa (Figure 3.1). The structure of VDAC was first published in 2008 and the protein folds into 19 β-strands and an N-terminal α-helix [22,24,26]. VDAC can modulate multiple cellular functions via interactions with other proteins [28–30]. However, despite these important roles, the effects of VDAC on mitochondrial bioenergetics have not been examined thoroughly.

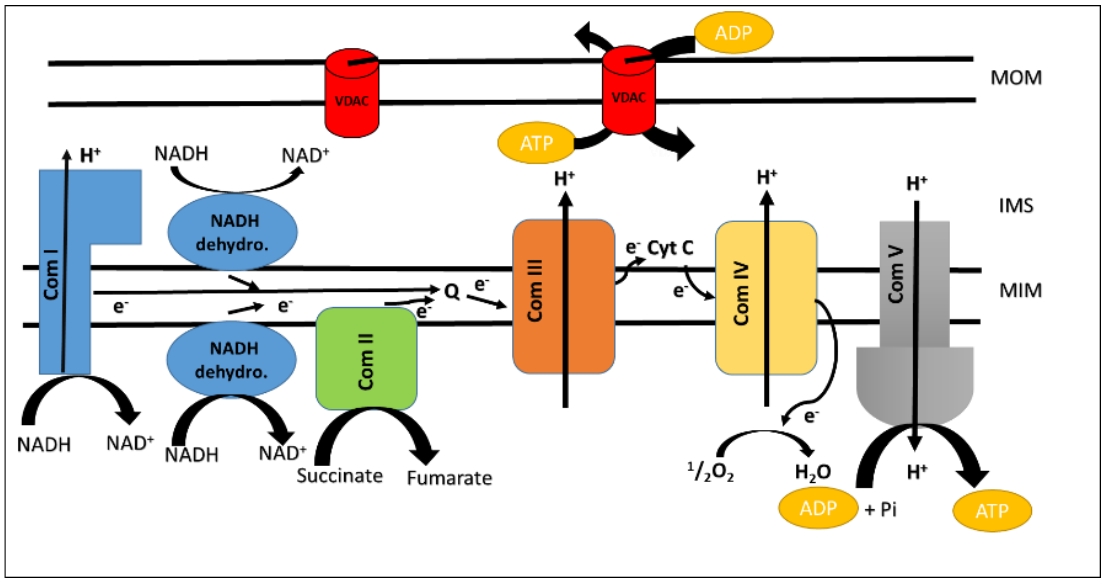


Figure 3.1: Electron transport and oxidative phosphorylation in *N. crassa* mitochondria. In WT cells CoQ (Q) shuttles electrons from complex I and complex II to complex III. *N. crassa* has four alternative NADH dehydrogenases (NADH dehyro.), one on the matrix side and three in the MIM. For the clarity of the figure one of each group is shown. VDAC are shown as red cylinders with black sticks that indicate the N-terminus of VDAC. MOM, mitochondrial outer membrane; MIM, mitochondrial inner membrane; IMS, inter membrane space.

In general, knockout of a protein coding gene from a cell provides a useful tool to study the role(s) of the protein in a cell [132]. In mammalian systems, understanding the effects of a knockout of VDAC is complicated because of the presence of multiple VDAC isoforms. In addition, deletion of the VDAC2 isoform is embryonically lethal [reviewed in 7]. *N. crassa* is a facultative aerobe and has canonical respiratory chain complexes (Figure 3.1; [154]). Moreover, isolation of mitochondria from *N. crassa* is straightforward; therefore, *N. crassa* has been used extensively for the study of mitochondrial biology and porin functions [111]. There is only one VDAC isoform in *N. crassa* making this organism a suitable and much simpler candidate than mammalian cells for studying the effect that loss of VDAC has on mitochondrial bioenergetics and reactive oxygen species (ROS) production. In *N. crassa*, VDAC is not essential but a strain lacking VDAC has severe mitochondrial abnormalities and alternative oxidase (AOX) is active [56]. Electrons can be received from ubiquinol (reduced CoQ) by AOX and thus bypass complex III and IV to donate electrons to terminal oxygen (Figure 3.2). Hence, energy from the electrons that pass through AOX contribute less to the formation of the protonmotive force across the inner membrane [81,155]. AOX has been proposed to reduce ROS production by allowing alternative electron flow in the inner membrane thereby lowering the reduction of CoQ [156].

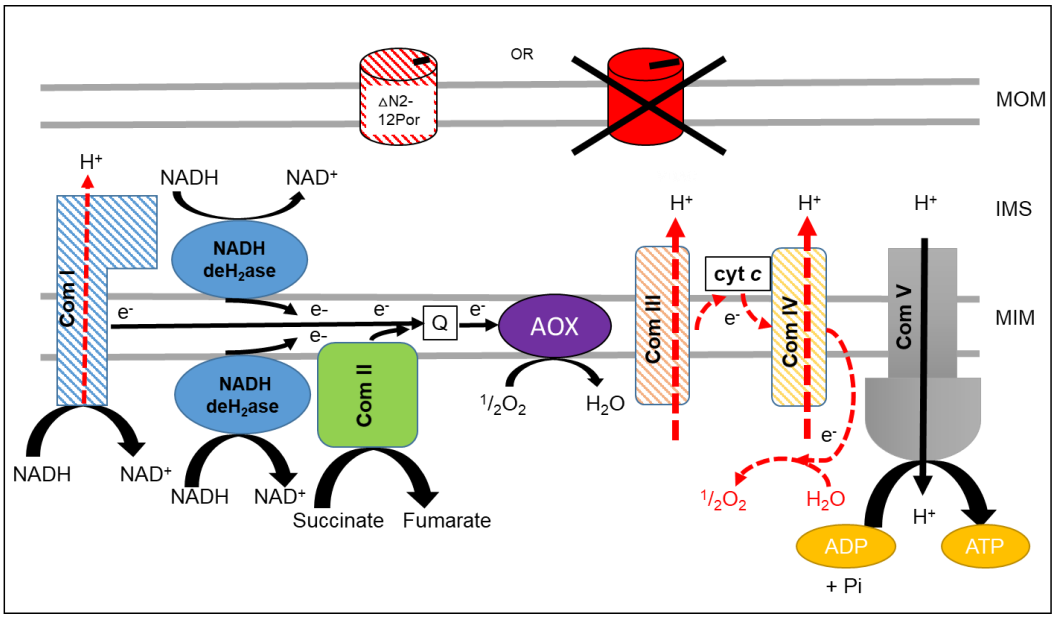


Figure 3.2: Mitochondrial OXPHOS in ΔPor-1 and ΔN2-12porin strains.

Both strains express AOX, which utilizes electrons from CoQ, thereby bypassing complex III to donate electrons to oxygen. The cross in the red cylinder indicates absence of VDAC and the cylinder with red dashed line indicates N-terminally truncated VDAC. Red dashed arrows indicate reduced electron flow in the mutant strains. Lower ETC complexes in ΔPor-1 (Com I, Com III and Com IV) compared to WT are shown as dashed shapes.

During mitochondrial energy transformation processes, electrons can leak and partially reduce oxygen to produce reactive oxygen species (ROS). In a broad term, ROS refers to oxygen molecules that are chemically reactive [89], meaning they can easily react with other molecules without the need for a catalyst. Examples of ROS are singlet oxygen, hydrogen peroxide, hydroxyl radical and superoxide anion. In mitochondria, ROS are produced from complex I, II and III of ETC and enzymes of the TCA cycle (Figure 3.3). In mitochondria, most of the ROS producing sites catalyze conversion of monovalent oxygen to generate superoxide which is rapidly dismuted to hydrogen peroxide by superoxide dismutase (SOD) activity in the matrix (SOD2) or the intermembrane space (SOD1); however, some sites can generate hydrogen peroxide from divalent reduction of oxygen [157]. Little is known about mitochondrial ROS production from *N. crassa*. Here, we use hydrogen peroxide efflux as a combined measurement of superoxide and hydrogen peroxide production, thus, we use "ROS production" term to mean hydrogen peroxide efflux.

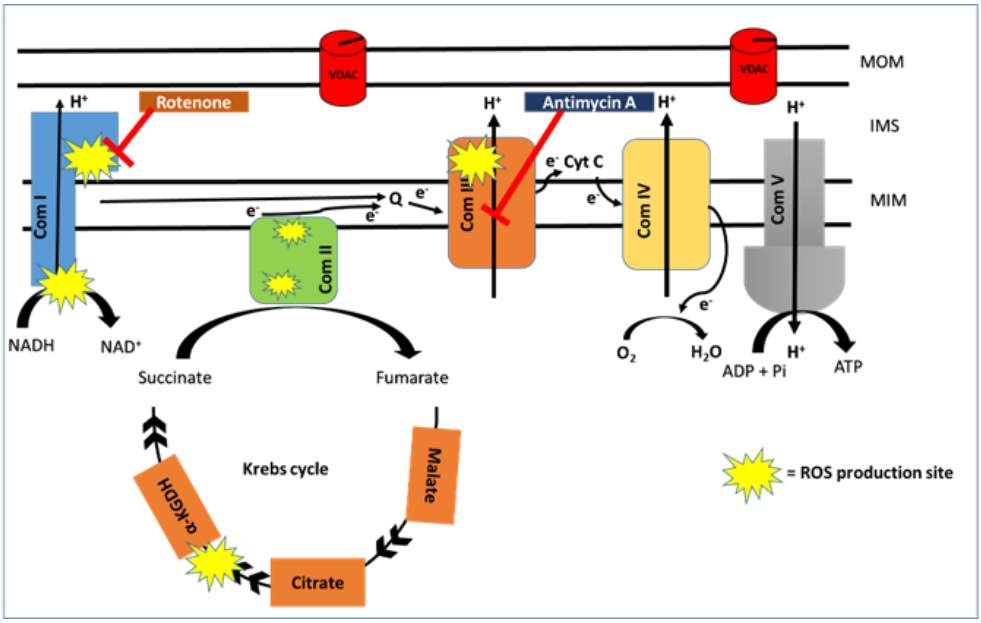


Figure 3.3: Mitochondrial ROS production sites.

Rotenone and antimycin A bind with complex I and complex III respectively. For clarity, some ROS producing sites and the alternative NADH dehydrogenases are not shown. α-KGDH, α-Ketoglutarate dehydrogenase; other abbreviations are as in Figure 3.1. Double arrows indicate other steps in the Krebs cycle; note that succinate and complex II are the part of Krebs cycle.

In this study, mitochondrial bioenergetics, including respiration rates and relative measurements of membrane potential, and ROS production were examined by comparing mitochondria isolated from wild-type *N. crassa* with VDAC knockdown and knockout strains and one expressing an N-terminally truncated variant of VDAC.

## 3.2 Materials and methods:

### 3.2.1 Chemicals:

All the chemicals were purchased from Thermo Fisher Scientific (Mississauga, ON, Canada), Sigma-Aldrich Canada (Oakville, ON, Canada) or BioShop Canada (Burlington, ON, Canada).

### 3.2.2 Strains and growth conditions:

*N. crassa* strains used in this study are listed in Table 3.1. Growth and handling of *N. crassa* strains were performed following the procedures described in [124] at 30$^{o}$C. Mitochondria were isolated following the protocol described in [136].

Table 3.1: *N. crassa* strains used in the study.

| **Strain name** | **Genotype/Comments** | **% respiration that can be mediated by AOX[1]** | **ETC defects** | **Reference** |
|---|---|---|---|---|
| FGSC 9718[2] (wild-type) | *Δmus-51::bar*$^{+}$ *mat a* | < 5% | None | [132] |
| ΔPor-1 | *Δpor::hph*$^{+}$ *Δmus51::bar*$^{+}$ *mat a* transformant of FGSC 9718 | 95% | Low levels of complexes I[3], III and IV | [56] |
| ΔN2-12porin | *hph*$^{+}$*, porΔ2-12, Δmus51::bar*$^{+}$ *mat a* transformant of FGSC 9718 | 80% | Low levels of complexes I, III and IV | [158] |
| LoPo | *hph*$^{+}$*, Δmus51::bar+ mat a, TOM40 promoter::por* transformant of FGSC 9718 | 8% | Increased complex II activity[3] | [158] |

[1] Measured as percentage of oxygen consumption that is resistant to cyanide

[2] Strains bearing FGSC names were obtained from the Fungal Genetics Stock Center [135]

[3] This work

### 3.2.3 Evaluation of mitochondrial outer membrane integrity:

Mitochondrial outer membrane integrity was evaluated based on the change in oxygen consumption in response to addition of exogenous cytochrome *c*. Briefly, 100 µg of mitochondrial protein was added to 2 ml of air-equilibrated SR buffer (modified from [130]; 50 mM $KH_2PO_4$, 5 mM $MgCl_2$, 10 mM MOPS, 250 mM sucrose, 0.3% fatty acid free BSA, pH 7.2) at 30$^oC$ in an Oxygraph-2k (Oroboros Instruments, Innsbruck, Austria). After stabilization of the signal, succinate and rotenone (the latter dissolved in DMSO) were added to final concentrations of 5 mM and 1 µM, respectively. The mitochondria reached a stable respiration rate under these non-phosphorylating conditions (state 2). Subsequent addition of 1 mM ADP initiated phosphorylating respiration (state 3). Lastly, 8 µM cytochrome *c* was added to determine the oxygen consumption rate to evaluate MOM integrity. The degree of broken mitochondrial outer membrane was determined by dividing the oxygen consumption rate in the presence of exogenous cytochrome *c* by the oxygen consumption rate in the presence of ADP [137]. The degree of mitochondrial breakage is proportional to the amount of exogenous cytochrome *c* that can enter mitochondrial intermembrane space to increase electron flux to complex IV, hence, increasing the respiration rate (Appendix 7.2 Figure 1).

### 3.2.4 Complex I level and complex II activity:

Relative levels of mitochondrial complex I activity were estimated following the in-gel detection protocol described in [55] with slight modification. 100 µg of mitochondrial protein were dissolved in 50 µl (1% w/v) n-dodecyl β-D-maltoside (DDM) and incubated on ice for 30 minutes followed by centrifugation at 16000 rpm (Beckman Coulter, optimaTM Max-E Ultracentrifuge, USA, rotor TLA100.3) for 30 minutes at 4°C. Complexes were separated in 4-10 % acrylamide

gradient Ponceau S native gels and an in-gel NADH-dehydrogenase activity assay was performed [159]. In brief, the gel was incubated at room temperature with 5 mM Tris-Cl, pH 7.4, 0.1 mg/ml NADH and 2.5 mg/ml NTB (NitroTetrazolium Blue). Good signals were obtained after overnight incubation of the gel with the solution in the dark. Mitochondrial complex II activity was measured with slight modification of the protocol described in [160]. Briefly, 50 µg of frozen mitochondrial protein was used in 1 ml of complex II buffer (50 mM $KH_2PO_4$, 10 mM succinate, 1 mM KCN, 2.5 µM rotenone, 10 µM antimycin A, pH 7.4). Mitochondria were incubated at 23°C in the buffer for 5 minutes to oxidize endogenous CoQ and reduce complex II. Next, the reaction was started by adding 20 µM coenzyme $Q_1$ ($CoQ_1$), which was oxidized from the reduced complex II. Absorbance was measured at 280 nm to detect consumption of reduced $CoQ_1$. The activity was calculated with the extinction coefficient for reduced $CoQ_1$ of 12 $mM^{-1}$ $cm^{-1}$ and then normalized to the amount of protein.

### 3.2.5 Simultaneous measurement of respiration rate and membrane potential:

Accumulation of the membrane-permeant fluorescent dye tetramethylrhodamine methyl ester (TMRM) was used to estimate membrane potential ($\Delta\Psi$). Briefly, combined respirometry and spectrofluorometry were conducted using 200 µg of freshly prepared whole mitochondrial protein in 2 ml of SR buffer containing 2.5 µM TMRM at 30°C in an Oxygraph-2k. In state 2 respiration, the oxygen consumption rate in the presence and absence of TMRM was measured in reaction medium containing 5 mM glutamate, 5 mM succinate and 5 mM malate (GMS), supporting electron entry into the electron transport system at complex I and complex II [161]. To initiate state 3 respiration, ADP was added to 800 µM, followed by oligomycin (1 µM) to measure the oligomycin-induced, non-phosphorylating respiration rate (state 4o). The respiratory control

ratio (RCR) was determined by dividing the oxygen consumption at state 3 by oxygen consumption rate at state 4o.

Mitochondrial membrane potential ($\Delta\Psi$) was estimated, by relating to the quenching of the fluorescence of TMRM in response to its migration into the organelle upon mitochondrial energization, while simultaneously monitoring respiration rate. Here we assume that TMRM has comparable non-specific binding and the matrix volumes per mg of mitochondria protein across strains are similar. Reaction conditions for measuring $\Delta\Psi$ were as described for determining respiration rate, except that 10 µM CCCP (Carbonyl cyanide 3-chlorophenylhydrazone) was introduced to depolarize the mitochondria at the end of the experiment. Relative TMRM fluorescence quenching was used to determine $\Delta\Psi$ in different conditions (Figure 3.4).

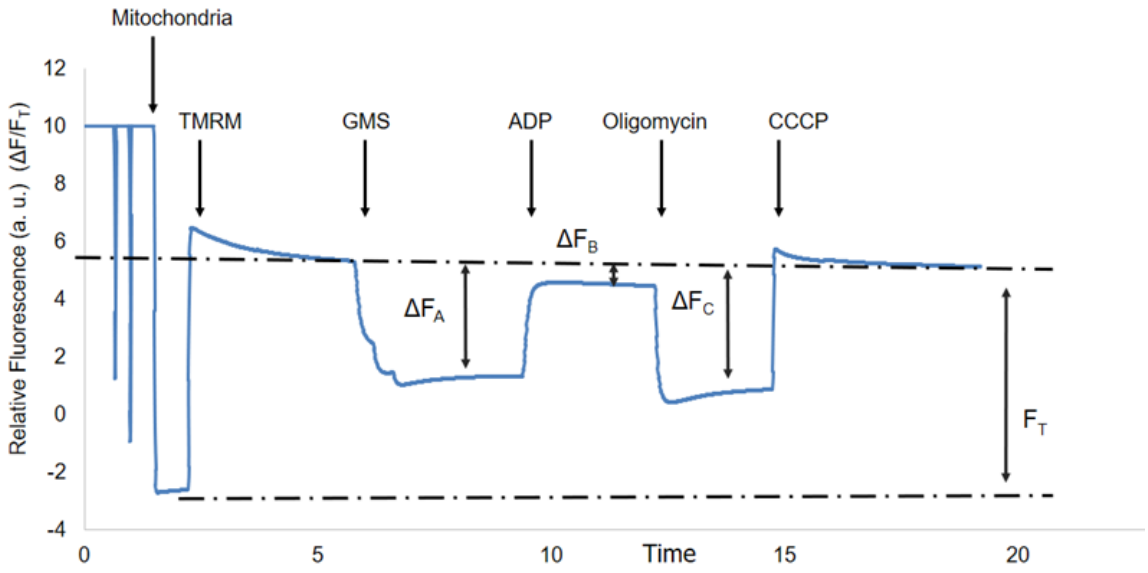


Figure 3.4: Measurement of relative ΔΨ in WT mitochondria by quenching of TMRM fluorescence.

The difference between deenergized and background fluorescence ($F_T$) was determined. The lowest fluorescence was observed in the closed chamber with mitochondria and buffer and without TMRM. When TMRM is introduced, fluorescence increases. In the presence of GMS mitochondria become energized and fluorescence is quenched ($\Delta F_A/F_T$). After that, ADP is used to depolarize the mitochondria ($\Delta F_B/F_T$). Later, oligomycin is used to inhibit the ATP synthesis from complex V ($\Delta F_C/F_T$). To obtain the full uncoupled stage CCCP was used. Arrows show times of addition of the indicated mitochondria and chemicals.

### 3.2.6 Mitochondrial $H_2O_2$ efflux measurement:

Mitochondrial ROS production, was measured as $H_2O_2$ efflux using the protocol described in [162]. Briefly, 200 µg of mitochondrial protein was suspended in 2 ml SR buffer. 25 $IUml^{-1}$ superoxide dismutase (SOD) (to convert superoxide to $H_2O_2$), 5 $IUml^{-1}$ horseradish peroxidase, which carries out the oxidation of Amplex Ultrared in the presence of $H_2O_2$, and 50 µM Amplex Ultrared were used in the reaction buffer. The fluorescence was measured at 30˚C with constant stirring, at an excitation wavelength of 550 nm and an emission wavelength of 590 nm in an Agilent Eclipse spectrofluorometer. After monitoring for a 5 minutes preincubation phase, GMS was added and the reaction was allowed to continue for at least 5 minutes to determine the rate of $H_2O_2$ efflux. Calibration curves were constructed by using at least 4 stepwise additions of 0.2 nmole of $H_2O_2$ to identical cuvettes with mitochondria in the presence or absence of respiratory substrates. In ΔPor-1, 150 arbitrary unit and 167 arbitrary unit per nmole of $H_2O_2$ were observed in the presence and absence of GMS respectively. The rate of increase in fluorescence was converted to nmole of $H_2O_2$ $min^{-1}$ mg $protein^{-1}$ based on this curve. To evaluate the possible role of specific enzyme complexes in ROS production, 0.5 µM rotenone and 10 µM antimycin A were used separately as inhibitors for complex I and complex III, respectively. Rotenone binds to the Q binding site of complex I and antimycin A blocks the transfer of electrons in the $Q_i$ site of complex III [163].

### 3.2.7 Statistical analysis:

The results are presented as mean ± SD (standard deviation) (n=3-4). Given the multiple differences (VDAC amount, activation of AOX) among the strains analyzed (see below), pairwise

comparisons between the WT and each variant were performed for complex II activity, membrane potential, ROS production and RCR. These data were analyzed using Student's t-test; $p< 0.05$ was considered significant. For analyzing the effect of TMRM on the overall RCR data, ANOVA was used, followed by the PAIRWISE Tukey test.

### 3.3 Results and Discussion:

#### 3.3.1 Fungal ETC complexes and VDAC.

As a first step toward understanding the impact of absence of VDAC on the fungal electron transport chain, the *N. crassa* FGSC 9718 strain (WT) was studied. In WT, the ETC is composed of canonical complexes and, in addition, there are four rotenone-insensitive, non-proton pumping alternative NADH dehydrogenases, one of which faces the matrix side of the mitochondrial inner membrane (Figure 3.1) [78]. The high abundance of VDAC [8] suggests that many pores are needed for its many normal functions; therefore to determine the effect of reducing the amount of VDAC on fungal ETC complexes, a strain (LoPo, [158]) expressing 40-50% of VDAC compared to WT was studied. In LoPo, the activity of complex II was increased compared to WT (WT= reduction of 3.27± 0.30 nmole $CoQ_1$ $min^{-1}$ $mg^{-1}$) (Figure 3.5 A); however, no difference was observed in complex I activity (Figure 3.5 B) or cytochrome spectrum in this strain [158]. Next, to understand the effect of the absence of VDAC on the ETC complexes, a knockout VDAC strain (ΔPor-1) was studied [56]. In this knockout strain, proteomic analysis predicted low levels of some of the subunits of complex I [56], and an in-gel activity assay for complex I (Figure 3.5 B), [55] supported this finding. Another proteomic study pointed out unchanged relative amounts of three of the four alternative NADH dehydrogenases in ΔPor-1; the fourth enzyme was not detected [55]. In ΔPor-1, complex II activity was unchanged compared to WT (Figure 3.5 B). Cytochrome

spectra analysis revealed that the cytochromes residing in complex III (cytochrome *b*) and complex IV (cytochrome $aa_3$) were low; moreover, this strain expresses alternative oxidase (AOX; Table 1), which can bypass complex III and complex IV to donate electrons to the terminal oxygen [56].

The N-terminus of VDAC resides in the lumen of the barrel, where it is hypothesized to control gating of the pore, and regulate interactions with ATP (reviewed by [2]). To understand the influence of truncating the N-terminus of VDAC on mitochondrial bioenergetics, an N-terminally truncated VDAC strain (ΔN2-12porin) was studied. The ΔN2-12porin strain has similar cytochrome deficiencies as ΔPor-1, but complex I levels are similar to WT (Figure 3.5 B). Thus, the presence of different amounts of wild-type VDAC or, low levels of the ΔN2-12porin variant of VDAC, is associated with multiple changes in ETC complexes in *N. crassa*.

A.

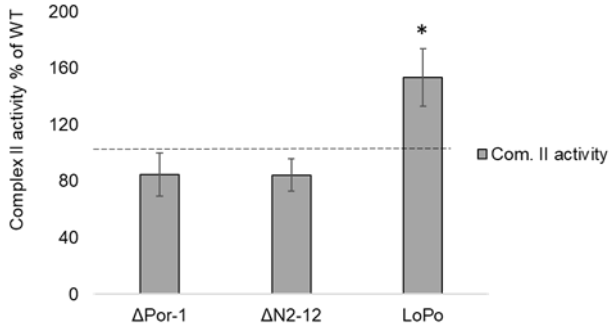


B.

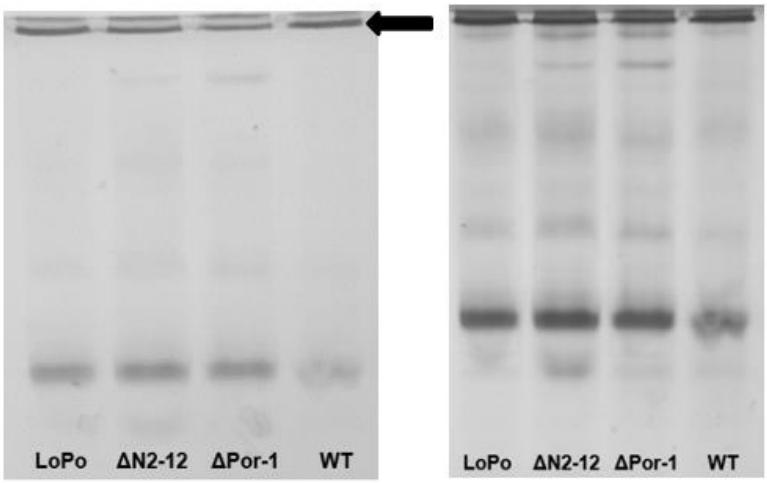


Figure 3.5: Characterization of the ETC complexes of strains harbouring different variants of VDAC.

(A) Complex II activity was determined as described in Materials and Methods and percentages of WT values are presented. The dashed line indicates 100%. (B) Complex I assay in pink native gel. The left panel shows an in-gel NADH dehydrogenase activity assay for complex I. The arrow indicates bands corresponding to complex I. The second panel shows Coomassie Brilliant

Blue staining of the same gel to confirm that similar amounts of protein were present in each lane.

### 3.3.2 Oxygen consumption and respiratory control ratios (RCR).

It was hypothesized that VDAC abnormalities in the MOM and deficiencies in ETC complexes may influence the substrate oxidation capacity in the corresponding mitochondria by limiting the substrate transport into mitochondria, or by reducing the oxidation capacity of the ETC complexes; this was tested by determining the oxygen consumption and respiratory control ratios of mitochondria isolated from the set of strains. To determine the RCR, oxygen consumption rates in phosphorylating and non-phosphorylating states were measured, and RCR was defined as the ratio of state 3 to state 4o respiration (Figure 3.6 A, Appendix 7.2 Figure 2).

In the presence of GMS at 30°C, the WT mitochondrial RCR was 1.98±0.08, which was on the lower side of the previously published results; the RCR for WT *N. crassa* was 1.4 to 6.2 in the presence of various substrates [164–166] (Table 3.2). However, in the presence of succinate (RCR=1.4) [164] the value is close to that reported here. Thus, the relatively low RCR suggests that, in the presence of GMS, the ratio of protons pumped to the IMS and the oxygen molecules reduced by electrons flowing through the ETC is low. This observation may suggest that a relatively high fraction of electrons is entering the ETC downstream of complex I. However, it has been observed that in the presence of exogenous NADH, the RCR for *N. crassa* mitochondria is also relatively low 2.0 [165]. Oxidation of NADH by by-passing complex I and instead using the non-proton-pumping alternative NADH dehydrogenases [165] may also contribute to this effect. The high RCR observed by others in the presence of α-ketoglutarate (6.2) was considered unusual for fungi [165].

In the presence of GMS, the oxygen consumption rate (OCR) for ΔPor-1 was low compared to WT (Figure 3.6, Appendix 7.2 Figure 2 & 3). in agreement with our observation that ΔPor-1 has low levels of complexes I, III and IV. Both strains responded to the addition of ADP by increasing OCR to a similar level. In the state 4o, oligomycin blocks the ATP synthase and reduced oxygen consumption to a similar level in WT and in ΔPor-1. However, when RCR was calculated using paired OCR data (state 3 over state 4o from the same preparation), a difference was observed. In ΔPor-1 mitochondria, RCR was 1.71 ± 0.15, which is slightly lower compared to WT (Table 2). It should be noted that, in contrast to WT, ΔPor-1 displays high AOX activity, and thus oxygen consumption likely occurs through both complex IV and AOX. Therefore, in comparison to the situation for mammalian cells, the RCR value is less useful for comparing coupling efficiency between fungal cells expressing and not expressing AOX. In comparison to WT, no differences were observed in OCR and RCR from ΔN2-12porin and LoPo mitochondria, despite a lower quantity of VDAC in the MOM compared to WT (Figure 3.6 B). The proportional increases in $O_2$ consumption upon the addition of ADP suggests that the electron flow increases to a similar degree in variant and wild-type mitochondria in response to utilization of the membrane potential for ATP synthesis.

A.

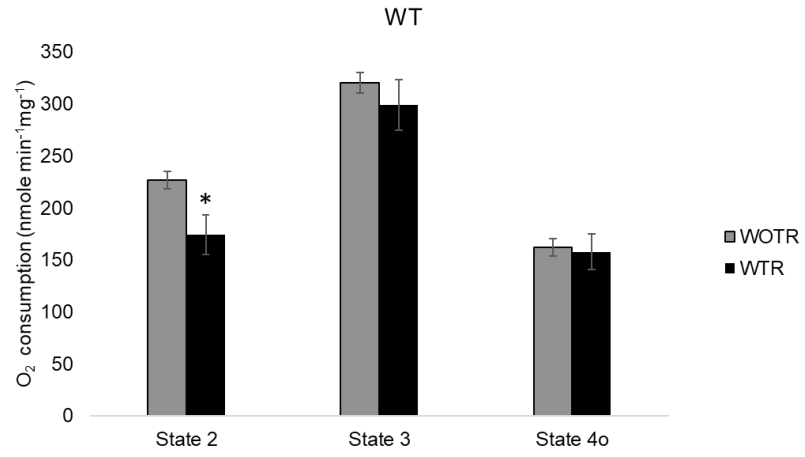


B.

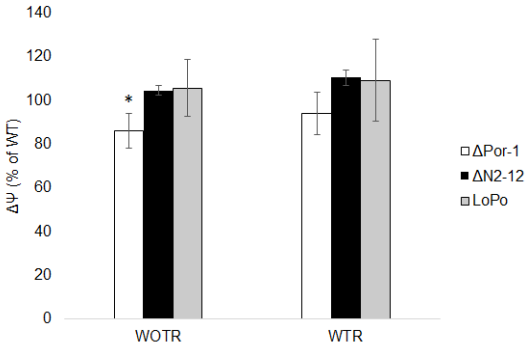


Figure 3.6: Oxygen consumption rates in the presence of GMS and RCR in the presence and absence of TMRM.

(A) WT mitochondrial oxygen consumption rates at the different respiratory states of mitochondria in the presence (WTR) and absence (WOTR) of TMRM. (B) RCR of mitochondria of different strains in the presence of TMRM (WTR) and in the absence of TMRM (WOTM). In both panels, average value (n=3-4) are presented with standard deviations.

### 3.3.3 Membrane potential.

Previous studies have reported that the knockdown of VDAC from HepG2 and HeLa cell lines resulted in lower mitochondrial ΔΨ [167,168]. Under normal conditions, in mammalian systems, there is a linear relationship between the rate of oxygen consumption and the total proton current [169]. However, in fungal species, because of branched respiration (Figure 3.2), there is not a direct correlation between the two. Here, *Neurospora* mitochondrial ΔΨ was studied by using VDAC knockout or VDAC variant mitochondria. Mitochondrial ΔΨ was measured by using a lipophilic cationic fluorescent dye, TMRM. However, to the best of our knowledge this is the first time TMRM was utilized to study the *N. crassa* mitochondrial ΔΨ and it was necessary to confirm that TMRM did not influence mitochondrial respiration. A moderate effect of TMRM on respiration was seen only in WT and LoPo (Figure 3.6 A, Appendix 7.2 Figure 2). In the presence of TMRM, WT and LoPo state 2 respiration was about 20-25% lower than that in the absence of TMRM; no deference was observed for ΔN2-12 and ΔPor-1 strains. The reason for this difference is not known. But, these observations might be linked to the fact that both of these strains have VDAC and absence of AOX activity. However, in the presence and absence of TMRM, the RCR was unchanged for each of the strains when evaluated using an oligomycin induced non-phosphorylating state of respiration (state 4o) (Figure 3.6 B). Thus, TMRM at above 2.5 μmol $l^{-1}$ does not interfere significantly with respiration and is a suitable tool for comparison of ΔΨ in *N. crassa*.

Interestingly, mitochondrial ΔΨ in the non-phosphorylating state 2 was similar in VDAC-mutated and WT strains (Figure 3.7), which is unexpected given the fact that VDAC is thought of as the primary transport mechanism across the MOM for the small organic anions added as respiratory substrates. ADP was then added to activate the phosphorylating state 3 of mitochondria.

It was hypothesized that the effect of externally-added ADP on ΔΨ would be reduced in the mitochondria lacking the normal amount of VDAC, because it has been proposed that VDAC functions as a regulating step in the control of the flow of ATP across the MOM [170]. Furthermore, a complex between VDAC and the inner membrane protein, adenine nucleotide translocator (ANT), has been proposed to be involved in the transportation of ADP/ATP between mitochondria and cytosol [23]. As expected, the degree of depolarization observed in ΔPor-1 mitochondria was blunted compared to WT in the presence of ADP (Figure 3.7). Conversely, no difference was observed in the ΔΨ between WT and ΔPor-1, when oligomycin was introduced to stop complex V activity.

Together, these analyses reveal several features of ΔPor-1 mitochondria that are not readily explained. First, a WT level of ΔΨ is maintained in state 2 organelles, in spite of the defects in the proton-pumping complexes of the ETC in the ΔPor-1 mitochondria. Second, an OCR less than that in WT organelles is able to maintain these WT levels of ΔΨ in state 2 ΔPor-1 mitochondria (Appendix 7.2 Figure 3.3). The abnormal levels of complex I (Figure 3.1) and the activity of AOX [55,114] would imply reduced proton translocation per oxygen consumed, and therefore would suggest a reduced ΔΨ or an increased OCR. The relative flux of electrons mediated by AOX and complex IV is not known, but it is assumed that the low levels of cytochromes $aa_3$ indicate a low level of active complex IV in ΔPor-1. Moreover, stimulation of AOX by ADP has been reported [58]. The steady state membrane potential is the equilibrium between proton translocation into the IMS, and the sum of proton return through processes such as ATP synthesis, protein import and transport of metabolites, as well as proton leak [40]. In isolated, state 2 mitochondria, it would be expected that proton leak is a significant component of proton return to the matrix, and therefore

ΔPor-1 mitochondria might be less prone to proton leak, through differences in lipid or protein composition of the inner membrane.

When ΔΨ was measured in different VDAC-variant mitochondria, no differences were observed in the ΔΨ in the LoPo and ΔN2-12porin strains compared to WT. Mitochondrial depolarization upon addition of ADP was like WT in the other two strains in the phosphorylation state, despite lesser amounts of VDAC (Figure 3.7). Presumably, VDAC molecules, alone or in contact sites with ANT, are present in sufficient amounts in ΔN2-12porin and LoPo mitochondria to ensure that ATP/ADP exchange and respiratory substrate supply were not limiting factors for respiration; thus, ΔΨ was like that of state 3 WT mitochondria. These observations also suggest that a low level (10%) of a N-terminally truncated VDAC provides for a sufficient level of ADP/ATP transport. This suggested that an alternative ADP/ATP transport mechanism may be present apart from currently recognized mechanism.

These results appear to differ from the lower mitochondrial ΔΨ observed in different VDAC1 knockdown mammalian cell lines [168,172]. It is difficult to compare these data with those from the current study because phosphorylation state of the organelles and the effect of knockdown of VDAC on ETC complexes were not presented. Furthermore, the mammalian system was further complicated by the presence of multiple VDAC isoforms.

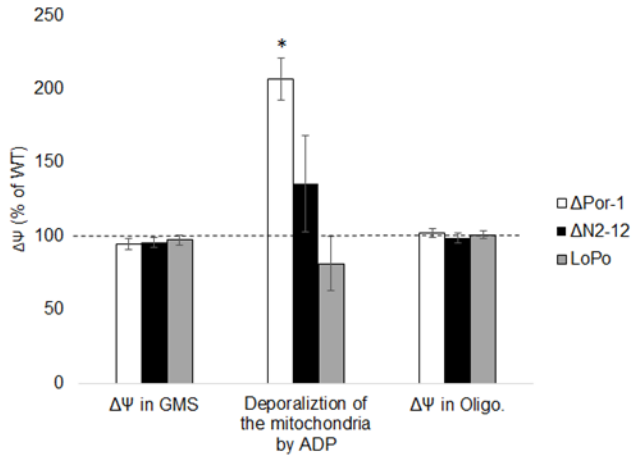


Figure 3.7: Mitochondrial ΔΨ as estimated by quenching of the fluorescent dye TMRM.

The first data set shows the ΔΨ in the presence of GMS ($\Delta F_A/F_T$ x 100; see Figure 4), the second data set shows ΔΨ remaining after mitochondria were depolarized by adding ADP. (retention of ΔΨ in the presence of ADP, $\Delta F_B/F_T$ x 100), and the third data set shows ΔΨ in the presence of oligomycin ($\Delta F_C/F_T$ x 100). All values are converted to percentage of WT. The dotted line indicates 100%.

### 3.3.4 Mitochondrial ROS production.

Increased intracellular and mitochondrial ROS were observed in yeast VDAC knockout strains, animal knockdown cell lines and yeast strains expressing different variants of VDAC [1,117,118]. Moreover, VDAC has been proposed to control the release of superoxide from mitochondria [173–175], and ROS may be involved in the modulation of VDAC for the release of

cytochrome *c* to initiate apoptosis in mammalian cells [reviewed in 7]. Thus, the ROS production capacity was measured from isolated mitochondria containing different variants or levels of VDAC. Here, hydrogen peroxide efflux was measured after dis-mutation of superoxide to hydrogen peroxide, which we use the general term ROS to describe. To study the ROS production from isolated mitochondria, the substrate mixture GMS and different inhibitors of ETC complexes were used (Figure 3.3). In WT *N. crassa*, mitochondrial ROS production capacity in the presence of the GMS substrate mixture was 74.00± 4.95 pmole $H_2O_2$ $min^{-1}$ $mg^{-1}$ (Table 3.2). To the best of our knowledge, this is the first-time $H_2O_2$ production from mitochondria from *N. crassa* was characterized. In the presence of GMS, the capacity of ΔPor-1 and ΔN2-12porin mitochondria to produce ROS was increased, compared to LoPo and WT (Figure 3.3). These data were supported by the fractional electron leak, which was estimated by the ratio of the rates of $H_2O_2$ production to $O_2$ consumption (Table 3.3). The fractional electron leak was highest in ΔPor-1 (Table 3.3).

Table 3.2: Characterization of *N. crassa* WT mitochondria.

| **RCR** | |
|---|---|
| RCR in the absence of TMRM[1] | 1.98±0.08 |
| RCR in the presence of TMRM[1] | 1.91±0.17 |
| **Relative TMRM fluorescence** | |

| | |
|---|---|
| In GMS ($\Delta F_A/ F_T$)[3] | 58.42±0.74 |
| In GMS + ADP ($\Delta F_B/F_T$)[3] | 5.50±1.26 |
| In GMS + ADP + Oligomycin ($\Delta F_C/F_T$) [3] | 62.63±1.94 |
| **ROS production (pmole $H_2O_2$ $min^{-1}$ $mg^{-1}$)** | |
| ROS in the presence of GMS | 74.00± 4.95 |
| ROS in GMS + rotenone | 50.00±13.08 |
| ROS in GMS + antimycin A | 442.00±13.42 |

[1]RCR, respiration control ratio in the presence of GMS

[2] values are averages and standard deviations (n=3-4)

[3]see Figure 3.2 for definitions of $\Delta F_A$, $\Delta F_B$, $\Delta F_C$, and $F_T$

Table 3.3: Fractional electron leak in the presence of GMS.

| **Strain** | **Electron leak relative to WT[1]** |
|---|---|
| WT | 100% |
| ΔPor-1 | 356 ± 130%[2] * |
| ΔN2-12porin | 153 ± 20 %[2] * |
| LoPo | 100 ± 2 %[2] |

[1] relative electron leak was determined as the ratio between $H_2O_2$ produced and oxygen consumed, per mg mitochondria; value for WT was $6.55*10^{-4}$ nmole $H_2O_2$/nmole O and was set to 100%

[2] % of WT;

* stars indicate values that are different from WT, p <= 0.05) (n=4-3)

To investigate the role of impaired electron flow in the ETC complexes in the increased ROS production, inhibitors that block electron flow were utilized. Rotenone blocks the electron transfer from NADH dehydrogenase (Complex I) to CoQ and blocks superoxide formation in the $I_Q$ site; in complex I, there may be two sites ($I_F$ and $I_Q$) for ROS production (Figure 3.3 [176]) . For mammalian mitochondria, in the presence of succinate, ROS is produced from the $I_Q$ site in complex I due to reverse electron flow from the reduced Q-pool. In the presence of rotenone and succinate, ROS production from the $I_Q$ site is decreased [163,177]. However, with mammalian mitochondria increased ROS production is often observed in the presence of NADH-generating substrates, such as malate and glutamate, in the presence of rotenone [163]. Therefore, in the presence of GMS and rotenone, ROS may be produced from the many NADH-

dependent sites or complexes II and III. Another inhibitor, antimycin A, was used to impair electron flow from complex III. Antimycin A binds to the $Q_i$ site of complex III, which may elevate superoxide formation from the $Q_o$ site and inhibits the mitochondrial electron transfer between cytochromes *b* and *c* (Figure 3.3) [178,179].

In the presence of GMS, and the complex I inhibitor rotenone, ROS production capacity was increased in all the strains compared to WT (Figure 3.8). A striking observation was that, although ΔPor-1 has low complex I, $H_2O_2$ efflux is elevated in mitochondria from this strain in the absence of inhibitors and is 9-fold elevated in the presence of rotenone. One possible explanation is that in the presence of rotenone, ROS production not only increased from the small amount of complex I, but also increased from other NADH-dependent sites (like pyruvate dehydrogenase and α-ketoglutarate dehydrogenase) in response to the increased NADH/$NAD^+$ that could result from blocking of complex I [90]. Another possibility is that the presence of rotenone increased electron flow into the CoQ pool via alternative NADH-dehydrogenases, which could increase ROS

production from complexes II and III. In LoPo, in the presence of complex I inhibitor rotenone, ROS production was increased around 3.5-fold. Interestingly, elevated ROS production in the presence of rotenone in LoPo indicates that some modifications may occur in the ETC complexes or other NADH-dependent ROS production sites that were not reflected in its growth and respiratory phenotypes [158]. In contrast, in ΔN2-12porin, a small 1.3-fold increase in ROS production rate was detected in the presence of rotenone compared to WT. Thus, the amount of VDAC or expression of the N-terminal deletion variant in the MOM influences the levels of ROS production capacity in the presence of rotenone.

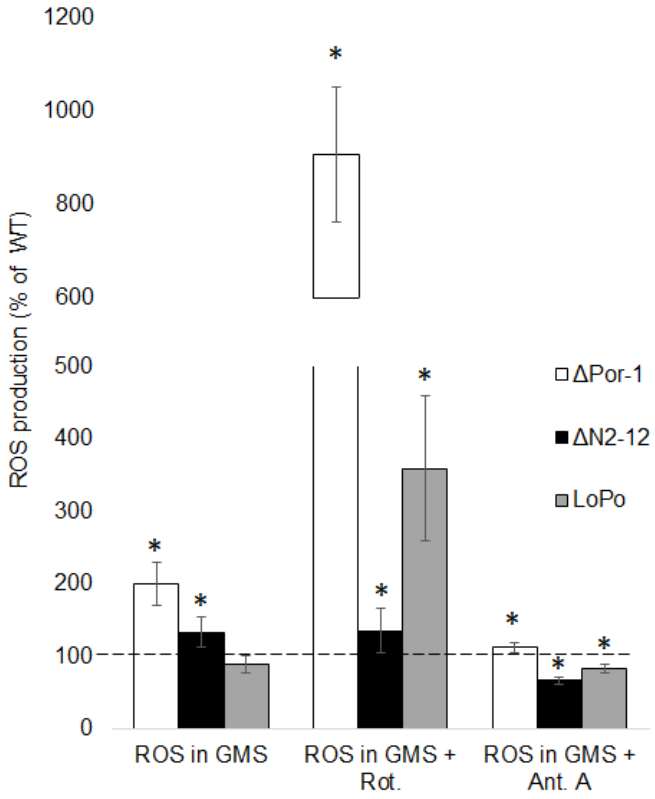


Figure 3.8: ROS production by mitochondria isolated from different VDAC mutants.

The first panel shows ROS production in the presence of GMS. The second panel shows ROS production in the presence of GMS and rotenone (ROS in GMS + Rot.) and the third panel shows ROS production in the presence of GMS and antimycin A (ROS in GMS + Ant. A). Values are shown as percentage of WT. The dotted line indicates 100%. N=3-4

Lastly, ROS production capacity was tested in the presence of antimycin A, which blocks complex III electron transport, and thus collapses part of the protonmotive force. In the cells having AOX activity, apart from conventional electron transport routes, some of the flux from alternative NADH dehydrogenase to AOX via complex I remains, this may lead to a highly-reduced Q-pool. This should magnify the ROS production from complex III because electrons can now enter complex III but are impaired from leaving it, leading to marked elevation in the production of ROS from $Q_o$ site of complex III. In antimycin A-treated WT mitochondria, the level of ROS production was significantly higher than that of the rotenone-treated organelles (Table 3.2). Similar to the situation in the presence of rotenone, higher ROS production capacity was detected in ΔPor-1 mitochondria in the presence of antimycin A, although, this strain has a low ratio of cytochrome *b* to cyto c compared to WT and high AOX expression [56]. It might be possible that, in ΔPor-1 mitochondria, the small number of electrons that were passing through low amount of complex III, in the presence of AOX were very prone to leakage when antimycin A was introduced into the reaction. As mentioned before, AOX can bypass complex III to transport electrons from CoQ; therefore oxidized CoQ can be reduced again by accepting electrons from complex I, alternative NADH dehydrogenase, and complex II. Thus, AOX is expected to maintain electron flow in the upstream ETC complexes and reduced ROS production relative to an equivalent system but in the absence of AOX. Hence, it was hypothesized that ROS production from complex III will be lower compared to WT in the strains that express AOX. In addition, in LoPo, decreased ROS production capacity was detected compared to WT in the presence of antimycin A, although LoPo has normal ETC complexes and does not express AOX [158]. However, the mechanism that LoPo utilizes to lower the ROS production from complex III is unclear. In ΔN2-12porin, ROS production capacity from complex III was lower compared to WT, although ΔN2-12porin has low complex III and

expresses AOX like ΔPor-1. The reason for this low level of ROS from ΔN2-12porin is unclear; but, again, this implies amount of VDAC indirectly associates with ROS production from mitochondria in the presence of antimycin A.

### 3.5 Concluding remarks:

Mitochondrial bioenergetics and normal levels of ROS production are important for proper functioning of the organelles and therefore of the cells. The results presented herein form the first detailed description of the impact of changes to the levels and variants of the most abundant MOM protein, VDAC, in mitochondrial bioenergetics and in the potential for ROS production by the organelles. The utilization of a fungal system with a single VDAC isoform has removed the complexities that result from investigating cells with multiple isoforms. In the presence of a lower level of VDAC, the activity of ETC complex II was increased, but the RCR and membrane potential were similar to those of WT. However, the potential ROS production was higher in the presence of inhibitors in this strain. Thus, mitochondrial bioenergetics are sensitive to a reduction in VDAC levels. In the complete absence of VDAC, normal $\Delta\Psi$ was perturbed, presumably due to reduced ADP/ATP flow. Mitochondrial ROS production capacity was increased in the strain, indicating abnormal ETC complexes and possibly contributions from other sites may lead to altered ROS metabolism in the absence of VDAC. These observations are relevant because different VDAC inhibitors have been proposed for use in the treatment of cancers [180], based on the role of the VDAC1 isoform in the increased metabolism and decrease apoptosis observed in these cells [1,175]. Partial blocking of VDAC via drugs might not result in any detectable phenotypic changes in the target or bystander cells, but the data presented herein indicate that careful examination of the ETC complexes for those mitochondria should be considered.

This study has extended the understanding of the requirements for the N-terminus of VDAC *in vivo* on mitochondrial functions. Mitochondria expressing VDAC with a truncated N-terminus showed an overall increase in the capacity to produce ROS, but maintained WT levels of $\Delta\Psi$ and OXPHOS and grew at almost normal rates. Therefore, this protein must retain some significant level of function in the absence of a complete N-terminus. This is noteworthy, particularly in light of the observation that it is present at levels about 10% of that of WT porin [158]. The retention of wild-type RCR in this strain, and in ΔPor-1, is intriguing, given the branched electron flow in these mutant strains. In conclusion, this study has revealed that VDAC has multiple impacts on mitochondrial bioenergetics and ROS production that are critical for a primary function of mitochondria, which is energy production.

**3.6 Acknowledgement:**

This work was supported by Discovery Grants from the Natural Sciences and Engineering Research Council of Canada (NSERC) to D.A.C and J. R. T. and the Canada Research Chairs program to J.R.T. S.R.S. acknowledges support from the Faculty of Graduate Studies at the University of Manitoba. L. M. W. was also supported from Discovery Grants and Canada Research Chairs grants.

# Chapter 4: The absence of VDAC from *Neurospora crassa* is associated with a differential protein expression profile and endoplasmic-reticulum unfolded protein response.

Sabbir R. Shuvo[1], Anna Motnenko[1§], Oleg V. Krokhin[2], Victor Spicer[3], Deborah A. Court[1*]

[1]Department of Microbiology, University of Manitoba,

[2]Department of Internal Medicine, University of Manitoba & Manitoba Centre for Proteomics and Systems Biology,

[3]Department of Physics and Astronomy, University of Manitoba,

[§]Current address: Department of Biochemistry, University of Oxford, Oxford, UK

*corresponding author
Deborah.Court@umanitoba.ca

Department of Microbiology

University of Manitoba

Winnipeg, MB Canada R3T 2N2

Phone (204) 474 8263

Fax (204) 474-7603

**Abstract:**

Mitochondrial porin forms voltage-dependent anion-selective channels (VDAC). To understand the global impact of the absence of VDAC, cytosolic and mitochondrial proteomic analyses were performed in a VDAC-less *Neurospora crassa* strain and its progenitor strain. The studies revealed proteins related to protein synthesis, and amino acid, nucleotide and sulfur metabolism that are less abundant in the VDAC-less strain. In contrast, some proteins involved in aerobic respiration, in the TCA cycle, carbohydrate and sugar metabolism and in oxidative stress responses were more abundant. Of particular interest, in the absence of VDAC, some proteins involved in the unfolded protein response (UPR) of the endoplasmic reticulum were high. Analysis of mitochondrial membranes revealed changes to the ratios of some acyl chains and the relative ergosterol levels in the VDAC-less strain. Thus, the absence of VDAC influences metabolism, particularly related to energy transformations, UPR and the composition of mitochondrial membranes.

## 4.1 Introduction:

The mitochondrial outer membrane (MOM) harbours mitochondrial porins, which are also known as voltage dependent anion-selective channels (VDAC). Mitochondrial VDAC, a member of the β-barrel protein family, is composed of 19 β-strands and an N-terminal α-helix [11,15,22,24,26]. VDAC works as a channel between the mitochondrial intermembrane space and the cytosol of the cell to transport metabolites [39]. In artificial membranes, the open conformation of VDAC is slightly anion-selective and the partially closed confirmation is slightly cation-selective [181,182]. The N-terminus of VDAC proposed to help the gating of VDAC between these two states [2] and the expression of VDAC with a truncated N-terminus is associated with abnormal electron transport chain (ETC) complexes and slow growth rate [54] (chapter 2).

The organism *Neurospora crassa* is an appropriate model to investigate the roles of VDAC in mitochondrial functions, as a single VDAC isoform is present [56,111]. An *N. crassa* strain containing VDAC-less mitochondria is viable, but temperature-sensitive and has a slow growth rate [56]. Moreover, mitochondria of the strain are small, have abnormal electron transport chain (ETC) complexes, and express alternative oxidase [56]. Furthermore, those mitochondria have dissimilar membrane potential and reactive oxygen species production capacity compared to wild-type (WT) organelles (chapter 3). Thus, absence of VDAC is associated with mitochondrial stresses.

Proteomic analyses of VDAC-less *N. crassa* mitochondria were previously performed using iTRAQ [56] and one-dimensional liquid chromatography followed by tandem mass spectroscopy methods (1D LC-MS/MS) [55]. In the iTRAQ analysis, 12 proteins were more abundant and 7 proteins were less abundant than in wild-type. In contrast, 1D LC-MS/MS analysis,

10 proteins were more abundant and 13 proteins were less abundant. Proteins involved in energy production, amino acid metabolism and transport were more abundant in ΔPor-1; in contrast, the amounts of protein components of the NADH:ubiquinone oxidoreductase (complex I) were shown to be reduced in the latter study [55]. Although the same strains were used in both studies, some of the intermembrane space proteins that were relatively in low amount in the iTRAQ experiments, were in similar relative levels as in WT in the 1D LC-MS/MS study. The additional flotation gradient purification step used to isolate pure mitochondria in the iTRAQ study might have caused more disruption of the MOM in the VDAC-less strain, and hence, loss of some of the intermembrane space proteins [55].

Mitochondrial stress responses and the modulation of other cellular pathways were not examined thoroughly in those studies as purified organelles were used. Multiple interactions of VDAC with both mitochondrial and cellular proteins have been detected [1,28,29] and therefore it is important to study the cytosolic protein expression profiles in the absence of VDAC. In the current study, cytosolic 1D LC-MS/MS protein expression profile was utilized. In addition, 2D LC-MS/MS proteomic analysis of isolated mitochondria was used to increase the coverage of mitochondrial proteins to further enhance our understanding of the protein expression profile of the VDAC knockout *N. crassa* cells.

## 4.2 Materials and methods:

### 4.2.1 Chemicals:

If otherwise not mentioned, chemicals were obtained from Thermo Fisher Scientific (Mississauga, ON, Canada), Sigma-Aldrich Canada (Oakville, ON, Canada) or BioShop Canada (Burlington, ON, Canada).

### 4.2.2 General growth and handling of *N. crassa:*

*N. crassa* strains WT FGSC 9718 (*Δmus-5::bar mat a*) and ΔPor-1 (*Δpor::hph+ Δmus51::bar+* transformant of FGSC 9718) were used in this study [56,132,135]. Growth and handling of the *N. crassa* strains were performed following the procedures described in [124] at 30˚C. Mitochondria from *N. crassa* were isolated following the protocol described in [136]. Light microscopy was performed with a Leica Wild M8 stereomicroscope (Wild Heerbrugg, Ontario, Canada).

### 4.2.2 Mitochondrial and cytosolic proteomic analysis:

Mitochondrial samples were prepared following the protocol described in [183] for proteomic analysis. To avoid damage of the mitochondrial membranes, crude mitochondria were isolated by differential centrifugation without a flotation gradient. In brief, samples were lysed with sodium dodecyl sulfate (SDS) and subsequently washed with urea buffer to remove SDS. Proteins were digested with trypsin at a ratio of 50:1 (w/w), and then were acidified using trifluoroacetic acid to a final concentration of 0.5 % and desalted using 1x100 mm column packed with 5 µm Luna C18(2) (Phenomenex, Torrance, CA). Purified peptide mixtures were lyophilized

and were subjected to 2D liquid chromatography (LC) and tandem mass spectroscopy (MS/MS) following the method described in [184].

Mass spectrometric (MS) acquisition was performed using an ABSciexTripleTOF 5600 TOF-MS system (Applied Biosystems, Foster City, CA) equipped with a Nano- sprayIII ionization source. Each acquisition cycle included a 250-ms survey, MS acquisition (m/z 400- 1500) and up to twenty 100-ms MS/MS measurements on the most intense parent ions (300 counts/s threshold, +2 to +4 charge state, m/z 100–1500 mass range for MS/MS).

For isolating cytosolic proteins, *N. crassa* cells were grown to the exponential phase and hyphae were harvested by filtration. Cells were ground with 1 g of sand per 1 g weight of hyphae in the presence of 1.5 ml of SEM buffer (250 mM Sucrose, 1 mM EDTA and 1 mM PMSF (Phenylmethylsulfonyl fluoride) per 1 g of hyphae. Cells were spun at 4000 rpm for 5 minutes in an SS34 rotor (Sorvall RC 6 plus) to remove the cell debris and sand. Supernatants were collected and further purified by spinning at 43000 rpm (Beckman Coulter, Optima$^{TM}$ Max-E Ultracentrifuge in a TLA100.3 rotor) for 45 minutes at 4°C; soluble proteins were collected in the supernatant [185].

For sample preparation for mass spectrometry the following protocol was used [186]. The soluble proteins were reduced (10 mM dithiothrietol, 30 min, 57°C), alkylated (50 mM iodoacetamide, 30 minutes in the dark at room temperature) and dialyzed against 100 mM $NH_4HCO_3$ for 6 hours. Then samples were digested overnight with modified trypsin (Promega, Madison, WI) with a ratio of 1 enzyme: 100 substrates (w/w) (determined by NanoDrop 2000, ThermoFisher) for 12 hours at 37°C. The resulting tryptic digest was acidified with trifluoroacetic acid (TFA) and purified by reversed-phase solid phase extraction (SPE). Approximately 50 µg of

each digest (determined by NanoDrop 2000, ThermoFisher) was sufficient for each LC-MS experiments [184].

1D LC-MS/MS analyses were performed for 3 hours of acquisition time for each sample. A splitless nano-flow 2D LC Ultra system (Eksigent, Dublin, CA) was used to deliver water/acetonitrile gradient at 500 nl/min flow rate through a 100 µm*200 mm analytical column packed with 3 µm Luna C18(2) (Phenomenex, Torrance, CA) at room temperature. Samples were injected (~1 µg of peptides in 10 µl of eluent A (water)) via a 300 µm*5 mm PepMap100 trap-column (ThermoFisher, CA). The gradient program included following steps: linear increase from 0.5 to 35 % of eluent B (acetonitrile) in 168 min followed by 5 minuets column wash with 90% buffer B and 7 minutes system equilibration using starting conditions of 0.5% buffer B. Both eluents A (water) and B (acetonitrile) contained 0.1 % formic acid as the ion-pairing modifier.

Data-dependent acquisition of TripleTOF5600 mass spectrometer (Sciex, Concord, ON) was performed using the following settings: 250 ms survey MS spectra (m/z 375-1500) was followed by up to 20 MS/MS measurements on the most intense parent ions (300 counts/sec threshold, +2 to +4 charge state, m/z 100-1500 mass range for MS/MS, 100 ms each, high sensitivity mode). Previously targeted parent ions were excluded from repetitive MS/MS acquisition for 12 seconds (50 mDa mass tolerance).

In both cases, the resulting raw WIFF files were processed using a standard conversion script, bundled with Analyst QS 1.6 into Mascot Generic File format (MGF). An in-house GPU-based peptide identification engine [187] was used for protein identification. These systems used the following search parameters: 20 ppm and 0.1 Da mass tolerance on the parent and fragment masses, respectively, and, fixed modification of cysteine residues +57.021 Da (cysteine protection

with iodoacetamide). Only tryptic peptides with expectation values of log(e) < -1.5 and up to one permitted missed cleavage were used for identification. Sequence data were obtained from the 7th annotated version of the *N. crassa* genome, obtained from the *Neurospora crassa* Sequencing Project, Broad Institute of Harvard and MIT (http://www.broadinstitute.org/).

MGF files contain information on charge, m/z, retention time of fragmented peptide as well as m/z values and intensities of fragment ions. Mass measurements for the parent and daughter ions were used for peptide identification, while intensities of the daughter ions were used for quantitation. TripleTOF 5600 provides very consistent MS/MS acquisition with good linearity between intensity of the parent peptide and daughter ions. Protein total ion counts (TIC) were used as a relative measure of protein expression within an experimental run; these values represent the sum of the MS/MS fragment ion intensities for every identified member peptide. This value is expressed in a log2 scale. Mitochondrial data were analyzed following the methods described in [55]. Relative abundance of cytosolic proteins were calculated from experiments carried out in duplicate following the protocol described in [188]. In brief, the differences between the relative abundances (TIC) for replicates from the same strain (R0, R1) and between strains (Z0 and Z1) were calculated. These populations of difference values were normalized to generate an average of 0, and the normalized populations were used to determine Wstat as a measure of the signal to noise ratio (S/N). A S/N value of 2.8 was chosen as the cut-off for significance, and represents $p<0.05$. The average TIC of the proteins within this group had a difference of at least two-fold ($-1 > \log2 > 1$) between wild-type and mutant samples, and were used for the current analysis [189].

### 4.2.3 Stress analysis:

To determine the sensitivity of the cells to tunicamycin (increased unfolded proteins accumulation in the cells), growth rates of the cells were measured by using race tubes. Cells were grown in race tubes in Vogel's media (VM) in the presence of 2 μg/ml tunicamycin [190].

Intracellular reactive oxygen species were measured following the protocol described in [191] with slight modifications. Cells were grown to exponential phase in 25 ml of VM at 30°C. Next, cells were incubated in 15 mM of 2',7'-dichlorofluorescein (DCF) in VM for 1 hour at 30°C. Cells were washed with 100 ml of water and then ground in the presence of liquid nitrogen. 15-25 mg of cell extracts were resuspended in 1 ml of phosphate buffer (10 mM $Na_2HPO_4$, 1.8 mM $KH_2PO_4$, 137 mM NaCl, 2.7 mM KCl, pH 7.4). The solution was diluted five-folds in the same buffer and fluorescence was measured at an excitation wavelength of 490 and an emission wavelength of 524 in a plate reader (SpectraMax Plus 384 Microplate Reader, Molecular Devices, USA) and normalized to the mass of proteins.

Catalase activity was determined by following the process described in [192] with slight modification. Hyphae of *N. crassa* were broken in a mortar and pestle as for the mitochondrial preparation. Cellular debris and sand were removed by centrifugation at 4000 rpm at 4°C for 5 minutes in an SS34 rotor (Sorvall RC 6 plus). Supernatant was collected and purified twice by spinning at 12000 and 13000 rpm for 12 minutes and 20 minutes at 4°C in a Sorvall RC 6 plus centrifuge (rotor SS34) and a table top micro-centrifuge respectively. Catalase activity was measured in a Gilson oxygraph equipped with Clark electrode. One unit of catalase is defined as the amount that decomposes 1 μmole of $H_2O_2$ in 1 minutes in a 60 mM $H_2O_2$ solution at pH 7.0 [193].

### 4.2.4 Acyl chain analysis:

Acyl chain analysis of whole mitochondrial lipid analysis was performed following the protocol described in [194] with slight modifications. Fatty acids were extracted from mitochondria (3 mg of protein) in 2 ml of 15% (v/v) concentrated methanolic sulphuric acid and 2 ml of chloroform. An internal standard of C17:1 was used (Nu-Chek Prep Inc., USA) in the chloroform for quantification. Samples were boiled at 90°C for 3 hours and 1 ml of deionized water was added to separate the 1 ml of organic phase. The data were presented are the percent lipid that was calculated from the total peak area (GC/MS) and peak area was correlated to that of the internal standard.

### 4.2.5 Sterol analysis:

Sterol analysis was performed following the protocol described in [195] with slight modification. Mitochondria (3 mg of protein) were heated in 3 ml of 10% methanolic KOH at 80°C for 90 minutes. After cooling, 5α-cholestanol (250 ng) was added as an internal standard followed by 1 ml of water. Then, 3 ml of hexane was added and mixed with the solution. 1 ml of the organic layer was collected and was used for analysis by gas chromatography [196].

## 4.3 Results and discussion:

Proteomic analyses of mitochondria and cytosol will be useful to understand the global responses associated with the absence of VDAC in cells (Table 4.1). Two strains were analyzed: ΔPor-1 [56] and its progenitor strain, FGSC 9718 (WT). In 1D LC-MS/MS analysis of cytosolic extracts, 1031 proteins were detected and 170 were differentially expressed in ΔPor-1 (Appendix 7.3 file 1). In 2D LC-MS/MS analysis of mitochondria, 867 proteins were detected and 60 proteins were differentially expressed in the two strains (Appendix 7.3 file 2). This increases the depth of the data available from ΔPor-1 mitochondria (Table 4.1) and provides new information about proteins in the cytosol. The data from cytosolic 1D LC-MS/MS and mitochondrial 2D-LC MS/MS analyses were combined and discussed.

Table 4.1: Summary of ΔPor-1 proteomic studies:

| Methods (Type of samples) | Number of proteins detected | Numbers of proteins more abundant in ΔPor-1[2] | Number of proteins less abundant in ΔPor-1[2] |
|---|---|---|---|
| 1D LC-MS/MS (Mitochondria)[1] | 500 | 10 | 13 |
| 2D LC-MS/MS (Mitochondria) | 867 | 23 | 37 |
| 1D LC-MS/MS (Cytosolic proteins) | 1035 | 108 | 139 |

[1]Data were collected from [55].

[2] $p < 0.05$

### 4.3.1 Less abundant proteins in ΔPor-1:

In the current study a total of 133 proteins were found to be less abundant in ΔPor-1 cells than in WT cells (Table 4.1). To determine the cellular functions associated with them, the proteins were sorted using the functional categorization (FunCat) system [197]. The majority of the less-abundant proteins reside in four FunCat main categories- protein synthesis (FunCat 12), proteins with binding function or cofactor requirement (FunCat 16), Energy (FunCat 02), and Metabolism (FunCat 01) (Figure 4.1 and Appendix 7.3 Table 1).

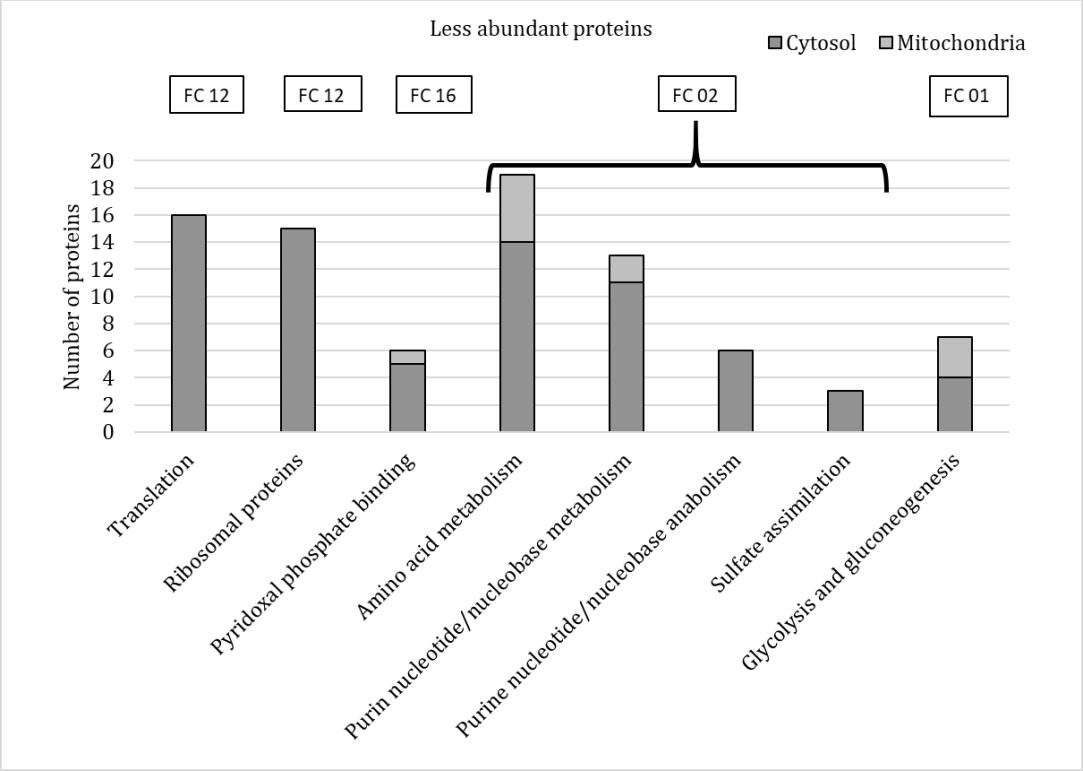


Figure 4.1**:** Less abundant proteins in ΔPor-1.

The proteins used in this analysis were at lower levels in the mutant than in WT cells (Appendix 7.3 Table 1). FungiFun2 (**https://elbe.hki-jena.de/fungifun/fungifun.php**) was used to predict the categories of the proteins highly represented among these less abundant proteins, by using the FunCat classification database [198]. Boxes above the bars indicate the main FunCat categories, protein synthesis (FunCat 12), protein with binding function (FunCat 16), energy (FunCat 02), and metabolism (FunCat 01). The dark grey section of each bar indicates the cytosolic proteins and the light grey section of the bar indicates the mitochondrial proteins.

The low levels of proteins involved in translation (category 12) likely are related to the growth rate of ΔPor-1 cells, which is slow compared to WT [56]. Protein synthesis depends on the external conditions and intracellular demands of cells [199]. It may be that the mitochondrial deficiencies in ΔPor-1 [55,56] lead to low cellular energy levels, thereby reducing the demand for protein synthesis. In support of this hypothesis, reductions in the levels of some ribosomal proteins and translational initiation factors (12.04), as well as those involved in amino acid (01.01) and purine nucleotide (01.03.01) metabolism are observed. Reduced need for purine nucleotides may reflect a combination of reduced needs for GTP due to reduced translation [200], and reduced requirements for adenine nucleotides for transcription and for ATP synthesis in mitochondria. Proteins linked to in the metabolism of alanine (NCU03973), lysine (NCU03010) and the sulfur-containing amino acids methionine (NCU06512) and cysteine (NCU05238) are present in reduced amounts. Enrichment of underrepresented proteins related to sulphur metabolism (categories in 01.02.03) may reflect a lower demand for sulphur-containing amino acids. In addition, two of the reactions involved in the uptake of inorganic sulphate require ATP [201] (Figure 4.2), and ATP is expected to be lower due to the ETC defects in ΔPor-1.

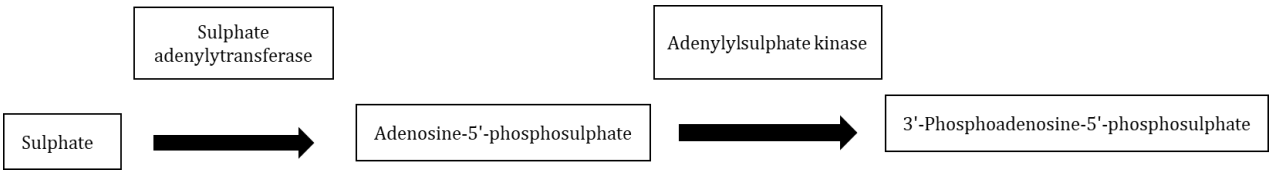


Figure 4.2: Initial steps of sulphur assimilation.

Sulphate adenylytransferease and adenylysulphate kinase are less abundant in ΔPor-1 and utilize ATP as less abundant proteins in sulphur assimilation. Figure was drawn following [195].

As seen in previous experiments, proteins related to pyridoxal phosphate binding (16.21.17) are reduced in ΔPor-1; the current analysis of the cytosolic proteome suggests that this observation is related to a reduced requirement for amino acid biosynthesis, because pyridoxal phosphate is involved in many reactions in amino acid metabolism [202].

In terms of metabolism (FunCat 02), in ΔPor-1 cells, a group of proteins involved in glycolysis and gluconeogenesis (02.01) is downregulated. In glycolysis, pyruvate is produced, which is then utilized by mitochondria to produce ATP. One of the possibilities is that transportation of pyruvate into mitochondria, which normally occurs through VDAC [30] is disrupted in ΔPor-1 mitochondria, resulting in the accumulation of pyruvate in the cytoplasm. This may play a negative role for the expression of proteins involved in glycolysis, which are also involved in the reverse reactions in gluconeogenesis.

### 4.3.2 More abundant proteins in ΔPor-1:

In the current analysis a total of 131 proteins were found to be more abundant in ΔPor-1 cells than in WT cells (Table 4.2). To determine the cellular functions associated with them, the proteins were sorted using the functional categorization (FunCat) system. Most of the most abundant proteins reside in four FunCat main categories- energy (FunCat 02), metabolism (FunCat 01), cellular transport, transport facilitation and transport route (FunCat 20), and cell rescue, defence and virulence (FunCat 32) (Figure 4.2 and Appendix 7.3 Table 2).

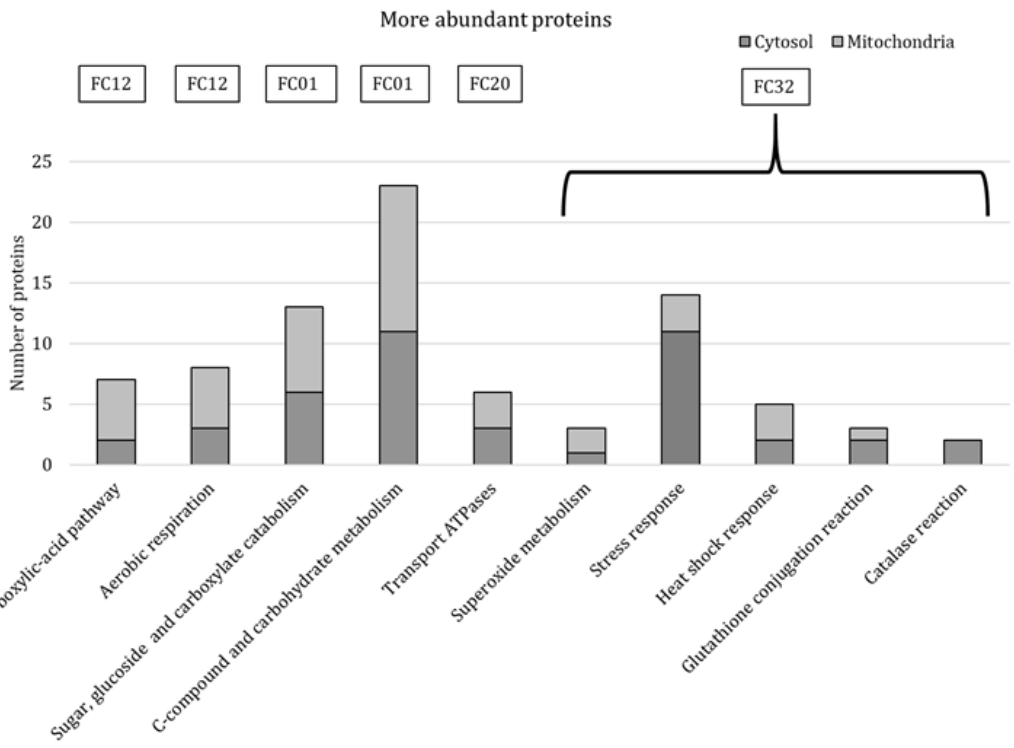


Figure 4.3**:** More abundant proteins in ΔPor-1.

FungiFun2 was used to predict protein categories by FunCat classification database. Boxes above the bars indicate the main FunCat categories. Energy (FunCat 02), Metabolism (FunCat 01), cellular transport, transport facilitation and transport routes (FunCat 20) and cell rescue, defense and virulence (FunCat 32). Dark grey sections of the bars indicate the cytosolic proteins and light grey sections indicates the proteins that are reside in mitochondria.

In the absence of VDAC, some of the more abundant proteins that are involved in metabolism (FunCat 01) are also part of tricarboxylic acid (TCA) pathway (FunCat 02.10), Appendix 7.3 Tables 1 and 2), so both energy and metabolism categories will be discussed together. Proteins involved in the TCA pathway and aerobic respiration are two main subgroups in the "energy" category, and there are two links with VDAC. First, VDAC has been proposed to help the movement of metabolites like succinate and pyruvate across the MOM [1] and hence, the absence of VDAC might cause deficiencies of those metabolites in mitochondria. To compensate for those deficiencies, cells may increase the TCA cycle proteins such as succinate-CoA ligase (NCU01227), citrate synthase (NCU01692), pyruvate dehydrogenase E1 component (NCU06482) and pyruvate dehydrogenase E2 component (NCU07659). Therefore, more pyruvate and succinate can be produced from the TCA cycle. Moreover, the absence of VDAC causes abnormally low levels of mitochondrial ETC complex I and of heme groups associated with complexes III and IV [55,56]. These defects are expected to reduce respiration rates in mitochondria. A relatively low oxygen consumption was recorded in ΔPor-1 mitochondria compared to WT (Chapter 3). Therefore, it may be possible that to compensate for the low respiration and the abnormal ETC complexes, the expression levels of some of the proteins (F-type $H^+$-transporting ATPase subunit alpha (NCU02514), F-type $H^+$-transporting ATPase subunit beta (NCU05430), protoheme IX farnesyltransferase (NCU06141)) involved in aerobic respiration (FunCat 02.13.03) were increased in ΔPor-1 mitochondria (Figure 4.3). One of them is cytochrome c (NCU01808), which was previously shown to be more abundant by biochemical analysis [56].

Metabolism (FunCat 02) is another Funcat category of interest, and the two enriched groups within this category are "C-compound and carbohydrate metabolism" (FunCat 01.05), and "sugar, glucoside, polyol and carboxylate catabolism" (FunCat 01.05.02.07). In the absence of

VDAC, cells may be deprived of optimum energy that is required for normal cellular activity, as the ΔPor-1 strain has a slow growth rate and abnormal mitochondria [56]. Therefore, cells may express proteins that help them to provide more energy by metabolizing sugar and carbohydrate.

A sub-set of proteins related to cellular transport, transport facilitation and transport routes (FunCat 20) was more abundant in ΔPor-1. In particular, transport ATPase (FunCat 20.03.22) is a part of this group [203]. Several subunits of vacuolar ATPases (vacuolar membrane ATPase-1 (NCU01207), vacuolar membrane ATPase-2 (NCU08515)) are increased in ΔPor-1. These proteins generate an electrochemical gradient to transport molecules across the vacuolar membranes and also create an acidic functional environment for the hydrolytic enzymes in the vacuoles [204]. It may be that degradation in vacuoles and recycling of the cellular materials [205], are may be important for the increased survival of ΔPor-1 cells. The remaining types of proteins are members of the ABC and multidrug transporter families of proteins. Their substrates are unknown, but presumably they are overexpressed to compensate for lower levels of their substrates reaching the intermembrane space due to the lack of VDAC.

The last main FunCat category includes proteins involved in cell rescue, defense and virulence (FunCat 32). This category can be sub-divided into stress response and heat shock response (FunCat 32.01.05), catalases (FunCat 32.07.07.01), proteins involved in superoxide metabolism (FunCat 32.07.07.07), and in the glutathione conjugate reaction (FunCat 32.07.07.03). There are several links between VDAC and ROS. Increased intracellular ROS has been observed in different VDAC variants yeast and animal cell lines [1,117,118]. Moreover, various groups have proposed a role for VDAC in the release of superoxide from mitochondria [173–175]. In addition to that, mitochondrial ROS production capacity also increases in ΔPor-1 mitochondria (Chapter

3). Although enhanced cytosolic catalase activity was detected in ΔPor-1 compared to WT cells (Figure 4.4), suggesting that anti-oxidant mechanisms try to limit ROS-induced stress.

Some heat shock proteins work as a quality control pathway for mitochondrial proteins [206]. Previously, it was shown that in *N. crassa* in the absence of VDAC, proteins involved in the misfolded protein response were more abundant [55]. Similarly, an increased expression of heat shock proteins was detected in the current study (Figure 4.3). The absence of VDAC may introduce misfolding of both cytoplasmic and mitochondrial proteins in the cells, because the level of ATP expected to be low, reducing the activity of ATP-dependent chaperones.

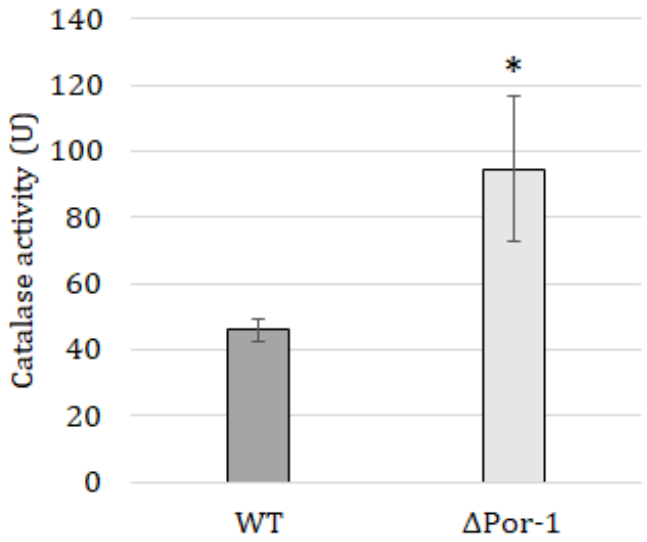


Figure 4.4: Catalase activity in cytoplasmic extracts.

Catalase activity was measured in the presence of $H_2O_2$ and cytosolic extract in a Clark type oxygen electrode. Catalase degrades the $H_2O_2$ and releases oxygen, which was converted to electrode current and recorded by a micrograph recorder [207]. One unit of catalase is defined as the amount that decomposes 1 µmole of $H_2O_2$ in 1 minute in a 60 mM $H_2O_2$ solution at pH 7.0 per mg of protein. * indicates significance at a p value of <0.05 based on a Student's t test (n= 3-4). Error bars indicate standard deviation. The graph shows the catalase activity (U) per mg of protein for each strain.

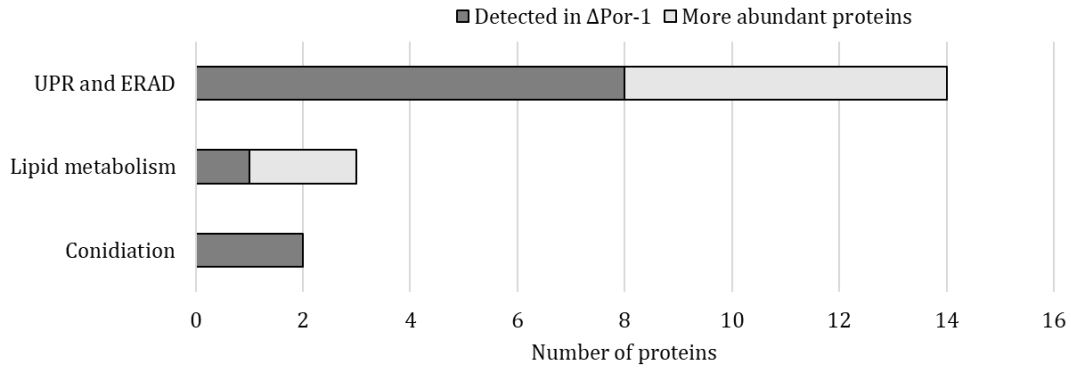


Figure 4.5: Summary of a subset of proteins expressed or upregulated in ΔPor-1.

Proteins involved in the ER-unfolded protein response (UPR) and the endoplasmic-reticulum associated degradation (ERAD), lipid metabolism and conidiation were identified by manual analysis of the dataset (Appendix 7.3 Table 3). Dark grey indicate proteins that were detected only in ΔPor-1 and grey bars indicate proteins that were more abundant in ΔPor-1.

There were few proteins that were detected only in ΔPor-1 (Appendix 7.3 table 3). Further analysis of those proteins and the proteins expressed at higher levels in the ΔPor-1 strain, revealed a group of proteins involved in the unfolded protein response (UPR) and endoplasmic reticulum-associated degradation (ERAD) pathways that were associated more with ΔPor-1 compared to WT (Figure 4.5). We hypothesized that in ΔPor-1, because misfolding of the proteins in ER is increased the expression of the proteins involved in that pathway is increased. To investigate this possibility, the sensitivity of ΔPor-1 to tunicamycin was examined. This drug blocks the glycosylation of proteins in the ER, thereby inducing their misfolding [190]. Assuming that ΔPor-1 has an increased level of misfolded proteins in drug-free conditions, it is predicted that this strain will be very sensitive to additional drug-induced misfolding of proteins in the ER. To test this hypothesis WT and ΔPor-1 cells were treated with tunicamycin. Slow growth was observed for WT (Table 4.2) in the presence of tunicamycin, indicating that the cell could function with the level of misfolded proteins induced by the drug. In contrast, no growth was observed in ΔPor-1 strain in the presence of tunicamycin. This observation suggests that the ΔPor-1 cells may not be able to cope with the extra misfolded proteins resulting from tunicamycin treatment, and that these levels exceed the capacity of UPR and ERAD, even when those pathways are upregulated.

Table 4.2: Growth rate of WT and ΔPor-1 in the presence and absence of (2 μg/ml) tunicamycin.

| | Growth rate at 30°C (cm/day)[1] | |
|---|---|---|
| | WT | ΔPor-1 |
| Presence of tunicamycin | 2.7 ± 0.8 | No growth |
| Absence of tunicamycin[2] | 11.7 ± 0.1 | 4.1 ± 0.7 |

[1]Growth rate was measured as linear growth on solid medium in a "race tube". Number of replicates is 3.

[2]Part of data were collected from [56]

Another interesting group of proteins are involved in lipid metabolism. VDAC is the most abundant MOM protein, and the deletion of VDAC is associated with cold sensitivity and altered mitochondrial morphology [56]. Moreover, in artificial membranes, VDAC can interact with different phospholipids, which can modulate pore activity [208]. Furthermore, an indirect effect of VDAC on mitochondrial phospholipids through associated increases in ROS was proposed [209] and knockout or knockdown of VDAC in different cell lines and model organisms causes increased mitochondrial ROS [41,117,168]. In support of above mentioned observations, proteomic analysis of VDAC knockout *N. crassa* cells detected changes in some of the proteins involved in lipid metabolism pathways (Figure 4.5). As an initial step in the analysis of mitochondrial membrane composition, acyl chains of whole mitochondrial phospholipids and relative ergosterol levels were measured. In the first analysis (Figure 4.6A), the predominant acyl chain content was very similar in the two strains. However, in the WT strain, the level of C18:1 (oleic acid) was higher relative to C18:3n3 than it was in ΔPor-1. Next, the relative ergosterol levels were measured between the strains. In ΔPor-1, the amount of ergosterol was lower compared to WT (Figure 4.6B). Thus, the absence of VDAC is associated with changes in the composition of mitochondrial membranes.

A.

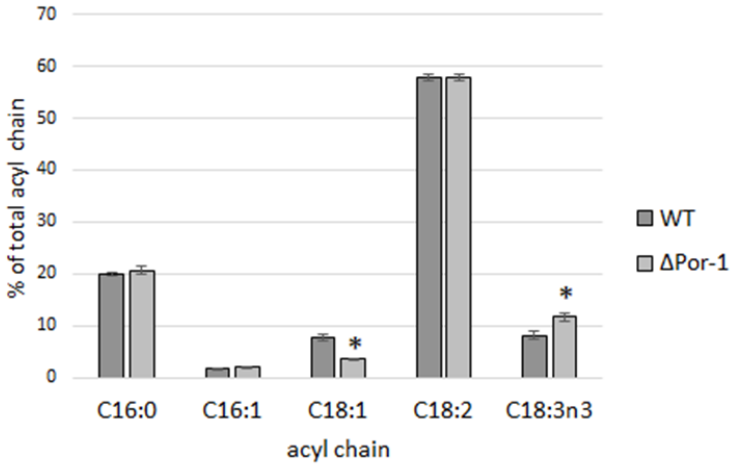


Figure 4.6 A**:** Acyl chain content of mitochondrial membrane fatty acids.

Most abundant acyl chain are shown in the graph. * indicates significance at a *P* value of <0.05 based on a Student's *t* test. (n=3-4). Error bars indicate standard deviation of the samples.

B.

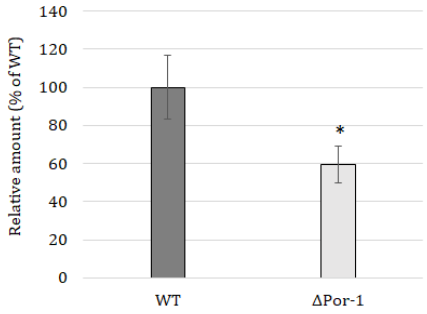


Figure 4.6 B**:** Relative ergosterol amount in the mitochondrial membrane of WT and ΔPor-1.

The amount of ergosterol in ΔPor-1 is express as a percent of WT, where the WT amount and the standard deviation of the replicates were set to 100%. * indicates significance at a *P* value of <0.05 based on a Student's *t* test. (n=2 (WT) and3 (ΔPor-1)). Error bars indicate standard deviation of the samples.

Several proteins showing differential expression are linked to the morphology of the strains. Two proteins were detected that are involved in conidiation, and are expressed more in ΔPor-1 compared to WT (Figure 4.5). However, ΔPor-1 generates less aerial hyphae compared to WT (Figure 4.7 A). Morphological analysis of the hyphae grown at 30°C did demonstrate a noticeable difference between two strains (Figure 4.7 B). Hyphae of the ΔPor-1 strain were highly branched compared to WT.


Figure 4.6 A: Lower number of aerial hyphae is observed in ΔPor-1 than WT.

*N. crassa* was grown in the dark to induce conidia formation at 30°C for 3 days and 7 days for WT and ΔPor-1 respectively in conidia flasks. For conidiation cells were kept in the light for 3 days.

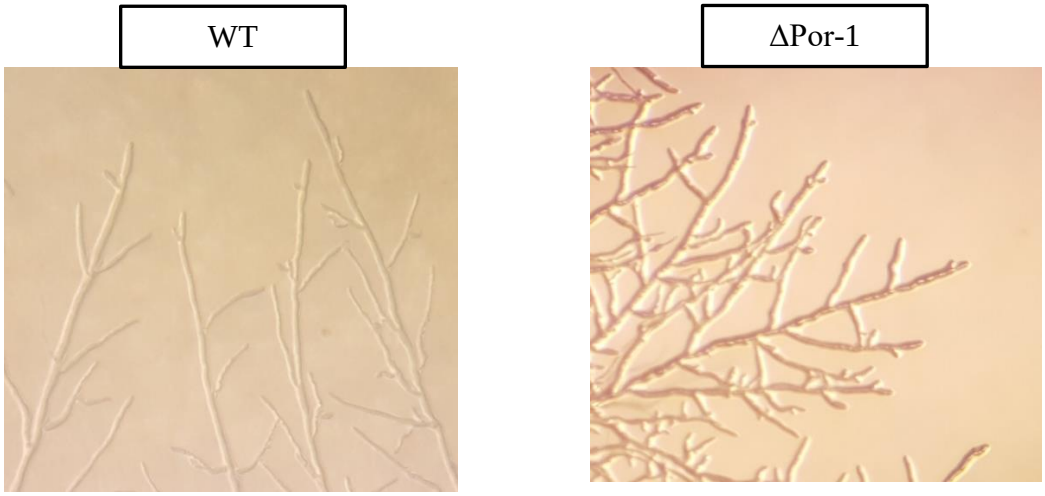


Figure 4.7 B: Hyphal morphology of WT and ΔPor-1.

Cells were grown on a VM plate for 12 hours and 24 hours at 30°C for WT and ΔPor-1, respectively. Plates were observed directly with a stereomicroscope and the resulting images are presented at 60X magnification.

## 4.4 Conclusions:

Using proteomic studies as a tool, here we try to elucidate the effect of the absence of VDAC on the cellular and mitochondrial functions. In this study, we have determined that proteins involved in proteins synthesis, amino acid metabolism, nucleotide and sulphur metabolism are less abundant in ΔPor-1 strains. This finding might relate to the slow growth rate of the ΔPor-1 cells, which leads to a lower demand for the proteins, amino acids and nucleotide involved in translation.

VDAC is the most abundant MOM protein. The primary energy transformation function of mitochondria hugely depends of the proper transport of the metabolites across the MOM into the mitochondria. Therefore, the absence of VDAC from mitochondrial membrane might disrupt this transport. Moreover, the absence of VDAC causes dysfunction ETC complexes (chapter 3) [55,56]. In the absence of VDAC proteins involved in TCA pathway, aerobic respiration and carbohydrate metabolism are more abundant. It may be possible that these proteins were more abundant to compensate the disruption of the flow of the metabolites and the dysfunctional mitochondrial ETC complexes.

It has been previously proposed that the absence of VDAC associated with elevated redox environment [30,210]. In our study, we have also detected proteins involved in anti-oxidant mechanisms and cellular stress are more abundant. Similar results also were observed in [211], where the authors induced oxidative stress in *N. crassa* by using menadione. The authors detected more abundant expression of a sub-set of anti-oxidant enzymes such as (NCU00355, catalase-3), (NCU0785, superoxide dismutase), and (NCU05780, glutathione S-transferase-1). Those proteins are also more abundant in our studies (Appendix 7.3 Table-2). This finding suggestes that in *N. crassa* the absence of VDAC induced oxidative stress.

The analysis of cytosolic proteome has revealed proteins involved in UPR and ERAD pathways are expressed more in ΔPor-1. Although, we could not establish a direct role of VDAC in the UPR and ERAD pathway, this is the first time that an association of VDAC with UPR and ERAD has been shown. It might be possible that increased redox environment in the cells in the absence of VDAC induced UPR [212].

In this study, a few proteins in lipid metabolism have changed. The absence of VDAC from MOM is association with decreased ratio of C18:1 unsaturated fatty acids to in abundance C18:3n3 unsaturated fatty acids ΔPor-1. Moreover, in ΔPor-1 the amount of ergosterol was lower than in WT. Mitochondrial membrane properties are important for normal cellular functions [213] and those changes might influence mitochondrial membrane properties like fluidity of the membrane. Therefore, VDAC might play important roles by maintaining normal membrane properties. In the future, it will be interesting to understand the pathways that are responsible for the differential membrane composition.

**4.5 Acknowledgements:**

This work was supported by a Discovery Grant from the Natural Sciences and Engineering Research Council of Canada (NSERC) to D.A.C; S.R.S. acknowledges support from the Faculty of Graduate Studies at the University of Manitoba; A.M. was supported by an NSERC PGS-M award and a Faculty of Science award from the University of Manitoba. We would like to thank Mr. Fraser Ferens, Department of Microbiology for his valuable comments. We would also like to thank Mr. Jacek Switala, Department of Microbiology, for his help with the catalase activity measurements, Mr. Dennis Labossiere, Department of Food and Human Nutritional Sciences for his help with lipid and sterol analysis and Mr. Peyman Ezzati, Manitoba Centre for Proteomics

and Systems Biology for help with proteomic analysis. We also express our gratitude to Dr. Ayush Kumar, Department of Microbiology, Dr. Georg Hausner, Department of Microbiology and Dr. Jason Treberg, Department of Biological Sciences for assistance with the stereomicroscope, plate reader and fluorimeter respectively.

# Chapter 5: The absence of Por1p in *Saccharomyces cerevisiae* is associated with a differential cytosolic protein expression profile and downregulation of the target of rapamycin pathway.

**Sabbir R. Shuvo[1] & Deborah A. Court[1*]**

**[1]Department of Microbiology, University of Manitoba, Winnipeg, Manitoba, Canada**

*corresponding author
Deborah.Court@umanitoba.ca

Department of Microbiology

University of Manitoba

Winnipeg, MB Canada R3T 2N2

Phone (204) 474 8263

Fax (204) 474-7603

One of my goals in this thesis was to understand the global roles of VDAC. Thus, another model organism *S. cerevisiae* was selected for the proteomic study. *N. crassa* and *S. cerevisiae* are two distinct organisms. Therefore, understanding the stress responses of *S. cerevisiae* in the absence of Por1p would help to elucidate global roles of VDAC.

**Abstract:**

Pore forming, functionally conserved mitochondrial porin, a voltage depended anion-selective channel (VDAC) works as a channel in the mitochondrial outer membrane (MOM) to transport metabolites across the MOM. In *Saccharomyces cerevisiae* Por1p is not essential but deletion of Por1p is associated with an impaired growth rate of the cells in non-fermentative media. Proteomic analysis of *por1Δ* cells revealed increased expression levels of some of the proteins involved in the process of actin complex formation, in anti-apoptotic events and in the assembly of protein complexes. In contrast, the absence of Por1p is associated with a lower abundance of proteins is involved in mitochondrial biogenesis, assembly of electron transport chain complexes, mitochondrial transport, and protein synthesis processes. In addition, loss of Por1p is associated with the downregulation of unfolded protein response and the target of rapamycin pathways. Therefore, the absence of Por1p influences multiple cellular pathways.

## 5.1 Introduction:

Mitochondrial porin, a voltage dependent anion-selective channel (VDAC), is a functionally conserved protein of the mitochondrial outer membrane (MOM) β-barrel family of proteins [11,15]. VDAC has 19 β-strands and a flexible N-terminal α-helix [22,24,26]. This pore forming protein works as a tunnel for the transport of small metabolites, such as pyruvate, malate, succinate, ATP/ADP and $Ca^{2+}$ across the MOM [1,39]. The N-terminus of VDAC is proposed to be associated with the movement of the metabolites by opening and partially closing the pore [2]. In artificial membrane experiments, the gating of recombinant VDAC depends on the electrical field across the membrane. In the open state, VDAC is slightly anion selective, and the semi-closed state of VDAC is cation selective [182].

In addition, VDAC interacts with other cellular proteins for maintaining normal cellular functions [1,28,30,33]. VDAC also interacts with various apoptosis related proteins to generate the mitochondrial permeability transition pore (MPTP) for releasing cytochrome c from the inter-membrane space (IMS) to induce apoptosis [52,175,214]. In various cell lines, the blocking of VDAC, with different compounds (such as itraconazole and aspirin (2-Acetoxybenzoic acid)) disrupts calcium and nucleotide homeostasis [41,168,180,215]. Moreover, knockout or variations in VDAC in different systems cause slow growth rates of the mutant cells, distort mitochondrial shape, reduce mitochondrial membrane potential, generate reactive oxygen species (ROS) and disrupt the mitochondrial electron transport chain (ETC) complexes [54,55,116,171, Chapter 3].

In the absence of VDAC, protein expression profiles of mitochondrial [56] and cytosolic proteins were changed in *N. crassa* (Chapter 4). Besides, in *N. crassa*, deletion of VDAC residues from 238-242 changed the expression level of subunits of NADH:ubiquinone oxidoreductase,

proteins involved in electron flow and mitochondrial biogenesis [55]. Another model organism *S. cerevisiae,* is used extensively for VDAC studies [117,118,216]. *S. cerevisiae* mitochondria have two VDAC isoforms Por1p and Por2p [117]. The channel forming properties of *S. cerevisiae* Por1p are highly conserved in other species [117]. A protein encoded by *POR2*, has 49% amino acid sequence identity with yeast Por1p. Overexpressed Por2p can functionally complement defects present in *por1Δ* strains [217]. However, *por2Δ* cells have no detectable phenotype. Moreover, no channel activity for Por2p was detected in artificial membrane experiments; Therefore, this suggests that Por2p may not function as a pore [217]. However, this does not role out the possibility that it makes a partially functional pore in mitochondria. Therefore, POR2 must be overexpressed to complement the *por1Δ* cells.

The aim of this study is to understand the cellular stress responses in the absence of Por1p and to create links between observed phenotypes of the cells with protein expression data. In this study, analysis of the cytosolic proteome of cells that are lacking Por1p was performed, to understand the influence of absence of VDAC on mitochondrial functions, pathways involved in mitochondrial metabolism and stress responses. A protein expression profile of *por1Δ* was elucidated previously [218]. The study was a part of large yeast knockout database project; hence, the authors of that study did analyze the data *por1Δ* data specially. Therefore, we combined our data with Y3K dataset and analyzed them together to get an over-all picture of the global roles of VDAC in the cells.

## 5.2 Materials and Methods:

### 5.2.1 Chemicals:

Chemicals and reagents were purchased from Thermo Fisher Scientific (Mississauga, ON, Canada), Sigma-Aldrich Canada (Oakville, ON, Canada), BioShop Canada (Burlington, ON, Canada), and VWR International (Mississauga, ON, Canada).

### 5.2.2 Strains and growth conditions:

*S. cerevisiae* strain BY 4741 (*his3Δ1 leu2Δ0 met15Δ0 ura3Δ0*, *mat a*) and the porin knockout cells were used in this study [126,219]. Deletion of *POR1* was confirmed by using *POR1* primers (Table 5.1) (data not shown). Cells were grown at 30°C in YPG (1% yeast extract, 2 % peptone and 3 % glycerol) and SC (synthetic complete) media supplemented with the required amino acids. *S. cerevisiae* transformations was performed using a lithium acetate method [220].

### 5.2.3 Quantification of mitochondrial DNA:

Mitochondrial DNA levels were determined semi-quantitatively following the protocol described in [221] by using actin and cytochrome c oxidase subunit 2 primers (Table 5.1). Briefly, cells were grown in YPG media in the exponential phase and subjected to genomic DNA isolation. Genomic DNA were isolated by using glass beads and DNA was serially diluted by half and PCR was performed. Analysis of the gel was performed with a Axygen Gel Documentation System BL, GDBL-1000.

### 5.2.4 Stress responses:

*S. cerevisiae* cells were grown in the presence of different chemicals (0.05 mM potassium tellurite, 3 mM nickel sulphate, 0.2% acetic acid, 1 mM hydrogen peroxide, 3.8% ethanol, 0.25 µg/ml tunicamycin, 25 mM aspirin or 0.6 µg/ml itraconazole, 3 µM rapamycin) in the exponential phase in YPG media at 30$^{o}$C. To study the temperature stress response cells were grown at 23$^{o}$C, 30$^{o}$C and 37$^{o}$C in YPG media in a plate reader (SpectraMax Plus 384 Microplate Reader, Molecular Devices, USA).

### 5.2.5 Isolation of cytosolic proteins:

Cytosolic proteins were isolated from *S. cerevisiae* WT and *por1Δ* cells grown in the exponential phase in YPG media following the protocol described in [222]. In brief, cells were isolated by centrifugation at 3000 rpm (sorvall RC 6 plus, SS34 rotor) for 5 minutes at room temperature and incubated in DTT buffer (100 mM Tris- $H_2SO_4$, pH 9.4 and 10 mM dithiothreitol) at the ratio of 2 ml/g wet weight cells for 20 minutes at 30$^{o}$C. Cells were washed with enzyme buffer (1.2 M sorbitol, 20 mM potassium phosphate, pH 7.4) at 7 ml/g wet weight cells and resuspended again with the enzyme buffer in the presence of 500 U/g wet weight cells of lyticase. Cells were slowly shaken at 30$^{\circ}$C for 45 minutes. Cells were harvested by centrifugation (SORVALL RC 6 PLUS, SS34 rotor) at 3000 rpm and resuspended in 6 ml of homogenization buffer (0.6 M sorbitol, 10 mM Tris-Cl, pH 7.4, 1 mM ethylenediaminetetraacetic acid (EDTA), 1 mM phenymethylsulfonyl fluoride (PMSF)) per/g wet weight cells. Yeast spheroplasts were generated by 20 strokes of glass-Teflon homogenizer and then centrifuged at 1500 rpm (sorvall RC 6 plus, SS34 rotor) for 5 minutes to remove cell debris and nuclei. Supernatants were collected and cellular organelles were removed by spinning again at 43000 rpm (Beckman Coulter,

Optima$^{TM}$ Max-E Ultracentrifuge, USA, TLA100.3 rotor) at 4$^{o}$C for 45 minutes [185]. Standardized per mg of proteins.

### 5.2.6 Proteomic analysis:

Samples were prepared following the protocol described in [186]. Proteomic analysis was performed following the protocol described in [187] using 1 dimensional liquid chromatography (LC) follow by tandem mass spectroscopy (MS/MS) (1D LC-MS/MS). Data were analyzed following the protocol described in [188].

### 5.2.7 Catalase activity:

Catalase activity was measured by following the protocol described in [223] with slight modifications. Cells were harvested in exponential phase and lysate was prepared by using glass beads in 50 mM phosphate buffer supplemented with 1 mM 4-benzenesulfonyl fluoride hydrochloride (AEBFS) as a protease inhibitor. Cellular debris was removed by centrifugation at 13000 rpm for 15 minutes in a micro-centrifuge at 4$^{o}$C with the supernatant and later supernatant was collected. Catalase activity was measured in a Gilson oxygraph equipped with Clark electrode. One unit of catalase is defined as the amount that decomposes 1 µmole of $H_2O_2$ in 1 minute in a 60 mM $H_2O_2$ solution at pH 7.0 [193].

### 5.2.8 Intracellular oxidative stress:

Intracellular oxidative stress was measured by using the fluorescent dye 2' 7'-dichlorofluorescein (DCF) following the protocol described in [192] with slight modification. Briefly, 2 ml cells were washed twice with 1 ml of water. They were resuspended in 400 µl of water in the presence of 100 µl of glass beads, subsequently vortexed for 1 minute. Cells were

centrifuged at 13000 rpm at 4°C in a table top centrifuge and the supernatant was collected. Fluorescence was measured, after 6-fold dilution of the samples in a plate reader at the excitation wavelength of 490 nm and at the emission wavelength of 524 nm.

### 5.2.9 β-galactosidase reporter assay:

WT and *por1Δ* strains were transformed with the pJC004 reporter plasmid [105,107]. In brief, pJ004 contains 4X unfolded protein response elements (UPRE) fused with a disabled *CYC1* promoter upstream of *lacZ*. Cells were grown at 30°C in SC-URA media to an $OD_{600}$ of 0.2-0.5. Then, 2 µg/ml tunicamycin was added to induce ER stress and incubated for 1.5 hours. Enzyme activity was measured following the protocol described in [224] with slight modification. Two $OD_{600}$ of cells were washed with 1 ml of Z buffer (40 mM $NaH_2PO_4$, 60 mM $Na_2HPO_4$, 10 mM KCl, 1 mM $MgSO_4$, 50 mM β-mercaptoethanol) collected by centrifugal force and resuspended in 50 µl buffer Z. 20 µl of 0.1% SDS and 50 µl chloroform were added and the samples were vortexed for 30 seconds. 700 µL 2 mg/ml *o*-nitrophenyl-β-galactopyranoside (ONPG) was added to the reaction mixture and incubated at 30°C.The reaction was stopped by adding 1 M $Na_2CO_3$ and the reaction time was recorded. The reaction mixture was spun at 13000 rpm for 1 min in a table top centrifuge, the supernatant was collected and the absorbance was measured at 420 nm. The enzyme activity was expressed as Miller units ($1000*A_{420}/t_{min}*V_{ml}*A_{600}$).

Table 5.1: List of primers used in this study.

| Primer name | Forward primer (5'-3') | Reverse primer (5'-3') |
|---|---|---|
| ACT1 | CCTTCTGTTTTGGGTTTGGA | CGGTGATTTCCTTTTGCATT |
| Cytochrome c oxidase 2 | GCTGATGTTATTCATGATTTTGCT | TGGCATATTTGCATGACCTG |
| POR1 | TTAAATTCTCGAGGGGCGCTTGTC GCGTGCC | ATTTTAATTTGGATCCTTAGT GGTGGTGGTGGTGGTGCGCA GACTCGAAGGTGAAGCTGG |

Table 5.2: Exponential growth rate in of WT and *por1Δ* cells at different temperatures in YPG. Note that *por1*Δ cells are both heat and cold sensitive.

| Temperatures | WT ($OD_{600}$/hour) | *por1Δ* ($OD_{600}$/hour) |
|---|---|---|
| 23°C | 0.126 ± 0.03 | 0.054 ± 0.006 |
| 30°C | 0.160 ± 0.01 | 0.130 ± 0.003 |
| 37°C | 0.273 ± 0.04 | 0.050 ± 0.003 |

Number of replicate=3-4

## 5.3 Results and discussion:

Mitochondria are the primary energy transforming organelles in cells and VDAC is the most functionally conserved MOM protein. Hence, VDAC plays a major role in mitochondrial biology. Therefore, the growth rate of *S. cerevisiae por1Δ* mutant was measured in the non-fermentative medium (YPG) at different temperatures (Table 5.2). WT growth was highest at 37°C; a similar result was observed in [225]. The growth rate of *por1Δ* cells were low compared to WT at all of temperatures, but, the differences were more pronounced at 37°C. These results also support the findings in [226], the authors observed slow growth of *por1Δ* cells at 37°C in glycerol after the adaptation of the cells to respiratory growth. However, in another study no growth was observed at 37°C in glycerol; it may be possible that there was no adaptation to the non-fermentative medium for cells in this study [217]. Therefore, the absence of Por1p causes impaired cellular growth. A similar growth defect was observed in *N. crassa* [56].

In the absence of Por1p, cellular homeostasis may be disrupted as the growth rate of the cells was slow compared to WT. Therefore, to understand the influence of Por1p on the cellular pathways, analysis of the cytosolic proteome was performed by 1D LC-MS/MS. Moreover, data from the Y3K database [218] were combined (Appendix 7.4 Table 1, Appendix 7.4 Figure 1, Appendix 7.4 Table 2-3) with this study to get more detailed insight about the stresses associated with absence of Por1p.

### 5.3.1 Proteins that were more abundant in *por1Δ* cells:

The Fungifun2 (https://elbe.hki-jena.de/fungifun/fungifun.php) server was used to predict the functional (FunCat) protein categories of differentially expressed proteins [198] to determine which cellular processes were influenced in the absence of Por1p.

**Table 5.3: Proteins that were more abundant in *por1Δ* cells:**

| **FunCat main category** | **FunCat description** | **Number of proteins** |
|---|---|---|
| Biogenesis of cellular components | actin cytoskeleton | 12 |
| Cell fate | anti-apoptosis | 4 |
| Cellular transport, transport facilitation and transport routes | cytoskeleton-dependent transport | 5 |
| Energy | energy conversion and regeneration | 4 |
| | anaplerotic reactions | 2 |
| Interaction with the environment | cell motility | 5 |
| Metabolism | lipid, fatty acid and isoprenoid metabolism | 17 |
| | biosynthesis of vitamins, cofactors, and prosthetic groups | 12 |
| | amino acid metabolism | 12 |
| | fatty acid metabolism | 6 |
| | purine nucleotide/nucleoside/nucleobase anabolism | 5 |
| | metabolism of derivatives of dehydroquinic acid, shikimic acid and chorismic acid | 3 |
| | metabolism of the cysteine - aromatic group | 4 |
| | aromate anabolism | 3 |
| Protein synthesis | aminoacyl-tRNA-synthetases | 11 |

| | | |
|---|---|---|
| Protein with binding function or cofactor | ATP binding | 25 |
| | nucleotide/nucleoside/nucleobase binding | 18 |
| | structural protein binding | 9 |
| | biotin binding | 3 |

One of the FunCat categories is biogenesis of cellular components, and the actin cytoskeleton is only subgroup in this category (Table 5.3). One of the proteins in this subgroup is actin, which is involved in mitochondrial morphology, motility and distribution [36,227], and, interacts with ATP in the process of actin polymerization [228]. Moreover, it has been proposed that actin can modulate the gating of VDAC [46]. The *N. crassa* cells expressing VDAC variants have abnormal mitochondrial distribution [55,56], further suggesting that interactions between VDAC and actin may important for intracellular organization [9,23]. Hence, in the absence of VDAC, cells might try to increase the expression of actin to maintain normal mitochondrial morphology and distribution. Another interesting observation is that some of the protein subunits of ARP 2/3 complexes (*ARC15, ARC19, ARC35, ACR40*) were more abundant in *por1Δ* compared to WT. The ARP2/3 complex interacts with ATP for the polymerization of actin [35], and cellular functions like adherence and migration of the cells. The absence of Por1p may cause low levels of ATP (discussed below); hence, expression of ARP 2/3 proteins may be increased to augment the polymerization of actin. ARP2/3 complex is a master regulatory system; therefore, those proteins (*ARC15, ARC19, ARC35, ACR40*) are also included in other FunCat categories such as cellular transport, transport facilitation and transport routes and interaction with the environment, cell motility, proteins folding, and structural protein binding. Actin is also involved in the process of endocytosis [36]. Endocytosis is a process that collects extra-cellular materials and plasma-membrane associated proteins and helps them to enter the cytosol. These coated vesicles then fuse with other internal compartments for recycling or for degrading their contents [36]. It may be possible that in the Por1p-knockout cells, some of the essential compounds (amino acids, vitamins, co-factors) are low; therefore, cells try to increase their endocytosis mediated recycling process for the survival.

The cell fate is another FunCat category, and anti-apoptosis related proteins are in this group. Involvement of VDAC in pro-apoptosis has been proposed previously [1,229]; however, it is interesting to detect anti-apoptosis proteins as more abundant in the Por1p knockout strain. One of the possibilities is that the absence of Por1p causes oxidative stress [117,168]. ROS may induce apoptosis by damaging DNA and proteins [230,231]; therefore, increased levels of an anti-apoptotic proteins may be required for the survival of the cells. Tsa2p is an oxidative stress response protein that was more abundant in *Δpor1*. Similar to Tsa2p, Stm1p has been proposed to work as an anti-apoptotic protein [232,233], and more abundant in *por1Δ*. However, other proteins in the cell fate group (Tef2p and Gln4p) are involved in the translation process, so, their roles in anti-apoptosis are not clear.

Another subset of more abundant proteins in the FunCat category of "energy" are encoded by genes *PYC1*, *PYC2*, *TKL1*, *ADH6*; and these proteins are particularly related to glycolysis. In the absence of VDAC, ATP production may be compromised, as some of the protein subunits of ATP synthase are less abundant (discussed below). Moreover, VDAC has been proposed to work as a rate limiting step for ADP/ATP flow [39]; therefore, the absence of VDAC will limit entry of ADP and exit of ATP from the organelle. Hence, cells may try to increase the production of ATP through glycolysis; thus, these proteins in the energy category are more abundant.

"Metabolism" is the next FunCat category. Most of the enriched proteins in the *por1Δ* cells in this subgroup are participate in amino acid metabolism. Intriguingly, a group of enzymes involved in pathways of amino acids synthesis from chorismate are more abundant (Figure 5.1). In contrast, proteins involved in biosynthesis of other amino acids were less abundant (Table 5.4). The reason(s) behind this observation is not clear, but suggest that the regulation is not at the level

of general control [234]. It might be possible that, *por1Δ* cells are trying to scavenge amino acids from media.

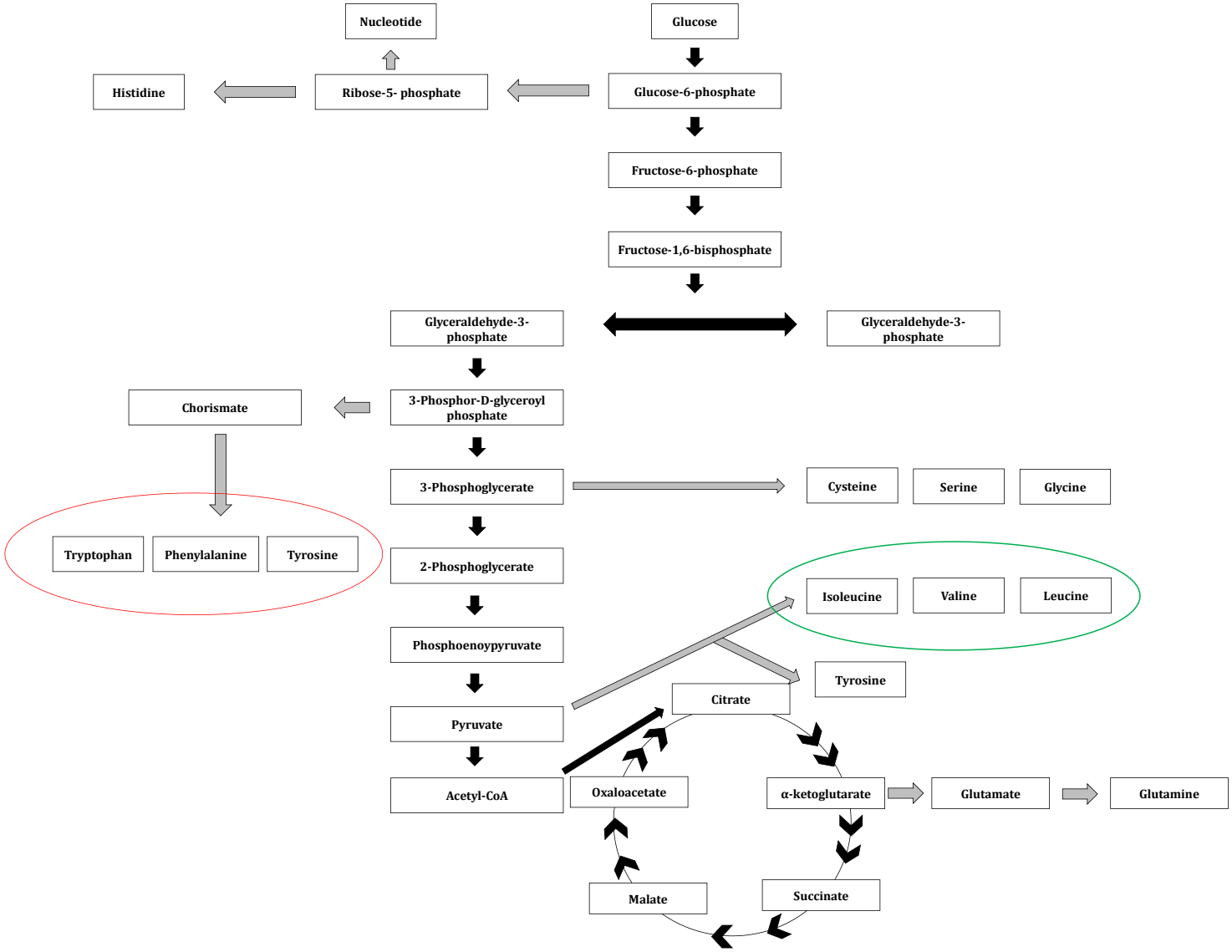
Nucleotide
Glucose
Histidine
Ribose-5- phosphate
Glucose-6-phosphate
Fructose-6-phosphate
Fructose-1,6-bisphosphate
Glyceraldehyde-3-phosphate
Glyceraldehyde-3-phosphate
Chorismate
3-Phosphor-D-glyceroyl phosphate
3-Phosphoglycerate
Cysteine
Serine
Glycine
Tryptophan
Phenylalanine
Tyrosine
2-Phosphoglycerate
Isoleucine
Valine
Leucine
Phosphoenoypyruvate
Tyrosine
Citrate
Pyruvate
Acetyl-CoA
Oxaloacetate
α-ketoglutarate
Glutamate
Glutamine
Malate
Succinate

Figure 5.1: Yeast glycolysis and amino acids synthesis pathways.

Red and green circles indicate the proteins that are involved in amino acids synthesis and were more abundant and that were less abundant in *por1Δ* respectively. Black arrows show the glycolysis pathway and grey arrows show amino acid synthesis pathways. Pathways are taken from KEGG database (http://www.genome.jp/kegg/pathway.html).

The next FunCat category is protein fate. In the absence of *POR1*, proteins involved in the assembly of protein complexes were more abundant. Many of these proteins are related to or part of the ARP 2/3 complex (Appendix 7.4 Table 4, discussed above). The other proteins are associated with various processes. One protein of interest is Uba1p, the E1 ubiquitin activating enzyme linked to an increase in unfolded proteins tagged for degradation [235]; the unfolded protein response will be discussed later.

Another group of overabundant proteins are in the FunCat category of "protein synthesis". Aminoacyl-tRNA-synthetases (*ALA1, DED8, DPS1, FRS1, FRS2, GLN4, GRS1, HST1, THS1, VAS1, YDR341C*) form the main sub group is this category. Those aminoacyl-tRNA-synthetases may be responding to a low level of charged tRNAs resulting from reduced synthesis of some amino acids. Moreover, some of those aminoacyl-tRNA-synthetases may have 'moonlight" functions [236] and may be involved in some non-translation functions that may be essential for *por1Δ* cells.

The last FunCat category to be discussed contains proteins with binding functions and requiring co-factors, which may not be unexpected given the multiple changes differences between the *por1Δ* and WT proteomes. For example, a biotin deficiency impairs heme synthesis [237] and in *por1Δ* mitochondria, proteins involved in heme synthesis are less abundant (Table 5.4).

Therefore, proteins (Pyc1p, Pyc2p and Acc1p) are involved in biotin synthesis may increase to compensate for the loss of heme synthesis.

In summary, proteins associated with amino acid synthesis, metabolite transport, anti-apoptotic, and protein synthesis are expressed more in the *por1Δ* strain likely to compensate for effects resulting from the absence of Por1p.

### 5.3.2 Validation of some of the potentially upregulated pathways:

#### 5.3.2.1 UPR pathway:

The absence of VDAC in *N. crassa* is associated with upregulation of some proteins associated with the endoplasmic reticulum (ER) unfolded protein response (UPR) (Chapter 4). Therefore, we hypothesized that in *S. cerevisiae,* the UPR will be high in the *por1Δ* strain. To test our hypothesis, cells were grown in the presence of tunicamycin. Tunicamycin blocks the glycosylation of the proteins in the ER; hence, the misfolding of the proteins is increased [105,238]. *por1Δ* was less sensitive compared to WT to the presence of tunicamycin (Figure 5.2). These results suggest that the absence of Por1p may induced a higher UPR response than WT; therefore, cells are resistant to tunicamycin. Another possibility is that protein synthesis may be decreased in *por1Δ* (Table 5.4), and therefore, cells are less sensitive to tunicamycin because the amount of protein is not enough to cause severe ER stress. Next, to confirm that UPR is upregulated an UPR driven β-galactosidase reporter plasmid was used [105,107]. If the UPR is high in *por1Δ* than WT, β-galactosidase activity will be high in *por1Δ* compared to WT. Interestingly, expression of the reporter gene is lower in *por1Δ* than WT (Figure 5.3), suggesting that the lower sensitivity to tunicamycin is not due to an active UPR. The proteomic analysis suggests that protein synthesis is decreased in *por1Δ*; therefore, it is possible that the level of

unfolded proteins induced by tunicamycin is insufficient to activate the UPR and, hence, expression of reporter gene is low.

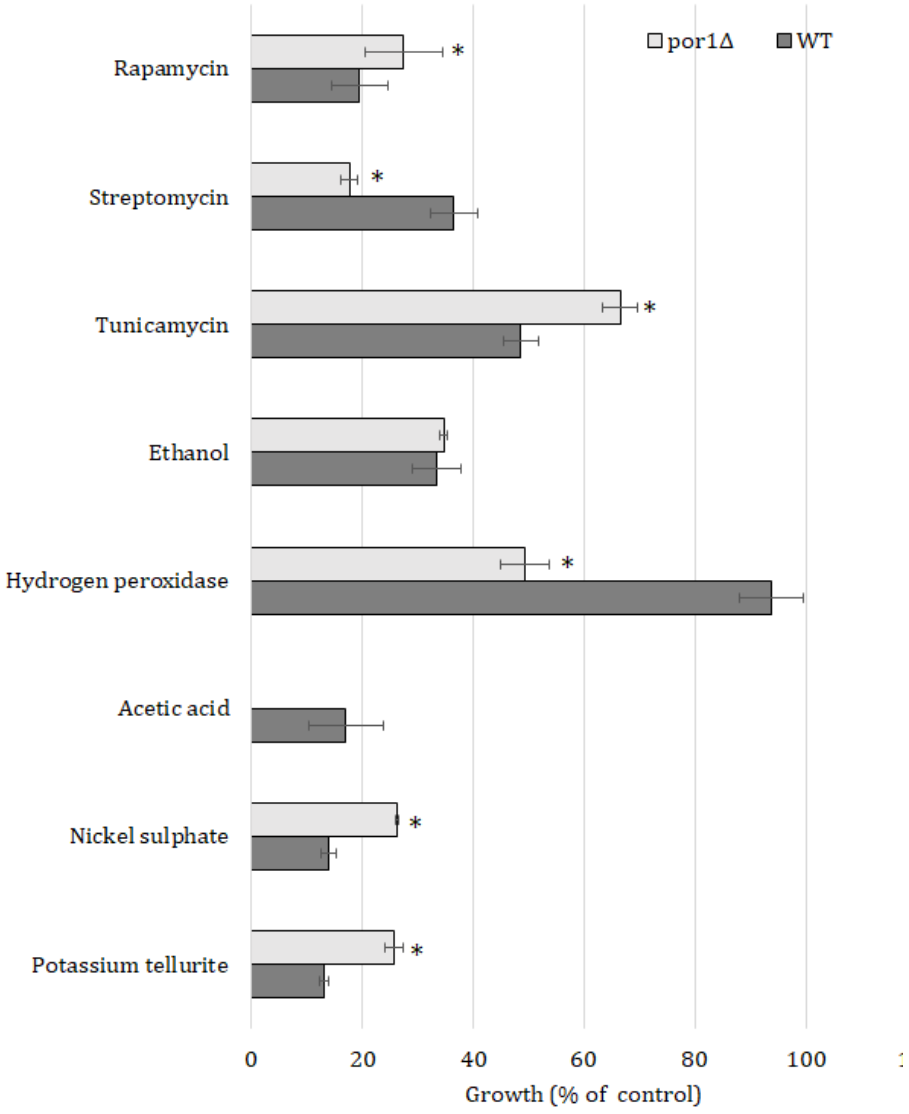


Figure 5.2: Maximum $OD_{600}$ in the presence of different chemical stresses.

Wild-type (dark bars) and *por1Δ* (light bars) cells were grown (14-20 hours) in the presence and absence of different chemicals in YPG media. Data are shown here as a percentage of that of non-treated cells. Statistical analysis was performed by using a students' *t* test. The results are presented as mean ± SD (standard deviation) (n=3-4). * indicates $P < 0.05$.

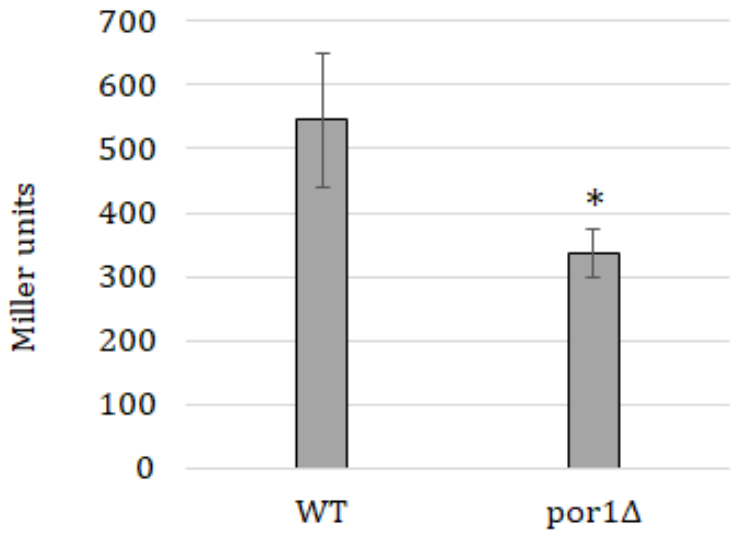


Figure 5.3: Expression of UPR regulated reporter gene induced by tunicamycin.

Cells containing the pJC004 reporter plasmid were treated with tunicamycin and the resulting β-galactosidase activity was measured. Statistical analysis was performed by using a students' *t* test. The results are presented as mean ± SD (standard deviation) (n=3). * indicates $P < 0.05$

#### 5.3.2.2 TOR pathway:

Human VDAC1 has been proposed to regulate a protein kinase – the mammalian target of rapamycin (mTOR), which controls cell growth, proliferation, and survival of mammalian cells [41,239]. In the absence of mammalian VDAC1, the mTOR pathway is downregulated, resulting in disrupted mitochondrial metabolism and an altered cellular AMP/ATP ratio [41]. Therefore, we hypothesized that in yeast *POR1* knockout cells the TOR pathway will be downregulated. To test this hypothesis, cells were grown in the presence of rapamycin. If the TOR pathway is active, sensitivity to the drug will be higher, and hence, growth of the cells will be lower. In support of this hypothesis, *por1Δ* cells are more resistant to rapamycin treatment compared to WT, as the growth of the *por1Δ* cells was higher in the presence of drug (Figure 5.2).

There is a link between VDAC and TOR revealed by drug (itraconazole) treatments. Studies have shown that itraconazole and aspirin could block human VDAC1 and downregulate the mTOR pathway and alter calcium homeostasis respectively [41,168]. Therefore, we wanted to test, if aspirin and itraconazole have an effect on Por1p of *S. cerevisiae*. Cells were grown in the presence of aspirin and itraconazole, but, no difference was observed in the maximum growth of the two strains (Figure 5.4) and (Appendix 7.4 Figure 2). Therefore, in yeast cells the mode of actions or the binding affinity for aspirin and itraconazole may be different from those in mammalian cells.

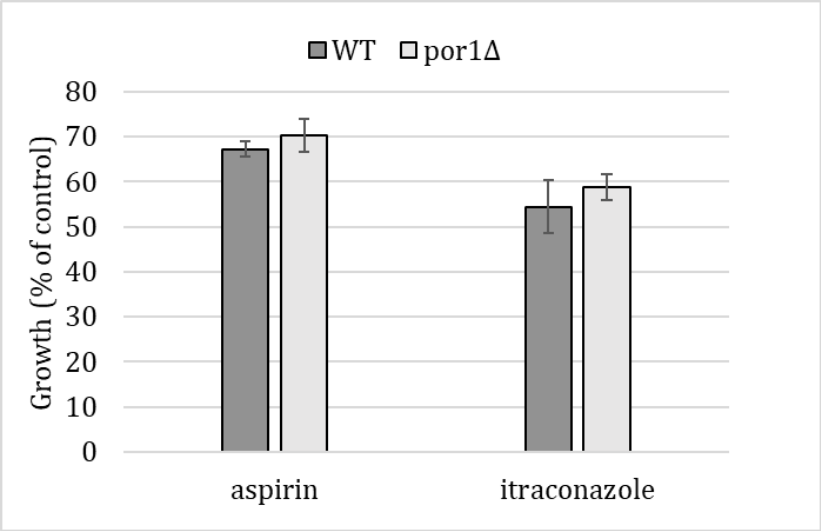


Figure 5.4: Cellular growth (maximum $OD_{600}$) in the presence of 25 mM aspirin and 0.6 µg/ml itraconazole. Statistical analysis was performed by using a students' *t* test. The results are presented as mean ± SD (standard deviation) (n=3).

#### 5.3.2.3 Oxidative stress response:

An interesting observation from the data in the Y3K database is that oxidative stress response proteins (Tsa2p, Ari1p, Gpp1p, Ahp1p and Gre1p) were more abundant in *por1Δ* cells (Appendix 7.4 Figure 1). Oxidative stress proteins were also observed in a proteomic analysis of porin-less *N. crassa* (Chapter 4). To determine whether the over-expression of stress response proteins made the *por1Δ* yeast cells more resistant to externally added oxidative stress, cells were grown in the presence of oxidative stressors hydrogen peroxide or acetic acid. In the presence either stress, WT cells were more resistant (Figure 5.2). In the presence of hydrogen peroxide, *por1Δ* growth was around 60% compared to untreated *por1Δ* cells, but, WT growth was around 90% compared to untreated WT cells. In contrast, no growth was observed in *por1Δ* in the presence of a concentration of acetic acid-which produced oxidative stress [240], but WT growth was reduced by 80%. The intracellular oxidative environment was measured by using the probe DFC (Figure 5.5). Oxidative environment was higher in *por1Δ* than WT (Figure 5.5). It was not surprising to detect a more oxidative environment in *por1Δ* than WT, as in the absence of VDAC, *N. crassa* mitochondria were abnormal and their ROS production capacity has increased (Chapter 3).

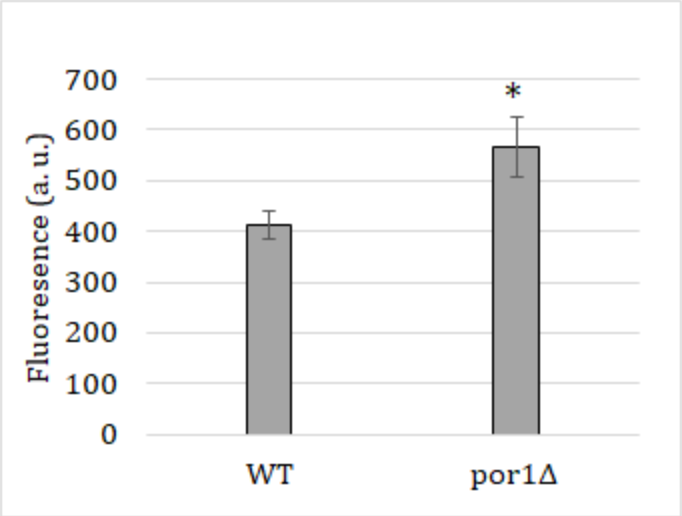


Figure 5.5: Intracellular oxidative environment measured by DFC.

Cells were grown in YPG in exponential phase. Following exponential growth, DFC was added to the media, the cells were lysed and fluorescence of oxidized DFC was measured and normalized against protein concentration. Statistical analysis was performed by using a students' *t* test. The results are presented as mean ± SD (standard deviation) (n=3). * indicates $P < 0.05$

### 5.3.3 Less abundant proteins in *por1Δ:*

The absence of Por1p is associated with some of proteins expressed in lower levels (Table 5.4). Most of the proteins are mitochondrial proteins and related to bioenergetics of mitochondria.

**Table 5.4: Less abundant proteins in *por1Δ***

| **FunCat main category** | **FunCat description** | **Number of proteins** |
|---|---|---|
| Biogenesis of cellular components | mitochondrion | 69 |
| | nucleolus | 3 |
| Cell rescue, defense and virulence | catalase reaction | 2 |
| Cellular transport, transport facilitation and transport routes | electron transport | 54 |
| | mitochondrial transport | 27 |
| | C4-dicarboxylate transport (e.g. malate, succinate, fumarate) | 6 |
| | transport facilities | 24 |
| | antiporter | 5 |
| | transport ATPases | 10 |
| | cation transport (H+, Na+, K+, Ca2+, NH4+, etc.) | 13 |

| | | |
|---|---|---|
| Energy | electron transport and membrane-associated energy conservation | 41 |
| | aerobic respiration | 42 |
| | tricarboxylic-acid pathway (citrate cycle, Krebs cycle, TCA cycle) | 26 |
| | respiration | 35 |
| | energy generation (e.g. ATP synthase) | 16 |
| | glycolysis and gluconeogenesis | 18 |
| | accessory proteins of electron transport and membrane-associated energy conservation | 11 |
| | pyruvate dehydrogenase complex | 5 |
| | alcohol fermentation | 7 |
| | anaerobic respiration | 4 |
| | energy conversion and regeneration | 6 |
| | lactate fermentation | 3 |
| | propionate fermentation | 3 |
| Interaction with the environment | homeostasis of protons | 11 |
| Metabolism | C-compound and carbohydrate metabolism | 56 |
| | sugar, glucoside, polyol and carboxylate catabolism | 28 |
| | sugar, glucoside, polyol and carboxylate anabolism | 19 |
| | biosynthesis of glutamate | 11 |
| | biosynthesis of leucine | 7 |

| | | |
|---|---|---|
| | metabolism of the pyruvate family (alanine, isoleucine, leucine, valine) and D-alanine | 6 |
| | biosynthesis of isoleucine | 6 |
| | degradation of threonine | 5 |
| | biosynthesis of valine | 5 |
| | C-2 compound and organic acid catabolism | 7 |
| | degradation of leucine | 4 |
| | metabolism of glycine | 2 |
| Protein synthesis | ribosomal proteins | 44 |
| Protein with binding function or cofactor requirement (structural or catalytic) | Fe/S binding | 9 |
| | NAD/NADP binding | 16 |
| | heme binding | 7 |
| | pyridoxal phosphate binding | 7 |
| | thiamine pyrophosphate binding | 3 |
| | FAD/FMN binding | 7 |
| Transcription | rRNA modification | 5 |

In the absence of VDAC, proteins involved in the biogenesis of some cellular components were less abundant. The less abundant proteins in this FunCat category can be sub-grouped into those involved in mitochondrial biogenesis and cellular biogenesis. VDAC is the most abundant mitochondrial MOM protein, and its absence is associated with a variety of mitochondria defects [55,56]. Moreover, the absence of VDAC can induce ROS production from mitochondria (Chapter 3), and oxidative stress may cause degradation of mitochondrial DNA [241]. Hence, we hypothesized that the amount of mitochondrial DNA may be low in *por1Δ* compared to WT and we tested the ratio of genomic DNA and mitochondrial DNA using semi-quantitative PCR amplification of *ACT1* and *COX2* genes (Figure 5.6).

.

A.

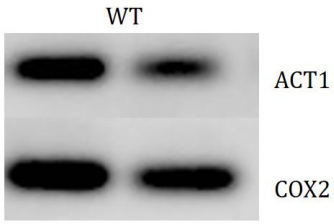


B.

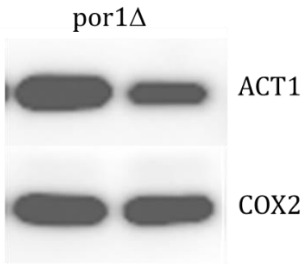


C.

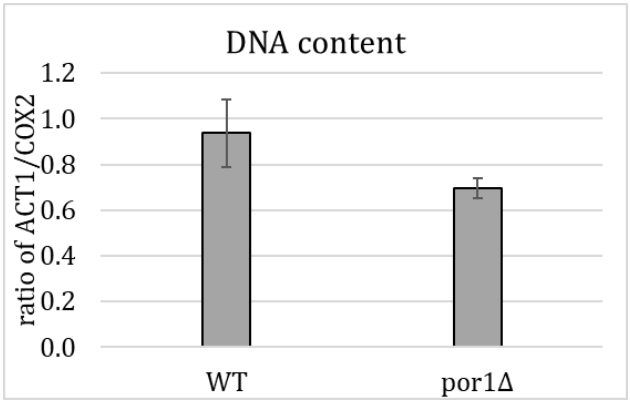


Figure 5.6: Ratio of ACT1, (nuclear) and COX2 (mitochondrial) DNA determined by PCR amplification.

Images of the gels from (A) WT PCR and (B) *por1Δ* PCR reactions. C. Ratio of genomic DNA and mitochondrial DNA was determined by using the intensity of the bands.

The next FunCat category to be discussed contains proteins involved in cell rescue, defense and virulence. Catalase proteins are the part of this group. However, it was surprising for us to detect low levels of catalase proteins (Table 5.4), as, other oxidative stress response proteins were more abundant in *por1Δ* (Appendix 7.4 Figure 2). To verify this finding, catalase activity was measured in the strains and catalase activity indeed was lower in *por1Δ* compared to WT (Figure 5.7).

The third main FunCat category includes cellular transport, transport facilitation and transport routes. The absence of VDAC causes lower levels of mitochondrial ETC complexes in *N. crassa* [55,56]. In agreement with this finding, proteins involved in electron transport were less abundant in *por1Δ* (Table 5.2). VDAC is also proposed to be involved in the transport of metabolites in the cells [1]. Proteins (Odc1p, Odc2p,) in the MIM of mitochondria [242], involved in the transport of 2-oxoglutarate are less abundant in *por1Δ*. Therefore, the absence of VDAC may influence the movement of 2-oxoglutarate in the cells. Next, another group of proteins are anti-porters that are encoded by the gene *AAC1, GGC1, PET9, SFC,* and *YHM2*. VDAC has been proposed to make complexes with the MIM protein adenine nucleotide translocator (Aac1p and Aac2p) [32] and the absence of VDAC would cause the absence of the protein complexes. Hence, it may be possible that the synthesis of Aac1p and Aac2p respond to a signal in the absence of Por1p and therefore, they were less abundant in *por1Δ*. Other antiporters are involved in GTP/GDP transport, mitochondrial succinate-fumarate transport and citrate-oxoglutarate transport [243,244]. Another sub-group of proteins contains transport ATPase and some of the subunits in complex V (Appendix 7.4 Table 5.5) are part of this group. Many of these complex V protein subunits are also categorized in the homeostasis of protons sub-group in the FunCat category of interaction with the environment. Therefore, in the absence of VDAC, protein abundance for complex V is

reduced. The growth rate of VDAC1-less *S. cerevisiae* in non-fermentative medium is low compared to WT (Table 5.2), which may reflect the energy and metabolic production of the cells. Therefore, proteins involved in energy production are predicted to be less abundant compared to WT. This idea also supported by the observation that, several proteins involved in the TCA were less abundant (Appendix 7.4 Table 6).

Another group of less-abundant proteins are in the FunCat category of "metabolism". As mentioned before, the absence of *POR1* causes impaired cellular growth; therefore, metabolism of some of the sugars, carbohydrates and amino acids may be low, and as expected, proteins involved in the metabolism of those compounds are less abundant. One of the sub-groups in this category is biosynthesis of glutamate. Some of the steps in glutamate synthesis are tightly regulated by mitochondria and depend on substrates from the TCA cycle [245]. Therefore, it was not surprising to observe that proteins involved in glutamate synthesis are less abundant. This observation is supported by the metabolomic analysis that revealed relatively lower levels of glutamate in *por1Δ* [218]. Another interesting observation was that proteins involved in the synthesis of the amino acids from pyruvate were also less abundant in *por1Δ* (Figure 5.1).

In the absence of *POR1*, proteins in the FunCat categories of protein synthesis and transcription are less abundant. Protein synthesis depends on the external conditions and intracellular demand of the cells [199]. Therefore, low cellular functions because of slow growth rate may generate low demand for protein synthesis or vice versa. Furthermore, as protein synthesis is downregulated, protein binding functions and co-factor requirements are low.

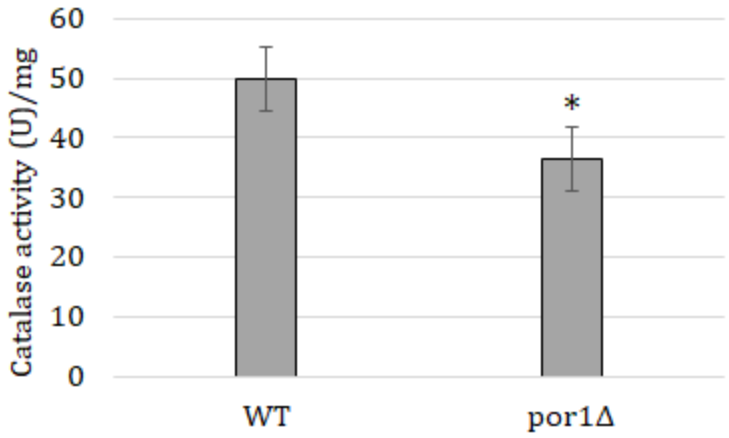


Figure 5.7: Catalase activity measured in the cytosol of WT and *por1Δ* cells.

Catalase activity was measured in the cytoplasmic extract of WT and *por1Δ* cells were grown in the exponential phase. One unit of catalase is defined as the amount that decomposes 1 µmole of $H_2O_2$ in 1 minutes in a 60 mM $H_2O_2$ solution at pH 7.0. Statistical analysis was performed by using a students' *t* test. The results are presented as mean ± SD (standard deviation) (n=3-4). * indicates $P < 0.05$

Table 5.5: Phenotypic characterization of *por1Δ* in the presence of different chemicals.

| Systematic (Gene) and descriptive names | Chemical stress | Null mutant phenotype[1] | *por1Δ* phenotype | More abundant /Less abundant in *por1Δ* | KEEG category |
|---|---|---|---|---|---|
| YOR374W (ALD4), Aldehyde dehydrogenase | Nickel sulphate | Resistant | Resistant | Less abundant | Glycolysis / Gluconeogenesis |
| YIL036W (CST6) Basic leucine zipper (bZIP) transcription factor | Ethanol | Sensitive | Resistant | Less abundant | Transcription |
| YBL024W (NCL1) tRNA (cytosine-C5-)-methyltransferase | Potassium Tellurite | Resistant | Resistant | More abundant | t-RNA biogenesis |

[1]Data were collected from *S. cerevisiae* genome database (https://www.yeastgenome.org/).

Resistance and sensitivity were determined by maximum growth at $OD_{600}$. Concentrations of the chemical were listed in materials and methods.

Next, *por1Δ* was grown in different chemicals, to test if the phenotypes of *por1Δ* matched those of the null mutants of the several of genes are over- or under-represented in *por1Δ* (Figure 5.1 and Table 5.5). The null mutant of *ALD4* is resistant to nickel sulphate; in *por1Δ*, this protein was less abundant and the strain also was resistant to nickel sulphate. However, the null mutant of *CST6* gene is sensitive to ethanol; in contrast, this protein was less abundant and *por1Δ c*ells were resistant to ethanol. One of the possibilities is that cells may utilize different resistant mechanisms when there is less protein compared to null proteins. The last gene was tested *NCL1;* the null mutant of this gene is resistant to potassium tellurite. However, in *por1Δ*, this protein is more abundant resulting in resistance to potassium tellurite stress. Therefore, other proteins may be involved in the potassium tellurite resistance.

**5.4 Conclusions:**

The data presented here indicate that mitochondrial bioenergetics across the MOM are disrupted in the absence of VDAC and that proteins involved those processes are expressed differentially in *por1Δ* compared to WT. In addition to that, in the absence of *POR1* in yeast, evidence suggests that TOR pathway is downregulated. In agreement with previously published results, the absence of VDAC causes oxidative stress; however, there was less cytosolic catalase activity in *por1Δ*. It might be possible that other antioxidant mechanisms can control the ROS in the cells and therefore, catalase activity was less abundant. In the future, it will be interesting to understand the pathways linking mitochondrial function with lower TOR activity and the UPR in the absence of VDAC.

## 5.5 Acknowledgements:

This work was supported by a Discovery Grant from the Natural Sciences and Engineering Research Council of Canada (NSERC) and funds from the University of Manitoba to D.A.C.; S.R.S. acknowledges support from the Faculty of Graduate Studies at the University of Manitoba. We would like to thank Dr. Troy Harkness, University of Saskatchewan and Dr. Dana Schroeder, University of Manitoba, for providing *S. cerevisiae* cells. We thank Dr. Davis Ng, Temasek Lifesciences Laboratory, Singapore and Dr. Peter Walter, University of California, San Francisco, USA for providing the pJC31, pJC004, and pJC005 plasmids. We thank Dr. Oleg V. Krokhin, Mr. Victor Spicer, and Mr. Peyman Ezzati, Manitoba Centre for Proteomics and Systems Biology for acquiring the LC-MS/MS data for the proteomic analysis.

# Chapter 6: Conclusion and future works

## 6.1 Conclusion:

In this thesis, the aim was to elucidate *in vivo* roles of N-terminus of VDAC and the global role of VDAC. The importance of N-terminus of VDAC has been proposed in various studies. To the best of my knowledge, this is the first time, the association of the N-terminus of VDAC in the efficient assembly of the VDAC protein in mitochondria, and maintenance of the standard electron transport chain and number of mitochondria are proposed. Moreover, the N-terminus of VDAC also associated with mitochondrial ROS production because mitochondria expressing VDAC with a truncated N-terminus showed an overall increase in the capacity to produce ROS, but maintained WT levels of membrane potential and oxidative phosphorylation. In summary, the N-terminus and lower level of VDAC are associated with mitochondrial redox state, mitochondrial number and other cellular functions.

The influence of VDAC on ROS was studied by using cells with different amounts of VDAC in the MOM. In the presence of almost 50% of the WT level of VDAC, mitochondrial ROS production capacity was similar to that of WT. However, in the presence of drugs (antimycin and rotenone) that inhibit mitochondrial ETC complexes, ROS production capacity was increased relative to WT. Therefore, the amount of VDAC in the MOM is associated with differential ROS production capacity from various sites. In the absence of VDAC, ROS production was increased with and without inhibitors of ETC complexes. This observation was not unexpected, as abnormal ETC complexes were observed in the absence of VDAC. The intracellular oxidative state was also higher in VDAC-less cells compared to WT. Therefore, the absence of VDAC is linked to elevated mitochondrial ROS production and the intracellular redox environment.

Human VDAC isoforms have been proposed to associate with cancers [174,179]; for example, human VDAC1 expression was higher in various cancer cell lines compared to a normal cell line [179]. Increased hexokinase expression was also detected in those cells. The interactions between VDAC-hexokinase have been shown previously [31,180]. These interactions are important for providing energy to the cells and blocking the apoptosis of the cells [179]. Therefore, different drugs like 4,4'-Diisothiocyanatostilbene-2,2'-disulfonate (DIDS), methyl jasmonate and erastin have been proposed to be used to block VDAC and interactions with hexokinase and slow the cancer [180,246]. My studies indicate that careful steps should be taken to use drugs against VDAC because of the changes in bioenergetics associated with partial reduction in VDAC amounts.

Mitochondria work as signalling hubs in the cells and mitochondrial redox environment can influence these signalling pathways. Hence, proteomic analysis of two model organisms provided some insights related to the mechanisms fungal cells implement to survive in the absence of VDAC. In general, proteins related to protein synthesis are less abundant; this includes those involved in amino acid, nucleotide and sulfur metabolism. In contrast, proteins involved in the TCA cycle and oxidative stress responses were more abundant. Intriguingly, in the absence of VDAC, proteins involved in the UPR were high in *N. crassa* but the UPR was low in *S. cerevisiae*. It might be possible that the two model systems implement distinct methods to reduce the stresses in the absence of VDAC; one of the mechanisms might be the expression of catalase. In *N. crassa*, expression of catalase was higher in ΔPor-1 than WT; but in *S. cerevisiae por1Δ*, it was lower. One explanation is that the oxidative stress might be different in two model systems; however, the ROS production capacity in *N. crassa* ΔPor-1 mitochondria was higher than WT, and higher intracellular oxidative environment was detected in *S. cerevisiae por1Δ*. To the best of my

knowledge, this is the first time, proteomic studies demonstrated the influence of VDAC on various cellular pathways, especially on UPR and mitochondrial membrane compositions.

Overall, these studies reveal that VDAC influences ROS production and various cellular pathways such as protein synthesis, amino acid synthesis, TCA cycle, UPR and lipid synthesis pathways; thus, VDACs play a global role in cells.

**6.2 Future works:**

Further experiments will be required to answer some interesting questions in this field. It will be interesting to generate strains with similar amount of VDAC as is found in ΔN2-12porin. These strains will help me to separate the influence of low amount of VDAC from the influence of truncated the N-terminal variants of VDAC. Phenotypic characterizations and bioenergetics characterization of these strains will help to understand the impact of N-terminus of VDAC. Moreover, it has been proposed that the N-terminus of VDAC interacts with VDAC proteins in the formation of dimers [2], and it will be important to assess dimerization of ΔN2-12porin to investigate this hypothesis. Once the strain with lower levels of VDAC is available, it will be interesting to do some proteomic analysis of the ΔN2-12porin strain to understand the roles of N-terminus of VDAC in cellular functions. Another approach that can be taken in future is to use different chemical crosslinkers to elucidate the proteins, such as hexokinase, that might be interacting with N-terminus of VDAC. This way, involvement of the N-terminus of VDAC in specific interactions can be studied.

In future, it will be interesting to use a mammalian cell line or mouse model to study mitochondrial bioenergetics and ROS production. As mentioned before, various isoforms of

human VDAC such, as VDAC1 have been proposed to be involved in gastric cancer, cervical cancer and myeloma [180]; therefore, a cancer cell line or mouse model knockout of VDAC isoforms will be helpful to understand the influence of VDAC on mitochondrial bioenergetics and ROS production in healthy and cancerous cells. In my thesis, I have studied the effect of VDAC on mitochondrial bioenergetics and ROS production in *N. crassa*; however, mammalian systems have several distinct features, like the absence of alternative oxidase and alternative NADH dehydrogenase. In the medical perspective, this type of study is very important.

Another interesting study can be the swapping of the N-terminus of different human VDAC isoforms with each other, and determining the effects on mitochondrial bioenergetics and ROS. In studies of yeast VDAC expressing the N-terminus of human VDACs, it has been shown that swapping the N-terminus of human VDAC1 with human VDAC3 increased the longevity of the yeast cells [117]. ROS has been proposed to be linked to aging [247], and therefore, it will be interesting to study those modified VDAC in mammalian cell lines for potential ROS production capacity and longevity.

Different isoforms of human VDAC have been proposed to be involved in various neurodegenerative diseases like Parkinson's Disease and Alzheimer’s disease [248]. Moreover, VDAC has been suggested to be involved in various bacterial and viral diseases [249–252]. Therefore, it will be interesting to perform multiomics analysis of various human VDAC knockout cells, comparing infected and uninfected cells. This type of study will help to elucidate the roles of VDAC in humans and may provide suggestions for the treatment of these diseases.

In *N. crassa*, the absence of VDAC is associated with distinct mitochondrial membrane properties compared to WT. VDAC is the most abundant MOM protein; therefore, it can be

hypothesized that, the influence of the absence of VDAC will be more in the MOM compositions. Membrane properties and composition impact various cellular functions like carrier-mediated transport, functions of certain enzyme and cell growth [211]. Therefore, it will be interesting to study isolated MOM from VDAC-less mitochondria and study the composition of the MOM, and different pathways related to mitochondrial membrane composition in the absence of VDAC.

These above-mentioned studies will be helpful and interesting to further elucidate the global of roles of VDAC in cells.

# References:


[1] V. Shoshan-Barmatz, V. De Pinto, M. Zweckstetter, Z. Raviv, N. Keinan, N. Arbel, VDAC, a multi-functional mitochondrial protein regulating cell life and death, Mol. Aspects Med. 31 (2010) 227–285. doi:10.1016/j.mam.2010.03.002.

[2] S.R. Shuvo, F.G. Ferens, D.A. Court, The N-terminus of VDAC: structure, mutational analysis, and a potential role in regulating barrel shape, Biochim. Biophys. Acta - Biomembr. 1858 (2016) 1350–1361. doi:10.1016/j.bbamem.2016.03.017.

[3] B. Alberts, A. Johnson, J. Lewis, M. Raff, K. Roberts, P. Walter, Molecular Biology of the Cell, 4th ed., Garland Science, New York, 2002.

[4] K. McCluskey, A.E. Wiest, I. V Grigoriev, A. Lipzen, J. Martin, W. Schackwitz, S.E. Baker, Rediscovery by whole genome sequencing: slassical sutations and genome polymorphisms in *Neurospora crassa*, G3 Genes, Genomes, Genet. 1 (2011) 303–316. doi:10.1534/g3.111.000307.

[5] K. McCluskey, Variation in mitochondrial genome primary sequence among whole-genome-sequenced strains of *Neurospora crassa*, IMA Fungus. 3 (2012) 93–98. doi:10.5598/imafungus.2012.03.01.10.

[6] K. Boengler, G. Heusch, R. Schulz, Nuclear-encoded mitochondrial proteins and their role in cardioprotection, Biochim. Biophys. Acta - Mol. Cell Res. 1813 (2011) 1286–1294. doi:10.1016/j.bbamcr.2011.01.009.

[7] L.D. Osellame, T.S. Blacker, M.R. Duchen, Cellular and molecular mechanisms of mitochondrial function, Best Pract. Res. Clin. Endocrinol. Metab. 26 (2012) 711–723.

doi:10.1016/j.beem.2012.05.003.

[8] S.J. Schein, M. Colombini, A. Finkelstein, Reconstitution in planar lipid bilayers of a voltage-dependent anion-selective channel obtained from paramecium mitochondria, J. Membr. Biol. 30 (1976) 99–120. doi:10.1007/BF01869662.

[9] R. Benz, Permeation of hydrophilic solutes through mitochondrial outer membranes: Review on mitochondrial porins, Biochim. Biophys. Acta - Rev. Biomembr. 1197 (1994) 167–196. doi:10.1016/0304-4157(94)90004-3.

[10] F. Homble, E.M. Krammer, M. Prevost, Plant VDAC: Facts and speculations, Biochim. Biophys. Acta - Biomembr. 1818 (2012) 1486–1501. doi:10.1016/j.bbamem.2011.11.028.

[11] M.J. Young, D.C. Bay, G. Hausner, D.A. Court, The evolutionary history of mitochondrial porins., BMC Evol. Biol. 7 (2007) 31. doi:10.1186/1471-2148-7-31.

[12] K. Mihara, R. Sato, Molecular cloning and sequencing of cDNA for yeast porin, an outer mitochondrial membrane protein: a search for targeting signal in the primary structure., EMBO J. 4 (1985) 769–74.

[13] R. Kleene, N. Pfanner, R. Pfaller, T.A. Link, W. Sebald, W. Neupert, M. Tropschug, Mitochondrial porin of *Neurospora crassa*: cDNA cloning, in vitro expression and import into mitochondria., EMBO J. 6 (1987) 2627–2633.

[14] J. Song, C. Midson, E. Blachly-Dyson, M. Forte, M. Colombini, The sensor regions of VDAC are translocated from within the membrane to the surface during the gating processes., Biophys. J. 74 (1998) 2926–2944. doi:10.1016/S0006-3495(98)78000-2.

[15] D.C. Bay, M. Hafez, M.J. Young, D.A. Court, Phylogenetic and coevolutionary analysis

of the B-barrel protein family comprised of mitochondrial porin (VDAC) and Tom40, Biochim. Biophys. Acta - Biomembr. 1818 (2012) 1502–1519. doi:10.1016/j.bbamem.2011.11.027.

[16] V. De Pinto, G. Prezioso, F. Thinnes, T. a Link, F. Palmieri, Peptide-specific antibodies and proteases as probes of the transmembrane topology of the bovine heart mitochondrial porin., Biochemistry. 30 (1991) 10191–10200. doi:10.1021/bi00106a017.

[17] S. Stanley, J.A. Dias, D. D'Arcangelis, C.A. Mannella, Peptide-specific antibodies as probes of the topography of the voltage-gated channel in the mitochondrial outer membrane of *Neurospora crassa*., J. Biol. Chem. 270 (1995) 16694–16700.

[18] B. Shanmugavadivu, H.-J.J. Apell, T. Meins, K. Zeth, J.H.J.H. Kleinschmidt, Correct folding of the β-Barrel of the human membrane protein VDAC requires a lipid bilayer, J. Mol. Biol. 368 (2007) 66–78. doi:10.1016/j.jmb.2007.01.066.

[19] T.J. Malia, G. Wagner, NMR structural investigation of the mitochondrial outer membrane protein VDAC and its interaction with antiapoptotic Bcl-XL, Biochemistry. 46 (2007) 514–525. doi:10.1021/bi061577h.

[20] D.C. Bay, J.D. O'Neil, D.A. Court, Two-Step folding of recombinant mitochondrial porin in detergent, Biophys. J. 94 (2008) 457–468. doi:10.1529/biophysj.107.115196.

[21] T. Raschle, S. Hiller, T.-Y. Yu, A.J. Rice, T. Walz, G. Wagner, Structural and functional characterization of the integral membrane protein VDAC-1 in lipid bilayer nanodiscs., J. Am. Chem. Soc. 131 (2009) 17777–9. doi:10.1021/ja907918r.

[22] R. Ujwal, D. Cascio, J.-P. Colletier, S. Faham, J. Zhang, L. Toro, P. Ping, J. Abramson,

The crystal structure of mouse VDAC1 at 2.3 A resolution reveals mechanistic insights into metabolite gating., Proc. Natl. Acad. Sci. U. S. A. 105 (2008) 17742–7. doi:10.1073/pnas.0809634105.

[23] J. Schredelseker, A. Paz, C.J. López, C. Altenbach, C.S. Leung, M.K. Drexler, J.-N. Chen, W.L. Hubbell, J. Abramson, High resolution structure and double electron-electron resonance of the zebrafish voltage-dependent anion channel 2 reveal an oligomeric population., J. Biol. Chem. 289 (2014) 12566–77. doi:10.1074/jbc.M113.497438.

[24] M. Bayrhuber, T. Meins, M. Habeck, S. Becker, K. Giller, S. Villinger, C. Vonrhein, C. Griesinger, M. Zweckstetter, K. Zeth, Structure of the human voltage-dependent anion channel, Proc. Natl. Acad. Sci. 105 (2008) 15370–15375. doi:10.1073/pnas.0808115105.

[25] R. Schneider, M. Etzkorn, K. Giller, V. Daebel, J. Eisfeld, M. Zweckstetter, C. Griesinger, S. Becker, A. Lange, The native conformation of the human VDAC1 N terminus, Angew. Chemie - Int. Ed. 49 (2010) 1882–1885. doi:10.1002/anie.200906241.

[26] S. Hiller, R.G. Garces, T.J. Malia, V.Y. Orekhov, M. Colombini, G. Wagner, Solution structure of the integral human membrane protein VDAC-1 in detergent micelles, Science (80). 321 (2008) 1206–1210. doi:10.1126/science.1161302.

[27] L.A. Kelley, S. Mezulis, C.M. Yates, M.N. Wass, M.J.E. Sternberg, The Phyre2 web portal for protein modeling, prediction and analysis, Nat. Protoc. 10 (2015) 845–858. doi:10.1038/nprot.2015.053.

[28] I. Roman, J. Figys, G. Steurs, M. Zizi, Hunting interactomes of a membrane protein: obtaining the largest set of Voltage-Dependent Anion Channel-interacting protein

epitopes, Mol. Cell. Proteomics. 5 (2006) 1667–1680. doi:10.1074/mcp.T600009-MCP200.

[29] K.S. McCommis, C.P. Baines, The role of VDAC in cell death: Friend or foe?, Biochim. Biophys. Acta - Biomembr. 1818 (2012) 1444–1450. doi:10.1016/j.bbamem.2011.10.025.

[30] J.J. Lemasters, E. Holmuhamedov, Voltage-dependent anion channel (VDAC) as mitochondrial governator—Thinking outside the box, Biochim. Biophys. Acta. 1782 (2005) 181–190. doi:10.1016/j.bbadis.2005.10.006.

[31] J.G. Pastorino, J.B. Hoek, Regulation of hexokinase binding to VDAC, J. Bioenerg. Biomembr. 40 (2008) 171–182. doi:10.1007/s10863-008-9148-8.

[32] M.Y. Vyssokikh, D. Brdiczka, The function of complexes between the outer mitochondrial membrane pore (VDAC) and the adenine nucleotide translocase in regulation of energy metabolism and apoptosis, Acta Biochim. Pol. 50 (2003) 389–404. doi:035002389.

[33] V. Shoshan-Barmatz, N. Keinan, H. Zaid, Uncovering the role of VDAC in the regulation of cell life and death, J. Bioenerg. Biomembr. 40 (2008) 183–191. doi:10.1007/s10863-008-9147-9.

[34] S. Abu-Hamad, H. Zaid, A. Israelson, E. Nahon, V. Shoshan-Barmatz, Hexokinase-I protection against apoptotic cell death is mediated via interaction with the voltage-dependent anion channel-1: Mapping the site of binding, J. Biol. Chem. 283 (2008) 13482–13490. doi:10.1074/jbc.M708216200.

[35] E.D. Goley, M.D. Welch, The ARP2/3 complex: an actin nucleator comes of age., Nat.

Rev. Mol. Cell Biol. 7 (2006) 713–26. doi:10.1038/nrm2026.

[36] B.L. Goode, J.A. Eskin, B. Wendland, Actin and endocytosis in budding yeast., Genetics. 199 (2015) 315–58. doi:10.1534/genetics.112.145540.

[37] T.K. Rostovtseva, S.M. Bezrukov, VDAC inhibition by tubulin and its physiological implications, Biochim. Biophys. Acta - Biomembr. 1818 (2012) 1526–1535. doi:10.1016/j.bbamem.2011.11.004.

[38] X. Xu, J.G. Forbes, M. Colombini, Actin modulates the gating of *Neurospora crassa* VDAC, J. Membr. Biol. 180 (2001) 73–81. doi:10.1007/s002320010060.

[39] T. Rostovtseva, M. Colombini, VDAC channels mediate and gate the flow of ATP: implications for the regulation of mitochondrial function., Biophys. J. 72 (1997) 1954–1962. doi:10.1016/S0006-3495(97)78841-6.

[40] S. Abu-Hamad, S. Sivan, V. Shoshan-Barmatz, The expression level of the voltage-dependent anion channel controls life and death of the cell., Proc. Natl. Acad. Sci. U. S. A. 103 (2006) 5787–92. doi:10.1073/pnas.0600103103.

[41] S.A. Head, W. Shi, L. Zhao, K. Gorshkov, K. Pasunooti, Y. Chen, Z. Deng, R.-J. Li, J.S. Shim, W. Tan, T. Hartung, J. Zhang, Y. Zhao, M. Colombini, J.O. Liu, Antifungal drug itraconazole targets VDAC1 to modulate the AMPK/mTOR signaling axis in endothelial cells., Proc. Natl. Acad. Sci. U. S. A. 112 (2015) E7276-85. doi:10.1073/pnas.1512867112.

[42] G. Yehezkel, S. Abu-Hamad, V. Shoshan-Barmatz, An N-terminal nucleotide-binding site in VDAC1: Involvement in regulating mitochondrial function, J. Cell. Physiol. 212 (2007)

551–561. doi:10.1002/jcp.21048.

[43] B.H. Graham, W.J. Craigen, Mitochondrial voltage-dependent anion channel gene family in *Drosophila melanogaste*r: complex patterns of evolution, genomic organization, and developmental expression., Mol. Genet. Metab. 85 (2005) 308–17. doi:10.1016/j.ymgme.2005.03.009.

[44] X.W. Guo, P.R. Smith, B. Cognon, D. D'Arcangelis, E. Dolginova, C.A. Mannella, Molecular Design of the Voltage-Dependent, Anion-Selective Channel in the Mitochondrial Outer Membrane, J. Struct. Biol. 114 (1995) 41–59. doi:10.1006/jsbi.1995.1004.

[45] V. De Pinto, F. Tomasello, A. Messina, F. Guarino, R. Benz, D. La Mendola, A. Magrì, D. Milardi, G. Pappalardo, Determination of the conformation of the human VDAC1 N-Terminal peptide, a protein moiety essential for the functional properties of the pore, ChemBioChem. 8 (2007) 744–756. doi:10.1002/cbic.200700009.

[46] C. Guardiani, M.A. Scorciapino, G.F. Amodeo, J. Grdadolnik, G. Pappalardo, V. De Pinto, M. Ceccarelli, M. Casu, The N-terminal peptides of the three human isoforms of the mitochondrial voltage-dependent anion channel have different helical propensities, Biochemistry. 54 (2015) 5646–5656. doi:10.1021/acs.biochem.5b00469.

[47] Z. Gattin, R. Schneider, Y. Laukat, K. Giller, E. Maier, M. Zweckstetter, C. Griesinger, R. Benz, S. Becker, A. Lange, Solid-state NMR, electrophysiology and molecular dynamics characterization of human VDAC2, J. Biomol. NMR. 61 (2015) 311–320. doi:10.1007/s10858-014-9876-5.

[48] R.P. Gonçalves, N. Buzhynskyy, V. Prima, J.N. Sturgis, S. Scheuring, Supramolecular assembly of VDAC in native mitochondrial outer membranes, J. Mol. Biol. 369 (2007) 413–418. doi:10.1016/j.jmb.2007.03.063.

[49] R. Zalk, A. Israelson, E.S. Garty, H. Azoulay-Zohar, V. Shoshan-Barmatz, Oligomeric states of the voltage-dependent anion channel and cytochrome c release from mitochondria., Biochem. J. 386 (2005) 73–83. doi:10.1042/BJ20041356.

[50] D.C. Bay, D.A. Court, Effects of ergosterol on the structure and activity of *Neurospora* mitochondrial porin in liposomes., Can. J. Microbiol. 55 (2009) 1275–1283. doi:10.1139/w09-088.

[51] S. Geula, D. Ben-Hail, V. Shoshan-Barmatz, Structure-based analysis of VDAC1: N-terminus location, translocation, channel gating and association with anti-apoptotic proteins, Biochem. J. 444 (2012) 475–485. doi:10.1042/BJ20112079.

[52] S. Abu-Hamad, N. Arbel, D. Calo, L. Arzoine, A. Israelson, N. Keinan, R. Ben-Romano, O. Friedman, V. Shoshan-Barmatz, The VDAC1 N-terminus is essential both for apoptosis and the protective effect of anti-apoptotic proteins., J. Cell Sci. 122 (2009) 1906–1916. doi:10.1242/jcs.040188.

[53] L. Arzoine, N. Zilberberg, R. Ben-Romano, V. Shoshan-Barmatz, Voltage-dependent anion channel 1-based peptides interact with hexokinase to prevent its anti-apoptotic activity, J. Biol. Chem. 284 (2009) 3946–3955. doi:10.1074/jbc.M803614200.

[54] S.R. Shuvo, U. Kovaltchouk, A. Zubaer, A. Kumar, W.A.T. Summers, L.J. Donald, G. Hausner, D.A. Court, Functional characterization of an N-terminally-truncated

mitochondrial porin expressed in *Neurospora crassa*, Can. J. Microbiol. 68 (2017) 730–738. doi:10.1139/cjm-2016-0764.

[55] F.G. Ferens, V. Spicer, O. V. Krokhin, A. Motnenko, W.A.T. Summers, D.A. Court, A deletion variant partially complements a porin-less strain of *Neurospora crassa*, Biochem. Cell Biol. 95 (2017) 318–327. doi:10.1139/bcb-2016-0166.

[56] W.A.T. Summers, J.A. Wilkins, R.C. Dwivedi, P. Ezzati, D.A. Court, Mitochondrial dysfunction resulting from the absence of mitochondrial porin in *Neurospora crassa*, Mitochondrion. 12 (2012) 220–229. doi:10.1016/j.mito.2011.09.002.

[57] M. Jastroch, A.S. Divakaruni, S. Mookerjee, J.R. Treberg, M.D. Brand, Mitochondrial proton and electron leaks., Essays Biochem. 47 (2010) 53–67. doi:10.1042/bse0470053.

[58] T. Joseph-Horne, D.W. Hollomon, P.M. Wood, Fungal respiration: a fusion of standard and alternative components, Biochim. Biophys. Acta. 1504 (2001) 179–195. doi:10.1016/S0005-2728(00)00251-6.

[59] L.A. Sazanov, REVIEWS A giant molecular proton pump : structure and mechanism of respiratory complex I, Nat. Publ. Gr. 16 (2015) 375–388. doi:10.1038/nrm3997.

[60] I. Marques, N.A. Dencher, A. Videira, F. Krause, Supramolecular organization of the respiratory chain in *Neurospora crassa* mitochondria, Eukaryot. Cell. 6 (2007) 2391–2405. doi:10.1128/EC.00149-07.

[61] F. Krause, C.Q. Scheckhuber, A. Werner, S. Rexroth, N.H. Reifschneider, N.A. Dencher, H.D. Osiewacz, Supramolecular organization of cytochrome c oxidase-and alternative oxidase-dependent respiratory chains in the filamentous fungus *Podospora anserina*,

(2004). doi:10.1074/jbc.M402756200.

[62] J. Zhu, K.R. Vinothkumar, J. Hirst, Structure of mammalian respiratory complex I., Nature. 536 (2016) 354–358. doi:10.1038/nature19095.

[63] L.A. Sazanov, A giant molecular proton pump: structure and mechanism of respiratory complex I, Nat. Publ. Gr. 16 (2015). doi:10.1038/nrm3997.

[64] C. Wirth, U. Brandt, C. Hunte, V. Zickermann, Mitochondrial complex I inhibitor rotenone induces apoptosis through enhancing mitochondrial reactive oxygen species production, J. Biol. Chem. 278 (2003) 1005–1011. doi:10.1042/BJ20081386.

[65] U. Schulte, Biogenesis of Respiratory Complex I, J. Bioenerg. Biomembr. 33 (2001) 205–212. doi:10.1023/A:1010730919074.

[66] G. Cecchini, Function and Structure of Complex II of the Respiratory Chain, Annu. Rev. Biochem. 72 (2003) 77–109. doi:10.1146/annurev.biochem.72.121801.161700.

[67] F. Sun, X. Huo, Y. Zhai, A. Wang, J. Xu, D. Su, M. Bartlam, Z. Rao, Crystal structure of mitochondrial respiratory membrane protein Complex II, Cell. 121 (2005) 1043–1057. doi:10.1016/j.cell.2005.05.025.

[68] D. Xia, L. Esser, W.-K.K. Tang, F. Zhou, Y. Zhou, L. Yu, C.-A.A. Yu, Structural analysis of cytochrome bc1 complexes: Implications to the mechanism of function, Biochim. Biophys. Acta - Bioenerg. 1827 (2013) 1278–1294. doi:10.1016/j.bbabio.2012.11.008.

[69] M. D'Aurelio, C.D. Gajewski, G. Lenaz, G. Manfredi, Respiratory chain supercomplexes set the threshold for respiration defects in human mtDNA mutant cybrids, Hum. Mol. Genet. 15 (2006) 2157–2169. doi:10.1093/hmg/ddl141.

[70] M. Duarte, A. Videira, Effects of mitochondrial complex III disruption in the respiratory chain of *Neurospora crassa*, Mol. Microbiol. 72 (2009) 246–258. doi:10.1111/j.1365-2958.2009.06643.x.

[71] F. Fontanesi, I.C. Soto, D. Horn, A. Barrientos, Assembly of mitochondrial cytochrome c-oxidase, a complicated and highly regulated cellular process, Am. J. Physiol. Cell Physiol. 291 (2006) C1129–C1147. doi:10.1152/ajpcell.00233.2006.

[72] I.C. Soto, F. Fontanesi, J. Liu, A. Barrientos, Biogenesis and assembly of eukaryotic cytochrome c oxidase catalytic core, Biochim. Biophys. Acta - Bioenerg. 1817 (2012) 883–897. doi:10.1016/j.bbabio.2011.09.005.

[73] Y. Chaban, E.J. Boekema, N. V. Dudkina, Structures of mitochondrial oxidative phosphorylation supercomplexes and mechanisms for their stabilisation, Biochim. Biophys. Acta - Bioenerg. 1837 (2014) 418–426. doi:10.1016/j.bbabio.2013.10.004.

[74] S.H. Ackerman, A. Tzagoloff, Function, Structure, and Biogenesis of Mitochondrial ATP Synthase, in: 2005: pp. 95–133. doi:10.1016/S0079-6603(05)80003-0.

[75] A.I. Jonckheere, J.A.M. Smeitink, R.J.T. Rodenburg, Mitochondrial ATP synthase: architecture, function and pathology, J. Inherit. Metab. Dis. 35 (2012) 211–225. doi:10.1007/s10545-011-9382-9.

[76] F.E. Nargang, K. Adames, C. Rüb, S. Cheung, N. Easton, C.E. Nargang, M.S. Chae, Identification of genes required for alternative oxidase production in the *Neurospora crassa* gene knockout library., G3 (Bethesda). 2 (2012) 1345–56. doi:10.1534/g3.112.004218.

[77] P. Carneiro, M. Duarte, A. Videira, The main external alternative NAD(P)H dehydrogenase of *Neurospora crassa* mitochondria, Biochim. Biophys. Acta - Bioenerg. 1608 (2004) 45–52. doi:10.1016/j.bbabio.2003.10.004.

[78] A.P. Gonçalves, A. Videira, Mitochondrial type II NAD(P)H dehydrogenases in fungal cell death., Microb. Cell (Graz, Austria). 2 (2015) 68–73. doi:10.15698/mic2015.03.192.

[79] M. Duarte, M. Peters, U. Schulte, A. Videira, The internal alternative NADH dehydrogenase of *Neurospora crassa* mitochondria, Biochem. J. 371 (2003) 1005–1011. doi:10.1042/BJ20021374.

[80] G.C. Vanlerberghe, L. McIntosh, Alternative oxidase: from gene to function, Annu. Rev. Plant Physiol. Plant Mol. Biol. 48 (1997) 703–734. doi:10.1146/annurev.arplant.48.1.703.

[81] L.L. Tanton, C.E. Nargang, K.E. Kessler, Q. Li, F.E. Nargang, Alternative oxidase expression in *Neurospora crassa*, Fungal Genet. Biol. 39 (2003) 176–190. doi:10.1016/S1087-1845(03)00002-1.

[82] A.E. Mcdonald, Alternative oxidase: an inter-kingdom perspective on the function and regulation of this broadly distributed “cyanide-resistant” terminal oxidase, (n.d.). doi:10.1071/FP08025.

[83] A.M. Lambowitz, J.R. Sabourin, H. Bertrand, R. Nickels, L. McIntosh, Immunological identification of the alternative oxidase of *Neurospora crassa* mitochondria., Mol. Cell. Biol. 9 (1989) 1362–4.

[84] A.T. Descheneau, I.A. Cleary, F.E. Nargang, Genetic evidence for a regulatory pathway controlling alternative oxidase production in *Neurospora crassa*, Genetics. 169 (2005)

123–135. doi:10.1534/genetics.104.034017.

[85] Z. Qi, K.M. Smith, E.L. Bredeweg, N. Bosnjak, M. Freitag, F.E. Nargang, Alternative oxidase transcription factors AOD2 and AOD5 of *Neurospora crassa* control the expression of genes involved in energy production and metabolism, G3: Genes|Genomes|Genetics. 7 (2017) 449–466. doi:10.1534/g3.116.035402.

[86] T. Magnani, F.M. Soriani, V. de P. Martins, A.C. de F. Policarpo, C.A. Sorgi, L.H. Faccioli, C. Curti, S.A. Uyemura, Silencing of mitochondrial alternative oxidase gene of *Aspergillus fumigatus* enhances reactive oxygen species production and killing of the fungus by macrophages, J. Bioenerg. Biomembr. 40 (2008) 631–636. doi:10.1007/s10863-008-9191-5.

[87] S. Akhter, H.C. McDade, J.M. Gorlach, G. Heinrich, G.M. Cox, J.R. Perfect, Role of alternative oxidase gene in pathogenesis of *Cryptococcus neoformans*., Infect. Immun. 71 (2003) 5794–802. doi:10.1128/IAI.71.10.5794-5802.2003.

[88] O. Hernández Ruiz, A. Gonzalez, A.J. Almeida, D. Tamayo, A.M. Garcia, A. Restrepo, J.G. McEwen, Alternative oxidase mediates pathogen resistance in *Paracoccidioides brasiliensis* infection, PLoS Negl. Trop. Dis. 5 (2011) e1353. doi:10.1371/journal.pntd.0001353.

[89] D. Munro, J.R. Treberg, A radical shift in perspective: mitochondria as regulators of reactive oxygen species, J. Exp. Biol. Online Mar (2017) 1170–1180. doi:10.1242/jeb.132142.

[90] R.J. Mailloux, Teaching the fundamentals of electron transfer reactions in mitochondria

and the production and detection of reactive oxygen species, Redox Biol. 4 (2015) 381–398. doi:10.1016/j.redox.2015.02.001.

[91] A.Y. Andreyev, Y.E. Kushnareva, A.N. Murphy, A.A. Starkov, Mitochondrial ROS metabolism: 10 Years later, Biochem. 80 (2015) 517–531. doi:10.1134/S0006297915050028.

[92] C.L. Quinlan, I. V. Perevoshchikova, M. Hey-Mogensen, A.L. Orr, M.D. Brand, Sites of reactive oxygen species generation by mitochondria oxidizing different substrates, Redox Biol. 1 (2013) 304–312. doi:10.1016/j.redox.2013.04.005.

[93] K.M. Holmström, T. Finkel, Cellular mechanisms and physiological consequences of redox-dependent signalling, Nat. Publ. Gr. 15 (2014). doi:10.1038/nrm3801.

[94] Q. Li, L.M. Harvey, B. McNeil, Oxidative stress in industrial fungi., Crit. Rev. Biotechnol. 29 (2009) 199–213. doi:10.1080/07388550903004795.

[95] T.C.M. Seah, A.R. Bhatti, J.G. Kaplan, Novel catalatic proteins of bakers' yeast. I. an atypical catalase, Can. J. Biochem. 51 (1973) 1551–1555. doi:10.1139/o73-208.

[96] V.Y. Petrova, T.V. Rasheva, A. V. Kujumdzieva, Catalase enzyme in mitochondria of *Saccharomyces cerevisiae*, Electron. J. Biotechnol. 5 (2002) 0–0.

[97] W. Schliebs, C. Würtz, W.H. Kunau, M. Veenhuis, H. Rottensteiner, A eukaryote without catalase-containing microbodies: *Neurospora crassa* exhibits a unique cellular distribution of its four catalases, Eukaryot. Cell. 5 (2006) 1490–1502. doi:10.1128/EC.00113-06.

[98] R.H. Davis, *Neurospora* : contributions of a model organism, Oxford University Press, 2000.

[99] V. Lushchak, H. Semchyshyn, S. Mandryk, O. Lushchak, Possible role of superoxide dismutases in the yeast *Saccharomyces cerevisiae* under respiratory conditions, Arch. Biochem. Biophys. 441 (2005) 35–40. doi:10.1016/j.abb.2005.06.010.

[100] M.J. Kwon, B.H. Kim, Y.S. Lee, T.Y. Kim, Role of superoxide dismutase 3 in skin inflammation, J. Dermatol. Sci. 67 (2012) 81–87. doi:10.1016/j.jdermsci.2012.06.003.

[101] M.B. Lewin, P.S. Timiras, Lipid changes with aging in cardiac mitochondrial membranes, Mech. Ageing Dev. 24 (1984) 343–351. doi:10.1016/0047-6374(84)90119-2.

[102] A.I.P.M. De Kroon, A. Mayer, R. Lill, B. De Kruijff, A.I. de Kroon, D. Dolis, A. Mayer, R. Lill, B. de Kruijff, Phospholipid composition of highly purified mitochondrial outer membranes of rat liver and *Neurospora crassa*. Is cardiolipin present in the mitochondrial outer membrane?, Biochim Biophys Acta. 1325 (1997) 108–116. doi:S0005-2736(96)00240-4 [pii].

[103] E.M. Mejia, G.M. Hatch, Mitochondrial phospholipids: role in mitochondrial function, J. Bioenerg. Biomembr. 48 (2016) 99–112. doi:10.1007/s10863-015-9601-4.

[104] H. Wu, B.S.H. Ng, G. Thibault, Endoplasmic reticulum stress response in yeast and humans., Biosci. Rep. 34 (2014) 321–330. doi:10.1042/BSR20140058.

[105] J.S. Cox, C.E. Shamu, P. Walter, Transcriptional induction of genes encoding endoplasmic reticulum resident proteins requires a transmembrane protein kinase., Cell. 73 (1993) 1197–206. http://www.ncbi.nlm.nih.gov/pubmed/8513503.

[106] P. Walter, D. Ron, The Unfolded Protein Response: from stress pathway to homeostatic regulation, Science (80-. ). 334 (2011) 1081–1086. doi:10.1126/science.1209038.

[107] J.S. Cox, P. Walter, A novel mechanism for regulating activity of a transcription factor that controls the unfolded protein response, Cell. 87 (1996) 391–404. doi:10.1016/S0092-8674(00)81360-4.

[108] B.M. Gardner, D. Pincus, K. Gotthardt, C.M. Gallagher, P. Walter, Endoplasmic Reticulum stress sensing in the unfolded protein response, Cold Spring Harb. Perspect. Biol. 5 (2013) a013169–a013169. doi:10.1101/cshperspect.a013169.

[109] K. Okamura, Y. Kimata, H. Higashio, A. Tsuru, K. Kohno, Dissociation of Kar2p/BiP from an ER Sensory Molecule, Ire1p, Triggers the Unfolded Protein Response in Yeast, Biochem. Biophys. Res. Commun. 279 (2000) 445–450. doi:10.1006/bbrc.2000.3987.

[110] D. Oikawa, Y. Kimata, K. Kohno, T. Iwawaki, Activation of mammalian IRE1α upon ER stress depends on dissociation of BiP rather than on direct interaction with unfolded proteins, Exp. Cell Res. 315 (2009) 2496–2504. doi:10.1016/j.yexcr.2009.06.009.

[111] F.E. Nargang, D. Rapaport, *Neurospora crassa* as a model organism for mitochondrial biogenesis, Mitochondria. 372 (2007) 107–123. http://dx.doi.org/10.1007/978-1-59745-365-3_8.

[112] S. Schmitt, H. Prokisch, T. Schlunck, D.G.C. Ii, B.A. Mayer, A. Driessen, W. Neupert, S. Schmitt, H. Prokisch, T. Schlunck, D.G. Camp, U. Ahting, T. Waizenegger, C. Scharfe, T. Meitinger, A. Imhof, W. Neupert, P.J. Oefner, D. Rapaport, D.G.C. Ii, Proteome analysis of mitochondrial outer membrane from *Neurospora crassa*, Proteomics. 6 (2006) 72–80. doi:10.1002/pmic.200402084.

[113] J.G. Wideman, N.E. Go, A. Klein, E. Redmond, S.W.K. Lackey, T. Tao, H. Kalbacher, D.

Rapaport, W. Neupert, F.E. Nargang, Roles of the Mdm10, Tom7, Mdm12, and Mmm1 proteins in the assembly of mitochondrial outer membrane proteins in *Neurospora crassa.*, Mol. Biol. Cell. 21 (2010) 1725–36. doi:10.1091/mbc.E09-10-0844.

[114] W.A.T. Summers, D.A. Court, Origami in outer membrane mimetics: correlating the first detailed images of refolded VDAC with over 20 years of biochemical data., Biochem. Cell Biol. 88 (2010) 425–438. doi:10.1139/o09-115.

[115] Q. Li, R.G. Ritzel, L. McLean, L. McIntosh, T. Ko, H. Bertrand, F.E. Nargang, Cloning and analysis of the alternative oxidase gene of *Neurospora crassa*., Genetics. 142 (1996) 129–140.

[116] K. Altmann, M. Dürr, B. Westermann, *Saccharomyces cerevisiae* as a model organism to study mitochondrial biology, in: Humana Press, 2007: pp. 81–90. doi:10.1007/978-1-59745-365-3_6.

[117] H. Galganska, M. Budzinska, M. Wojtkowska, H. Kmita, Redox regulation of protein expression in *Saccharomyces cerevisiae* mitochondria: Possible role of VDAC, Arch. Biochem. Biophys. 479 (2008) 39–45. doi:10.1016/j.abb.2008.08.010.

[118] S. Reina, V. Palermo, A. Guarnera, F. Guarino, A. Messina, C. Mazzoni, V. De Pinto, Swapping of the N-terminus of VDAC1 with VDAC3 restores full activity of the channel and confers anti-aging features to the cell, FEBS Lett. 584 (2010) 2837–2844. doi:10.1016/j.febslet.2010.04.066.

[119] H.W. Mager, J. Winderickx, Yeast as a model for medical and medicinal research, TRENDS Pharmacol. Sci. 26 (2005) 265–273.

[120] J.E. Galagan, S.E. Calvo, K.A. Borkovich, E.U. Selker, N.D. Read, D. Jaffe, W. FitzHugh, L.-J. Ma, S. Smirnov, S. Purcell, B. Rehman, T. Elkins, R. Engels, S. Wang, C.B. Nielsen, J. Butler, M. Endrizzi, D. Qui, P. Ianakiev, D. Bell-Pedersen, M.A. Nelson, M. Werner-Washburne, C.P. Selitrennikoff, J.A. Kinsey, E.L. Braun, A. Zelter, U. Schulte, G.O. Kothe, G. Jedd, W. Mewes, C. Staben, E. Marcotte, D. Greenberg, A. Roy, K. Foley, J. Naylor, N. Stange-Thomann, R. Barrett, S. Gnerre, M. Kamal, M. Kamvysselis, E. Mauceli, C. Bielke, S. Rudd, D. Frishman, S. Krystofova, C. Rasmussen, R.L. Metzenberg, D.D. Perkins, S. Kroken, C. Cogoni, G. Macino, D. Catcheside, W. Li, R.J. Pratt, S.A. Osmani, C.P.C. DeSouza, L. Glass, M.J. Orbach, J.A. Berglund, R. Voelker, O. Yarden, M. Plamann, S. Seiler, J. Dunlap, A. Radford, R. Aramayo, D.O. Natvig, L.A. Alex, G. Mannhaupt, D.J. Ebbole, M. Freitag, I. Paulsen, M.S. Sachs, E.S. Lander, C. Nusbaum, B. Birren, The genome sequence of the filamentous fungus *Neurospora crassa*, Nature. 422 (2003) 859–868. doi:10.1038/nature01554.

[121] A. Goffeau, B.G. Barrell, H. Bussey, R.W. Davis, B. Dujon, H. Feldmann, F. Galibert, J.D. Hoheisel, C. Jacq, M. Johnston, E.J. Louis, H.W. Mewes, Y. Murakami, P. Philippsen, H. Tettelin, S.G. Oliver, Life with 6000 genes., Science. 274 (1996) 546, 563–7.

[122] W. Beadle, L. Tatum, Genetic control of biochemical reactions in *Neurospora*, Proc. Natl. Acad. Sci. 27 (1941) 499–506.

[123] C.M. Roche, J.J. Loros, K. McCluskey, N.L. Glass, N. Louise Glass, *Neurospora crassa:* Looking back and looking forward at a model microbe, Am. J. Bot. 101 (2014) 2022–2035. doi:10.3732/ajb.1400377.

[124] R.H. Davis, F.J. de Serres, Genetic and microbiological research techniques for *Neurospora crassa,* Methods Enzymol. 17 (1970) 79–143. doi:10.1016/0076-6879(71)17168-6.

[125] R.D. Gietz, R.H. Schiestl, High-efficiency yeast transformation using the LiAc/SS carrier DNA/PEG method, Nat. Protoc. 2 (2007) 31–34. doi:10.1038/nprot.2007.13.

[126] G. Giaever, C. Nislow, The yeast deletion collection: a decade of functional genomics., Genetics. 197 (2014) 451–65. doi:10.1534/genetics.114.161620.

[127] T. Hodge, M. Colombini, Regulation of metabolite flux through voltage-gating of VDAC channels, J. Membr. Biol. 157 (1997) 271–279. doi:10.1007/s002329900235.

[128] D.A. Koppel, K.W. Kinnally, P. Masters, M. Forte, E. Blachly-Dyson, C.A. Mannella, Bacterial expression and characterization of the mitochondrial outer membrane channel. Effects of n-terminal modifications, J Biol Chem. 273 (1998) 13794–13800. doi:10.1074/jbc.273.22.13794.

[129] V. De Pinto, S. Reina, F. Guarino, A. Messina, Structure of the voltage dependent anion channel: State of the art, J. Bioenerg. Biomembr. 40 (2008) 139–147. doi:10.1007/s10863-008-9140-3.

[130] B. Popp, D.A. Court, R. Benz, W. Neupert, R. Lill, The role of the N and C termini of recombinan*t Neurospora* mitochondrial porin in channel formation and voltage-dependent gating, J. Biol. Chem. 271 (1996) 13593–13599. doi:10.1074/jbc.271.23.13593.

[131] D.A. Court, R. Kleene, W. Neupert, R. Lill, Role of the N- and C-termini of porin in import into the outer membrane of *Neurospora* mitochondria, FEBS Lett. 390 (1996) 73–

77. doi:10.1016/0014-5793(96)00629-1.

[132] H. V Colot, G. Park, G.E. Turner, C. Ringelberg, C.M. Crew, L. Litvinkova, R.L. Weiss, K.A. Borkovich, J.C. Dunlap, A high-throughput gene knockout procedure for *Neurospora* reveals functions for multiple transcription factors., Proc. Natl. Acad. Sci. U. S. A. 103 (2006) 10352–7. doi:10.1073/pnas.0601456103.

[133] Y. Ninomiya, K. Suzuki, C. Ishii, H. Inoue, Highly efficient gene replacements in *Neurospora* strains deficient for nonhomologous end-joining., Proc. Natl. Acad. Sci. U. S. A. 101 (2004) 12248–53. doi:10.1073/pnas.0402780101.

[134] C. Staben, B. Jensen, M. Singer, J. Pollock, M. Schechtman, J. Kinsey, E. Selker, Use of a bacterial hygromycin B resistance gene as a dominant selectable marker in *Neurospora crassa* transformation., Fungal Genet. Newsl. 36 (1989) 79–81.

[135] K. McCluskey, A. Wiest, M. Plamann, The Fungal Genetics Stock Center: a repository for 50 years of fungal genetics research., J. Biosci. 35 (2010) 119–26.

[136] T.A.A. Harkness, F.E. Nargang, I. Van Der Klei, W. Neupert, R. Lill, A crucial role of the mitochondrial protein import receptor MOM19 for the biogenesis of mitochondria, J. Cell Biol. 124 (1994) 637–648.

[137] S. Banh, L. Wiens, E. Sotiri, J.R. Treberg, Mitochondrial reactive oxygen species production by fish muscle mitochondria: Potential role in acute heat-induced oxidative stress., Comp. Biochem. Physiol. B. Biochem. Mol. Biol. 191 (2015) 99–107. doi:10.1016/j.cbpb.2015.10.001.

[138] A. V Kuznetsov, V. Veksler, F.N. Gellerich, V. Saks, R. Margreiter, W.S. Kunz, Analysis

of mitochondrial function in situ in permeabilized muscle fibers, tissues and cells., Nat. Protoc. 3 (2008) 965–976. doi:10.1038/nprot.2008.61.

[139] H. Bertrand, B.S. Chan, A.J. Griffiths, Insertion of a foreign nucleotide sequence into mitochondrial DNA causes senescence in *Neurospora intermedia*., Cell. 41 (1985) 877–84. doi:10.1016/S0092-8674(85)80068-4.

[140] D. Coil, G. Jospin, A.E. Darling, A5-miseq: an updated pipeline to assemble microbial genomes from Illumina MiSeq data, Bioinformatics. 31 (2015) 587–589. doi:10.1093/bioinformatics/btu661.

[141] A. Tritt, J.A. Eisen, M.T. Facciotti, A.E. Darling, An Integrated Pipeline for de Novo Assembly of Microbial Genomes, PLoS One. 7 (2012) e42304. doi:10.1371/journal.pone.0042304.

[142] K. Rutherford, J. Parkhill, J. Crook, T. Horsnell, P. Rice, M.-A. Rajandream, B. Barrell, Artemis: sequence visualization and annotation, Bioinformatics. 16 (2000) 944–945. doi:10.1093/bioinformatics/16.10.944.

[143] L.A. Gautheret Daniel, Direct RNA motif definition and identification from multiple sequence alignments using secondary structure profiles1, J. Mol. Biol. 313 (2001) 1003–1011. doi:10.1006/JMBI.2001.5102.

[144] B.F. Lang, M.-J. Laforest, G. Burger, Mitochondrial introns: a critical view, Trends Genet. 23 (2007) 119–125. doi:10.1016/j.tig.2007.01.006.

[145] K. Katoh, K. Misawa, K. Kuma, T. Miyata, MAFFT: a novel method for rapid multiple sequence alignment based on fast Fourier transform., Nucleic Acids Res. 30 (2002) 3059–

66.

[146] A. Shevchenko, H. Tomas, J. Havli\[sbreve], J. V Olsen, M. Mann, In-gel digestion for mass spectrometric characterization of proteins and proteomes, Nat. Protoc. 1 (2007) 2856–2860. doi:10.1038/nprot.2006.468.

[147] A. V. Loboda, A.N. Krutchinsky, M. Bromirski, W. Ens, K.G. Standing, A tandem quadrupole/time-of-flight mass spectrometer with a matrix-assisted laser desorption/ionization source: design and performance, Rapid Commun. Mass Spectrom. 14 (2000) 1047–1057. doi:10.1002/1097-0231(20000630)14:12<1047::AID-RCM990>3.0.CO;2-E.

[148] H. Towbin, T. Staehelin, J. Gordon, Electrophoretic transfer of proteins from polyacrylamide gels to nitrocellulose sheets: procedure and some applications., Proc. Natl. Acad. Sci. 76 (1979) 4350–4354. doi:10.1073/pnas.76.9.4350.

[149] A. Infanger, H. Bertrand, Inversions and recombinations in mitochondrial DNA of the (SG-1) cytoplasmic mutant in two *Neurospora species*., Curr. Genet. 10 (1986) 607–17.

[150] A.M. Lambowitz, C.W. Slayivan, B.D.W.J. Slayman, Clifford L, The electron transport components of wild type and poky strains of *Neurospora crassa,* J. Biol. Chem. 247 (1972) 1536–1545.

[151] E. Agsteribbe, M. Hartog, H. de Vries, Duplication of the tRNA M Met and tRNACys genes and of fragments of a gene encoding a subunit of the NADH dehydrogenase complex in *Neurospora grassa* mitochondrial DNA, Curr. Genet. 15 (1989) 57–62. doi:10.1007/BF00445752.

[152] A.B. Desaulniers, The role of YVH1, a dual specificity phosphatase, in the production of alternative oxidase in the filamentous fungus *Neurospora crassa,* M.Sc. thesis, University of Alberta, Edmonton

[153] J. Dukanovic, D. Rapaport, Multiple pathways in the integration of proteins into the mitochondrial outer membrane, Biochim. Biophys. Acta - Biomembr. 1808 (2011) 971–980. doi:10.1016/j.bbamem.2010.06.021.

[154] P. Carneiro, M. Duarte, A. Videira, Disruption of alternative NAD(P)H dehydrogenases leads to decreased mitochondrial ROS in *Neurospora crassa,* Free Radic. Biol. Med. 52 (2012) 402–409. doi:10.1016/j.freeradbiomed.2011.10.492.

[155] I.M. Møller, Plant mitochondria and oxidative stress: electron transport, NADPH turnover, and metabolism of reactive oxygen species, Annu. Rev. Plant Physiol. Plant Mol. Biol. 52 (2001) 561–91.

[156] D.P. Maxwell, Y. Wang, L. Mcintosh, H.J. Kende, The alternative oxidase lowers mitochondrial reactive oxygen production in plant cells, Plant Biol. 96 (1999) 8271–8276.

[157] M.D. Brand, The sites and topology of mitochondrial superoxide production, Exp. Gerontol. 45 (2010) 466–472. doi:10.1016/j.exger.2010.01.003.

[158] S.R. Shuvo, U. Kovaltchouk, A. Zubaer, A. Kumar, W.A.T. Summers, L.J. Donald, G. Hausner, D.A. Court, Functional characterization of an N-terminally truncated mitochondrial porin expressed in *Neurospora crassa*, Can. J. Microbiol. 68 (2017) 730–738. doi:10.1139/cjm-2016-0764.

[159] T. Dráb, J. Kračmerová, I. Tichá, E. Hanzlíková, M. Tichá, H. Ryšlavá, V. Doubnerová,

P. Maňásková-Postlerová, J. Liberda, Native Red Electrophoresis - A new method suitable for separation of native proteins, Electrophoresis. 32 (2011) 3597–3599. doi:10.1002/elps.201100310.

[160] A.E. Frazier, D.R. Thorburn, Biochemical analyses of the electron transport chain complexes by spectrophotometry, Methods Mol Biol. (2012) 49–62. doi:10.1007/978-1-61779-504-6_4.

[161] D.L. Hoffman, P.S. Brookes, Oxygen sensitivity of mitochondrial reactive oxygen species generation depends on metabolic conditions, J. Biol. Chem. 284 (2009) 16236–16245. doi:10.1074/jbc.M809512200.

[162] S. Banh, J.R. Treberg, The pH sensitivity of H2O2 metabolism in skeletal muscle mitochondria, FEBS Lett. 587 (2013) 1799–1804. doi:10.1016/j.febslet.2013.04.035.

[163] Y. Liu, G. Fiskum, D. Schubert, Generation of reactive oxygen species by the mitochondrial electron transport chain, J Neurochem. 80 (2002) 780–787. doi:10.1046/j.0022-3042.2002.00744.x.

[164] E.W. Lambowitz, Alan. M. & Smith, C.W. Slaymany, Oxidative Phosphorylation in *Neurospora* Mitochondria Studies on wild type,poky and chloramphenicol- induced wild type., J. Biol. CHBMISTRY. 247 (1972) 4859–4865.

[165] E.P. Isakova, L.V. Gorpenko, E.I. Shurubor, T.A. Belozerskaya, R.A. Zvyagilskaya, Isolation and characterization of tightly-coupled mitochondria from wild type and nap-mutant of *Neurospora crassa*, Biokhimiya. 67 (2002) 260–264.

[166] P.J.M. Schwitzguebel Jean-paul, Rotenone and cyanide-insensitive respiration in

mitochondria from *Neurospora crassa*, *J*. Gen. Microbiol. 129 (1983) 2387–2397.

[167] E.N. Maldonado, K.L. Sheldon, D.N. DeHart, J. Patnaik, Y. Manevich, D.M. Townsend, S.M. Bezrukov, T.K. Rostovtseva, J.J. Lemasters, Voltage-dependent anion channels modulate mitochondrial metabolism in cancer cells: regulation by free tubulin and erastin., J. Biol. Chem. 288 (2013) 11920–9. doi:10.1074/jbc.M112.433847.

[168] D. Tewari, D. Majumdar, S. Vallabhaneni, A.K. Bera, P. Pinton, Aspirin induces cell death by directly modulating mitochondrial voltage-dependent anion channel (VDAC), Sci. Rep. 7 (2017) 45184. doi:10.1038/srep45184.

[169] M.D. Brand, D.G. Nicholls, Assessing mitochondrial dysfunction in cells., Biochem. J. 435 (2011) 297–312. doi:10.1042/BJ20110162.

[170] M. Klingenberg, The ADP and ATP transport in mitochondria and its carrier, Biochim. Biophys. Acta - Biomembr. 1778 (2008) 1978–2021. doi:10.1016/j.bbamem.2008.04.011.

[171] M. Klingenberg, The ADP-ATP translocation in mitochondria, a membrane potential controlled transport, J. Membr. Biol. 56 (1980) 97–105. doi:10.1007/BF01875961.

[172] S. Reina, F. Guarino, A. Magri, V. De Pinto, VDAC3 As a potential marker of mitochondrial status is involved in cancer and pathology, Front. Oncol. 6 (2016) 264. doi:10.3389/fonc.2016.00264.

[173] A. Phillip West, G.S. Shadel, S. Ghosh, Mitochondria in innate immune responses, Nat. Publ. Gr. 11 (2011). doi:10.1038/nri2975.

[174] M. Madesh, G. Hajnóczky, VDAC-dependent permeabilization of the outer mitochondrial membrane by superoxide induces rapid and massive cytochrome c release, J. Cell Biol.

155 (2001).

[175] V. Shoshan-Barmatz, D. Mizrachi, VDAC1: from structure to cancer therapy., Front. Oncol. 2 (2012) 164. doi:10.3389/fonc.2012.00164.

[176] J.R. Treberg, C.L. Quinlan, M.D. Brand, Evidence for two sites of superoxide production by mitochondrial NADH-ubiquinone oxidoreductase (complex I)., J. Biol. Chem. 286 (2011) 27103–10. doi:10.1074/jbc.M111.252502.

[177] A.J. Lambert, M.D. Brand, Superoxide production by NADH:ubiquinone oxidoreductase (complex I) depends on the pH gradient across the mitochondrial inner membrane, Biochem. J. 382 (2004) 511–517.

[178] X. Ma, M. Jin, Y. Cai, H. Xia, K. Long, J. Liu, Q. Yu, J. Yuan, Mitochondrial electron transport chain complex III is required for antimycin A to inhibit autophagy., Chem. Biol. 18 (2011) 1474–81. doi:10.1016/j.chembiol.2011.08.009.

[179] C.L. Quinlan, A.A. Gerencser, J.R. Treberg, M.D. Brand, The mechanism of superoxide production by the antimycin-inhibited mitochondrial Q-cycle., J. Biol. Chem. 286 (2011) 31361–72. doi:10.1074/jbc.M111.267898.

[180] N.M. Mazure, VDAC in cancer, BBA - Bioenerg. 1858 (2017) 665–673. doi:10.1016/j.bbabio.2017.03.002.

[181] R. Benz, A. Schmid, M. Dihanich, Pores from mitochondrial outer membranes of yeast and a porin-deficient yeast mutant: A comparison, J. Bioenerg. Biomembr. 21 (1989) 439–450. doi:10.1007/BF00762516.

[182] C.A. Mannella, Minireview: on the structure and gating mechanism of the mitochondrial

channel, VDAC., J. Bioenerg. Biomembr. 29 (1997) 525–31. http://www.ncbi.nlm.nih.gov/pubmed/9559853 (accessed August 9, 2017).

[183] J.R. Wiśniewski, A. Zougman, N. Nagaraj, M. Mann, Universal sample preparation method for proteome analysis, Nat. Methods. 6 (2009) 359–362. doi:10.1038/nmeth.1322.

[184] R.C. Dwivedi, V. Spicer, M. Harder, M. Antonovici, W. Ens, K.G. Standing, J.A. Wilkins, O. V. Krokhin, Practical implementation of 2D HPLC scheme with accurate peptide retention prediction in both dimensions for high-throughput bottom-up proteomics, Anal. Chem. 80 (2008) 7036–7042. doi:10.1021/ac800984n.

[185] N. Rodriguez-Cousino, R. Lill, W. Neupert, D.A. Court, Identification and initial characterization of the cytosolic protein Ycr77p, Yeast. 11 (1995) 581–585. doi:10.1002/yea.320110608.

[186] R. Craig, R.C. Beavis, TANDEM: matching proteins with tandem mass spectra, Bioinformatics. 20 (2004) 1466–1467. doi:10.1093/bioinformatics/bth092.

[187] P. Mcqueen, V. Spicer, T. Rydzak, R. Sparling, D. Levin, J.A. Wilkins, O. Krokhin, Information-dependent LC-MS/MS acquisition with exclusion lists potentially generated on-the-fly: Case study using a whole cell digest of Clostridium thermocellum, Proteomics. 12 (2012) 1160–1169. doi:10.1002/pmic.201100425.

[188] P. Mcqueen, V. Spicer, J. Schellenberg, O. Krokhin, R. Sparling, D. Levin, J.A. Wilkins, Whole cell, label free protein quantitation with data independent acquisition: Quantitation at the MS2 level, Proteomics. 15 (2015) 16–24. doi:10.1002/pmic.201400188.

[189] S. Wushke, V. Spicer, X.L. Zhang, B. Fristensky, O. V. Krokhin, D.B. Levin, N. Cicek, R.

Sparling, Understanding aerobic/anaerobic metabolism in *Caldibacillus debilis* through a comparison with model organisms, Syst. Appl. Microbiol. 40 (2017) 245–253. doi:10.1016/j.syapm.2017.03.004.

[190] A. Montenegro-Montero, A. Goity, L.F. Larrondo, The bZIP transcription factor HAC-1 is involved in the unfolded Protein response and is necessary for growth on cellulose in *Neurospora crassa,* PLoS One. 10 (2015) e0131415. doi:10.1371/journal.pone.0131415.

[191] L. Karaffa, K. Váczy, E. Sándor, S. Biró, A. Szentirmai, I. Pócsi, Cyanide-resistant alternative respiration is strictly correlated to intracellular peroxide levels in *Acremonium Chrysogenum*, Free Radic. Res. 34 (2001) 405–416. doi:10.1080/10715760100300341.

[192] P.N. Fernandes, S.C. Mannarino, C.G. Silva, M.D. Pereira, A.D. Panek, E.C.A. Eleutherio, Oxidative stress response in eukaryotes: effect of glutathione, superoxide dismutase and catalase on adaptation to peroxide and menadione stresses in *Saccharomyces cerevisiae*, Redox Rep. 12 (2007) 236–244. doi:10.1179/135100007X200344.

[193] P.C. Loewen, J. Villanueva, J. Switala, L.J. Donald, A. Ivancich, Unprecedented access of phenolic substrates to the heme active site of a catalase: Substrate binding and peroxidase-like reactivity of *Bacillus pumilus* catalase monitored by X-ray crystallography and EPR spectroscopy, Proteins Struct. Funct. Bioinforma. 83 (2015) 853–866. doi:10.1002/prot.24777.

[194] R. Sestric, G. Munch, N. Cicek, R. Sparling, D.B. Levin, Growth and neutral lipid synthesis by Yarrowia lipolytica on various carbon substrates under nutrient-sufficient and nutrient-limited conditions, Bioresour. Technol. 164 (2014) 41–46.

doi:10.1016/j.biortech.2014.04.016.

[195] L. Larsson, A. Saraf, Use of gas chromatography-ion trap tandem mass spectrometry for the detection and characterization of microorganisms in complex samples, Mol. Biotechnol. 7 (1997) 279–287. doi:10.1007/BF02740818.

[196] M.H. Moghadasian, P. Moghadasian, K. Le, A. Hydamaka, P. Zahradka, Lipid Analyses of Four Types of Fish from Manitoba Lakes, ECronicon. 1 (2015) 41–48. https://ecronicon.com/ecnu/pdf/ECNU-01-00008.pdf (accessed August 15, 2017).

[197] A. Ruepp, A. Zollner, D. Maier, K. Albermann, J. Hani, M. Mokrejs, I. Tetko, U. Güldener, G. Mannhaupt, M. Münsterkötter, H.W. Mewes, The FunCat, a functional annotation scheme for systematic classification of proteins from whole genomes, Nucleic Acids Res. 32 (2004) 5539–5545. doi:10.1093/nar/gkh894.

[198] S. Priebe, C. Kreisel, F. Horn, R. Guthke, J. Linde, FungiFun2: a comprehensive online resource for systematic analysis of gene lists from fungal species., Bioinformatics. 31 (2015) 445–6. doi:10.1093/bioinformatics/btu627.

[199] M. Kafri, E. Metzl-Raz, G. Jona, N. Barkai, The cost of protein production., Cell Rep. 14 (2016) 22–31. doi:10.1016/j.celrep.2015.12.015.

[200] A.G. Hinnebusch, The Scanning Mechanism of Eukaryotic Translation Initiation, Annu. Rev. Biochem. 83 (2014) 779–812. doi:10.1146/annurev-biochem-060713-035802.

[201] G.A. Marzluf, Molecular Genetics of sulphur assimilation in filamentus fungi and yeast, Annu. Rev. Microbiol. 51 (1997) 73–96.

[202] R.S. Phillips, Chemistry and diversity of pyridoxal-5-phosphate dependent enzymes,

Biochim. Biophys. Acta - Proteins Proteomics. 1854 (2015) 1167–1174. doi:10.1016/j.bbapap.2014.12.028.

[203] P.L. Pedersen, Transport ATPases: Structure, motors, mechanism and medicine: A brief overview, J. Bioenerg. Biomembr. 37 (2005) 349–357. doi:10.1007/s10863-005-9470-3.

[204] E. Margolles-Clark, K. Tenney, E.J. Bowman, B.J. Bowman, The Structure of the Vacuolar ATPase in Neurospora crassa, J. Bioenerg. Biomembr. 31 (1999) 29–37. doi:10.1023/a:1005403427848.

[205] N. Plesofsky, L. Higgins, T. Markowski, R. Brambl, Glucose starvation alters heat shock response, leading to death of wild type cells and survival of MAP kinase signaling mutant, PLoS One. 11 (2016) e0165980. doi:10.1371/journal.pone.0165980.

[206] W. Wang, B. Vinocur, O. Shoseyov, A. Altman, Role of plant heat-shock proteins and molecular chaperones in the abiotic stress response, Trends Plant Sci. 9 (2004) 244–252. doi:10.1016/j.tplants.2004.03.006.

[207] P.J. M Rørth, Determination of catalase activity by means of the Clark oxygen electrode, Biochim. Biophys. Acta - Enzymol. 39 (1967) 171–173.

[208] T.K. Rostovtseva, S.M. Bezrukov, VDAC regulation: Role of cytosolic proteins and mitochondrial lipids, J. Bioenerg. Biomembr. 40 (2008) 163–170. doi:10.1007/s10863-008-9145-y.

[209] Z.A. Ma, The role of peroxidation of mitochondrial membrane phospholipids in pancreatic β -cell failure., Curr. Diabetes Rev. 8 (2012) 69–75.

[210] A. Messina, S. Reina, F. Guarino, V. De Pinto, VDAC isoforms in mammals, Biochim.

Biophys. Acta - Biomembr. 1818 (2012) 1466–1476. doi:10.1016/j.bbamem.2011.10.005.

[211] J. Zhu, X. Yu, B. Xie, X. Gu, Z. Zhang, S. Li, Transcriptomic profiling-based mutant screen reveals three new transcription factors mediating menadione resistance in Neurospora crassa, Fungal Biol. 117 (2013) 422–430. doi:10.1016/j.funbio.2013.04.006.

[212] R. Ozgur, B. Uzilday, A.H. Sekmen, I. Turkan, The effects of induced production of reactive oxygen species in organelles on endoplasmic reticulum stress and on the unfolded protein response in arabidopsis, Ann. Bot. 116 (2015) 541–553. doi:10.1093/aob/mcv072.

[213] A.A. Spector, M.A. Yorek, Membrane lipid composition and cellular function, J. Lipid Res. 26 (1985) 1015–1035. doi:3906008.

[214] W. Tan, VDAC blockage by phosphorothioate oligonucleotides and its implication in apoptosis, Biochim. Biophys. Acta - Biomembr. 1818 (2012) 1555–1561. doi:10.1016/j.bbamem.2011.12.032.

[215] S.P. Mathupala, P.L. Pedersen, Voltage dependent anion channel-1 (VDAC-1) as an anti-cancer target., Cancer Biol. Ther. 9 (2010) 1053–6. http://www.ncbi.nlm.nih.gov/pubmed/20581475 (accessed August 9, 2017).

[216] M.J. kamita Hanna, Stobienia Olgierd, The access of metabolites into yeast mitochondria in the presence and absence of voltage dependent anion selective channel (YVDAC1), Acta Biochim. Pol. 46 (1999) 991–1000.

[217] E. Blachly-Dyson, J. Song, W.J. Wolfgang, M. Colombini, M. Forte, Multicopy suppressors of phenotypes resulting from the absence of yeast VDAC encode a VDAC-like protein, Mol Cell Biol. 17 (1997) 5727–5738.

http://www.ncbi.nlm.nih.gov/pubmed/9315631 (accessed August 21, 2017).

[218] J.A. Stefely, N.W. Kwiecien, E.C. Freiberger, A.L. Richards, A. Jochem, M.J.P. Rush, A. Ulbrich, K.P. Robinson, P.D. Hutchins, M.T. Veling, X. Guo, Z.A. Kemmerer, K.J. Connors, E.A. Trujillo, J. Sokol, H. Marx, M.S. Westphall, A.S. Hebert, D.J. Pagliarini, J.J. Coon, Mitochondrial protein functions elucidated by multi-omic mass spectrometry profiling., Nat. Biotechnol. 34 (2016) 1191–1197. doi:10.1038/nbt.3683.

[219] E.A. Winzeler, D.D. Shoemaker, A. Astromoff, H. Liang, K. Anderson, B. Andre, R. Bangham, R. Benito, J.D. Boeke, H. Bussey, A.M. Chu, C. Connelly, K. Davis, F. Dietrich, S.W. Dow, M. El Bakkoury, F. Foury, S.H. Friend, E. Gentalen, G. Giaever, J.H. Hegemann, T. Jones, M. Laub, H. Liao, N. Liebundguth, D.J. Lockhart, A. Lucau-Danila, M. Lussier, N. M'Rabet, P. Menard, M. Mittmann, C. Pai, C. Rebischung, J.L. Revuelta, L. Riles, C.J. Roberts, P. Ross-MacDonald, B. Scherens, M. Snyder, S. Sookhai-Mahadeo, R.K. Storms, S. Véronneau, M. Voet, G. Volckaert, T.R. Ward, R. Wysocki, G.S. Yen, K. Yu, K. Zimmermann, P. Philippsen, M. Johnston, R.W. Davis, Functional characterization of the *S. cerevisiae* genome by gene deletion and parallel analysis., Science. 285 (1999) 901–6.

[220] S.D. Finlayson, C. Fleming, D.R. Berry, J.R. Johnston, An improved lithium acetate method for yeast transformation, Biotechnol. Tech. 5 (1991) 13–18. doi:10.1007/BF00152747.

[221] S.K. Sariki, P.K. Sahu, U. Golla, V. Singh, G.K. Azad, R.S. Tomar, Sen1, the homolog of human Senataxin, is critical for cell survival through regulation of redox homeostasis, mitochondrial function, and the TOR pathway in *Saccharomyces cerevisiae*, FEBS J. 283

(2016) 4056–4083. doi:10.1111/febs.13917.

[222] C. Meisinger, N. Pfanner, K.N. Truscott, isolation of yeast mitochondria.pdf, Humana Press, New Jersey, 2006. doi:10.1385/1-59259-958-3:033.

[223] N.Q. Torelli, J.R. Ferreira-Júnior, A.J. Kowaltowski, F.M. da Cunha, F. Marques, D. Cunha, RTG1- and RTG2-dependent retrograde signaling controls mitochondrial activity and stress resistance in *Saccharomyces cerevisiae*, Free Radic. Biol. Med. 81 (2015) 30–37. doi:10.1016/j.freeradbiomed.2014.12.025.

[224] G. Thibault, N. Ismail, D.T.W. Ng, The unfolded protein response supports cellular robustness as a broad-spectrum compensatory pathway., Proc. Natl. Acad. Sci. U. S. A. 108 (2011) 20597–602. doi:10.1073/pnas.1117184109.

[225] N.R. Merritt, The influence of temperature on some properties of yeast., J. Inst. Brew. 72 (1966) 374–383. doi:10.1002/j.2050-0416.1966.tb02977.x.

[226] M. Dihanich, K. Suda, G. Schatz, A yeast mutant lacking mitochondrial porin is respiratory-deficient, but can recover respiration with simultaneous accumulation of an 86-kd extramitochondrial protein., EMBO J. 6 (1987) 723–728. doi:10.1002/J.1460-2075.1987.TB04813.X.

[227] V.R. Simon, T.C. Swayne, L.A. Pon, Actin-dependent mitochondrial motility in mitotic yeast and cell-free systems: Identification of a motor activity on the mitochondrial surface, J. Cell Biol. 130 (1995) 345–354. doi:10.1083/jcb.130.2.345.

[228] D.S. Kudryashov, E. Reisler, ATP and ADP actin states., Biopolymers. 99 (2013) 245–56. doi:10.1002/bip.22155.

[229] R. Kumarswamy, S. Chandna, Putative partners in Bax mediated cytochrome-c release: ANT, CypD, VDAC or none of them?, Mitochondrion. 9 (2009) 1–8. doi:10.1016/j.mito.2008.10.003.

[230] M.L. Circu, T.Y. Aw, Reactive oxygen species, cellular redox systems, and apoptosis., Free Radic. Biol. Med. 48 (2010) 749–62. doi:10.1016/j.freeradbiomed.2009.12.022.

[231] H.-U. Simon, A. Haj-Yehia, F. Levi-Schaffer, Role of reactive oxygen species (ROS) in apoptosis induction, APOPTOSIS. 5 (2000) 415–418. doi:10.1023/A:1009616228304.

[232] M. Rinnerthaler, S. Jarolim, G. Heeren, E. Palle, S. Perju, H. Klinger, E. Bogengruber, F. Madeo, R.J. Braun, L. Breitenbach-Koller, M. Breitenbach, P. Laun, MMI1 (YKL056c, TMA19), the yeast orthologue of the translationally controlled tumor protein (TCTP) has apoptotic functions and interacts with both microtubules and mitochondria, Biochim. Biophys. Acta - Bioenerg. 1757 (2006) 631–638. doi:10.1016/j.bbabio.2006.05.022.

[233] L. Kazemzadeh, M. Cvijovic, D. Petranovic, Boolean model of yeast apoptosis as a tool to study yeast and human apoptotic regulations, Front. Physiol. 3 DEC (2012) 1–18. doi:10.3389/fphys.2012.00446.

[234] J.R. Murguía, R. Serrano, New functions of protein kinase Gcn2 in yeast and mammals, IUBMB Life. 64 (2012) 971–974. doi:10.1002/iub.1090.

[235] R.J. Dohmen, R. Stappen, J.P. McGrath, H. Forrova, J. Kolarov, A. Goffeau, A. Varshavsky, H. Forrová, J. Kolarov, A. Goffeau, A. Varshavsky, An essential yeast gene encoding a homolog of ubiquitin-activating enzyme, J. Biol. Chem. 270 (1995) 18099–18109. doi:10.1074/jbc.270.30.18099.

[236] M. Guo, P. Schimmel, Essential nontranslational functions of tRNA synthetases., Nat. Chem. Biol. 9 (2013) 145–53. doi:10.1038/nchembio.1158.

[237] H. Atamna, J. Newberry, R. Erlitzki, C.S. Schultz, B.N. Ames, Biotin deficiency inhibits heme synthesis and impairs mitochondria in human lung fibroblasts., J. Nutr. 137 (2007) 25–30. http://www.ncbi.nlm.nih.gov/pubmed/17182796.

[238] F. Torres-Quiroz, S. García-Marqués, R. Coria, F. Randez-Gil, J.A. Prieto, The activity of yeast Hog1 MAPK is required during endoplasmic reticulum stress induced by tunicamycin exposure, J. Biol. Chem. 285 (2010) 20088–20096. doi:10.1074/jbc.M109.063578.

[239] L.M. Ballou, R.Z. Lin, Rapamycin and mTOR kinase inhibitors., J. Chem. Biol. 1 (2008) 27–36. doi:10.1007/s12154-008-0003-5.

[240] G. Farrugia, R. Balzan, Oxidative Stress and Programmed Cell Death in Yeast, Front. Oncol. 2 (2012) 1–21. doi:10.3389/fonc.2012.00064.

[241] I. Shokolenko, N. Venediktova, A. Bochkareva, G.L. Wilson, M.F. Alexeyev, Oxidative stress induces degradation of mitochondrial DNA, Nucleic Acids Res. 37 (2009) 2539–2548. doi:10.1093/nar/gkp100.

[242] M. de Taffin de Tilques, D. Tribouillard-Tanvier, E. Tétaud, E. Testet, J.-P. di Rago, J.-P. Lasserre, Overexpression of mitochondrial oxodicarboxylate carrier (ODC1) preserves oxidative phosphorylation in a yeast model of Barth syndrome., Dis. Model. Mech. 10 (2017) 439–450. doi:10.1242/dmm.027540.

[243] A. Vozza, E. Blanco, L. Palmieri, F. Palmieri, Identification of the mitochondrial

GTP/GDP transporter in *Saccharomyces cerevisiae.*, J. Biol. Chem. 279 (2004) 20850–7. doi:10.1074/jbc.M313610200.

[244] A. Castegna, P. Scarcia, G. Agrimi, L. Palmieri, H. Rottensteiner, I. Spera, L. Germinario, F. Palmieri, Identification and functional characterization of a novel mitochondrial carrier for citrate and oxoglutarate in *Saccharomyces cerevisiae.*, J. Biol. Chem. 285 (2010) 17359–70. doi:10.1074/jbc.M109.097188.

[245] F. Frigerio, M. Casimir, S. Carobbio, P. Maechler, Tissue specificity of mitochondrial glutamate pathways and the control of metabolic homeostasis, (2008). doi:10.1016/j.bbabio.2008.04.031.

[246] E. Benítez-Rangel, M. López-Méndez, L. García, A. Guerrero-Hernández, DIDS (4,4'-Diisothiocyanatostilbene-2,2'-disulfonate) directly inhibits caspase activity in HeLa cell lysates, Cell Death Discov. 1 (2015) 15037. doi:10.1038/cddiscovery.2015.37.

[247] P. Davalli, T. Mitic, A. Caporali, A. Lauriola, D. D'Arca, ROS, Cell Senescence, and Novel Molecular Mechanisms in Aging and Age-Related Diseases, Oxid. Med. Cell. Longev. 2016 (2016). doi:10.1155/2016/3565127.

[248] A. Magrì, A. Messina, Interactions of VDAC with proteins involved in neurodegenerative aggregation: an opportunity for advancement on therapeutic molecules, Curr. Med. Chem. 24 (2017) 1–18. doi:10.2174/0929867324666170601073920.

[249] K. Jitobaom, N. Tongluan, D.R. Smith, Involvement of voltage-dependent anion channel (VDAC) in dengue infection, Sci. Rep. 6 (2016) 1–12. doi:10.1038/srep35753.

[250] W. Lin, Z. Zhang, Z. Xu, B. Wang, X. Li, H. Cao, Y. Wang, S.J. Zheng, The association

of receptor of activated protein kinase C 1(RACK1) with infectious bursal disease virus viral protein VP5 and voltage-dependent anion channel 2 (VDAC2) inhibits apoptosis and enhances viral replication, J. Biol. Chem. 290 (2015) 8500–8510. doi:10.1074/jbc.M114.585687.

[251] L. Danelishvili, J.J.J. Chinison, T. Pham, R. Gupta, L.E. Bermudez, The Voltage-Dependent Anion Channels (VDAC) of Mycobacterium avium phagosome are associated with bacterial survival and lipid export in macrophages, Sci. Rep. 7 (2017) 1–14. doi:10.1038/s41598-017-06700-3.

[252] K. Guan, Z. Zheng, T. Song, X. He, C. Xu, Y. Zhang, S. Ma, Y. Wang, Q. Xu, Y. Cao, J. Li, X. Yang, X. Ge, C. Wei, H. Zhong, MAVS regulates apoptotic cell death by decreasing K48-linked ubiquitination of voltage-dependent anion channel 1., Mol. Cell. Biol. 33 (2013) 3137–49. doi:10.1128/MCB.00030-13.

[253] J.S. Lee, W.K. Huh, B.H. Lee, Y.U. Baek, C.S. Hwang, S.T. Kim, Y.R. Kim, S.O. Kang, Mitochondrial NADH-cytochrome b(5) reductase plays a crucial role in the reduction of D-erythroascorbyl free radical in *Saccharomyces cerevisiae.*, Biochim. Biophys. Acta. 1527 (2001) 31–8.

[254] G.I. Belogrudov, P.T. Lee, T. Jonassen, A.Y. Hsu, P. Gin, C.F. Clarke, Yeast COQ4 Encodes a Mitochondrial Protein Required for Coenzyme Q Synthesis, Arch. Biochem. Biophys. 392 (2001) 48–58. doi:10.1006/abbi.2001.2448.

[255] P. Carneiro, M. Duarte, A. Videira, G. Henrique Goldman, U. de Sao Paulo, Characterization of apoptosis-related oxidoreductases from *Neurospora crassa*, PLoS One. 7 (2012). doi:10.1371/journal.pone.0034270.

[256] B. Gehl, C.P. Lee, P. Bota, M.R. Blatt, L.J. Sweetlove, An *Arabidopsis* stomatin-like protein affects mitochondrial respiratory supercomplex organization, PLANT Physiol. 164 (2014) 1389–1400. doi:10.1104/pp.113.230383.

[257] P. Mitsopoulos, Y.-H. Chang, T. Wai, T. König, S.D. Dunn, T. Langer, J. Madrenas, Stomatin-Like protein 2 is required for *in vivo* mitochondrial respiratory chain supercomplex formation and optimal cell function, Mol. Cell. Biol. 35 (2015) 1838–1847. doi:10.1128/MCB.00047-15.

[258] J. Sun, C. Tian, S. Diamond, N.L. Glass, Deciphering transcriptional regulatory mechanisms associated with hemicellulose degradation in *Neurospora crassa*, Eukaryot. Cell. 11 (2012) 482–493. doi:10.1128/EC.05327-11.

# Chapter 7: Appendix

## Appendix 7.1

Table 1. Observed intensity of the MALDI-produced monoisotopic ions from VDAC and ANT. Manual peak pick using the expected ions list as a guide.

| STRAIN | WT | | LoPo | | ΔN2-12-1 | | ΔN2-12-2 | | ΔPor-1 | | | | | | |
|---|---|---|---|---|---|---|---|---|---|---|---|---|---|---|---|
| SAMPLE | SR15 | | SR16 | | SR17 | | SR18 | | SR19 | | | | | | |
| SPECTRUM II | 10986 | 11004 | 10985 | 11006 | 10984 | 11007 | 10983 | 11008 | 10982 | 11009 | | expected ion | from | to | sequence |
| xpected ions | intensity | intensity | intensity | intensity | intensity | intensity | intensity | intensity | intensity | intensity | | | | | |
| VDAC | | | | | | | | | | | | VDAC | | | |
| 845.402 | 6462 | 4905 | 0 | 0 | 0 | 0 | 0 | 0 | 0 | 0 | | 845.402 | 119 | 125 | QSNFHGR |
| 974.447 | 7167 | 4343 | 3157 | 0 | 0 | 0 | 0 | 0 | 0 | 0 | | 974.447 | 275 | 283 | VGTSFTFES |
| 1018.517 | 6077 | 4747 | 4050 | 3977 | 0 | 0 | 0 | 0 | 0 | 0 | | 1018.517 | 197 | 206 | VNSQVEAGSK |
| 1091.549 | 5317 | 3535 | 0 | 0 | 0 | 0 | 0 | 0 | 0 | 0 | | 1091.549 | 33 | 42 | SNTPNNVAFK |
| 1189.643 | 10223 | 6864 | 7260 | 7871 | 5040 | 4676 | 4007 | 6106 | 0 | 0 | | 1189.643 | 213 | 224 | TGNTVGLEVATK |
| 1259.748 | 19277 | 14967 | 5403 | 6027 | 0 | 0 | 0 | 0 | 0 | 0 | | 1259.748 | 241 | 252 | GVAAIAYNVLLR |
| 1493.775 | 42465 | 29260 | 14379 | 15018 | 0 | 0 | 0 | 0 | 0 | 0 | | 1493.775 | 96 | 109 | AEGIFSFLPATNAR |
| 1758.003 | 10178 | 8336 | 4232 | 4784 | 0 | 0 | 0 | 0 | 0 | 0 | | 1758.003 | 237 | 252 | INDRGVAAIAYNVLLR |
| 2045.042 | 4685 | 3895 | 4657 | 4746 | 3153 | 2986 | 4115 | 5089 | 0 | 0 | | 2045.042 | 33 | 51 | SNTPNNVAFKVTGKSTHDK |
| 2302.168 | 13011 | 9961 | 0 | 5126 | 0 | 0 | 0 | 0 | 0 | 0 | | 2302.168 | 253 | 274 | EGVTLGVGASFDTQKLDQATHK |
| 2319.199 | 25589 | 17129 | 6683 | 6697 | 0 | 0 | 0 | 0 | 0 | 0 | | 2319.199 | 12 | 32 | SANDLLNKDFYHLAAGTIEVK |
| 2658.316 | 5422 | 3669 | 0 | 0 | 0 | 0 | 0 | 0 | 0 | 0 | | 2658.316 | 133 | 159 | GPTANIDAIVGHEGFLAGASAGYDVQK |
| 3257.597 | 3000 | 2126 | 0 | 0 | 0 | 0 | 0 | 0 | 0 | 0 | | 3257.597 | 253 | 283 | EGVTLGVGASFDTQKLDQATHKVGTSFTFES |
| 3492.78 | 4470 | 2769 | 916 | 1001 | 0 | 0 | 0 | 0 | 0 | 0 | | 3492.78 | 126 | 159 | AFFDLLKGPTANIDAIVGHEGFLAGASAGYDVQK |
| 3521.759 | 3597 | 2279 | 1212 | 1052 | 0 | 0 | 0 | 0 | 0 | 0 | | 3521.759 | 61 | 92 | FTDKPNGLTVTQTWNTANALETKVEMADNLAK |
| 3839.856 | 2667 | 2020 | 942 | 775 | 0 | 0 | 0 | 0 | 0 | 0 | | 3839.856 | 160 | 196 | AAITGYSAAVGYHAPTYSAAITATDNLSVFSASYYHK |
| VDAC | 169607 | 120805 | 52891 | 57074 | 8193 | 7662 | 8122 | 11195 | 0 | 0 | | | | | |

| ANT | | | | | | | | | | | | ANT | | | |
|---|---|---|---|---|---|---|---|---|---|---|---|---|---|---|---|
| 1045.601 | 6022 | 3116 | 3840 | 4151 | 2706 | 3431 | 0 | 0 | 0 | 0 | | 1045.601 | 146 | 155 | LANDAKSAKK |
| 1210.622 | 25812 | 17583 | 17513 | 15372 | 11459 | 10274 | 8136 | 10838 | 8736 | 8929 | | 1210.622 | 160 | 169 | QFNGLVDVYR |
| 1236.659 | 28521 | 20571 | 23803 | 16080 | 11044 | 10376 | 6341 | 6070 | 13035 | 8068 | | 1236.659 | 171 | 182 | TIASDGIAGLYR |
| 1285.636 | 30298 | 14043 | 25430 | 21954 | 14553 | 17641 | 11907 | 14847 | 8658 | 11943 | | 1285.636 | 57 | 66 | YNGIIDCFKR |
| 1321.727 | 82659 | 53755 | 64637 | 53182 | 37222 | 38126 | 16740 | 22017 | 24971 | 37331 | | 1321.727 | 183 | 195 | GFGPSVAGIVVYR |
| 1338.717 | 41184 | 27072 | 30682 | 23628 | 22028 | 18313 | 14189 | 20204 | 16690 | 17717 | | 1338.717 | 160 | 170 | QFNGLVDVYRK |
| 1349.652 | 47574 | 30205 | 38645 | 35374 | 23277 | 22449 | 21069 | 33846 | 14273 | 23273 | | 1349.652 | 67 | 78 | TTADEGVMALWR |
| 1358.71 | 32059 | 23344 | 18493 | 17870 | 13965 | 12342 | 7294 | 10666 | 9494 | 11688 | | 1358.71 | 39 | 49 | LLVQNQDEMIR |
| 1364.754 | 14843 | 10806 | 10677 | 8717 | 5800 | 5490 | 4329 | 5044 | 7409 | 6375 | | 1364.754 | 170 | 182 | KTIASDGIAGLYR |
| 1441.737 | 11933 | 6655 | 13173 | 11049 | 7891 | 9660 | 8173 | 12120 | 5096 | 6385 | | 1441.737 | 56 | 66 | RYNGIIDCFKR |
| 1474.748 | 79114 | 48152 | 54906 | 42089 | 32893 | 30986 | 21804 | 24341 | 21713 | 26785 | | 1474.748 | 87 | 98 | YFPTQALNFAFR |
| 1599.889 | 25165 | 18198 | 15270 | 14021 | 11096 | 10390 | 11457 | 14076 | 9964 | 10579 | | 1599.889 | 37 | 49 | IKLLVQNQDEMIR |
| 1717.87 | 42844 | 23849 | 30256 | 23125 | 17830 | 17054 | 13268 | 14513 | 12019 | 16745 | | 1717.87 | 87 | 100 | YFPTQALNFAFRDK |
| 2193.145 | 15474 | 8078 | 11060 | 8665 | 8041 | 6917 | 10469 | 11455 | 8709 | 10401 | | 2193.145 | 7 | 28 | VLGMPPFVADFLMGGVSAAVSK |
| 2409.329 | 7306 | 5653 | 5741 | 5460 | 4321 | 4220 | 5640 | 6608 | 6228 | 5900 | | 2409.329 | 29 | 49 | TAAAPIERIKLLVQNQDEMIR |
| ANT | 490808 | 311080 | 364126 | 300737 | 224126 | 217669 | 160816 | 206645 | 166995 | 202119 | | | | | |
| VDAC/ANT | 0.35 | 0.39 | 0.15 | 0.19 | 0.04 | 0.04 | 0.05 | 0.05 | 0.00 | 0.00 | | | | | |
| % of WT | 100 | | 46 | | 10 | | 14 | | 0 | | | | | | |
| (average of two spectra) | | | | | | | | | | | | | | | |

**Appendix 7.1 Table 2**. Descriptions of ORFs for which mRNA levels were analyzed by qRT-PCR.

| **ORF*** | **Annotation** | **Relative mRNA expression level i) ΔPor-1† ii) Δ2-12porin** | **Putative function and comments** | **Reference** |
|---|---|---|---|---|
| NCU07953 | Alternative oxidase-1 | i) n/d‡ ii) 0.9 | Expressed when electron flow through electron transport chain is prevented | [115] |
| NCU06518 | NADH-cytochrome $b_5$ reductase | i) n/d ii) 0.5 | Ergosterol biosynthesis and oxidative stress response | [253] |
| NCU02157 | COQ4 | i) 3.7 ii) 0.2 | Ubiquinone biosynthesis | [254] |
| NCU05850 | Rubredoxin-NAD(+) reductase | i) 14.9 ii) 2.5 | Identified as apoptosis-inducing factor -1 (*aif-1)* | [255] |
| NCU05633 | Stomatin family protein | i) 7.0 ii) 1.0 | Related to SLP2 of mouse and AtSLP1 of *Arabidopsis thaliana*, which are involved in the assembly of respiratory super complexes in the inner membrane | [256,257] |
| NCU04173 | β-Actin | n/a§ | Used to normalize qRT-PCR data | [258] |
| NCU08476 | Conserved hypothetical protein | i) 9.2 ii) 2.0 | Unknown function | |
| NCU11655/ NCU04304 | Porin | i) n/a ii) 2.0 | Voltage dependent anion channel | [13] |

*ORF numbers are taken from *Neurospora crassa* Sequencing Project, Broad Institute of Harvard and MIT (http://www.broadinstitute.org/)

**Appendix 7.2:**

Figure 1.

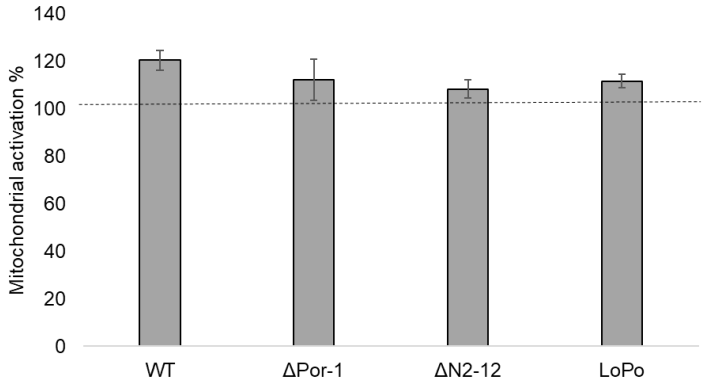


Appendix 7.2 Figure 1. Activation of mitochondrial oxygen consumption in the presence of succinate by exogenous cytochrome *c* in different strains. Intactness was estimated based on the ratio of OCR in the presence of exogenous cytochrome to state, as the degree of activation of oxygen consumption by exogenous cytochrome *c* is indicative of level of damage to the outer membrane. The dotted line indicates 100%.

Appendix 7.2 Figure 2

A.

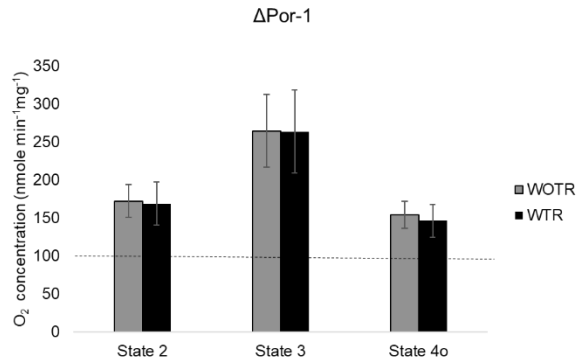


B.

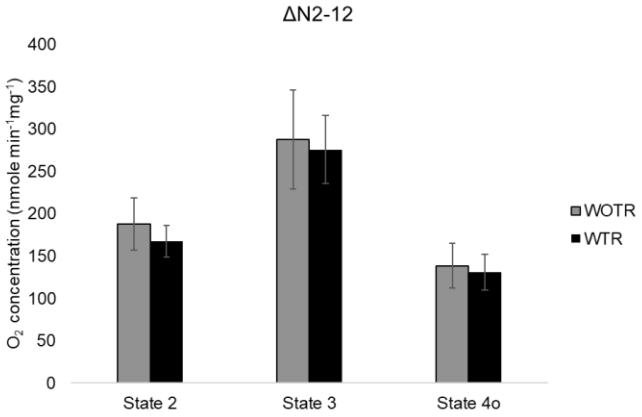


C.

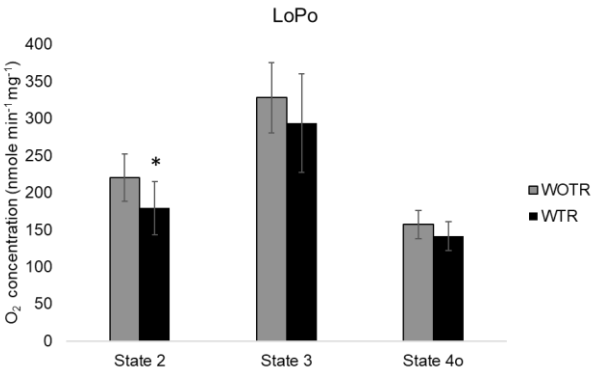

Appendix 7.2 Figure 2: Mitochondrial respiration rates in different states in the presence of GMS. (A) ΔPor-1, (B) ΔN2-12porin, (C) LoPo, with (WTR) and without (WOTR) TMRM. Rates were measured as described in materials and methods.

Appendix 7.2 Figure 3:

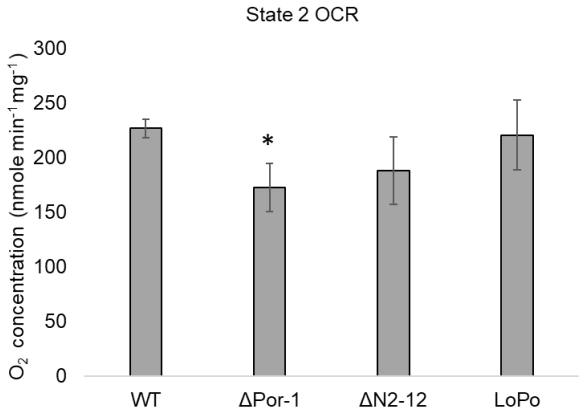


Appendix 7.2 Figure 3: Mitochondrial state 2 respiration in the presence of GMS.

**Appendix 7.3:**

**Appendix 7.3 Table 1.** Categories of proteins enriched the pool of down-regulated proteins in ΔPor-1.

Proteins in functional category 1.01 amino acid metabolism

| | |
|---|---|
| NCU01300 | imidazoleglycerol-phosphate dehydratase |
| NCU01439 | 2-oxoglutarate reductase |
| NCU01652 | O-acetylserine sulfhydrylase |
| NCU01985 | sulfate adenylyltransferase |
| NCU02274 | glycine hydroxymethyltransferase |
| NCU02325 | guanine-3 |
| NCU02704 | branched-chain alpha-keto acid dehydrogenase E2 component |
| NCU02936 | proline oxidase |
| NCU03010 | lysine-3 |
| NCU03425 | threonine synthase |
| NCU03973 | alanine transaminase |
| NCU04292 | branched-chain amino acid aminotransferase |
| NCU05238 | cysteine-4 |
| NCU06512 | methionine-8 |
| NCU07117 | ornithine-N5-oxygenase |
| NCU07930 | 4-aminobutyrate aminotransferase |
| NCU08998 | 4-aminobutyrate aminotransferase |
| NCU09864 | 2-oxoisovalerate dehydrogenase alpha subunit |
| NCU09896 | adenylyl-sulfate kinase |

Proteins in functional category 01.03.01 purin nucleotide/nucleoside/nucleobase metabolism

| | |
|---|---|
| NCU00177 | phosphoribosylformylglycinamidine cyclo-ligase |
| NCU01550 | adenylate kinase cytosolic |
| NCU01985 | cysteine-11 |
| NCU02274 | glycine hydroxymethyltransferase |
| NCU02325 | guanine-3 |
| NCU02979 | AMP deaminase |
| NCU03117 | inosine-5'-monophosphate dehydrogenase IMD2 |
| NCU03194 | phosphoribosylaminoimidazole |
| NCU03488 | pyrimidine-4 |
| NCU08685 | phosphoribosylformylglycinamidine synthase |
| NCU09789 | adenine-8 |
| NCU09896 | adenylyl-sulfate kinase |
| NCU10007 | acetate utilization-9 |

Proteins in functional category 12.04. translation

| | |
|---|---|
| NCU00475 | 40S ribosomal protein S18 |
| NCU00489 | cytoplasmic ribosomal protein-10 |
| NCU00971 | ribosomal protein S12 |
| NCU02810 | eukaryotic translation initiation factor 2 gamma subunit |
| NCU03757 | 60S ribosomal protein L4-A |
| NCU03806 | cycloheximide resistant-2 |
| NCU04640 | eukaryotic translation initiation factor 2 beta subunit |
| NCU04799 | polyadenylate-binding protein |
| NCU06843 | 60S ribosomal protein L3 |
| NCU07014 | cytoplasmic ribosomal protein-3 |
| NCU07830 | cytoplasmic ribosomal protein-2 |
| NCU08277 | eukaryotic translation initiation factor 2 alpha subunit |
| NCU08502 | 40S ribosomal protein S6 |
| NCU08620 | 40S ribosomal protein S16 |
| NCU08963 | 60S ribosomal protein L30 |
| NCU09475 | 40s ribosomal protein s5 |

Proteins in functional category 12.01.01 ribosomal proteins

| | |
|---|---|
| NCU00475 | 40S ribosomal protein S18 |
| NCU00489 | cytoplasmic ribosomal protein-10 |
| NCU00971 | ribosomal protein S12 |
| NCU03757 | 60S ribosomal protein L4-A |
| NCU03806 | cycloheximide resistant-2 |
| NCU06843 | 60S ribosomal protein L3 |
| NCU07014 | cytoplasmic ribosomal protein-3 |
| NCU07826 | 40S ribosomal protein S19 |
| NCU07830 | cytoplasmic ribosomal protein-2 |
| NCU08277 | eukaryotic translation initiation factor 2 alpha subunit |
| NCU08502 | 40S ribosomal protein S6 |
| NCU08620 | 40S ribosomal protein S16 |
| NCU08963 | 60S ribosomal protein L30 |
| NCU09475 | 40s ribosomal protein s5 |
| NCU09539 | 40S ribosomal protein S13 |

Proteins in functional category 01.03.01.03 purine nucleotide/nucleoside/nucleobase anabolism

| | |
|---|---|
| NCU00177 | phosphoribosylformylglycinamidine cyclo-ligase |
| NCU02325 | guanine-3 |
| NCU03117 | inosine-5'-monophosphate dehydrogenase |
| NCU03194 | phosphoribosylaminoimidazole |
| NCU08685 | phosphoribosylformylglycinamidine synthase |
| NCU09789 | adenine-8 |

Proteins in functional category 16.21.17 pyridoxal phosphate binding

| | |
|---|---|
| NCU01652 | O-acetylhomoserine |
| NCU03973 | alanine |
| NCU04292 | branched-chain-amino-acid aminotransferase |
| NCU08216 | cystathionine beta-synthase |
| NCU08998 | 4-aminobutyrate aminotransferase |
| NCU09116 | aromatic aminotransferase Aro8 |

Proteins in functional category 01.02.03.04 conjunction of sulfate

| | |
|---|---|
| NCU01985 | cysteine-11 |
| NCU09896 | adenylyl-sulfate kinase |

Proteins in functional category 01.02.03.01 sulfate assimilation

| | |
|---|---|
| NCU01985 | cysteine-11 |
| NCU05238 | cysteine-4 |
| NCU09896 | adenylyl-sulfate kinase |

Proteins in functional category 02.01 glycolysis and gluconeogenesis

| | |
|---|---|
| NCU01528 | glyceraldehyde-3-phosphate dehydrogenase-1 |
| NCU01754 | alcohol dehydrogenase-1 |
| NCU02704 | branched-chain alpha-keto acid dehydrogenase E2 component |
| NCU06075 | acetate-8 |
| NCU09873 | acetate utilization-6 |
| NCU10007 | acetate utilization-9 |
| NCU10042 | enolase |

**Appendix 7.3 Supplementary Table 2**: Categories of proteins enriched the pool of up-regulated proteins in ΔPor-1.

Proteins in functional category 01.05 C-compound and carbohydrate metabolism

| | |
|---|---|
| NCU00350 | epoxide hydrolase |

| | |
|---|---|
| NCU01092 | 3-oxoacyl-(acyl-carrier-protein) reductase |
| NCU03068 | pyridoxine-3 |
| NCU03949 | Nitronate monooxygenase |
| NCU05041 | Trehalose 6-phosphate synthase |
| NCU06482 | Pyruvate dehydrogenase E1 component alpha subunit |
| NCU07008 | Carotenoid oxygenase-1 |
| NCU07659 | Pyruvate dehydrogenase E2 component |
| NCU07737 | Salicylate hydroxylase |
| NCU08044 | Malonic semialdehyde reductase |
| NCU08402 | Zinc-binding alcohol dehydrogenase |
| NCU09798 | aryl-alcohol dehydrogenase |
| NCU10572 | short chain oxidoreductase |
| NCU00720 | L-lactate dehydrogenase |
| NCU00865 | oxalate decarboxylase |
| NCU01227 | Succinyl-CoA synthetase alpha subunit |
| NCU01272 | mitochondrial presequence protease |
| NCU01692 | Citrate synthesis |
| NCU02097 | short chain dehydrogenase |
| NCU02366 | Aconitate hydratase |
| NCU04483 | epoxide hydrolase |
| NCU07008 | Carotenoid oxygenase 1 |
| NCU06441 | 2-hydroxyglutarate---pyruvate transhydrogenase |
| NCU09519 | 2,5-diketo-D-gluconic acid reductase A |
| NCU09559 | clock-controlled gene-9 |

Proteins in functional category 01.05.02.07 sugar, glucoside, polyol and carboxylate catabolism

| | |
|---|---|
| NCU00720 | L-lactate dehydrogenase |
| NCU00865 | oxalate decarboxylase |
| NCU01227 | Succinyl-CoA synthetase alpha subunit |
| NCU01692 | Citrate synthesis |
| NCU02097 | short chain dehydrogenase |
| NCU02366 | Aconitate hydratase |
| NCU04483 | epoxide hydrolase |
| NCU05594 | L-galactose dehydrogenase |
| NCU06441 | 2-hydroxyglutarate---pyruvate transhydrogenase |
| NCU06687 | glycogen synthase-1 |
| NCU07240 | Aflatoxin B1 aldehyde reductase member 2 |
| NCU08384 | xylose reductase |
| NCU09519 | 2,5-diketo-D-gluconic acid reductase A |

Proteins in functional category 02.1 tricarboxylic-acid pathway (citrate cycle, Krebs cycle, TCA cycle)

| | |
|---|---|
| NCU00461 | glutamate dehydrogenase-1 |
| NCU00720 | L-lactate dehydrogenase |
| NCU01227 | succinate--CoA ligase |
| NCU01692 | citrate synthase |
| NCU02366 | Aconitate hydratase |
| NCU06482 | pyruvate dehydrogenase E1 component alpha subunit |
| NCU07659 | pyruvate dehydrogenase E2 component |

Proteins in functional category 32.01 stress response

| | |
|---|---|
| NCU00355 | catalase-3 |
| NCU00465 | chaperone dnaJ |
| NCU01589 | heat shock protein 60 |
| NCU01808 | cytochrome c-1 |
| NCU02113 | ubiquitin-conjugating enzyme E2 13 |
| NCU03068 | pyridoxine-3 |
| NCU03739 | ERP38 protein |
| NCU03786 | serine/threonine-protein phosphatase 2A regulatory subunit B |
| NCU04069 | 3'-phosphoadenosine 5'-phosphatase isoform B |
| NCU05041 | trehalose-phosphatase |
| NCU05143 | rds1 |
| NCU06372 | ubiquitin hydrolase L3 |
| NCU08693 | heat shock protein 70-5 |
| NCU09559 | clock-controlled gene-9 |

Proteins in functional category 02.13.03 aerobic respiration

| | |
|---|---|
| NCU01808 | cytochrome c-1 |
| NCU02162 | SURF-family protein |
| NCU02514 | ATPase-1 |
| NCU02549 | mitochondrial-processing peptidase subunit beta |
| NCU05430 | ATPase-2 |
| NCU06086 | Q subcomponent-binding protein, mitochondrial |
| NCU06141 | protoheme IX farnesyltransferase |
| NCU08004 | electron transfer flavoprotein alpha subunit |

Proteins in functional category 32.07.07.07 superoxide metabolism

| | |
|---|---|
| NCU00350 | epoxide hydrolase |
| NCU07851 | superoxide dismutase 1 copper chaperone |
| NCU09560 | superoxide dismutase |

Proteins in functional category 32.07.07.03 glutathione conjugation reaction

| | |
|---|---|
| NCU00173 | esterase D |
| NCU00549 | glutathione transferase omega-1 |
| NCU05780 | glutathione S-transferase-1 |

Proteins in functional category 32.01.05 heat shock response

| | |
|---|---|
| NCU00465 | chaperone dnaJ |
| NCU01166 | cAMP-dependent protein kinase regulator |
| NCU01589 | heat shock protein 60 |
| NCU08384 | xylose reductase |
| NCU08693 | heat shock protein 70-5 |

Proteins in functional category 32.07.07.01 catalase reaction

| | |
|---|---|
| NCU00355 | catalase-3 |
| NCU05770 | catalase-2 |

Proteins in functional category 20.03.22 transport ATPases

| | |
|---|---|
| NCU01207 | vacuolar membrane ATPase-1 |
| NCU02514 | ATPase-1 |
| NCU05430 | ATPase-2 |
| NCU07546 | multidrug resistance protein MDR |
| NCU08515 | vacuolar membrane ATPase-2 |
| NCU09975 | multidrug resistance protein 3 |

**Appendix 7.3 Table 3:** List of proteins that were differentially expressed and are part of UPR and ERAD pathways

**A. Proteins detected only in ΔPor-1**

| | |
|---|---|
| NCU00465 | chaperone dnaJ , also known as Hsp40 |
| NCU03732 | SIS1 |

| | |
|---|---|
| NCU09485 | chaperone dnaK |
| NCU02349 | UDP-glucose:glycoprotein glucosyltransferase |
| NCU02113 | ubiquitin-conjugating enzyme E2 13 |
| NCU09290 | proteasome catalytic beta-1 |
| NCU07257 | F-box domain-containing protein |
| NCU00879 | WD domain-containing protein |

**B. More abundant in both strains**

| | |
|---|---|
| NCU06738 | protein transporter sec-31 |
| NCU00880 | phospholipase A-2-activating protein |
| NCU03739 | ERP38 protein |
| NCU04404 | coatomer beta subunit |
| NCU01919 | ubiquitin C-terminal hydrolase |
| NCU06372 | ubiquitin hydrolase L3 |

**Appendix 7.3 Table 4:** List of proteins involved in A. lipid metabolism and B. conidiation

**A. Lipid metabolism**

| **A. Lipid Metabolism** | |
|---|---|
| **ORF designation** | **Predicted protein** |
| NCU09409 | arylesterase/monooxygenase |
| NCU03596 | CRAL/TRIO domain-containing protein |
| NCU01004 | phosphatidylserine decarboxylase proenzyme |
| **B. Conidiation** | |
| NCU05841 | UMTA |
| NCU06205 | regulator of conidiation-1 |
| NCU01797 | non-repressor of conidiation-2 |

Appendix 7.3 file 1:

*N. crassa* cytosolic proteins:

R0, R1 = Inter-replicate differences; Z0, Z1 = Replicates comparing different strains; NR0, NR1 = normalized, NZ0, NZ1 = combined vector of Z0 and Z1.

## More abundant proteins in ΔPor-1:

| Protein | Description | WT | WT-1 | ΔPor | ΔPor-1 | R0 | R1 | Z0 | Z1 | NR0 | NR1 | NZ0 | NZ1 | SN |
|---|---|---|---|---|---|---|---|---|---|---|---|---|---|---|
| NCU00021 | hypothetical protein | 17.2 | 16.06 | 19.6 | 20.2 | -1.2 | 0.62 | 2.35 | 4.13 | -1.176 | 0.493 | 2.07 | 3.743 | 3.35582 |
| NCU05780 | glutathione S-transferase-1 | 14.4 | 14.48 | 20.1 | 19.3 | 0.09 | -0.8 | 5.7 | 4.85 | 0.074 | -0.887 | 5.42 | 4.463 | 7.891538 |
| NCU09519 | 2,5-diketo-D-gluconic acid reductase A | 13.1 | 13.24 | 17.8 | 17.1 | 0.16 | -0.7 | 4.71 | 3.88 | 0.144 | -0.797 | 4.43 | 3.493 | 6.969454 |
| NCU10572 | short chain oxidoreductase | 17.4 | 19.04 | 21.9 | 22 | 1.64 | 0.07 | 4.48 | 2.91 | 1.624 | -0.057 | 4.2 | 2.523 | 3.017214 |
| NCU01272 | mitochondrial presequence protease | 16 | 16.84 | 20.3 | 20.1 | 0.83 | -0.2 | 4.29 | 3.23 | 0.814 | -0.357 | 4.01 | 2.843 | 5.533954 |
| NCU02549 | processing enhancing protein | 16.4 | 17.08 | 20.6 | 20.9 | 0.71 | 0.27 | 4.23 | 3.79 | 0.694 | 0.143 | 3.95 | 3.403 | 7.362274 |
| NCU09533 | NAD binding Rossmann fold oxidoreductase | 14.6 | 15.25 | 18.7 | 18.7 | 0.7 | 0.08 | 4.1 | 3.48 | 0.684 | -0.047 | 3.82 | 3.093 | 7.173574 |
| NCU02514 | ATPase-1 | 18.4 | 18.17 | 22.3 | 21.4 | -0.3 | -0.9 | 3.84 | 3.19 | 0.286 | -1.047 | 3.56 | 2.803 | 4.177596 |
| NCU09559 | clock-controlled gene-9 | 14.2 | 14.61 | 18 | 18.8 | 0.46 | 0.82 | 3.84 | 4.2 | 0.444 | 0.693 | 3.56 | 3.813 | 6.341533 |
| NCU03737 | elongation factor Tu | 15.8 | 15.65 | 19.5 | 19.7 | -0.1 | 0.23 | 3.71 | 4.08 | 0.156 | 0.103 | 3.43 | 3.693 | 26.97651 |
| NCU09560 | superoxide dismutase | 16.1 | 16.18 | 19.8 | 18.7 | 0.12 | -1 | 3.69 | 2.54 | 0.104 | -1.157 | 3.41 | 2.153 | 3.474485 |
| NCU05770 | catalase-2 | 18.7 | 18.88 | 22.3 | 22.5 | 0.18 | 0.17 | 3.58 | 3.57 | 0.164 | 0.043 | 3.3 | 3.183 | 27.05972 |
| NCU03739 | ERP38 protein | 14.8 | 15.96 | 18.4 | 18.1 | 1.16 | -0.3 | 3.55 | 2.11 | 1.144 | -0.407 | 3.27 | 1.723 | 3.046923 |
| NCU04930 | hypothetical protein | 15.4 | 16.03 | 19 | 19.3 | 0.63 | 0.27 | 3.54 | 3.31 | 0.584 | 0.243 | 3.26 | 2.923 | 6.926866 |
| NCU06441 | D-lactate dehydrogenase 2 | 15.6 | 16.49 | 18.9 | 18.8 | 0.89 | -0.2 | 3.33 | 2.27 | 0.884 | -0.287 | 3.05 | 1.883 | 3.860294 |
| NCU08130 | hypothetical protein | 17.6 | 17.87 | 20.9 | 20.7 | 0.26 | -0.2 | 3.32 | 2.87 | 0.244 | -0.317 | 3.04 | 2.483 | 9.819882 |
| NCU02809 | hypothetical protein | 11.3 | 11.09 | 14.5 | 16.6 | -0.2 | 2.1 | 3.24 | 5.55 | 0.226 | 1.973 | 2.96 | 5.163 | 2.997786 |
| NCU01589 | heat shock protein 60 | 18.7 | 18.83 | 21.8 | 21.6 | 0.13 | -0.2 | 3.11 | 2.81 | 0.114 | -0.297 | 2.83 | 2.423 | 11.72048 |
| NCU06086 | regulatory protein suaprga1 | 14.9 | 14.13 | 18 | 17.9 | -0.8 | -0.1 | 3.11 | 3.72 | 0.766 | -0.267 | 2.83 | 3.333 | 5.393221 |
| NCU00355 | catalase-3 | 19 | 19.52 | 22 | 22.4 | 0.48 | 0.42 | 2.96 | 2.9 | 0.464 | 0.293 | 2.68 | 2.513 | 6.700155 |
| NCU00549 | glutathione transferase omega-1 | 15.7 | 14.97 | 18.6 | 18.1 | -0.7 | -0.6 | 2.95 | 3.1 | 0.736 | -0.697 | 2.67 | 2.713 | 3.757953 |
| NCU09674 | O-methyltransferase family 3 | 17.8 | 18.46 | 20.8 | 21 | 0.64 | 0.22 | 2.94 | 2.52 | 0.624 | 0.093 | 2.66 | 2.133 | 5.409338 |
| NCU04483 | sedoheptulose-1,7-bisphosphatase | 15.2 | 16 | 18.1 | 18.4 | 0.79 | 0.31 | 2.91 | 2.42 | 0.774 | 0.173 | 2.63 | 2.033 | 4.195341 |
| NCU03611 | chitin synthase-1 | 13.3 | 13.88 | 16.2 | 17 | 0.54 | 0.87 | 2.82 | 3.15 | 0.524 | 0.743 | 2.54 | 2.763 | 4.130944 |
| NCU02812 | uridylate kinase | 16.4 | 16.03 | 19.2 | 19.1 | -0.4 | -0.1 | 2.78 | 3.03 | 0.376 | -0.237 | 2.5 | 2.643 | 8.191519 |
| NCU02771 | uroporphyrinogen decarboxylase | 19.8 | 20.67 | 22.6 | 22.5 | 0.83 | -0.1 | 2.74 | 3.18 | 0.814 | -0.207 | 2.46 | 3.443 | 3.399708 |
| NCU08402 | zinc-binding alcohol dehydrogenase | 17.9 | 18 | 20.6 | 20.8 | 0.12 | 0.22 | 2.72 | 2.84 | 0.084 | 0.093 | 2.44 | 2.453 | 27.63102 |
| NCU02899 | hypothetical protein | 14.4 | 14.51 | 17.1 | 16.3 | 0.13 | -0.8 | 2.69 | 1.78 | 0.114 | -0.907 | 2.41 | 1.393 | 3.048873 |
| NCU03795 | cell division control protein 12 | 16.5 | 16.27 | 19.1 | 18.9 | -0.2 | -0.2 | 2.66 | 2.65 | 0.226 | -0.347 | 2.38 | 2.263 | 7.937647 |
| NCU08044 | oxidoreductase | 17.4 | 18.1 | 20 | 19.6 | 0.73 | -0.5 | 2.65 | 1.46 | 0.714 | -0.587 | 2.37 | 1.073 | 2.818537 |
| NCU08693 | heat shock protein 70-5 | 20.4 | 20.3 | 23.1 | 23.4 | -0.1 | 0.33 | 2.65 | 3.06 | 0.126 | 0.173 | 2.37 | 2.673 | 16.70408 |
| NCU00720 | tricarboxylic acid-17 | 14 | 14.92 | 16.6 | 16.8 | 0.93 | 0.17 | 2.64 | 1.88 | 0.914 | 0.043 | 2.36 | 1.493 | 3.055687 |
| NCU03949 | nitropropane dioxygenase-1 | 18.8 | 19.16 | 21.4 | 21.5 | 0.39 | 0.06 | 2.62 | 2.29 | 0.374 | -0.067 | 2.34 | 1.903 | 7.946303 |
| NCU05430 | ATPase-2 | 19.9 | 19.6 | 22.4 | 22 | -0.3 | -0.4 | 2.53 | 2.36 | 0.296 | -0.577 | 2.25 | 1.973 | 4.619219 |
| NCU04129 | gamma-tocopherol methyltransferase | 15.8 | 15.68 | 18.3 | 18.2 | -0.1 | -0.1 | 2.46 | 2.54 | 0.156 | -0.187 | 2.18 | 2.153 | 12.59331 |
| NCU05881 | DUF500 and UBA/TS-N domain-containing protein | 15.4 | 14.83 | 17.8 | 17.3 | -0.5 | -0.5 | 2.44 | 2.5 | 0.556 | -0.607 | 2.16 | 2.113 | 3.674288 |
| NCU10810 | mRNA splicing protein | 14.3 | 14.89 | 16.7 | 16.5 | 0.61 | -0.2 | 2.44 | 1.6 | 0.594 | -0.357 | 2.16 | 1.213 | 3.579634 |
| NCU02727 | glycine cleavage system T protein | 15.9 | 16.14 | 18.2 | 17.7 | 0.28 | -0.5 | 2.36 | 1.59 | 0.264 | -0.617 | 2.08 | 1.203 | 3.585562 |

| | | | | | | | | | | | | | | |
|---|---|---|---|---|---|---|---|---|---|---|---|---|---|---|
| NCU06738 | protein transporter sec-31 | 15.6 | 15.77 | 17.9 | 17.5 | 0.15 | -0.4 | 2.32 | 1.73 | 0.134 | -0.567 | 2.04 | 1.343 | 4.197816 |
| NCU07008 | carotenoid oxygenase-1 | 14.9 | 13.8 | 17.2 | 18 | -1.1 | 0.8 | 2.3 | 4.22 | -1.136 | 0.673 | 2.02 | 3.833 | 3.282797 |
| NCU03786 | serine/threonine protein phosphatase 2A | 13.3 | 13.87 | 15.6 | 15.7 | 0.57 | 0.1 | 2.28 | 1.81 | 0.554 | -0.027 | 2 | 1.423 | 4.431263 |
| NCU02464 | neuronal-specific septin-3 | 16.6 | 16.91 | 18.9 | 18.5 | 0.31 | -0.4 | 2.26 | 1.56 | 0.294 | -0.517 | 1.98 | 1.173 | 3.875286 |
| NCU09090 | phosphopantothenate-cysteine ligase | 15.6 | 16.03 | 17.8 | 17.8 | 0.47 | 0.0 | 2.21 | 1.78 | 0.454 | -0.087 | 1.93 | 1.393 | 5.15606 |
| NCU01166 | microcycle blastoconidiation | 16.1 | 16.13 | 18.3 | 17.9 | 0.02 | -0.4 | 2.16 | 1.78 | 0.004 | -0.487 | 1.88 | 1.393 | 4.811038 |
| NCU01258 | cyanase | 18.3 | 17.77 | 20.5 | 20.5 | -0.5 | 0.05 | 2.16 | 2.75 | -0.556 | -0.077 | 1.88 | 2.363 | 5.384086 |
| NCU06915 | hypothetical protein | 15.4 | 14.84 | 17.5 | 18.2 | -0.5 | 0.67 | 2.14 | 3.35 | -0.556 | 0.543 | 1.86 | 2.963 | 4.504266 |
| NCU03068 | pyridoxine-3 | 16.6 | 16.62 | 18.8 | 18.3 | -0 | -0.4 | 2.13 | 1.71 | -0.026 | -0.557 | 1.85 | 1.323 | 4.084673 |
| NCU00880 | phospholipase A-2-activating protein | 16.3 | 14.99 | 18.4 | 18.8 | -1.3 | 0.38 | 2.11 | 3.76 | -1.286 | 0.253 | 1.83 | 3.373 | 2.929354 |
| NCU09798 | aryl-alcohol dehydrogenase | 15.4 | 16.13 | 17.5 | 17.6 | 0.75 | 0.11 | 2.1 | 1.46 | 0.734 | -0.017 | 1.82 | 1.073 | 2.882334 |
| NCU03596 | CRAL/TRIO domain-containing protein | 14.2 | 14.41 | 16.2 | 15.8 | 0.2 | -0.5 | 2.02 | 1.34 | 0.184 | -0.607 | 1.74 | 0.953 | 3.133335 |
| NCU02113 | ubiquitin-conjugating enzyme E2 13 | 15.8 | 16.37 | 17.8 | 17.8 | 0.53 | -0.1 | 2 | 1.42 | 0.514 | -0.177 | 1.72 | 1.033 | 3.697039 |
| NCU07659 | acetate-4 | 17.6 | 17.11 | 19.6 | 20 | -0.5 | 0.42 | 1.99 | 2.91 | -0.516 | 0.293 | 1.71 | 2.523 | 5.140235 |
| NCU08004 | electron transfer flavoprotein alpha-subunit | 15 | 14.51 | 17 | 16.5 | -0.5 | -0.5 | 1.96 | 1.98 | -0.536 | -0.627 | 1.68 | 1.593 | 2.81021 |
| NCU04216 | adenine-7 | 16.7 | 16.4 | 18.6 | 18.6 | -0.3 | 0.02 | 1.93 | 2.21 | -0.276 | -0.107 | 1.65 | 1.823 | 8.315494 |
| NCU06974 | histidinol-phosphatase | 15.4 | 15.77 | 17.3 | 17.5 | 0.34 | 0.22 | 1.91 | 1.79 | 0.324 | 0.093 | 1.63 | 1.403 | 6.389186 |
| NCU00488 | protein phosphatase PP2A regulatory subunit A | 18.5 | 18.23 | 20.4 | 20.5 | -0.3 | 0.07 | 1.89 | 2.26 | -0.316 | -0.057 | 1.61 | 1.873 | 7.700019 |
| NCU01424 | DUF636 domain-containing protein | 18.6 | 19.03 | 20.5 | 21.1 | 0.42 | 0.62 | 1.87 | 2.05 | 0.404 | 0.473 | 1.59 | 1.663 | 3.703186 |
| NCU05143 | rds1 | 15.7 | 15.23 | 17.4 | 17.3 | -0.4 | -0.1 | 1.71 | 2.03 | -0.456 | -0.247 | 1.43 | 1.643 | 3.087854 |
| NCU00864 | TIM-barrel enzyme family protein | 17.1 | 17.54 | 18.8 | 18.9 | 0.41 | 0.03 | 1.7 | 1.32 | 0.394 | -0.097 | 1.42 | 0.933 | 4.195607 |
| NCU01919 | ubiquitin C-terminal hydrolase | 17.3 | 17.15 | 19 | 18.7 | -0.1 | -0.3 | 1.7 | 1.57 | -0.156 | -0.397 | 1.42 | 1.183 | 4.34014 |
| NCU07737 | salicylate hydroxylase | 18.2 | 18.51 | 19.8 | 20.4 | 0.35 | 0.53 | 1.68 | 1.86 | 0.334 | 0.403 | 1.4 | 1.473 | 3.887785 |
| NCU09223 | protein disulfide-isomerase | 17.2 | 16.58 | 18.8 | 18.7 | -0.6 | -0.1 | 1.67 | 2.12 | -0.606 | -0.267 | 1.39 | 1.733 | 3.358559 |
| NCU06372 | ubiquitin hydrolase L3 | 17.2 | 16.56 | 18.7 | 18.8 | -0.7 | 0.22 | 1.52 | 2.19 | -0.666 | -0.107 | 1.24 | 1.803 | 3.247414 |
| NCU10360 | hypothetical protein | 16.2 | 16.26 | 17.7 | 17.9 | 0.05 | 0.16 | 1.52 | 1.63 | 0.034 | 0.033 | 1.24 | 1.243 | 37.11527 |
| NCU08515 | vacuolar membrane ATPase-2 | 19.6 | 19.46 | 21.1 | 21.2 | -0.1 | 0.13 | 1.51 | 1.76 | -0.136 | 0.003 | 1.23 | 1.373 | 13.57056 |
| NCU01207 | vacuolar membrane ATPase-1 | 20.7 | 20.81 | 22.2 | 22.1 | 0.07 | -0.1 | 1.46 | 1.24 | 0.054 | -0.277 | 1.18 | 0.853 | 5.170779 |
| NCU05495 | clock-controlled gene-16 | 16.8 | 16.63 | 18.2 | 19 | -0.2 | 0.72 | 1.45 | 2.32 | -0.166 | 0.593 | 1.17 | 1.933 | 3.672618 |
| NCU01004 | phosphatidylserine decarboxylase proenzyme | 17.2 | 17.35 | 18.6 | 18.7 | 0.18 | 0.04 | 1.44 | 1.33 | 0.164 | -0.087 | 1.16 | 0.913 | 7.968575 |
| NCU07282 | hypothetical protein | 15.3 | 15.23 | 16.7 | 16.9 | -0.1 | 0.16 | 1.46 | 1.66 | -0.116 | 0.033 | 1.12 | 1.273 | 14.081 |
| NCU11369 | BAR domain-containing protein | 18.2 | 18.35 | 19.6 | 19.7 | 0.11 | 0.06 | 1.38 | 1.33 | 0.094 | -0.067 | 1.1 | 0.943 | 12.57791 |
| NCU08384 | xylose reductase | 15 | 15.37 | 16.3 | 16.8 | 0.41 | 0.45 | 1.38 | 1.42 | 0.394 | 0.323 | 1.1 | 1.033 | 2.967605 |
| NCU00173 | esterase D | 18.3 | 18.72 | 19.6 | 19.8 | 0.44 | 0.16 | 1.36 | 1.08 | 0.424 | 0.033 | 1.08 | 0.693 | 3.025253 |
| NCU01227 | tricarboxylic acid-8 | 17.5 | 16.84 | 18.8 | 18.9 | -0.6 | 0.06 | 1.36 | 2.06 | -0.656 | -0.067 | 1.08 | 1.673 | 3.023123 |
| NCU01820 | exportin-1 | 18.5 | 18.66 | 19.8 | 19.8 | 0.19 | -0 | 1.36 | 1.16 | 0.174 | -0.137 | 1.08 | 0.773 | 6.011823 |
| NCU00685 | casein kinase I isoform delta | 16.4 | 16.25 | 17.8 | 17.8 | -0.2 | 0.07 | 1.35 | 1.59 | -0.186 | -0.057 | 1.07 | 1.203 | 8.289715 |
| NCU05291 | polyamine acetyltransferase | 15.4 | 15.16 | 16.7 | 16.7 | -0.2 | -0.1 | 1.34 | 1.49 | -0.226 | -0.187 | 1.06 | 1.103 | 5.224584 |
| NCU01808 | cytochrome c-1 | 17.5 | 17.55 | 18.8 | 18.6 | 0.07 | -0.2 | 1.32 | 1.06 | 0.054 | -0.317 | 1.04 | 0.673 | 3.862721 |
| NCU00350 | epoxide hydrolase | 19.2 | 19.26 | 20.5 | 21 | 0.02 | 0.54 | 1.23 | 1.75 | 0.004 | 0.413 | 0.95 | 1.363 | 4.028131 |

## Less abundant proteins in ΔPor-1:

| Protein | Description | WT | WT-1 | ΔPor | ΔPor-1 | R0 | R1 | Z0 | Z1 | NR0 | NR1 | NZ0 | NZ1 | SN |
|---|---|---|---|---|---|---|---|---|---|---|---|---|---|---|
| NCU04385 | leucine-2 | 22.5 | 22.67 | 21.8 | 21.9 | 0.19 | 0.01 | -0.64 | -0.82 | 0.174 | 0.117 | -0.9 | -1.21 | 7.226424 |
| NCU04411 | tryptophan-4 | 17.9 | 18.07 | 17.2 | 17.3 | 0.2 | 0.09 | -0.64 | -0.75 | 0.184 | 0.037 | -0.9 | -1.14 | 7.779475 |
| NCU07826 | 40S ribosomal protein S19 | 21.8 | 22.03 | 21.2 | 21.2 | 0.23 | 0.04 | -0.64 | -0.83 | 0.214 | 0.087 | -0.9 | -1.22 | 6.593702 |
| NCU09475 | 40s ribosomal protein s5 | 22.8 | 22.8 | 22.2 | 22.5 | -0.04 | 0.32 | -0.64 | -0.32 | 0.036 | 0.173 | -0.9 | -0.71 | 6.548226 |
| NCU08685 | phosphoribosylformylglycinamidine synthase | 21.8 | 22 | 21.1 | 20.8 | 0.19 | -0.3 | -0.68 | -1.18 | 0.174 | -0.437 | -1 | -1.57 | 3.902484 |
| NCU16368 | hypothetical protein | 17.4 | 17.01 | 16.7 | 16.6 | -0.3 | -0.1 | -0.68 | -0.43 | -0.356 | -0.217 | -1 | -0.82 | 3.016256 |
| NCU07307 | chain elongation-2 | 23.3 | 23.34 | 22.6 | 22.9 | 0.08 | 0.33 | -0.68 | -0.43 | 0.064 | -0.203 | -1 | -0.82 | 5.908146 |
| NCU01195 | amination-deficient | 26.1 | 26.25 | 25.4 | 25.3 | 0.14 | -0.1 | -0.69 | -0.92 | 0.124 | -0.217 | -1 | -1.31 | 6.502781 |
| NCU00475 | 40S ribosomal protein S18 | 22.3 | 22.44 | 21.6 | 21.8 | 0.11 | 0.22 | -0.74 | -0.63 | -0.084 | -0.073 | -1 | -0.99 | 12.47281 |
| NCU09116 | aromatic aminotransferase Aro8 | 17.5 | 17.31 | 16.8 | 16.8 | -0.2 | -0.04 | -0.74 | -0.55 | -0.246 | -0.157 | -1 | -0.89 | 4.519208 |
| NCU03608 | isoleucine + valine-2 | 21.8 | 21.77 | 21.1 | 20.7 | -0.04 | 0.44 | -0.74 | -1.09 | -0.056 | -0.537 | -1 | -1.48 | 3.299509 |
| NCU01824 | UDP-galactopyranose mutase | 22.2 | 22.35 | 21.4 | 20.9 | 0.19 | -0.5 | -0.75 | -1.47 | -0.174 | -0.657 | -1 | -1.86 | 3.121582 |
| NCU08277 | eukaryotic translation initiation factor 2 alpha subunit | 19.8 | 19.6 | 19.1 | 19.1 | -0.2 | 0 | -0.75 | -0.53 | -0.236 | -0.127 | -1 | -0.92 | 5.134549 |
| NCU07014 | cytoplasmic ribosomal protein-3 | 22 | 21.79 | 21.2 | 21.5 | -0.2 | 0.32 | -0.76 | -0.62 | -0.196 | -0.193 | -1 | -0.96 | 4.440411 |
| NCU01439 | D-3-phosphoglycerate dehydrogenase 1 | 24 | 23.97 | 23.2 | 23.3 | 0.02 | 0.15 | -0.77 | -0.64 | -0.004 | -0.023 | -1 | -1.03 | 62.79202 |
| NCU06075 | acetate-8 | 25 | 24.66 | 24.2 | 24.5 | 0.44 | -0.2 | -0.77 | -0.18 | -0.366 | -0.113 | -1 | -0.57 | 3.106125 |
| NCU03922 | hydroxymethylglutaryl-CoA synthase | 21.6 | 22.09 | 20.8 | 20.5 | 0.49 | -0.4 | -0.78 | -1.63 | -0.474 | -0.487 | -1.1 | -2.02 | 3.350119 |
| NCU09194 | nuclease S1 | 17.6 | 17.35 | 16.8 | 16.6 | -0.2 | -0.2 | -0.79 | -0.74 | -0.236 | -0.297 | -1.1 | -1.13 | 4.089344 |
| NCU07735 | Grp1p | 22.8 | 22.59 | 22 | 21.8 | -0.2 | -0.2 | -0.79 | -0.66 | -0.206 | -0.287 | -1.1 | -1.15 | 4.432422 |
| NCU03010 | lysine-3 | 22.4 | 22.59 | 21.6 | 21.4 | 0.15 | -0.2 | -0.84 | -1.16 | -0.134 | -0.337 | -1.1 | -1.55 | 5.196013 |
| NCU03118 | hypothetical protein | 23.8 | 23.67 | 22.9 | 23.1 | -0.1 | 0.15 | -0.85 | -0.92 | -0.096 | -0.023 | -1.1 | -0.98 | 14.87331 |
| NCU06843 | 60S ribosomal protein L3 | 22.8 | 22.9 | 22 | 21.9 | 0.1 | -0.1 | -0.85 | -1.14 | -0.084 | -0.197 | -1.1 | -1.35 | 8.349011 |
| NCU00999 | hypothetical protein | 15.6 | 16.08 | 14.7 | 14.7 | 0.53 | -0.03 | -0.85 | -1.42 | -0.516 | -0.167 | -1.1 | -1.81 | 3.939528 |
| NCU05238 | cysteine-4 | 22.9 | 22.98 | 22.1 | 22.5 | 0.05 | 0.39 | -0.85 | -0.51 | -0.034 | -0.263 | -1.1 | -0.87 | 5.428637 |
| NCU02274 | formate | 24.4 | 24.19 | 23.6 | 23.9 | -0.2 | 0.33 | -0.86 | -0.32 | -0.256 | -0.173 | -1.1 | -0.71 | 4.330582 |
| NCU04449 | prolyl-tRNA synthetase | 20.9 | 20.85 | 20 | 20.4 | 0 | 0.39 | -0.86 | -0.47 | -0.016 | -0.263 | -1.1 | -0.86 | 5.400683 |
| NCU00971 | ribosomal protein S12 | 22 | 21.96 | 21.1 | 21.6 | -0.04 | 0.49 | -0.87 | -0.73 | -0.026 | -0.363 | -1.1 | -0.76 | 3.773941 |
| NCU09794 | NAD-binding Rossmann fold oxidoreductase | 18.3 | 18.93 | 17.4 | 17.5 | 0.66 | 0.11 | -0.87 | -1.42 | -0.636 | -0.007 | -1.1 | -1.81 | 3.321449 |
| NCU02979 | AMP deaminase | 18.2 | 18.27 | 17.3 | 17.7 | 0.07 | 0.33 | -0.88 | -0.62 | -0.054 | -0.203 | -1.2 | -1.01 | 7.298391 |

| | | | | | | | | | | | | | | |
|---|---|---|---|---|---|---|---|---|---|---|---|---|---|---|
| NCU01754 | alcohol dehydrogenase-1 | 24 | 24.1 | 23.1 | 22.7 | 0.08 | -0.4 | -0.89 | -1.41 | 0.064 | -0.567 | -1.2 | -1.8 | 3.754185 |
| NCU03425 | threonine synthase | 22.4 | 22.38 | 21.5 | 21.6 | -0 | 0.03 | -0.9 | -0.83 | 0.056 | -0.097 | -1.2 | 1.22 | 15.10971 |
| NCU08502 | 40S ribosomal protein S6 | 22.7 | 22.7 | 21.8 | 22.3 | 0.03 | 0.53 | -0.9 | -0.4 | 0.014 | 0.403 | -1.2 | -0.79 | 3.509155 |
| NCU09896 | adenylyl-sulfate kinase | 21.4 | 21.15 | 20.5 | 20.5 | -0.3 | 0.02 | -0.93 | -0.65 | -0.276 | -0.107 | -1.2 | -1.04 | 5.373157 |
| NCU01985 | cysteine-11 | 24.3 | 23.93 | 23.3 | 23.6 | -0.3 | 0.31 | -0.94 | -0.33 | -0.346 | -0.183 | -1.2 | -0.69 | 3.568215 |
| NCU08998 | 4-aminobutyrate aminotransferase | 19.5 | 19.1 | 18.5 | 18.8 | -0.4 | 0.34 | -0.94 | -0.28 | -0.376 | -0.173 | -1.2 | -0.67 | 3.350936 |
| NCU11356 | phenazine biosynthesis PhzC/PhzF protein | 19.9 | 20.2 | 19 | 19.4 | 0.29 | 0.44 | -0.95 | -0.88 | -0.274 | -0.313 | -1.2 | -1.19 | 4.102225 |
| NCU07930 | cysteine-18 | 25.5 | 25.16 | 24.5 | 24.3 | -0.3 | -0.2 | -0.97 | -0.84 | -0.346 | -0.327 | -1.2 | -1.23 | 3.673236 |
| NCU06110 | thiazole biosynthetic enzyme | 26.4 | 27.05 | 25.4 | 25.2 | 0.65 | -0.2 | -1 | -1.86 | 0.634 | -0.337 | -1.3 | -2.25 | 3.598917 |
| NCU09789 | adenine-8 | 21.3 | 21.36 | 20.3 | 21 | 0.03 | 0.64 | -1 | -0.39 | 0.014 | 0.513 | -1.3 | -0.78 | 2.911111 |
| NCU07719 | isopentenyl-diphosphate delta-isomerase | 20 | 20.29 | 19 | 19.5 | 0.26 | 0.55 | -1.04 | -0.88 | 0.244 | 0.373 | -1.3 | -1.19 | 3.976136 |
| NCU01632 | aromatic-1 gene cluster | 22.8 | 22.91 | 21.8 | 22.1 | 0.11 | 0.36 | -1.06 | -0.84 | 0.084 | 0.233 | -1.3 | -1.19 | 7.215538 |
| NCU07467 | hypothetical protein | 18.7 | 18.67 | 17.6 | 17.8 | 0 | 0.22 | -1.06 | -0.86 | 0.016 | 0.073 | -1.3 | -1.25 | 24.45431 |
| NCU03897 | RNA binding effector protein Scp160 | 18.1 | 18.46 | 17 | 17.4 | 0.36 | 0.41 | -1.07 | -1.02 | 0.344 | 0.283 | -1.3 | -1.41 | 4.371189 |
| NCU08859 | hypothetical protein | 16.7 | 17.22 | 15.6 | 15.6 | 0.55 | 0.02 | -1.07 | -1.61 | 0.534 | 0.107 | -1.3 | -1.99 | 4.406742 |
| NCU02571 | acetyl-CoA acetyltransferase | 22.8 | 23.54 | 21.8 | 22.2 | 0.74 | 0.44 | -1.08 | -1.34 | 0.684 | 0.313 | -1.4 | -1.73 | 2.919036 |
| NCU06512 | methionine-8 | 27.2 | 27.13 | 26.1 | 26.1 | -0 | 0.01 | -1.09 | -1.06 | 0.036 | 0.117 | -1.4 | -1.45 | 16.25572 |
| NCU02533 | DNA-directed RNA polymerase I and III polypeptide | 16.4 | 16.67 | 15.3 | 15 | 0.28 | -0.3 | -1.18 | -1.68 | 0.264 | -0.427 | -1.4 | -2.07 | 4.946244 |
| NCU09345 | no message in thiamine-1 | 26.9 | 27.09 | 25.8 | 25.8 | 0.18 | 0.04 | -1.12 | -1.26 | 0.164 | 0.087 | -1.4 | -1.65 | 11.62975 |
| NCU01300 | imidazoleglycerol-phosphate dehydratase | 18.8 | 19 | 17.7 | 18.2 | 0.18 | 0.49 | -1.13 | -0.82 | 0.164 | 0.363 | -1.4 | -1.21 | 4.651999 |
| NCU05620 | proteasome activator subunit 4 | 16.7 | 16.21 | 15.6 | 15.9 | -0.5 | 0.26 | -1.13 | -0.34 | 0.546 | -0.133 | -1.4 | -0.73 | 2.816605 |
| NCU00396 | pre-mRNA-splicing factor rse-1 | 17.3 | 17.09 | 16.2 | 15.5 | -0.2 | -0.7 | -1.15 | -1.57 | -0.256 | -0.787 | -1.4 | -1.96 | 2.925882 |
| NCU04292 | branched-chain-amino-acid aminotransferase | 20.4 | 20.64 | 19.3 | 19.6 | 0.24 | 0.39 | -1.15 | -1 | 0.224 | 0.263 | -1.4 | -1.39 | 5.758301 |
| NCU00635 | nascent polypeptide-associated complex subunit alpha | 20.9 | 20.75 | 19.7 | 20 | -0.1 | 0.26 | -1.18 | -0.77 | -0.166 | -0.133 | -1.5 | -1.16 | 8.743069 |
| NCU06417 | uracil-5-carboxylate decarboxylase | 19.1 | 18.94 | 17.9 | 18.3 | -0.2 | -0.4 | -1.18 | -0.66 | -0.176 | -0.293 | -1.5 | -0.99 | 5.146354 |
| NCU03973 | alanine | 19.1 | 19.47 | 17.9 | 18.1 | 0.39 | 0.18 | -1.19 | -1.44 | 0.374 | -0.053 | -1.5 | -1.79 | 6.119052 |
| NCU11381 | diphosphomevalonate decarboxylase | 20.1 | 20.1 | 18.9 | 19.3 | -0 | 0.39 | -1.21 | -0.81 | 0.026 | -0.263 | -1.5 | -1.22 | 7.220096 |
| NCU04799 | polyadenylate-binding protein | 22.1 | 21.92 | 20.9 | 21.3 | -0.2 | 0.41 | -1.23 | -0.66 | -0.176 | -0.283 | -1.5 | -1.05 | 5.503706 |
| NCU06459 | differentiation regulator | 16.1 | 15.62 | 14.9 | 15.1 | -0.5 | 0.22 | -1.23 | -0.52 | -0.506 | -0.093 | -1.5 | -0.91 | 3.417139 |
| NCU08295 | RNA-binding La domain-containing protein | 18.3 | 18.35 | 17 | 17.3 | 0.06 | 0.31 | -1.26 | -1.01 | 0.044 | -0.183 | -1.5 | -1.47 | 11.03137 |
| NCU04640 | eukaryotic translation initiation factor 2 beta subunit | 19.4 | 19.78 | 18.2 | 18.5 | 0.36 | 0.38 | -1.27 | -1.25 | 0.344 | -0.253 | -1.5 | -1.64 | 5.272931 |

| | | | | | | | | | | | | | | |
|---|---|---|---|---|---|---|---|---|---|---|---|---|---|---|
| NCU01550 | adenylate kinase cytosolic | 18 | 18.07 | 16.7 | 17.3 | 0.03 | 0.63 | -1.33 | -0.73 | 0.014 | 0.503 | -1.6 | -1.12 | 3.88766 |
| NCU08216 | cystathionine beta-synthase | 21.6 | 21.25 | 20.2 | 20.3 | -0.3 | 0.04 | -1.33 | -0.97 | 0.336 | 0.087 | -1.6 | -1.36 | 6.05779 |
| NCU04611 | transcription elongation factor spt-6 | 17 | 17.69 | 15.6 | 14.8 | 0.72 | -0.8 | -1.34 | -2.93 | 0.704 | 0.967 | -1.6 | -3.29 | 3.06220 |
| NCU05485 | casein kinase II regulatory beta subunit-1 | 17.7 | 17.37 | 16.4 | 16.9 | -0.4 | 0.59 | -1.39 | -0.43 | 0.386 | 0.463 | -1.7 | -0.82 | 3.07822 |
| NCU00692 | chaperone dnaK | 19.8 | 19.42 | 18.4 | 19.1 | -0.4 | 0.66 | -1.39 | -0.37 | 0.376 | 0.533 | -1.7 | -0.76 | 2.80543 |
| NCU01571 | hypothetical protein | 16 | 15.64 | 14.6 | 15.1 | -0.4 | 0.52 | -1.44 | -0.55 | 0.386 | 0.393 | -1.7 | -0.94 | 3.54928 |
| NCU08269 | pyridoxine-4 | 18.7 | 19.03 | 17.3 | 18 | 0.31 | 0.71 | -1.45 | -1.05 | 0.294 | 0.583 | -1.7 | -1.44 | 3.43968 |
| NCU07267 | blue light-induced-3 | 18.9 | 18.24 | 17.4 | 17 | -0.7 | -0.4 | -1.53 | -1.29 | 0.676 | 0.547 | -1.8 | -1.68 | 2.83414 |
| NCU02810 | eukaryotic translation initiation factor 2 gamma subunit | 20.6 | 20.83 | 19 | 19.8 | 0.28 | 0.83 | -1.57 | -1.02 | 0.264 | 0.703 | -1.8 | -1.41 | 3.09090 |
| NCU02435 | histone H2B | 20 | 20.35 | 18.4 | 18.3 | 0.39 | -0.1 | -1.58 | -2.05 | 0.374 | 0.207 | -1.9 | -2.44 | 7.16618 |
| NCU06603 | ThiJ/PfpI family protein | 21.1 | 20.64 | 19.5 | 19.5 | -0.4 | 0.05 | -1.59 | -1.13 | 0.426 | 0.077 | -1.9 | -1.52 | 5.55514 |
| NCU05305 | DNA-directed RNA polymerase II polypeptide | 16.2 | 16.28 | 14.5 | 15.3 | 0.11 | 0.82 | -1.68 | -0.97 | 0.094 | 0.693 | -2 | -1.36 | 3.40407 |
| NCU08183 | hypothetical protein | 18.3 | 18.93 | 16.6 | 16.9 | 0.6 | 0.3 | -1.69 | -1.99 | 0.584 | 0.173 | -2 | -2.38 | 5.06445 |
| NCU03194 | phosphoribosylaminoimidazole carboxylase | 21.3 | 21.07 | 19.6 | 20.4 | -0.3 | 0.78 | -1.71 | -0.66 | 0.286 | 0.653 | -2 | -1.05 | 3.14929 |
| NCU07936 | NMDA receptor-regulated protein 1 | 18.9 | 18.97 | 17.1 | 17.3 | 0.04 | 0.16 | -1.8 | -1.68 | 0.024 | 0.033 | -2.1 | -2.07 | 71.7949 |
| NCU07774 | GTP cyclohydrolase-1 | 17.3 | 17.27 | 15.5 | 15.2 | 0.11 | 0.33 | -1.81 | -2.06 | 0.076 | 0.437 | -2.1 | -2.45 | 7.24922 |
| NCU02688 | ubiquitin-conjugating enzyme E2Z | 15.1 | 14.88 | 13.2 | 13.7 | 0.24 | -0.4 | -1.84 | -1.22 | 0.196 | 0.313 | -2.1 | -1.61 | 7.19475 |
| NCU01428 | hydroxyisourate hydrolase | 18.7 | 18.58 | 16.8 | 17 | -0.1 | 0.21 | -1.87 | -1.58 | 0.096 | 0.083 | -2.1 | -1.97 | 22.9389 |
| NCU01652 | O-acetylhomoserine | 21.1 | 20.85 | 19.2 | 19.3 | -0.3 | 0.05 | -1.89 | -1.44 | 0.316 | 0.077 | -2.2 | -1.93 | 8.91361 |
| NCU09132 | tubulin alpha-1 | 20.9 | 20.29 | 19 | 19.2 | -0.7 | 0.22 | -1.89 | -0.98 | 0.706 | 0.093 | -2.2 | -1.37 | 3.59682 |
| NCU05512 | copper resistance protein Crd2 | 19.5 | 20.05 | 17.6 | 18.1 | 0.53 | 0.53 | -1.92 | -1.92 | 0.514 | 0.403 | -2.2 | -2.31 | 4.87647 |
| NCU05974 | cell wall glucanosyltransferase Mwg1 | 20.1 | 20.74 | 18.1 | 17.6 | 0.64 | -0.5 | -2.08 | -3.18 | 0.584 | 0.627 | -2.4 | -3.57 | 4.98903 |
| NCU04187 | cap binding protein | 17.3 | 16.97 | 15.2 | 15.2 | -0.4 | -0.0 | -2.09 | -1.75 | 0.366 | 0.137 | -2.4 | -2.14 | 8.15817 |
| NCU09873 | acetate utilization-6 | 21.3 | 21.67 | 19.2 | 20 | 0.34 | 0.77 | -2.14 | -1.71 | 0.324 | 0.643 | -2.4 | -2.13 | 4.44313 |
| NCU01438 | nucleosome assembly factor-1 | 22.5 | 22.38 | 20.4 | 21.4 | -0.1 | 1 | -2.14 | -1 | 0.156 | 0.873 | -2.4 | -1.39 | 3.14133 |
| NCU07192 | hypothetical protein | 17.9 | 17.77 | 15.7 | 15.4 | -0.1 | 0.33 | -2.15 | -2.37 | 0.116 | 0.447 | -2.4 | -2.76 | 7.95225 |
| NCU09821 | oxidoreductase | 17.9 | 17.56 | 15.7 | 16.5 | 0.34 | 0.55 | -2.16 | -1.11 | 0.326 | 0.623 | -2.4 | -1.49 | 4.05892 |
| NCU07437 | eukaryotic translation initiation factor 1A | 18.5 | 18.21 | 16.3 | 16.6 | -0.3 | 0.55 | -2.21 | -1.59 | 0.286 | 0.223 | -2.5 | -1.98 | 8.75818 |
| NCU08767 | serine/threonine protein kinase-52 | 15.6 | 14.61 | 13.2 | 13.4 | -1.0 | 0.22 | -2.46 | -1.23 | 1.026 | 0.093 | -2.7 | -1.62 | 3.08492 |
| NCU01638 | DNA-directed RNA polymerase I subunit RPA1 | 17.5 | 16.66 | 14.9 | 15.5 | -0.8 | 0.22 | -2.66 | -1.16 | 0.836 | 0.493 | -2.9 | -1.55 | 3.3648 |
| NCU04720 | nitrate nonutilizer-6 | 19.7 | 19.77 | 16.2 | 13.9 | 0.03 | -2.3 | -3.53 | -5.85 | 0.014 | 2.417 | -3.8 | -6.24 | 3.02293 |

| | | | | | | | | | | | | | | |
|---|---|---|---|---|---|---|---|---|---|---|---|---|---|---|
| NCU11027 | zinc metalloprotease | 19.8 | 19.38 | 16.3 | 17.6 | -0.4 | 1.3 | -3.54 | -1.79 | 0.466 | 1.173 | -3.8 | -2.18 | 3.480747 |
| NCU07117 | ornithine-N5-oxygenase | 19.2 | 19.85 | 15.5 | 15.2 | 0.63 | 0.3 | -3.73 | -4.69 | 0.614 | 0.457 | -4 | -5.08 | 8.449316 |
| NCU02684 | chromatin remodelling factor 4-3 | 20.1 | 20.1 | 16 | 17.9 | 0.05 | 1.94 | -4.09 | -2.29 | 0.034 | 1.813 | -4.4 | -2.59 | 2.798676 |
| NCU02668 | cell wall synthesis protein-Penicillium chrysogenum | 18.1 | 18.09 | 12.6 | 13.1 | -0.53 | 0.38 | -5.52 | -4.98 | 0.026 | 0.403 | -5.8 | -5.37 | 19.56047 |

Appendix 7.3 file-2

***N. crassa* mitochondrial proteomic:**

Less abundant proteins in ΔPor-1:

| locus | description | WT | ΔPor-1 | ΔPor-1- WT | z |
|---|---|---|---|---|---|
| NCU00160 | NADH:ubiquinone oxidoreductase 6.6kD subunit | 22.26 | 16.10 | -6.16 | -5.14 |
| NCU00712 | 3-hydroxy-3-methylglutaryl-coenzyme A reductase | 21.93 | 16.99 | -4.94 | -3.99 |
| NCU00336 | U3 small nucleolar RNA-associated protein 10 | 22.24 | 17.55 | -4.69 | -3.75 |
| NCU02704 | branched-chain alpha-keto acid dehydrogenase E | 21.85 | 17.32 | -4.53 | -3.60 |
| NCU01145 | hypothetical protein | 18.91 | 14.44 | -4.47 | -3.54 |
| NCU01501 | mitochondrial peptidyl-tRNA hydrolase Pth2 | 22.49 | 18.29 | -4.20 | -3.29 |
| NCU08961 | hypothetical protein, variant | 19.34 | 15.17 | -4.17 | -3.26 |
| NCU04781 | NADH:ubiquinone oxidoreductase 9.8 kDa subunit | 23.22 | 19.13 | -4.09 | -3.18 |
| NCU06740 | hypothetical protein | 21.02 | 17.27 | -3.75 | -2.86 |
| NCU00528 | FHA domain-containing protein | 20.04 | 16.47 | -3.57 | -2.69 |
| NCU09460 | NADH:ubiquinone oxidoreductase 20.1kD subunit | 23.75 | 20.29 | -3.46 | -2.59 |
| NCU00670 | NADH:ubiquinone oxidoreductase 9.5kD subunit | 24.07 | 20.62 | -3.45 | -2.58 |
| NCU01324 | hypothetical protein | 19.22 | 15.79 | -3.43 | -2.56 |
| NCU07489 | serine/threonine-protein phosphatase PP-Z | 18.99 | 15.60 | -3.39 | -2.52 |
| NCU01296 | hypothetical protein | 20.31 | 17.00 | -3.31 | -2.45 |
| NCU06110 | thiazole biosynthetic enzyme | 25.24 | 21.98 | -3.26 | -2.40 |
| NCU09539 | 40S ribosomal protein S13 | 23.20 | 19.97 | -3.23 | -2.37 |
| NCU09291 | FAD dependent sulfhydryl oxidase Erv2 | 20.82 | 17.61 | -3.21 | -2.35 |
| NCU00107 | mitochondrial inner membrane protease ATP-23 | 23.45 | 20.26 | -3.19 | -2.33 |

| | | | | | |
|---|---|---|---|---|---|
| NCU08397 | hypothetical protein | 19.41 | 16.24 | -3.17 | -2.31 |
| NCU01024 | hypothetical protein | 24.44 | 21.29 | -3.15 | -2.29 |
| NCU01854 | hypothetical protein | 21.23 | 18.10 | -3.13 | -2.28 |
| NCU04653 | LCCL domain-containing protein | 18.37 | 15.27 | -3.10 | -2.25 |
| NCU09864 | 2-oxoisovalerate dehydrogenase alpha subunit | 20.09 | 17.02 | -3.07 | -2.22 |
| NCU07062 | protein kinase | 17.15 | 14.10 | -3.05 | -2.20 |
| NCU04907 | hypothetical protein | 22.28 | 19.26 | -3.02 | -2.17 |
| NCU09536 | hypothetical protein | 23.59 | 20.58 | -3.01 | -2.16 |
| NCU08940 | ubiquinol-cytochrome c reductase comple | 24.26 | 21.25 | -3.01 | -2.16 |
| NCU00347 | peroxin-26 Pex26-Penicillium chrysogenum | 21.12 | 18.11 | -3.01 | -2.16 |
| NCU09345 | thiamine biosynthesis protein NMT-1, variant 2 | 26.30 | 23.39 | -2.91 | -2.07 |
| NCU02472 | NADH:ubiquinone oxidoreductase 20.8kD subunit | 26.39 | 23.51 | -2.88 | -2.04 |
| NCU05338 | hypothetical protein | 26.18 | 23.31 | -2.87 | -2.03 |
| NCU07988 | ATPase family AAA domain-containing protein 1 | 22.62 | 19.78 | -2.84 | -2.00 |
| NCU05009 | NADH-quinone oxidoreductase chain I, variant | 25.07 | 22.30 | -2.77 | -1.93 |
| NCU02936 | proline oxidase | 23.76 | 21.04 | -2.72 | -1.89 |
| NCU02669 | signal sequence binding protein | 20.40 | 17.69 | -2.71 | -1.88 |
| NCU03561 | mitochondrial carrier protein | 27.25 | 24.55 | -2.70 | -1.87 |

More abundant proteins in Δ Por-1:

| | | | | | |
|---|---|---|---|---|---|
| NCU00893 | folC protein | 16.69 | 18.00 | 1.31 | 1.92 |
| NCU02162 | SURF-family protein | 22.22 | 23.53 | 1.31 | 1.92 |
| NCU07546 | multidrug resistance protein MDR | 20.20 | 21.57 | 1.37 | 1.98 |
| NCU05495 | CVNH domain-containing protein | 19.57 | 21.00 | 1.43 | 2.04 |
| NCU07407 | MutS2 protein | 18.08 | 19.51 | 1.43 | 2.04 |
| NCU06141 | protoheme IX farnesyltransferase | 16.95 | 18.39 | 1.44 | 2.05 |
| NCU05695 | hypothetical protein | 18.40 | 19.87 | 1.47 | 2.07 |
| NCU04368 | glutathione S-transferase Gst3 | 21.12 | 22.61 | 1.49 | 2.09 |
| NCU09182 | stress responsive A/B barrel domain-containin | 17.86 | 19.35 | 1.49 | 2.09 |
| NCU00865 | oxalate decarboxylase oxdC | 21.56 | 23.13 | 1.57 | 2.17 |
| NCU00276 | DNA polymerase gamma | 18.43 | 20.01 | 1.58 | 2.18 |
| NCU02097 | short chain dehydrogenase | 21.51 | 23.15 | 1.64 | 2.23 |
| NCU07851 | superoxide dismutase 1 copper chaperone | 18.61 | 20.30 | 1.69 | 2.28 |
| NCU07481 | morphogenesis protein | 15.58 | 17.30 | 1.72 | 2.31 |
| NCU04594 | 4-carboxymuconolactone decarboxylase | 17.89 | 19.71 | 1.82 | 2.41 |
| NCU01092 | 3-oxoacyl- | 20.74 | 22.80 | 2.06 | 2.63 |
| NCU01914 | sorting nexin-3 | 17.12 | 19.28 | 2.16 | 2.73 |
| NCU00465 | chaperone dnaJ | 17.70 | 19.88 | 2.18 | 2.75 |
| NCU08954 | hypothetical protein | 21.01 | 23.20 | 2.19 | 2.75 |
| NCU06687 | glycogen synthase, variant 3 | 20.58 | 23.21 | 2.63 | 3.17 |
| NCU09975 | multidrug resistance protein 3 | 17.65 | 20.29 | 2.64 | 3.18 |
| NCU05005 | HHE domain-containing protein | 21.09 | 24.28 | 3.19 | 3.70 |
| NCU06043 | GPR/FUN34 family protein | 18.50 | 22.22 | 3.72 | 4.20 |

**Appendix 7.4:**

Appendix Table 1: More abundant proteins in *por1Δ* knockout cells:

| **FunCat main category** | **FunCat description** | **No of proteins** |
|---|---|---|
| Biogenesis of cellular components | Nucleolus | 3 |
| | Mitochondrion | 13 |
| Cell rescue, defense and virulence | Catalase reaction | 2 |
| | Defense related proteins | 3 |
| | Oxidative stress response | 7 |
| Cellular transport, transport facilitation and transport routes | Electron transport | 21 |
| | Mitochondrial transport | 11 |
| Energy | Tricarboxylic-acid pathway (citrate cycle, Krebs cycle, TCA cycle) | 17 |
| | Pyruvate dehydrogenase complex | 4 |
| | Electron transport and membrane-associated energy conservation | 10 |
| | Glycolysis and gluconeogenesis | 8 |
| | Respiration | 9 |
| | Energy generation (e.g. ATP synthase) | 5 |
| | Lactate fermentation | 2 |
| | Propionate fermentation | 2 |
| Metabolism | C-compound and carbohydrate metabolism | 35 |
| | Sugar, glucoside, polyol and carboxylate catabolism | 17 |
| | Biosynthesis of glutamate | 8 |
| | Biosynthesis of leucine | 6 |
| | Biosynthesis of valine | 5 |
| | Biosynthesis of isoleucine | 5 |
| | Sugar, glucoside, polyol and carboxylate anabolism | 10 |
| | C-2 compound and organic acid catabolism | 5 |
| | Degradation of leucine | 3 |
| | Aminoadipic acid pathway | 3 |
| | Biosynthesis of lysine | 3 |

| | | |
|---|---|---|
| | Metabolism of the pyruvate family (alanine, isoleucine, leucine, valine) and D-alanine | 3 |
| | Degradation of glycine | 3 |
| | Degradation of isoleucine | 2 |
| | C-1 compound catabolism | 3 |
| | Degradation of valine | 2 |
| Protein fate (folding, modification, destination) | Lysosomal and vacuolar protein degradation | 5 |
| | Vacuolar protein degradation | 4 |
| | Cytoplasmic and nuclear protein degradation | 8 |
| | NAD/NADP binding | 11 |
| | Thiamine pyrophosphate binding | 3 |
| Transcription | rRNA modification | 4 |
| | rRNA synthesis | 8 |

Appendix Figure 1: More abundant proteins in *por1Δ* knockout in Y3K database:

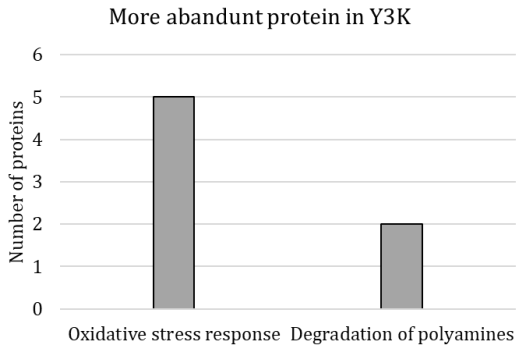

Appendix Table 2: Less abundant proteins in *por1Δ* knockout cells:

| **FunCat main category** | **FunCat description** | **No of proteins** |
|---|---|---|
| Biogenesis of cellular components | Nucleolus | 3 |
| | Catalase reaction | 3 |
| Cell rescue, defense and virulence | Electron transport | 2 |
| Cellular transport, transport facilitation and transport routes | Mitochondrial transport | 21 |
| | Tricarboxylic-acid pathway | 11 |
| Energy | Pyruvate dehydrogenase complex | 17 |
| | Electron transport and energy conservation | 4 |
| | Glycolysis and gluconeogenesis | 10 |
| | Respiration | 8 |
| | Energy generation (e.g. ATP synthase) | 9 |
| | C-compound and carbohydrate metabolism | 5 |
| Metabolism | Sugar, glucoside, polyol and carboxylate catabolism | 35 |
| | Biosynthesis of glutamate | 17 |
| | Biosynthesis of leucine | 8 |
| | Biosynthesis of valine | 6 |
| | Biosynthesis of isoleucine | 5 |
| | sugar, glucoside, polyol and carboxylate anabolism | 5 |
| | C-2 compound and organic acid catabolism | 10 |
| | Lysosomal and vacuolar protein degradation | 5 |
| Protein fate (folding, modification, destination) | NAD/NADP binding | 5 |
| Protein with binding function or cofactor requirement (structural or analytic) | Thiamine pyrophosphate binding | 11 |

Appendix Table 3: Less abundant proteins in *por1Δ* knockout cells in Y3K database:

| **FunCat main category** | **FunCat description** | **No of proteins** |
|---|---|---|
| Biogenesis of cellular components | Mitochondrion | 63 |
| Cellular transport, transport facilitation and transport routes | Electron transport | 44 |
| | Mitochondrial transport | 22 |
| | C4-dicarboxylate transport (e.g. malate, succinate, fumarate) | 6 |
| | Transport facilities | 23 |
| | Antiporter | 5 |
| | Cation transport (H+, Na+, K+, Ca2+ , NH4+, etc.) | 13 |
| | Transport ATPases | 10 |
| | C-compound and carbohydrate transport | 9 |
| Energy | Electron transport and membrane-associated energy conservation | 40 |
| | Aerobic respiration | 42 |
| | Respiration | 34 |
| | Energy generation (e.g. ATP synthase) | 16 |
| | Tricarboxylic-acid pathway (citrate cycle, Krebs cycle, TCA cycle) | 17 |
| | Accessory proteins of electron transport and membrane-associated energy conservation | 11 |
| | Glycolysis and gluconeogenesis | 13 |
| | Anaerobic respiration | 4 |
| | Lactate fermentation | 3 |
| | Propionate fermentation | 3 |
| | Alcohol fermentation | 5 |
| | Energy conversion and regeneration | 4 |
| Interaction with the environment | Homeostasis of protons | 11 |
| | Homeostasis of phosphate | 3 |
| Metabolism | Sugar, glucoside, polyol and carboxylate catabolism | 21 |
| | Sugar, glucoside, polyol and carboxylate anabolism | 15 |
| | C-compound and carbohydrate metabolism | 38 |
| | Degradation of threonine | 5 |

| | | |
|---|---|---|
| | Biosynthesis of glutamate | 5 |
| | Metabolism of the pyruvate family (alanine, isoleucine, leucine, valine) and D-alanine | 3 |
| | C-2 compound and organic acid catabolism | 4 |
| Protein synthesis | Ribosomal proteins | 43 |
| Protein with binding function or cofactor requirement (structural or analytic) | Fe/S binding | 9 |
| | FAD/FMN binding | 7 |
| | Heme binding | 5 |
| | Pyridoxal phosphate binding | 5 |

Appendix Figure 2:

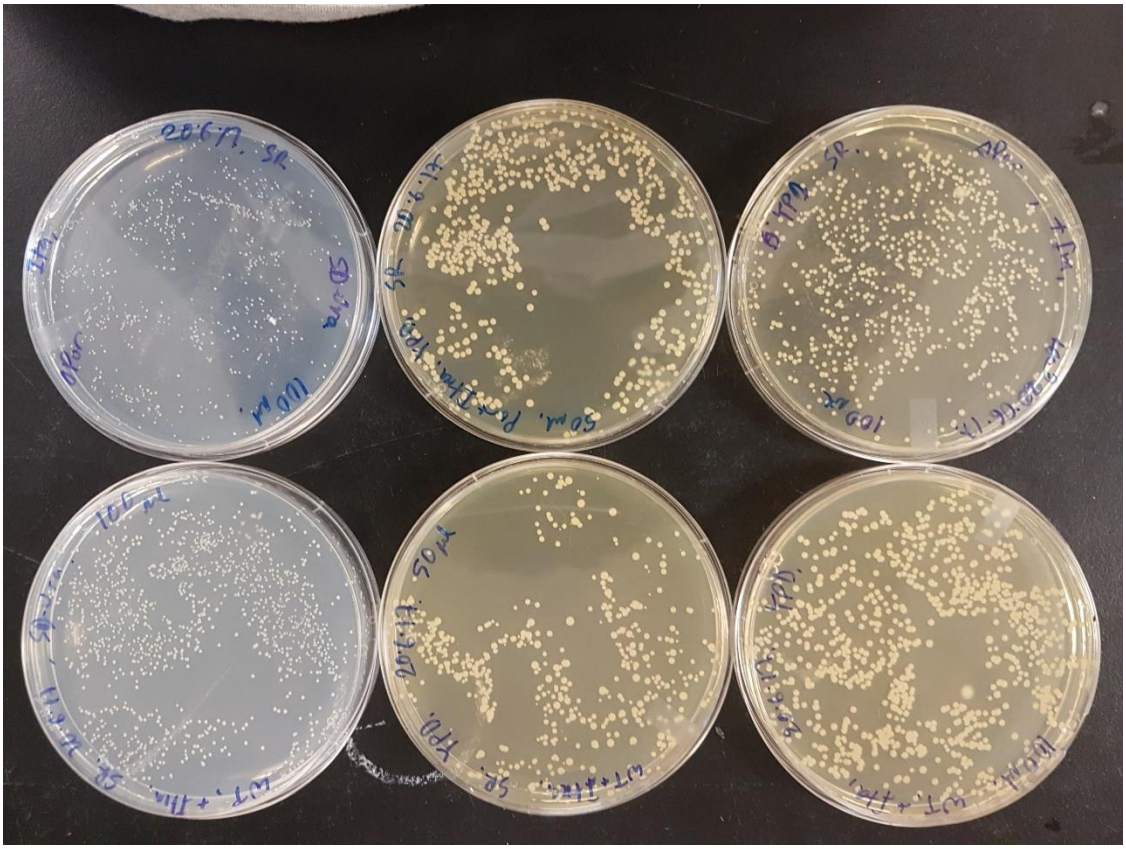

Appendix Figure 2:  Cells viability test after growing in itraconazole.

Cells were grown in the presence of 0.6 µg/ ml itraconazole and plated on YPG and YPD plates.

Appendix Table 4: Proteins involved in protein fate (folding, modification, destination) that are more abundant in *por1Δ* cells

| Gene | Protein |
|---|---|
| ARC15 | Subunit of the ARP2/3 complex |
| ARC19 | Subunit of the ARP2/3 complex |
| ARC35 | Subunit of the ARP2/3 |
| ARC40 | Subunit of the ARP2/3 complex |
| PAN1 | binds to and activates Arp2/3 complex in vitro |
| ARP3 | Essential component of the Arp2/3 complex |
| CRN1 | cortical actin cytoskeletal component that associates with the Arp2p/Arp3p complex to regulate |
| COF1 | Cofilin, involved in pH-dependent actin filament depolarization |
| SLA1 | Cytoskeletal protein binding protein |
| NCL1 | S-adenosyl-L-methionine-dependent tRNA: |
| UBA1 | Ubiquitin activating enzyme (E1) |
| NAP1 | Histone chaperone; involved in histone exchange by removing and replacing histone H2A-H2B dimers o |
| SEC31 | Component of the Sec13p-Sec31p complex of the COPII vesicle coat |
| NOP15 | Constituent of 66S pre-ribosomal particles; involved in 60S ribosomal subunit biogenesis |
| VMA4 | Subunit E of the V1 domain of the vacuolar H+-ATPase |
| FAS2 | Alpha subunit of fatty acid synthetase |

Appendix Table 5: Less abundant proteins in “energy production” in p*or1Δ*

| Protein | Description |
|---|---|
| ATP1 | Alpha subunit of the F1 sector of mitochondrial F1F0 ATP synthase |
| ATP14 | Subunit h of the F0 sector of mitochondrial F1F0 ATP synthase |
| ATP15 | Epsilon subunit of the F1 sector of mitochondrial F1F0 ATP synthase |
| ATP16 | Delta subunit of the central stalk of mitochondrial F1F0 ATP synthase; |
| ATP17 | Subunit f of the F0 sector of mitochondrial F1F0 ATP synthase |
| ATP18 | Subunit of the mitochondrial F1F0 ATP synthase |

| | |
|---|---|
| ATP19 | Subunit k of the mitochondrial F1F0 ATP synthase |
| ATP2 | Beta subunit of the F1 sector of mitochondrial F1F0 ATP synthase |
| ATP20 | Subunit g of the mitochondrial F1F0 ATP synthase |
| ATP21/TIM11 | Subunit e of mitochondrial F1F0-ATPase |
| ATP3 | Gamma subunit of the F1 sector of mitochondrial F1F0 ATP synthase |
| ATP4 | Subunit b of the stator stalk of mitochondrial F1F0 ATP synthase |
| ATP5 | Subunit 5 of the stator stalk of mitochondrial F1F0 ATP synthase |
| ATP7 | Subunit d of the stator stalk of mitochondrial F1F0 ATP synthase |
| CYT1 | Cytochrome c1; component of the mitochondrial respiratory chain |
| INH1 | Protein that inhibits ATP hydrolysis by the F1F0-ATP synthase |

Appendix Table 6: Less abundant proteins that are in part of TCA

| **Protein name** | **Description** |
|---|---|
| ACO2 | Putative mitochondrial aconitase isozyme |
| CIT1 | Citrate synthase |
| CIT3 | Dual specificity mitochondrial citrate and methylcitrate synthase |
| FUM1 | Fumarase; converts fumaric acid to L-malic acid in the TCA cycle; |
| GDH1 | NADP(+)-dependent glutamate dehydrogenase |
| GDH2 | NAD(+)-dependent glutamate dehydrogenase |
| IDH1 | Subunit of mitochondrial NAD(+)-dependent isocitrate dehydrogenase |
| IDH2 | Subunit of mitochondrial NAD(+)-dependent isocitrate dehydrogenase |
| IDP1 | Mitochondrial NADP-specific isocitrate dehydrogenase; |
| IDP2 | Cytosolic NADP-specific isocitrate dehydrogenase |
| KGD2 | Dihydrolipoyl transsuccinylase; component of the mitochondrial alpha-ketoglutarate dehydrogenase complex, which catalyzes the oxidative decarboxylation of alpha-ketoglutarate to succinyl-CoA in the TCA cycle; phosphorylated |
| LPD1 | Dihydrolipoamide dehydrogenase |
| LSC1 | Alpha subunit of succinyl-CoA ligase |
| LSC2 | Beta subunit of succinyl-CoA ligase; succinyl-CoA |
| LYS12 | Homo-isocitrate dehydrogenase |
| LYS4 | Homoaconitase |
| MDH1 | Mitochondrial malate dehydrogenase |
| SDH1 | Flavoprotein subunit of succinate dehydrogenase; |
| SDH2 | Iron-sulfur protein subunit of succinate dehydrogenase |

| | |
|---|---|
| SDH3 | Subunit of succinate dehydrogenase and of TIM22 translocase; functions as cytochrome b subunit of succinate dehydrogenase |
| SDH4 | succinate dehydrogenase (SDH) |

Appendix File 1:

R0, R1 = Inter-replicate differences; Z0, Z1 = Replicates comparing different strains; NR0, NR1 = normalized, NZ0, NZ1 = combined vector of Z0 and Z1.

**More abundant proteins:**

| protein | GENE | WTyeast | WTyeast2 | dportyeast | dPoryeast2 | R0 | R1 | Z0 | Z1 | NR0 | NR1 | NZ0 | NZ1 | SN |
|---|---|---|---|---|---|---|---|---|---|---|---|---|---|---|
| YKR097W | PCK1 | 21.17 | 20.93 | 22.18 | 22.03 | -0.24 | -0.15 | 1.01 | 1.1 | 0.04 | -0.02 | 1.178 | 1.119 | 36.33074 |
| YBR218C | PYC2 | 13.94 | 13.73 | 16.65 | 16.43 | -0.21 | -0.22 | 2.71 | 2.7 | 0.07 | -0.09 | 2.878 | 2.719 | 34.72512 |
| YDR127W | ARO1 | 17.27 | 16.9 | 19.2 | 19.07 | -0.37 | -0.13 | 1.93 | 2.17 | -0.09 | 9.99E-16 | 2.098 | 2.189 | 33.68944 |
| YBR118W | TEF2 | 23.41 | 23.1 | 24.19 | 24.11 | -0.31 | -0.08 | 0.78 | 1.01 | -0.03 | 0.05 | 0.948 | 1.029 | 23.99476 |
| YGR234W | YHB1 | 18.79 | 18.43 | 21.05 | 21.07 | -0.36 | 0.02 | 2.26 | 2.64 | -0.08 | 0.15 | 2.428 | 2.659 | 21.18093 |
| YER165W | PAB1 | 19.3 | 19.11 | 20.46 | 20.34 | -0.19 | -0.12 | 1.16 | 1.23 | 0.09 | 0.01 | 1.328 | 1.249 | 20.13244 |
| YIL041W | GVP36 | 18.08 | 17.85 | 19.66 | 19.65 | -0.23 | -0.01 | 1.58 | 1.8 | 0.05 | 0.12 | 1.748 | 1.819 | 19.40577 |
| YGR124W | ASN2 | 15.99 | 15.84 | 17.8 | 17.73 | -0.15 | -0.07 | 1.81 | 1.89 | 0.13 | 0.06 | 1.978 | 1.909 | 19.19955 |
| | | | | | | | | | | | | | | |
| YOR209C | NPT1 | 14.47 | 14.34 | 16.31 | 16.11 | -0.13 | -0.2 | 1.84 | 1.77 | 0.15 | -0.07 | 2.008 | 1.789 | 16.24694 |
| YMR217W | GUA1 | 16.08 | 15.88 | 17.56 | 17.32 | -0.2 | -0.24 | 1.48 | 1.44 | 0.08 | -0.11 | 1.648 | 1.459 | 16.18238 |
| YPR033C | HTS1 | 14.35 | 14.03 | 16.51 | 16.18 | -0.32 | -0.33 | 2.16 | 2.15 | -0.04 | -0.2 | 2.328 | 2.169 | 15.60028 |
| YHL034C | SBP1 | 17.93 | 17.78 | 19.75 | 19.51 | -0.15 | -0.24 | 1.82 | 1.73 | 0.13 | -0.11 | 1.988 | 1.749 | 15.54875 |
| YJR105W | ADO1 | 17.29 | 17.06 | 18.95 | 19 | -0.23 | 0.05 | 1.66 | 1.94 | 0.05 | 0.18 | 1.828 | 1.959 | 14.34258 |
| sp\|GAG_SCVLA\| | | 18.53 | 17.85 | 22.21 | 22.16 | -0.68 | -0.05 | 3.68 | 4.31 | -0.4 | 0.08 | 3.848 | 4.329 | 14.19883 |
| YLR174W | IDP2 | 19.54 | 19.25 | 20.36 | 20.34 | -0.29 | -0.02 | 0.82 | 1.09 | -0.01 | 0.11 | 0.988 | 1.109 | 13.447 |
| YNR016C | ACC1 | 18.69 | 18.04 | 21.85 | 21.69 | -0.65 | -0.16 | 3.16 | 3.65 | -0.37 | -0.03 | 3.328 | 3.669 | 13.34404 |
| YMR226C | YMR226C | 17.25 | 17.06 | 18.22 | 18.17 | -0.19 | -0.05 | 0.97 | 1.11 | 0.09 | 0.08 | 1.138 | 1.129 | 13.31239 |
| YDL055C | PSA1 | 19.65 | 19.28 | 20.86 | 20.61 | -0.37 | -0.25 | 1.21 | 1.33 | -0.09 | -0.12 | 1.378 | 1.349 | 12.85593 |
| YOR335C | ALA1 | 17.72 | 17.53 | 18.7 | 18.49 | -0.19 | -0.21 | 0.98 | 0.96 | 0.09 | -0.08 | 1.148 | 0.979 | 12.52954 |
| | | | | | | | | | | | | | | |

| | | | | | | | | | | | | | | |
|---|---|---|---|---|---|---|---|---|---|---|---|---|---|---|
| YJL167W | ERG20 | 17.86 | 17.68 | 18.83 | 18.79 | -0.18 | -0.04 | 0.97 | 1.11 | 0.1 | 0.09 | 1.138 | 1.129 | 11.91518 |
| YJL020C | BBC1 | 16.92 | 16.53 | 18.69 | 18.36 | -0.39 | -0.33 | 1.77 | 1.83 | -0.11 | -0.2 | 1.938 | 1.849 | 11.73495 |
| YDR035W | ARO3 | 14.54 | 14.24 | 16.1 | 16.2 | -0.3 | 0.1 | 1.56 | 1.96 | -0.02 | 0.23 | 1.728 | 1.979 | 11.37987 |
| YJL111W | CCT7 | 14.66 | 14.46 | 15.57 | 15.56 | -0.2 | -0.01 | 0.91 | 1.1 | 0.08 | 0.12 | 1.078 | 1.119 | 10.77355 |
| YDR432W | NPL3 | 16.88 | 16.43 | 18.94 | 18.57 | -0.45 | -0.37 | 2.06 | 2.14 | -0.17 | -0.24 | 2.228 | 2.159 | 10.54868 |
| YJR065C | ARP3 | 17.32 | 17.04 | 18.65 | 18.33 | -0.28 | -0.32 | 1.33 | 1.29 | -1.1E-15 | -0.19 | 1.498 | 1.309 | 10.47023 |
| YNL208W | YNL208W | 17.82 | 17.71 | 19.11 | 18.88 | -0.11 | -0.23 | 1.29 | 1.17 | 0.17 | -0.1 | 1.458 | 1.189 | 9.538833 |
| YDR321W | ASP1 | 13.41 | 13.3 | 14.78 | 14.8 | -0.11 | 0.02 | 1.37 | 1.5 | 0.17 | 0.15 | 1.538 | 1.519 | 9.534705 |
| YLL018C | DPS1 | 17.86 | 17.54 | 18.79 | 18.51 | -0.32 | -0.28 | 0.93 | 0.97 | -0.04 | -0.15 | 1.098 | 0.989 | 9.518981 |
| YGR037C | ACB1 | 18.14 | 18.05 | 19.58 | 19.34 | -0.09 | -0.24 | 1.44 | 1.29 | 0.19 | -0.11 | 1.608 | 1.309 | 9.444251 |
| YBL024W | NCL1 | 15.28 | 14.88 | 17.67 | 17.95 | -0.4 | 0.28 | 2.39 | 3.07 | -0.12 | 0.41 | 2.558 | 3.089 | 9.388213 |
| YLR429W | CRN1 | 16.47 | 16.21 | 17.37 | 17.42 | -0.26 | 0.05 | 0.9 | 1.21 | 0.02 | 0.18 | 1.068 | 1.229 | 8.990281 |
| YDR037W | KRS1 | 14.53 | 13.99 | 16.66 | 16.85 | -0.54 | 0.19 | 2.13 | 2.86 | -0.26 | 0.32 | 2.298 | 2.879 | 8.934219 |
| YGL234W | ADE5,7 | 17.39 | 17.01 | 18.38 | 18.1 | -0.38 | -0.28 | 0.99 | 1.09 | -0.1 | -0.15 | 1.158 | 1.109 | 8.893982 |
| YNR035C | ARC35 | 17.19 | 16.95 | 17.92 | 17.95 | -0.24 | 0.03 | 0.73 | 1 | 0.04 | 0.16 | 0.898 | 1.019 | 8.235426 |
| YGL206C | CHC1 | 18.33 | 18.15 | 19.57 | 19.68 | -0.18 | 0.11 | 1.24 | 1.53 | 0.1 | 0.24 | 1.408 | 1.549 | 8.051117 |
| YGL062W | PYC1 | 18.19 | 17.89 | 19.69 | 19.89 | -0.3 | 0.2 | 1.5 | 2 | -0.02 | 0.33 | 1.668 | 2.019 | 7.921496 |
| | | | | | | | | | | | | | | |
| YPL028W | ERG10 | 18.46 | 17.86 | 19.84 | 19.72 | -0.6 | -0.12 | 1.38 | 1.86 | -0.32 | 0.01 | 1.548 | 1.879 | 7.6042 |
| YEL037C | RAD23 | 13.72 | 13.47 | 15.05 | 15.25 | -0.25 | 0.2 | 1.33 | 1.78 | 0.03 | 0.33 | 1.498 | 1.799 | 7.064886 |
| YFL039C | ACT1 | 22.05 | 21.57 | 23.04 | 22.77 | -0.48 | -0.27 | 0.99 | 1.2 | -0.2 | -0.14 | 1.158 | 1.219 | 6.887062 |
| YKL182W | FAS1 | 20.48 | 20.34 | 21.65 | 21.77 | -0.14 | 0.12 | 1.17 | 1.43 | 0.14 | 0.25 | 1.338 | 1.449 | 6.883266 |
| YMR315W | YMR315W | 16.28 | 15.68 | 17.47 | 17.4 | -0.6 | -0.07 | 1.19 | 1.72 | -0.32 | 0.06 | 1.358 | 1.739 | 6.776962 |
| YFL037W | TUB2 | 13.98 | 14.47 | 17.74 | 17.68 | 0.49 | -0.06 | 3.76 | 3.21 | 0.77 | 0.07 | 3.928 | 3.229 | 6.576572 |
| YNL030W | HHF2 | 17.81 | 17.24 | 19.2 | 18.87 | -0.57 | -0.33 | 1.39 | 1.63 | -0.29 | -0.2 | 1.558 | 1.649 | 6.439807 |
| YHR146W | CRP1 | 16.52 | 16.52 | 17.76 | 17.7 | 0 | -0.06 | 1.24 | 1.18 | 0.28 | 0.07 | 1.408 | 1.199 | 6.407589 |
| YHR137W | ARO9 | 18.6 | 18.09 | 19.33 | 19.26 | -0.51 | -0.07 | 0.73 | 1.17 | -0.23 | 0.06 | 0.898 | 1.189 | 6.268512 |
| YGR061C | ADE6 | 15.92 | 15.25 | 17.48 | 17.19 | -0.67 | -0.29 | 1.56 | 1.94 | -0.39 | -0.16 | 1.728 | 1.959 | 6.196767 |
| YPR069C | SPE3 | 16.38 | 16.28 | 17.38 | 17.45 | -0.1 | 0.07 | 1 | 1.17 | 0.18 | 0.2 | 1.168 | 1.189 | 6.194304 |

| | | | | | | | | | | | | | | |
|---|---|---|---|---|---|---|---|---|---|---|---|---|---|---|
| YPR160W | GPH1 | 18.21 | 17.59 | 19.62 | 19.31 | -0.62 | -0.31 | 1.41 | 1.72 | -0.34 | -0.18 | 1.578 | 1.739 | 6.103945 |
| YLR231C | BNA5 | 14.16 | 13.93 | 15.55 | 15.1 | -0.23 | -0.45 | 1.39 | 1.17 | 0.05 | -0.32 | 1.558 | 1.189 | 6.051168 |
| YPL231W | FAS2 | 20.13 | 20.08 | 21.11 | 21.09 | -0.05 | -0.02 | 0.98 | 1.01 | 0.23 | 0.11 | 1.148 | 1.029 | 6.046925 |
| YDR388W | RVS167 | 15.13 | 14.45 | 16.56 | 16.65 | -0.68 | 0.09 | 1.43 | 2.2 | -0.4 | 0.22 | 1.598 | 2.219 | 5.990061 |
| YDL195W | SEC31 | 15.57 | 15.07 | 16.68 | 16.85 | -0.5 | 0.17 | 1.11 | 1.78 | -0.22 | 0.3 | 1.278 | 1.799 | 5.931744 |
| YJL080C | SCP160 | 16.5 | 16.57 | 18.05 | 17.82 | 0.07 | -0.23 | 1.55 | 1.25 | 0.35 | -0.1 | 1.718 | 1.269 | 5.86765 |
| YER063W | THO1 | 15.55 | 14.92 | 16.64 | 16.63 | -0.63 | -0.01 | 1.09 | 1.71 | -0.35 | 0.12 | 1.258 | 1.729 | 5.778986 |
| YHR025W | THR1 | 16.93 | 16.32 | 18.22 | 17.9 | -0.61 | -0.32 | 1.29 | 1.58 | -0.33 | -0.19 | 1.458 | 1.599 | 5.682742 |
| YOR168W | GLN4 | 15 | 14.21 | 16.72 | 16.47 | -0.79 | -0.25 | 1.72 | 2.26 | -0.51 | -0.12 | 1.888 | 2.279 | 5.6486 |
| YBR115C | LYS2 | 14.65 | 14.57 | 16.19 | 15.74 | -0.08 | -0.45 | 1.54 | 1.17 | 0.2 | -0.32 | 1.708 | 1.189 | 5.514909 |
| YJL130C | URA2 | 16.99 | 16.57 | 18.57 | 18.04 | -0.42 | -0.53 | 1.58 | 1.47 | -0.14 | -0.4 | 1.748 | 1.489 | 5.418265 |
| YBL058W | SHP1 | 15.03 | 14.99 | 16.01 | 16.05 | -0.04 | 0.04 | 0.98 | 1.06 | 0.24 | 0.17 | 1.148 | 1.079 | 5.356801 |
| YMR125W | STO1 | 14.66 | 13.82 | 16.29 | 16.25 | -0.84 | -0.04 | 1.63 | 2.43 | -0.56 | 0.09 | 1.798 | 2.449 | 5.356546 |
| YLL050C | COF1 | 16.02 | 15.54 | 17.35 | 16.89 | -0.48 | -0.46 | 1.33 | 1.35 | -0.2 | -0.33 | 1.498 | 1.369 | 5.259016 |
| YOR095C | RKI1 | 15.26 | 15.32 | 16.54 | 16.34 | 0.06 | -0.2 | 1.28 | 1.02 | 0.34 | -0.07 | 1.448 | 1.039 | 5.134074 |
| YIL109C | SEC24 | 16.33 | 15.65 | 17.39 | 17.22 | -0.68 | -0.17 | 1.06 | 1.57 | -0.4 | -0.04 | 1.228 | 1.589 | 4.995608 |
| YER156C | YER156C | 13.89 | 13.07 | 15.33 | 15.19 | -0.82 | -0.14 | 1.44 | 2.12 | -0.54 | -0.01 | 1.608 | 2.139 | 4.954709 |
| YGR094W | VAS1 | 18.22 | 17.69 | 19.29 | 18.91 | -0.53 | -0.38 | 1.07 | 1.22 | -0.25 | -0.25 | 1.238 | 1.239 | 4.954 |
| YPR074C | TKL1 | 18.23 | 17.71 | 19.88 | 19.31 | -0.52 | -0.57 | 1.65 | 1.6 | -0.24 | -0.44 | 1.818 | 1.619 | 4.857149 |
| YGR205W | TDA10 | 14.82 | 13.8 | 16.78 | 16.66 | -1.02 | -0.12 | 1.96 | 2.86 | -0.74 | 0.01 | 2.128 | 2.879 | 4.837514 |
| YGL048C | RPT6 | 14.59 | 14.53 | 15.57 | 15.71 | -0.06 | 0.14 | 0.98 | 1.18 | 0.22 | 0.27 | 1.148 | 1.199 | 4.766177 |
| YPR181C | SEC23 | 17.23 | 16.44 | 18.49 | 18.39 | -0.79 | -0.1 | 1.26 | 1.95 | -0.51 | 0.03 | 1.428 | 1.969 | 4.761011 |
| YKL007W | CAP1 | 13.69 | 13.19 | 15.61 | 14.94 | -0.5 | -0.67 | 1.92 | 1.75 | -0.22 | -0.54 | 2.088 | 1.769 | 4.69327 |
| YDL084W | SUB2 | 16.6 | 16.77 | 18.12 | 17.96 | 0.17 | -0.16 | 1.52 | 1.19 | 0.45 | -0.03 | 1.688 | 1.209 | 4.603782 |
| | | | | | | | | | | | | | | |
| YHR019C | DED81 | 18.05 | 17.34 | 19.03 | 19.03 | -0.71 | 0 | 0.98 | 1.69 | -0.43 | 0.13 | 1.148 | 1.709 | 4.583 |
| YBR249C | ARO4 | 16.54 | 15.73 | 17.89 | 17.66 | -0.81 | -0.23 | 1.35 | 1.93 | -0.53 | -0.1 | 1.518 | 1.949 | 4.580334 |
| YLR153C | ACS2 | 15.96 | 15.29 | 17.17 | 17.45 | -0.67 | 0.28 | 1.21 | 2.16 | -0.39 | 0.41 | 1.378 | 2.179 | 4.556168 |
| YLR258W | GSY2 | 16.23 | 16.29 | 17.39 | 17.47 | 0.06 | 0.08 | 1.16 | 1.18 | 0.34 | 0.21 | 1.328 | 1.199 | 4.477163 |
| YMR092C | AIP1 | 15.68 | 15.46 | 17.23 | 16.63 | -0.22 | -0.6 | 1.55 | 1.17 | 0.06 | -0.47 | 1.718 | 1.189 | 4.409569 |

| | | | | | | | | | | | | | | |
|---|---|---|---|---|---|---|---|---|---|---|---|---|---|---|
| YLR060W | FRS1 | 16.66 | 15.8 | 17.91 | 17.88 | -0.86 | -0.03 | 1.25 | 2.08 | -0.58 | 0.1 | 1.418 | 2.099 | 4.303888 |
| YKR001C | VPS1 | 15.57 | 15.59 | 16.61 | 16.75 | 0.02 | 0.14 | 1.04 | 1.16 | 0.3 | 0.27 | 1.208 | 1.179 | 4.18224 |
| YBR035C | PDX3 | 16.23 | 15.6 | 17.16 | 16.82 | -0.63 | -0.34 | 0.93 | 1.22 | -0.35 | -0.21 | 1.098 | 1.239 | 4.055975 |
| YBL003C | HTA2 | 18.46 | 17.9 | 19.42 | 19.78 | -0.56 | 0.36 | 0.96 | 1.88 | -0.28 | 0.49 | 1.128 | 1.899 | 3.913742 |
| YMR318C | ADH6 | 14.92 | 14.48 | 16.89 | 16.08 | -0.44 | -0.81 | 1.97 | 1.6 | -0.16 | -0.68 | 2.138 | 1.619 | 3.839027 |
| YER091C | MET6 | 16.64 | 16.56 | 18.1 | 18.64 | -0.08 | 0.54 | 1.46 | 2.08 | 0.2 | 0.67 | 1.628 | 2.099 | 3.79905 |
| YFL022C | FRS2 | 16.69 | 16.09 | 18.02 | 17.45 | -0.6 | -0.57 | 1.33 | 1.36 | -0.32 | -0.44 | 1.498 | 1.379 | 3.7424 |
| YFR044C | DUG1 | 19.51 | 18.77 | 20.32 | 20.16 | -0.74 | -0.16 | 0.81 | 1.39 | -0.46 | -0.03 | 0.978 | 1.409 | 3.720699 |
| YFL030W | AGX1 | 14.19 | 14.4 | 17.07 | 16.13 | 0.21 | -0.94 | 2.88 | 1.73 | 0.49 | -0.81 | 3.048 | 1.749 | 3.712092 |
| YLR150W | STM1 | 19.67 | 19.36 | 20.23 | 20.46 | -0.31 | 0.23 | 0.56 | 1.1 | -0.03 | 0.36 | 0.728 | 1.119 | 3.695441 |
| | | | | | | | | | | | | | | |
| YIL062C | ARC15 | 16.64 | 15.76 | 17.89 | 17.54 | -0.88 | -0.35 | 1.25 | 1.78 | -0.6 | -0.22 | 1.418 | 1.799 | 3.584411 |
| | | | | | | | | | | | | | | |
| YBR111C | YSA1 | 14.7 | 14.19 | 15.78 | 15.24 | -0.51 | -0.54 | 1.08 | 1.05 | -0.23 | -0.41 | 1.248 | 1.069 | 3.495482 |
| YNL010W | YNL010W | 15.27 | 15.37 | 16.68 | 17.12 | 0.1 | 0.44 | 1.41 | 1.75 | 0.38 | 0.57 | 1.578 | 1.769 | 3.460361 |
| YOR259C | RPT4 | 14.7 | 13.88 | 15.54 | 15.4 | -0.82 | -0.14 | 0.84 | 1.52 | -0.54 | -0.01 | 1.008 | 1.539 | 3.406313 |
| YOR323C | PRO2 | 15.88 | 14.93 | 16.93 | 16.79 | -0.95 | -0.14 | 1.05 | 1.86 | -0.67 | -0.01 | 1.218 | 1.879 | 3.341767 |
| YDR341C | YDR341C | 16.7 | 15.67 | 17.92 | 17.74 | -1.03 | -0.18 | 1.22 | 2.07 | -0.75 | -0.05 | 1.388 | 2.089 | 3.3367 |
| YIL078W | THS1 | 17.1 | 17.11 | 17.96 | 18.17 | 0.01 | 0.21 | 0.86 | 1.06 | 0.29 | 0.34 | 1.028 | 1.079 | 3.334937 |
| YER025W | GCD11 | 14.35 | 12.67 | 16.57 | 16.79 | -1.68 | 0.22 | 2.22 | 4.12 | -1.4 | 0.35 | 2.388 | 4.139 | 3.31129 |
| YLL024C | SSA2 | 17.5 | 17.65 | 18.79 | 19.14 | 0.15 | 0.35 | 1.29 | 1.49 | 0.43 | 0.48 | 1.458 | 1.509 | 3.25601 |
| YBR234C | ARC40 | 15.56 | 15.92 | 17.75 | 17.1 | 0.36 | -0.65 | 2.19 | 1.18 | 0.64 | -0.52 | 2.358 | 1.199 | 3.207932 |
| YOR184W | SER1 | 15.42 | 15.88 | 17.25 | 17.09 | 0.46 | -0.16 | 1.83 | 1.21 | 0.74 | -0.03 | 1.998 | 1.229 | 3.167302 |
| YGL009C | LEU1 | 14.23 | 14.28 | 16.35 | 15.47 | 0.05 | -0.88 | 2.12 | 1.19 | 0.33 | -0.75 | 2.288 | 1.209 | 3.158183 |
| YGL040C | HEM2 | 15.75 | 15.92 | 18.37 | 17.35 | 0.17 | -1.02 | 2.62 | 1.43 | 0.45 | -0.89 | 2.788 | 1.449 | 3.150579 |
| YLR270W | DCS1 | 14.86 | 14.26 | 15.86 | 16.46 | -0.6 | 0.6 | 1 | 2.2 | -0.32 | 0.73 | 1.168 | 2.219 | 3.146105 |
| | | | | | | | | | | | | | | |
| YHR179W | OYE2 | 15.69 | 15.91 | 17.05 | 17.44 | 0.22 | 0.39 | 1.36 | 1.53 | 0.5 | 0.52 | 1.528 | 1.549 | 3.016157 |
| YKL013C | ARC19 | 16.28 | 14.87 | 17.81 | 17.72 | -1.41 | -0.09 | 1.53 | 2.85 | -1.13 | 0.04 | 1.698 | 2.869 | 2.948438 |
| YER003C | PMI40 | 15.95 | 14.88 | 17.14 | 16.81 | -1.07 | -0.33 | 1.19 | 1.93 | -0.79 | -0.2 | 1.358 | 1.949 | 2.914937 |

| | | | | | | | | | | | | | | |
|---|---|---|---|---|---|---|---|---|---|---|---|---|---|---|
| **YLR109W** | **AHP1** | **15.93** | **14.95** | **17.54** | **16.84** | **-0.98** | **-0.7** | **1.61** | **1.89** | **-0.7** | **-0.57** | **1.778** | **1.909** | **2.889881** |
| **YNR050C** | **LYS9** | **19.66** | **18.99** | **20.12** | **20.34** | **-0.67** | **0.22** | **0.46** | **1.35** | **-0.39** | **0.35** | **0.628** | **1.369** | **2.874243** |
| **YGR155W** | **CYS4** | **18.13** | **17.86** | **18.64** | **18.97** | **-0.27** | **0.33** | **0.51** | **1.11** | **0.01** | **0.46** | **0.678** | **1.129** | **2.862232** |

**Less abundant proteins in *por1Δ***

| protein | GENE | WTyeast | WTyeast2 | dportyeast | dPoryeast2 | R0 | R1 | Z0 | Z1 | NR0 | NR1 | NZ0 | NZ1 | SN |
|---|---|---|---|---|---|---|---|---|---|---|---|---|---|---|
| YBL099W | ATP1 | 20.56 | 20.3 | 18.91 | 18.79 | -0.26 | -0.12 | -1.65 | -1.51 | 0.02 | 0.01 | -1.482 | -1.491 | 94.0 |
| YNL071W | LAT1 | 18.25 | 17.92 | 13.04 | 12.8 | -0.33 | -0.24 | -5.21 | -5.12 | -0.05 | -0.11 | -5.042 | -5.101 | 59.4 |
| YOR374W | ALD4 | 25.92 | 25.62 | 24.74 | 24.59 | -0.3 | -0.15 | -1.18 | -1.03 | -0.02 | -0.02 | -1.012 | -1.011 | 50.6 |
| YJR121W | ATP2 | 21.13 | 20.82 | 19.74 | 19.64 | -0.31 | -0.1 | -1.39 | -1.18 | -0.03 | 0.03 | -1.222 | -1.161 | 39.7 |
| YDR258C | HSP78 | 19.07 | 18.82 | 16.72 | 16.7 | -0.25 | -0.02 | -2.35 | -2.12 | 0.03 | 0.11 | -2.182 | -2.101 | 26.6 |
| YKL103C | APE1 | 20.07 | 19.88 | 17.67 | 17.64 | -0.19 | -0.03 | -2.4 | -2.24 | 0.09 | 0.1 | -2.232 | -2.221 | 23.4 |
| YER178W | PDA1 | 19.54 | 19.08 | 16.25 | 16.22 | -0.46 | -0.03 | -3.29 | -2.86 | -0.18 | 0.1 | -3.122 | -2.841 | 20.5 |
| YEL060C | PRB1 | 20.81 | 20.4 | 17.87 | 17.87 | -0.41 | 0 | -2.94 | -2.53 | -0.13 | 0.13 | -2.772 | -2.511 | 20.3 |
| YHR037W | PUT2 | 19.77 | 19.65 | 17.07 | 17.04 | -0.12 | -0.03 | -2.7 | -2.61 | 0.16 | 0.1 | -2.532 | -2.591 | 19.2 |
| YDR233C | RTN1 | 18.22 | 17.99 | 15.87 | 15.89 | -0.23 | 0.02 | -2.35 | -2.1 | 0.05 | 0.15 | -2.182 | -2.081 | 19.1 |
| YGR130C | YGR130C | 19.13 | 18.68 | 15.18 | 14.77 | -0.45 | -0.41 | -3.95 | -3.91 | -0.17 | -0.28 | -3.782 | -3.891 | 16.6 |
| YDR256C | CTA1 | 18.83 | 18.45 | 15.03 | 14.59 | -0.38 | -0.44 | -3.8 | -3.86 | -0.1 | -0.31 | -3.632 | -3.841 | 16.2 |
| YMR072W | ABF2 | 19.01 | 18.62 | 16.78 | 16.78 | -0.39 | 0 | -2.23 | -1.84 | -0.11 | 0.13 | -2.062 | -1.821 | 16.2 |
| YKR066C | CCP1 | 19.47 | 19.18 | 17.34 | 17.38 | -0.29 | 0.04 | -2.13 | -1.8 | -0.01 | 0.17 | -1.962 | -1.781 | 15.6 |
| YOR136W | IDH2 | 19.57 | 19.49 | 17.34 | 17.17 | -0.08 | -0.17 | -2.23 | -2.32 | 0.2 | -0.04 | -2.062 | -2.301 | 15.1 |
| YMR169C | ALD3 | 19.08 | 18.79 | 17.7 | 17.68 | -0.29 | -0.02 | -1.38 | -1.11 | -0.01 | 0.11 | -1.212 | -1.091 | 14.8 |
| YLR175W | CBF5 | 19.22 | 19.08 | 17.44 | 17.22 | -0.14 | -0.22 | -1.78 | -1.86 | 0.14 | -0.09 | -1.612 | -1.841 | 14.7 |
| YBR286W | APE3 | 20.98 | 20.8 | 18.6 | 18.66 | -0.18 | 0.06 | -2.38 | -2.14 | 0.1 | 0.19 | -2.212 | -2.121 | 14.3 |
| YBR269C | SDH8 | 16.72 | 16.49 | 15.12 | 14.84 | -0.23 | -0.28 | -1.6 | -1.65 | 0.05 | -0.15 | -1.432 | -1.631 | 13.7 |
| YGR086C | PIL1 | 17.54 | 17.2 | 14.86 | 14.97 | -0.34 | 0.11 | -2.68 | -2.23 | -0.06 | 0.24 | -2.512 | -2.211 | 13.5 |
| YGL156W | AMS1 | 19.36 | 19.26 | 16.88 | 16.54 | -0.1 | -0.34 | -2.48 | -2.72 | 0.18 | -0.21 | -2.312 | -2.701 | 12.9 |
| YDL014W | NOP1 | 19.1 | 18.72 | 17.38 | 17.38 | -0.38 | 0 | -1.72 | -1.34 | -0.1 | 0.13 | -1.552 | -1.321 | 12.4 |
| YIL125W | KGD1 | 21.49 | 21.14 | 20.09 | 20.07 | -0.35 | -0.02 | -1.4 | -1.07 | -0.07 | 0.11 | -1.232 | -1.051 | 12.4 |
| YJL172W | CPS1 | 20.17 | 20.26 | 16.36 | 16.51 | 0.09 | 0.15 | -3.81 | -3.75 | 0.37 | 0.28 | -3.642 | -3.731 | 11.2 |
| YIL160C | POT1 | 18.49 | 17.81 | 14.88 | 14.61 | -0.68 | -0.27 | -3.61 | -3.2 | -0.4 | -0.14 | -3.442 | -3.181 | 11.1 |
| YML128C | MSC1 | 19.87 | 19.48 | 14.3 | 13.44 | -0.39 | -0.86 | -5.57 | -6.04 | -0.11 | -0.73 | -5.402 | -6.021 | 11.0 |
| YPL223C | GRE1 | 19.65 | 19.69 | 16.56 | 16.65 | 0.04 | 0.09 | -3.09 | -3.04 | 0.32 | 0.22 | -2.922 | -3.021 | 10.8 |
| YBR221C | PDB1 | 19.52 | 19.21 | 15.93 | 15.31 | -0.31 | -0.62 | -3.59 | -3.9 | -0.03 | -0.49 | -3.422 | -3.881 | 10.5 |
| YDR050C | TPI1 | 17.06 | 16.64 | 14.48 | 14.04 | -0.42 | -0.44 | -2.58 | -2.6 | -0.14 | -0.31 | -2.412 | -2.581 | 10.4 |

| | | | | | | | | | | | | | | |
|---|---|---|---|---|---|---|---|---|---|---|---|---|---|---|
| YPL262W | FUM1 | 21.9 | 21.51 | 20.33 | 20.03 | -0.39 | -0.3 | -1.57 | -1.48 | -0.11 | -0.17 | -1.402 | -1.461 | 10.0 |
| YDR234W | LYS4 | 18.45 | 17.94 | 16.42 | 16.38 | -0.51 | -0.04 | -2.03 | -1.56 | -0.23 | 0.09 | -1.862 | -1.541 | 9.8 |
| YPR002W | PDH1 | 20.16 | 19.81 | 17.32 | 16.78 | -0.35 | -0.54 | -2.84 | -3.03 | -0.07 | -0.41 | -2.672 | -3.011 | 9.7 |
| YJR016C | ILV3 | 20.42 | 20.3 | 17.91 | 18.08 | -0.12 | 0.17 | -2.51 | -2.22 | 0.16 | 0.3 | -2.342 | -2.201 | 9.5 |
| YBL015W | ACH1 | 22.31 | 21.85 | 20.87 | 20.69 | -0.46 | -0.18 | -1.44 | -1.16 | -0.18 | -0.05 | -1.272 | -1.141 | 9.1 |
| YPR006C | ICL2 | 17.75 | 17.47 | 14.57 | 14.88 | -0.28 | 0.31 | -3.18 | -2.59 | -1.1E-15 | 0.44 | -3.012 | -2.571 | 9.0 |
| YMR090W | YMR090W | 16.31 | 15.82 | 14.16 | 14.22 | -0.49 | 0.06 | -2.15 | -1.6 | -0.21 | 0.19 | -1.982 | -1.581 | 9.0 |
| YOR187W | TUF1 | 19.26 | 19.14 | 18.11 | 17.9 | -0.12 | -0.21 | -1.15 | -1.24 | 0.16 | -0.08 | -0.982 | -1.221 | 8.8 |
| YML054C | CYB2 | 20.29 | 20.09 | 18.74 | 18.37 | -0.2 | -0.37 | -1.55 | -1.72 | 0.08 | -0.24 | -1.382 | -1.701 | 8.7 |
| YJL066C | MPM1 | 16.49 | 15.81 | 13.13 | 13.25 | -0.68 | 0.12 | -3.36 | -2.56 | -0.4 | 0.25 | -3.192 | -2.541 | 8.6 |
| YOR142W | LSC1 | 21.12 | 20.93 | 19.89 | 19.91 | -0.19 | 0.02 | -1.23 | -1.02 | 0.09 | 0.15 | -1.062 | -1.001 | 8.3 |
| YMR297W | PRC1 | 19.27 | 18.82 | 16.01 | 15.33 | -0.45 | -0.68 | -3.26 | -3.49 | -0.17 | -0.55 | -3.092 | -3.471 | 8.1 |
| YHR089C | GAR1 | 18.63 | 18.47 | 15.96 | 15.35 | -0.16 | -0.61 | -2.67 | -3.12 | 0.12 | -0.48 | -2.502 | -3.101 | 8.1 |
| YBR222C | PCS60 | 18.33 | 18.16 | 16.18 | 15.64 | -0.17 | -0.54 | -2.15 | -2.52 | 0.11 | -0.41 | -1.982 | -2.501 | 7.5 |
| YNL104C | LEU4 | 19.85 | 19.41 | 18.55 | 18.28 | -0.44 | -0.27 | -1.3 | -1.13 | -0.16 | -0.14 | -1.132 | -1.111 | 7.5 |
| YHR005C-A | TIM10 | 16.74 | 16.19 | 14.5 | 14.06 | -0.55 | -0.44 | -2.24 | -2.13 | -0.27 | -0.31 | -2.072 | -2.111 | 7.2 |
| YDR148C | KGD2 | 21.05 | 20.53 | 19.51 | 19.43 | -0.52 | -0.08 | -1.54 | -1.1 | -0.24 | 0.05 | -1.372 | -1.081 | 7.1 |
| YNL239W | LAP3 | 18.7 | 18.68 | 15.5 | 15.93 | -0.02 | 0.43 | -3.2 | -2.75 | 0.26 | 0.56 | -3.032 | -2.731 | 6.6 |
| YNR001C | CIT1 | 23.58 | 23.52 | 22.4 | 22.36 | -0.06 | -0.04 | -1.18 | -1.16 | 0.22 | 0.09 | -1.012 | -1.141 | 6.4 |
| YHR208W | BAT1 | 18.12 | 18.08 | 15.54 | 15.87 | -0.04 | 0.33 | -2.58 | -2.21 | 0.24 | 0.46 | -2.412 | -2.191 | 6.3 |
| YPR001W | CIT3 | 17.8 | 17.09 | 13.98 | 14.43 | -0.71 | 0.45 | -3.82 | -2.66 | -0.43 | 0.58 | -3.652 | -2.641 | 6.2 |
| YDL223C | HBT1 | 21.47 | 21.42 | 20.36 | 20.3 | -0.05 | -0.06 | -1.11 | -1.12 | 0.23 | 0.07 | -0.942 | -1.101 | 6.0 |
| YDL182W | LYS20 | 17.9 | 17.98 | 16.02 | 15.5 | 0.08 | -0.52 | -1.88 | -2.48 | 0.36 | -0.39 | -1.712 | -2.461 | 5.6 |
| YMR083W | ADH3 | 19.83 | 19.22 | 17.95 | 18 | -0.61 | 0.05 | -1.88 | -1.22 | -0.33 | 0.18 | -1.712 | -1.201 | 5.6 |
| YDL225W | SHS1 | 15.38 | 15.52 | 13.13 | 13.34 | 0.14 | 0.21 | -2.25 | -2.18 | 0.42 | 0.34 | -2.082 | -2.161 | 5.6 |
| YHR132C | ECM14 | 17.83 | 17.71 | 13.88 | 14.62 | -0.12 | 0.74 | -3.95 | -3.09 | 0.16 | 0.87 | -3.782 | -3.071 | 5.5 |
| YPR187W | RPO26 | 17.17 | 16.54 | 15.49 | 15.36 | -0.63 | -0.13 | -1.68 | -1.18 | -0.35 | -7.8E-16 | -1.512 | -1.161 | 5.4 |
| YAL044C | GCV3 | 19.79 | 19.3 | 17.45 | 17.76 | -0.49 | 0.31 | -2.34 | -1.54 | -0.21 | 0.44 | -2.172 | -1.521 | 5.4 |
| YIR038C | GTT1 | 17.86 | 18.03 | 14.74 | 13.77 | 0.17 | -0.97 | -3.12 | -4.26 | 0.45 | -0.84 | -2.952 | -4.241 | 5.4 |
| YML010W | SPT5 | 17.21 | 16.46 | 14.38 | 14.66 | -0.75 | 0.28 | -2.83 | -1.8 | -0.47 | 0.41 | -2.662 | -1.781 | 5.1 |

| | | | | | | | | | | | | | | |
|---|---|---|---|---|---|---|---|---|---|---|---|---|---|---|
| **YGR282C** | **BGL2** | **19.38** | **19.39** | **17.28** | **17.59** | **0.01** | **0.31** | **-2.1** | **-1.8** | **0.29** | **0.44** | **-1.932** | **-1.781** | **5.0** |
| **YDL066W** | **IDP1** | **21.05** | **21.11** | **19.88** | **19.65** | **0.06** | **-0.23** | **-1.17** | **-1.46** | **0.34** | **-0.1** | **-1.002** | **-1.441** | **5.0** |
| **YOR341W** | **RPA190** | **18.84** | **18.29** | **16.96** | **16.38** | **-0.55** | **-0.58** | **-1.88** | **-1.91** | **-0.27** | **-0.45** | **-1.712** | **-1.891** | **4.9** |
| **YJL076W** | **NET1** | **15.18** | **15.35** | **13.33** | **13.46** | **0.17** | **0.13** | **-1.85** | **-1.89** | **0.45** | **0.26** | **-1.682** | **-1.871** | **4.8** |
| **YJL159W** | **HSP150** | **19.51** | **19.1** | **15.68** | **16.47** | **-0.41** | **0.79** | **-3.83** | **-2.63** | **-0.13** | **0.92** | **-3.662** | **-2.611** | **4.8** |
| **YDL140C** | **RPO21** | **19.34** | **19.13** | **18.29** | **17.84** | **-0.21** | **-0.45** | **-1.05** | **-1.29** | **0.07** | **-0.32** | **-0.882** | **-1.271** | **4.7** |
| **YCL043C** | **PDI1** | **20.89** | **20.97** | **19.19** | **19.36** | **0.08** | **0.17** | **-1.7** | **-1.61** | **0.36** | **0.3** | **-1.532** | **-1.591** | **4.7** |
| **YLR259C** | **HSP60** | **21.92** | **21.75** | **20.1** | **20.41** | **-0.17** | **0.31** | **-1.82** | **-1.34** | **0.11** | **0.44** | **-1.652** | **-1.321** | **4.7** |
| **YLR355C** | **ILV5** | **22.84** | **22.93** | **21.19** | **21.34** | **0.09** | **0.15** | **-1.65** | **-1.59** | **0.37** | **0.28** | **-1.482** | **-1.571** | **4.7** |
| **YLR027C** | **AAT2** | **20.19** | **20.36** | **18.84** | **18.73** | **0.17** | **-0.11** | **-1.35** | **-1.63** | **0.45** | **0.02** | **-1.182** | **-1.611** | **4.4** |
| **YCR028C-A** | **RIM1** | **18.38** | **18.11** | **16.11** | **16.59** | **-0.27** | **0.48** | **-2.27** | **-1.52** | **0.01** | **0.61** | **-2.102** | **-1.501** | **4.2** |
| **YBL075C** | **SSA3** | **19.62** | **19.19** | **16.04** | **14.56** | **-0.43** | **-1.48** | **-3.58** | **-4.63** | **-0.15** | **-1.35** | **-3.412** | **-4.611** | **4.2** |